eman ta zabal zazu

Universidad del País Vasco
Euskal Herriko Unibertsitatea

Doktorego tesia

Promotion of membrane interactions as a pathway for HIV antibody optimization

Sara Insausti Gonzalez

2021

Zuzendaria: José Luis Nieva Escandón

Biofisika Institutua (CSIC/EHU)

Biokimika eta Biologia Molekularra saila

Etxekoei,

Acknowledgements

The present thesis was performed at Instituto Biofisika (CSIC, UPV/EHU) under the supervision of Professor José Luis Nieva. The work was supported by the Basque Government (IT838-13 and IT1196-19), the Spanish MINECO (BIO2015-64421-R (MINECO/AEI/FEDER, UE)); and MCIU (RTI2018-095624-B-C21 (MCIU/AEI/FEDER, UE)). The author was a recipient of a predoctoral fellowship from the Basque Government.

Aitorpena

Tesi hau Biosifiska Institutuan (CSIC, UPV/EHU) burutua izan da, José Luis Nieva katedradunaren zuzendaritzapean. Lanak Eusko Jaurlaritzaren (IT838-13 and IT1196-19) eta Espainiako Gobernuaren MINECO (BIO2015-64421-R (MINECO/AEI/FEDER, UE)) eta MCIU (RTI2018-095624-B-C21 (MCIU/AEI/FEDER, UE)) diru-laguntzak jaso ditu. Autorea Eusko Jaurlaritzaren ikertzaile ez-doktoreen prestakuntzarako doktoratu aurreko laguntzaren onuraduna izan da.

Autorearen argitalpenak

Rujas, E.*, Insausti, S.*, Leaman, D. P., Carravilla, P., González-Resines, S., Monceaux, V., Sánchez-Eugenia, R., García-Porras, M., Iloro, I., Zhang, L., Elortza, F., Julien, J. P., Saéz-Cirión, A., Zwick, M. B., Eggeling, C., Ojida, A., Domene, C., Caaveiro, J., & Nieva, J. L. (2020). Affinity for the Interface Underpins Potency of Antibodies Operating In Membrane Environments. *Cell Reports*, *32*(7), 108037. https://doi.org/10.1016/j.celrep.2020.108037

Torralba, J., de la Arada, I., Carravilla, P., Insausti, S., Rujas, E., Largo, E., Eggeling, C., Arrondo, J., Apellániz, B., & Nieva, J. L. (2020). Cholesterol Constrains the Antigenic Configuration of the Membrane-Proximal Neutralizing HIV-1 Epitope. *ACS infectious diseases*, *6*(8), 2155–2168. https://doi.org/10.1021/acsinfecdis.0c00243

Carravilla, P., Chojnacki, J., Rujas, E., Insausti, S., Largo, E., Waithe, D., Apellaniz, B., Sicard, T., Julien, J. P., Eggeling, C., & Nieva, J. L. (2019). Molecular recognition of the native HIV-1 MPER revealed by STED microscopy of single virions. *Nature communications*, *10*(1), 78. https://doi.org/10.1038/s41467-018-07962-9

Rujas, E., Leaman, D. P., Insausti, S., Ortigosa-Pascual, L., Zhang, L., Zwick, M. B., & Nieva, J. L. (2018). Functional Optimization of Broadly Neutralizing HIV-1 Antibody 10E8 by Promotion of Membrane Interactions. *Journal of virology*, *92*(8), e02249-17. https://doi.org/10.1128/JVI.02249-17

Rujas, E., Insausti, S., García-Porras, M., Sánchez-Eugenia, R., Tsumoto, K., Nieva, J. L., & Caaveiro, J. M. (2017). Functional Contacts between MPER and the Anti-HIV-1 Broadly Neutralizing Antibody 4E10 Extend into the Core of the Membrane. *Journal of molecular biology*, *429*(8), 1213–1226. https://doi.org/10.1016/j.jmb.2017.03.008

Rujas, E., Caaveiro, J. M., Insausti, S., García-Porras, M., Tsumoto, K., & Nieva, J. L. (2017). Peripheral Membrane Interactions Boost the Engagement by an Anti-HIV-1 Broadly Neutralizing Antibody. *The Journal of biological chemistry*, *292*(13), 5571–5583. https://doi.org/10.1074/jbc.M117.775429

- **Aurkibidea**

LABURDUREN ETA SINBOLOEN ZERRENDA

6-HB	6-helix bundle / 6-helize sorta
ADA	Anti-Drug Antibody / Botika-aurkako Antigorputza
ADCC	Antibody-Dependent Cellular Cytotoxicity / Antigorputzen menpeko zitotoxizitate zelularra
ADP	Antibody-Dependent Phagocytosis / Antigorputzen Menpeko Fagozitosia
AIDS / HIES	Acquired Immune Deficiency Syndrome / Hartutako ImmunoEskasiaren Sindromea
ANA	Anti-Nuclear Antibodies / Nukleoaren aurkako Antigorputza
AP	Alkaline phosphatase
ATP	Adenosine triphosphate
AZT	Zidovudin
BCR	B-cell receptor / B-zelulen hartzailea
bnAb	Broadly neutralizing antibody / Espektro zabaleko antigorputz neutralizatzailea
BN-PAGE	Blue-native polyacrylamide gel electrophoresis
BSA	Bovine serum albumin / Behi-gazur albumina
CA	Capsid / Kapsidea
CD4bs	CD4-binding site / CD4-ren batuketa gunea
CDC^1	Center for Disease Control / Gaixotasunen Kontrolerako Zentroa
CDC^2	Complement Dependent Cytotoxicity / Konplementuaren menpeko zitotoxizitatea
CD	Circular Dichroism / Dikroismo zirkularra
CDR	Complementarity determining region / Osagarritasuna determinatzen duen eskualdea
C_H	Constant heavy / Konstante-astuna
Chol	Cholesterol / Kolesterol
C_L	Constant light / Konstantea-arina

CR	Chemokine Receptor / Kimiokina-hartzaile
CSR	Class Switch Recombination / Klase-aldaketa berkonbinaketa
CT	Cytoplasmic Tail / Itsats zitoplasmikoa
CTL	Control / Kontrola
DDM	n-dodecyl- -D-maltoside
DEAE	Diethylaminoethyl-dextran hydrochloride
DMEM	Dulbecco's Modified Eagle's Medium / Medioa
DMPC	1,2-dimyristoyl-sn-glycero-3-phosphocholine
DHPC	1,2-dihexanoyl-sn-glycero-3-phosphocholine
DMSO	Dimethylsulfoxide
DNA	Deoxyribonucleic acid
DOPC	1,2-dioleoyl-*sn*-glycero-3-phosphatidylcholine
DOPE	1,2-dioleoyl-*sn*-glycero-3-phosphatidylethanolamine
DOPS	1,2-dioleoyl-*sn*-glycero-3- phosphatidylserine
DPC	n-dodecylphosphocholine
EDTA	Ethylenediaminetetraacetic acid
ELISA	Enzyme linked immunosorbent assay
EM	Electron Microscopy / Mikroskopia Elektronikoa
Env	Envelope glycoprotein / Bildukiko glukoproteina
ER	Endoplasmic Reticulum / Erretikulu endoplasmatikoa
F/F_0	Fluorescence intensity/Initial fluorescence intensity / Fluoreszentzia intentsitatea/Haserako intentsitatea
Fab	Fragment, antigen-binding / Antigenoa batzen duen fragmentua
FACS	Fluorescence-activated cell sorting / Fluoreszentziaz aktibatutako zelula sailkapena
Fc	Fragment crystallizable of Immunoglobulins / Immunoglobulinen fragment kristalizagarria
FcγR	Fc gamma receptors / Fc gamma hartzaileak
FcRn	Neonatal Fc receptor / Fcn hartzailea
FDA	Food and Drug Administration / Elikagai eta botiken administrazioa
FITC	Fluorescein isothiocyanate

FP^1	Fusion peptide
FP^2	FectoPro
Fv	Variable fragment / Fragmentu aldakorra
FWR	Framework regions
GC	Germinal centre / Zentro germinala
GFP	Green fluorescent protein / Proteina fluoresezente berdea
Grx	Glutaredoxin
Gp41	HIV glycoprotein 41 kDa (transmembrane subunit) / GIB 41 kDa glukoproteina (transmintz azpiunitatea)
Gp120	HIV glycoprotein 120 kDa (surface subunit) / GIB 120 kDa glukoproteina (gainazaleko azpiunitatea)
HAART	Highly active antiretroviral therapy / Terapia anti-erretrobiral oso aktiboa
HC	Heavy chain / Kate astuna
HEPES	4-(2-hydroxyethyl)piperazine-1-ethanesulfonic acid
HIV-1/GIB-1	Human immunodeficiency virus type 1 / 1. Motako Giza Immunoeskasiaren Birusa
HIV-2/GIB-2	Human immunodeficiency virus type 2 / 2. Motako Giza Immunoeskasiaren Birusa
HPLC	High performance liquid chromatography / Etekin altuko kromatografia likidoa
HR	Heptad repeated region / Heptada errepikakorren eskualdea
HRP	Horseradish peroxidase
IACUC	Institutional Animal Care and Use Committee / Animalien zaintza eta erabileraren komite instituzionala
IC_{50}	50% inhibitory concentration / %50 kontzentrazio inhibitzailea
IEC	Ion exchange chromatography / Ioi-trukeko kromatografia
Ig	Immunoglobulin
IGH	Immunoglobulin Heavy gene / Immunoglobulinen gene astuna
IGκ	Immunoglobulin Kappa Light gene / Immunoglobulinen Kappa gene arina

IGλ	Immunoglobulin Gamma light gene / Immunoglobulinen Gamma kate arina
IMP	Intrinsic mannose patch / Berezko manosa adabakia
iMab	Ibalizumab
IN	Integrase / Integrasa
IPTG	Isopropyl-D-thiogalactopyranoside
Kn	Kanamycin / Kanamizina
LC	Light chain / Kate Arina
LDH	Lactate Dehydrogenase
LUVs	Large unilamellar vesicles / Lamela bakarreko besikula handiak
MA	Matrix / Matrizea
Man	Mannose / Manosa
MAb	Monoclonal antibody / Antigorputz monoklonala
MALDI-TOF	Matrix-assisted laser desorption/ionization time-of-flight / Matrizean egindako laser desortzio/ionizazio hegaldi-denbora
MCS	Multiple cloning site / Klonazio gune anizkoitza
MHC	Major Histocompatibility Complex / Histokonpatibilitate konplexu nagusia
MLV	Multilamellar vesicles / Lamela ugaridun besikulak
MPER	Membrane-proximal external región / Mintzaren hurbileko kanpo-eskualdea
nAb	Neutralizing Antibody / Antigorputz neutralizatzailea
NBD	7-nitro-1,2,3-benzoxadiazole
NC	Nucleocapsid / Nukleokapsidea
NIAID	National Institute of Allergy and Infectious Diseases / Alergia eta gaixotasun infekziosoen instituto nazionala
NIH	National Institute of Health / Osasunaren instituto nazionala
Ni-NTA	Nickel-nitrilotriacetic acid
NMR	Nuclear magnetic resonance / Erresonantzia nuklear magnetikoa
ORF	Open reading frame / Irakurketa irekiko sekuentzia

OD	Optical density / Dentsitate optikoa
o/n	Overnight / Gauean zehar
PBS	Phosphate-buffered saline / Fosfatodun indargetzailea
PBST	Phosphate-buffered saline, %0.05 Tween20
PBMC	Peripheral Blood Mononuclear Cells / Odol periferikoko nukleo bakarreko zelulak
PCR	Polymerase chain reaction / Polimerasa kate-erreakzioa
POPC	1-palmitoyl-2-oleoyl-sn-glycero-3-phosphocholine
PR	Protease / Proteasa
PS	Phosphatidylserine
PsV	Pseudovirus
PVDF	Polyvinylidene difluoride
PTM	Post-translational modification / Itzulpen ondoko aldaketa
Rho	Lissamine rhodamine B sulfonyl chloride
RLU	Relative luminescence units / Lumineszentzia unitate erlatiboa
RT^1	Reverse transcriptase / Alderantzizko transkriptasa
RT^2	Room temperature / Giro tenperatura
scFv	Single-chain variable fragment / Kate bakarreko fragmentu aldakorra
SDS	Sodium dodecyl sulfate
SDS-PAGE	Sodium dodecyl sulfate polyacrylamide gel electrophoresis
SEC	Size-Exclusion Chromatography / Gel iragazpen kromatografia
SHIV	Simian-human immunodeficiency virus / Tximino-Giza immunoeskasiaren birusa
SHM	Somatic hypermutation / Hipermutazio somatikoa
SIV	Simian immunodeficiency virus / Tximinoen immunoeskasiaren birusa
SM	Sphingomyelin / Esfingomielina
SP	Signal Peptide / Seinale peptidoa
STED	Stimulated emission depletion microscopy / Igorpen-murriztuko kitzikapen mikroskopia

TdT	Deoxynucleotidyl Transferase
TEV	Tobacco Etch Virus / Birusa
T_{agg}	Aggregation transition temperature / Agregazio trantsizio tenperatura
T_M	Melting temperature / Urtze tenperatura
TMB	3,3',5,5'- tetramethylbenzidine
TMD	Transmembrane domain / Transmintz domeinua
Trx	Thioredoxin
Tween 20	Polyethyleneglycol sorbitan monolaurate
UCA	Unmutated Common Ancestors / Mutatu gabeko aitzindari komuna
UNAIDS	The Joint United Nations Programme on HIV and AIDS / GIB eta HIESaren Nazio Batuen programa
UV	Ultraviolet / Ultramore
V_H	Variable heavy / Aldakor astuna
V_L	Variable light / Aldakor arina
VL	Virus-like / Birus-antzeko
Vpr	Viral Protein R / R proteina birala
WB	Western blot

LABURPENA

SARRERA

Giza Immunoeskasiaren birusa (GIB), Hartutako Immuno Eskasiaren Sindromearen (HIES) eragilea, 1983an isolatu zuten lehen aldiz (Barré-Sinoussi et al., 1983) Parisko Pasteur Institutuan. UNAIDS-en arabera, GIBak 75 millioi pertsona kutsatu ditu pandemia hasi zenetik, eta munduan 32 milioi inguru hil dira HIESari lotutako gaixotasunek eraginda. 25 urte baino gehiagoren ondoren birus honen transmisio, prebentzio eta tratamenduaren inguruan egindako aurrerapenak ugariak izanagatik ere, oraindik ez dago gaixotasuna sendatu edo saihesteko gai den tratamendu ezta txertorik. Gaur egun, terapia antierretrobiralean oinarritzen da infektatutako banakoen tratamendua (ingelesetik, *"Highly Active Antiretroviral Therapy"* edo HAART), eta GIBa ezabatzen ez badu ere, honi esker hasiera batean hilgarria zen gaixotasun hau kroniko bilakatzea lortu da.

GIBak CD4 hartzailea adierazten duten zelulak infektatzen ditu, T_h linfozitoak batez ere. Hartzaile honi atxiki ondoren, birusaren eta zelularen mintzen arteko fusioa gertatzen da; azkenik, birusaren material genetikoa zelula ostalariaren genoman txertatzen denean amaitzen da infekzio prozesua. Momentu honetan, birusa latentzia fasean sar daiteke denbora zehaztugabe batez, edota aktibatu, proteina biralak ekoitzi eta partikula berriak sortuz. Linfozitoak suntsituz joan ahala, tratamendurik jasotzen ez duten banakoek immunoeskasia larria pairatuko dute, HIESa karakterizatzen duten gaixotasun oportunistei bidea irekiz (Simon et al., 2006).

GIBaren aurkako txerto baten diseinua eta gaixoen tratamendua bereziki zaila suertatzen da birusak ostalariaren immunitate sistemari ihes egiteko mekanismo ugari garatu dituelako (Johnson & Desrosiers, 2002). Zelula Env glukoproteinaz baliatzen da $CD4^+$ zelulak ezagutzeko, immunitate sistemarentzat ikusgai dagoen antigeno bakarra. Env gp120 eta gp41 azpiunitateek eratutako hiru heterodimeroz osaturiko transmintz glukoproteina da; lehenengo azpiunitateak zelula ostalariaren ezagumenduan parte hartzen duen bitartean, bigarrenak mintzen arteko fusioa eragiten du. Proteina oso dinamikoa eta ezegonkorra da, eta oso kopuru txikian adierazten da GIBaren gainazalean. Horrez gain, sekuentzian etengabe akatsak sartzen dituen erretrotranskiptasa entzimak eragindako aniztasun genetiko izugarriak trimeroaren ezagumendua zailtzen du. Bestalde, glukosilazio maila altuaz eta mintz lipidikoaz

baliatzen da birusa Env proteinan ezinbesteko funtzioak betetzen dituzten domeinu kontserbakorrak ezkutatzeko. Azken urteetan, hala ere, antigorputzen isolamendu tekniketan emandako hobekuntzek eta etekin-altuko neutralizazio saiotan izandako aurrerapenek, GIBaren infekzioa blokeatzeko gai diren, neutralizazio potentzia altua eta espektro zabala erakusten duten antigorputzen isolamendua ahalbidetu dute zenbait pazienteren gazurretik (Sok & Burton, 2018). Env glukoproteinan aurkitzen diren zenbait domeinu kontserbakor ezagutzen dituzten antigorputz hauei, birus andui ugari eta klinikan isolatutako partikula biral desberdinak neutralizatzeko gai direnez, espektro zabaleko antigorputz neutralizatzaile deitu zaie (ingelesetik, *"broadly neutralizing antibodies"* edo bnAb). Etengabe immunitate sistemak ezarritako presio selektiboaren ondorioz mutatzen ari den birusaren, eta honekin batera eboluzionatzen ari den erantzun immune humoralaren emaitza dira bnAb-ak (Liao et al., 2013). Hori dela eta, hipermutazio somatiko (SHM) tasa altua eta kate astunean CDR3 begizta luzeak bezalako ezohiko ezaugarriak aurkezten dituzte, eta oso zailak dira txertaketa bidez induzitzeko.

Antigorputzek terapian erabiltzeko desiragarriak diren ezaugarriak aurkezten dituzte; besteak beste, immunitate sistemaren gainontzeko elementuekin elkar eragiteko gaitasuna, "erdibizitza" luzea eta profil kliniko seguruak. Azken urteetan deskribatutako potentzia altuko zenbait bnAb-ek, gainera, balio farmakozinetiko itxaropentsuak erakutsi dituzte gizakietan egindako entsegu klinikoetan (Bar-On et al., 2018; Mendoza et al., 2018), eta konbinatuta erabili direnean, GIBarekin infektatutako gaixoen karga birala apaldu eta mantentzeko gai izan dira, mutazio erresistenteen sorrera eragotziz.

GIB1-aren aurkako bnAb-en artean, birusaren mintz lipidikoan murgilduta aurkitzen den MPER (ingelesetik, "*Membrane Proximal External Region"*) eskualdea ezagutzen dutenak dira espektro zabalena dutenak. Izan ere, MPER ezinbestekoa da mintzen arteko fusioa eragiteko (B. Apellániz, Rujas, et al., 2014) eta beraz, bere sekuentzia oso kontserbatuta dago andui ezberdinen artean. 4E10 eta 10E8 dira talde honetan hobekien deskribatuak izan diren antigorputzak. Biek ere, itu duten epitopo helikoidalaren ezagumenduan glukoproteinaren ektodomienuak eta birusaren mintzak eragiten dituzten eragozpen esterikoei egokitzeko gainazalak garatu dituzte. Halaber, antigorputzak, Env trimeroak eta mintzak osatutako konplexuaren modelo estrukturalek MPER helizeak, mintz biralaren lipidoek eta Env-en ektodomeinuko zenbait kontaktuk osatutako epitopo kuaternarioa definitu dute (1. Irudia).

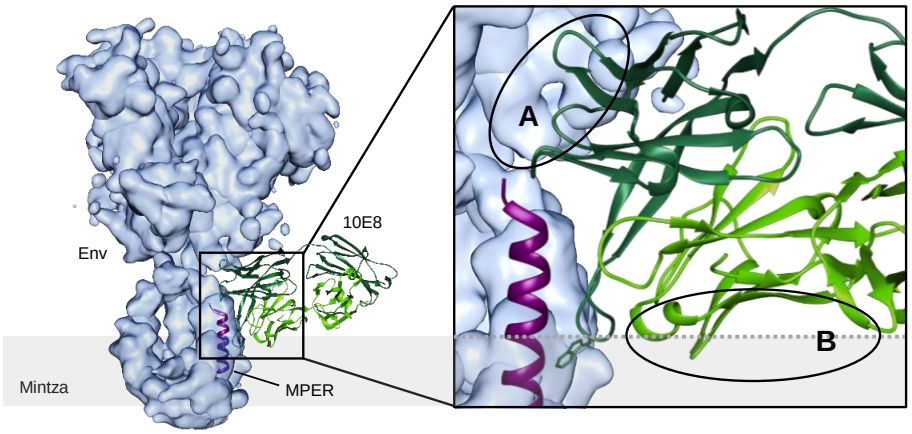

1. Irudia. 10E8 bnAb-aren eta Env trimeroan mintzetik hurbil aurkitzen den MPER epitopoaren arteko elkarrekintza. Ezkerrean: 10E8 Fab-a (PDB kodea: 5SY8) Env trimerikoari (EMDB-3308) lotuta. Eskuinean: antigorputzak garatutako bi gainazalak, mintzean txertatutako bere epitopoaren ezagumenduan trimeroaren ektodomeinuak (A) eta birusaren mintzak (B) ezartzen dituzten oztopoei egokitzeko.

Tesi honen helburu nagusia espezifitate eta potentzia altuko antigorputz neutralizatzaileak eskuratzea izan da, anti-MPER espektro zabaleko antigorputz errekonbinanteak plataforma gisa erabiliz. Horretarako, afinitate altuko batuketa gunetik urrun dagoen gainazalaren eta mintz biralaren arteko elkarrekintzak indartu nahi izan dira, ingeniaritza genetiko arrazionalaz baliatuz.

EMAITZAK ETA EZTABAIDA

Lehenik eta behin, mutagenesi tradizionala erabili da 10E8 eta 4E10 Fab-ek MPER lotzean birusaren mintzarekin kontaktuan gelditzen diren gainazalean Arg hondarrak gehitzeko (2. Irudia, I). Gainazal hauen karga neto positiboa handitzean birusaren bildukiarekin elkarrekintza elektrostatikoak sustatzea lortu da; izan ere, birusaren mintzaren kanpoaldeak karga neto negatiboa erakusten du, PS fosfolipido anionikoaren eraginez (Carravilla et al., 2019). 10E8 basatiak ez du espontaneoki mintzekin elkarrekiten, diseinatutako 10E8-3R mutante berriak, ordea, gaitasun hau izateaz gain, aktibitate antibiralaren emendioa erakutsi du (neutralizazio saioetan lortutako bataz-besteko IC_{50} balioak antigorputz basatiarenak baino 5-10 aldiz baxuagoak izan dira). Ez hori bakarrik, 3R mutazioak HC.S100cF ordezkapenarekin konbinatuz 10E8 basatia baino 20 aldiz hobea den antigorputza eskuratu da. Mintzarekiko elkarrekintza elektrostatikoak indartzeak, bestalde, ez du 4E10-3R antigorputzaren potentzian eraginik izan.

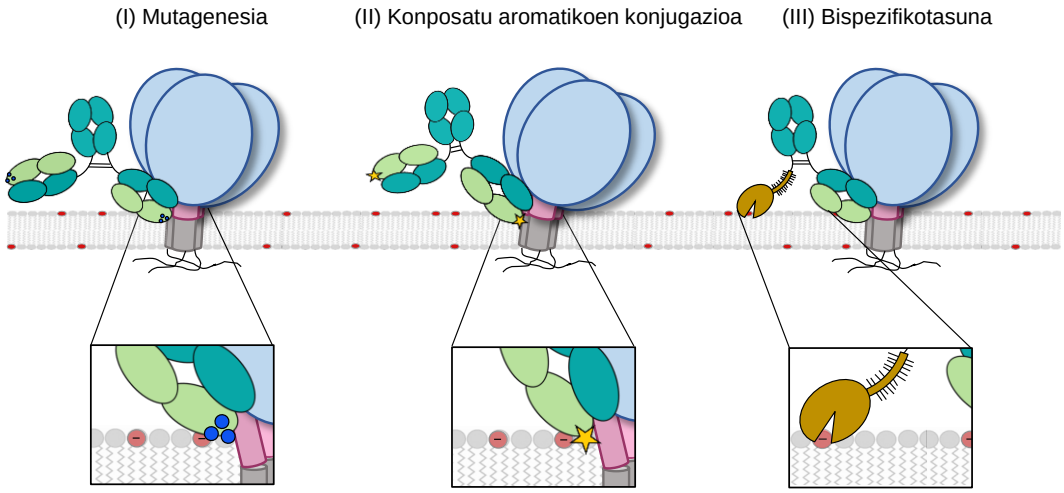

2. Irudia. Tesi honetan anti-MPER antigorputzak optimizatzeko erabilitako estrategia desberdinak. Anti-MPER antigorputzak mutagenesi konbentzionala erabiliz (I), zuzendutako konposatu aromatikoen konjugazioaren bidez (II) eta espezifitate desberdineko bigarren batuketa-bloke bat erantsiz (III) eraldatuak izan dira tesi lan honetan, beren funtzio biologikoa emendatzeko asmoz. MPER kolore arrosaz irudikatu da, antigorputzaren kateak berde argiz (LC) eta ilunez (HC), eta TIM hartzailearen ektodomeinua horiz.

Bestetik, konposatu aromatikoen erabileran oinarritzen den metodologia berri bat erabili da: Arrazoia erabiliz diseinatutako molekulen zuzendutako konjugazio kimikoak MPER epitopoari batu ondoren mintz biralarekin kontaktuan gelditzen den Fab-aren gainazaleko interfasearekiko hidrofobizitatea emendatzen du, ondorioz antigorputzaren potentzian zuzenki eraginez (2. Irudia, II). Horrela, posizio eta molekula egokiak aukeratu ondoren, 10E8 eta 4E10 antigorputzen funtzio biologikoa modu esanguratsuan emendatzea lortu da. Eraldatutako antigorputz batzuen kasuan, bataz besteko IC_{50} balioak basatiarenak baino 100 adliz txikiagoak izan dira, gaur egun terapian erabiltzeko aukeratuak izan diren GIB1-aren aurkako bnAb potenteenen balioetara asko hurbilduz.

Ondoren, eta perfil terapeutiko interesgarriena duen antigorputza 10E8-a izanik, kimikoki eraldaktutako bi aldaeren ezaugarri biologikoak aztertuak izan dira, *in vitro* (lerro zelularrekin toxizitatea eta poliespezifikotasuna aztertuz) eta *in vivo* (Balb/c xaguak erabiliz antigorputzek gazurrean denboran zehar duten eskuragarritasuna neurtuz). Emaitzek optimizatutako antigorputz bakoitzaren polierreaktibitatea, toxizitatea eta bioeskuragarritasuna erabilitako eraldaketa kimiko konkretuaren menpekoa izan daitekela iradokitzen dute; konsposatu bakoitzaren egitura eta ezaugarri fisiko-kimikoak soilik aztertuz ondorioztatzeko zaila.

Azkenik, anti-MPER antigorputzen abidezia, eta horrekin batera potentzia, emendatzeko erreminta gisa fosfolipidoen ezagumendu espezifikoaren erabilera aztertua izan da (2.III. Irudia). Hasierako emaitzek anti-MPER Fab-ak eta PS-batuketa domeinuak konbinatuz

molekula bi-espezifikoak sortzea posible dela baieztatu badute ere, ez da metodologia honekin antigorputzen potentzia emendatzea lortu, eta esperimentu gehiagoren beharra nabarmentzen da ondorio esanguratsuak atera ahal izateko.

PhD tesi lan honetan, antigorputzen eta mintzen interfasearen arteko elkarrekintzen sustapena erabili da GIBaren infekzioaren inhibitzaile ahaltsuak eskuratzeko. Mintzetik gertu aurkitzen diren epitopoak Influenza edo Ebola birusak bezalako giza-patogeno garrantzitsuen glukoproteinetan ere aurkituak izan dira, eta tumoreekin erlazionatutako antigenoa ugarik (CD20 edo CD37 hartzaileak) (Hendriks et al., 2017), ioi-kanalen familia desberdinaek (Hutchings et al., 2019) edota G-proteinei akoplatutako hartzaileek ere (Hutchings et al., 2017) antigorputz terapeutikoren itu diren eta mintzaz inguratuta dauden eskualde kontserbakorrak aurkezten dituzte.

Antigorputz terapeutikoen eta mintzen arteko elkarrekintzak bultzatzea, beraz, prozedura orokorra izan daiteke itu terapeutiko desberdinetan, mintzetik gertu edo mintzez inguratuta dauden epitopoen ezagumendu molekularra hobetu eta horrela antigorputzen funtzio biologikoa emendatzeko.

1. Kapitulua

SARRERA ETA HELBURUAK

1. SARRERA ETA HELBURUAK

1981. urtean, Amerikako Gaixotasunen Kontrolerako Zentroak (ingelesez *Center for Disease Control, CDC*) jatorri ezezaguneko immunoeskasia larria pairatzen zuten lehen kasuen berri eman zuen New York eta San Franciscon, Hartutako Immuno Eskasiaren Sindromea (HIES) izenarekin ezagutuko zen sindromea lehen aldiz deskribatuz.

Bi urte beranduago, Luc Montagnier eta Pasteur Institutuko lankideek giza erretrobirus berri bat isolatu zuten linfoadenopatia akutua jasaten zuen paziente batetik (Barré-Sinoussi et al., 1983). Erretrobirus hau HIESaren eragile bezala deskribatua izan zen (Gallo et al., 1984), eta Giza Immunoeskasiaren Birusa (GIB) izena eman zitzaion (Coffin et al., 1986). Aurkikuntza honen ondoren, Estatu Batuetako Osasun eta Gizarte Zerbitzuen Sailak bi urteren buruan GIBaren aurkako txerto bat eskuragarri egongo zela iragarri zuen. Ia lau hamarkadetako lanaren ondoren GIBaren transmisio eta epidemiologiaren inguruan zein immunologiaren arloan egindako aurrerapenak ikusgarriak izan badira ere, oraindik ez da lortu HIESa sendatuko duen botikarik, ez eta GIBaren aurkako txertorik ere.

Pandemia hasi zenetik, munduan 75 milioi pertsona kutsatu ditu GIBak, eta 32 milioi pertsona inguru hil dira HIESak eragindako gaitzen ondorioz (UNAIDS, 2018). Bestalde, joan den urtean 37.9 milioi pertsona bizi ziren GIBarekin, batez ere Afrikako hego-ekialdean.

1.1. 1 MOTAKO GIZA IMMUNOESKASIAREN BIRUSA (GIB-1)

GIBa *Lentivirus* generoaren *Retroviridae* familiaren barruan sailkatzen da. Bi mota bereizten dira (GIB-1, GIB-2), ustez espezieen artean emandako transmisio-gertakizun desberdinen ondorioz sortuak (Keele et al., 2006). Lehen motakoa da ezagunena, kutsakorrena, eta mundu mailako pandemiaren eragilea; bigarrena batez ere mendebaldeko Afrikan zabaltzen da. Azken honen transmisio maila baxuagoa da, eta gaixotasunaren progresioa eta immunoeskasiaren garapena modu geldoagoan ematen dira infektatutako banakoetan (Nyamweya et al., 2013).

GIB-1ak eragindako infekzioa sei aste inguru irauten dituen fase akutu batekin hasten da. Fase honetan birusaren erreplikazio azkarra ematen da infektatutako zeluletan eta beraz, karga biral altuak eta $CD4^+$ motako T linfozitoen beherakada azkarrak definitzen

dute (Hansasuta & Rowland-Jones, 2001). Fase honi sintomarik gabeko denboraldi batek jarraitzen dio. Bitarte horretan, maila baxuagoan bada ere, birusaren erreplikazioak dirau, immunitate sistema kronikoki aktibatuta mantenduz. Honen eraginez, $CD4^+$ zelulen zenbaketak beheranzko joeran jarraituko du. Azkenean, T linfozitoen murrizketak babesik gabe utziko du banakoa, HIESaren bereizgarri diren "infekzio oportunista" deiturikoei bidea irekiz (Simon et al., 2006).

Birusa guztiz desagerraraziko duen txerto zein sendagairik ez dagoen arren, HIESaren tratamenduan aurrerapen handiak egin dira lehenengo aldiz deskribatu zenetik. Azidotimidina (AZT) izan zen erretrobirusaren aurka erabilitako lehen botika, 1987an (Cohen et al., 2008). Ordutik, FDAk (ingelesetik, *Food and Drug Administration*) beste 222 tratamenduren erabilera onartu du. Gaur egun infekzioa kontrolatzeko erabiltzen den HAARTa (ingelesetik, *Highly Active Antiretroviral Therapy*) botika ezberdinen konbinaziotik dator, eta honi esker, HIESa gaixotasun kroniko bilakatzea lortu da. Tratamendu honen eskuragarritasuna, ordea, ez da unibertsala: batez ere Saharaz hegoaldeko Afrikan egiten du huts. Horrez gain, HAARTa ez da gai latentzia fasean dagoen birusa ezabatzeko, eta gaixoek bizitza guztian zehar jaso behar dute tratamendua, albo-ondorio ugarirekin.

1.1.1. GIB-1aren infekzio zikloa

GIBa mintz lipidiko batez inguratutako 100-150 nm-ko diametroa duen erretrobirus esferikoa da (1.1. irudia). Bi RNA molekula eta alderantzizko transkriptasa, (RT), eta integrasa (IN) entzimak dira birusaren nukleokapsidaren (NC) barnean aurkitzen diren elementu garrantzitsuenak. Nukleokapsidea inguratuz, kono itxura hartzen duen kapsidea (CA) aurkitzen da, CA proteina hexamerikoz osatuta. Matrizeak (MA), azkenik, birusaren egitura zentrala eta hau inguratzen duen bigeruza lipidikoa lotzen ditu. GIB-1aren mintzean fusio proteina (gp120/41) eta zenbait proteina zelular aurki daitezke (Ganser-Pornillos et al., 2012).

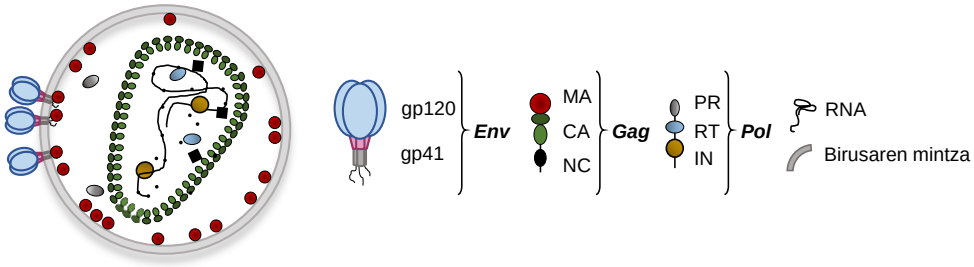

1.1. irudia: GIB-1 birioi helduaren modelo eskematikoa. Elementu garrantzitsuenak eskematikoki irudikatu dira. Irudia (Chojnacki et al., 2017)tik moldatua izan da.

GIB-1aren genoma bederatzi irakurketa irekiko sekuentzia (ingelesetik, *Open Reading Frame* edo ORF) kodetzen duten kate bakarreko bi RNA molekula identikok osatzen dute. *Gag, pol* eta *env* dira birusaren gene garrantzitsuenak: *Gag* egiturazko proteinen aitzindaria da, eta birus partikula eratuko duten MA, CA eta NC kodetzen ditu; *pol*-ek berriz, PR, RT eta IN osagai entzimatikoak kodetzen ditu. *Env* geneak, azkenik, GIB-1aren gainazalean dagoen gp160 fusio glukoproteina (Env) trimerikoa kodetzen du. Gp120 eta gp41 azpiunitateek osatzen duten aitzindari proteiko hau itu zelularen hartzaile eta kohartzailearen batuketaren, eta jarraian ematen den zelula eta birusaren mintzen arteko fusioaren erantzulea da (Freed, 2015).

GIB-1ak CD4 hartzailea adierazten duten zelulak infektatzen ditu: Batez ere $CD4^+$ T linfozitoak, baina baita monozito eta makrofagoen leinuko zelulak ere. Itzu zelula eta birusaren mintzen arteko fusioaren ondoren, birusaren kapsidea zelula ostalariaren zitoplasmara sartzen da, eta alderantzizko transkriptasak RNA birala kate bikoitzeko DNA bilakatuko du. Entzima honek akats ugari sortzen ditu nukleotido sekuentzian (Preston et al., 1988), birusaren dibertsitate tasa asko emendatuz. DNA probirala nukleora garraiatua izango da, eta integrasak itu zelularen genoman txertatuko du. Momentu honetan bi bide har ditzake GIB-1ak: batetik, latentzia fasean sar daiteke denbora mugagabez, eta bestetik, DNA transkripzioari ekin eta erreplikazio prozesua has dezake. Azken kasu honetan, egitura funtzioa betetzen duten MA, CA eta NC, eta Env proteinak ekoiztuak eta mintz plasmatikora garraiatuak izango dira, zeinetik gemazio bidez partikula biral heldugabeak sortuko diren. Birusaren proteasak Gag eta Gag-Pol polipeptido aitzindariak ebakiko ditu, infekzio ziklo berri bat hasteko prest egongo diren birus berrien heltze prozesua amaitutzat emanez (Briggs & Kräusslich, 2011; Checkley et al., 2011).

1.1.1.1 Zelula eta birusaren mintzen arteko fusioa

GIB-1aren Env glukoproteina trimerikoa, 1 motako mintz-fusio tresna, itu zelulara sartzeko baliatzen du birusak (White et al., 2008). Infekzio prozesua hasteko, Env proteinaren gp120 azpiunitateak CD4 zelula hartzailea ezagutzen du (Klatzmann et al., 1984), bere egituran konformazio aldaketa bat eraginez eta CXCR4 edo CCR5 (Deng et al., 1996; Feng et al., 1996) kimioerrezeptoreen ezagumendua ahalbidetuz. Kohartzailearen batuketak birusaren eta zelula mintzaren nahasketarekin amaituko diren berrantolaketa konformazionalak eragingo ditu gp41 azpiunitatean.

Gp41en egitura natibo eta metaegonkorra gp120 azpiunitatearekin egiten dituen kontaktuek egonkortzen dute (Mao et al., 2013). Gp120ak bere hartzailearekin elkarrekin ondoren (1.2B irudia, a), gp41aren amino muturrean aurkitzen den fusio peptidoak (FP)

konformazio aldaketa bat jasaten du, askatu eta itu zelularen mintzean txertatzen da. Gp41ak zelula mintza ainguratzen du, aldi berean hau desegonkortuz, eta modu iragankorrean bi mintzen osagai integrala bilakatzen da. Bi mintzen arteko zubi gisa jarduten duen egitura honi “urkila-aurreko bitartekari” (ingelesez, *pre-hairpin intermediate*) deritzo (1.2B irudia, b). Gp-41en N muturrean errepikatzen den heptadak (NHR) hiru harizpiz osatutako *coiled-coil* egitura zentral α-helikoidala eratzen du. Egitura honek hondar hidrofobiko kontserbakorrak uzten ditu ikusgai, azpiunitate beraren C muturreko heptada errepikakorra (CHR) zirrikitu horien artean paketatzea ahalbidetuz. Horrela, sei-helize sorta (ingelesetik, *six-helix bundle,* 6HB) deituriko egitura antiparaleloa sortzen da (1.2B irudia, c).

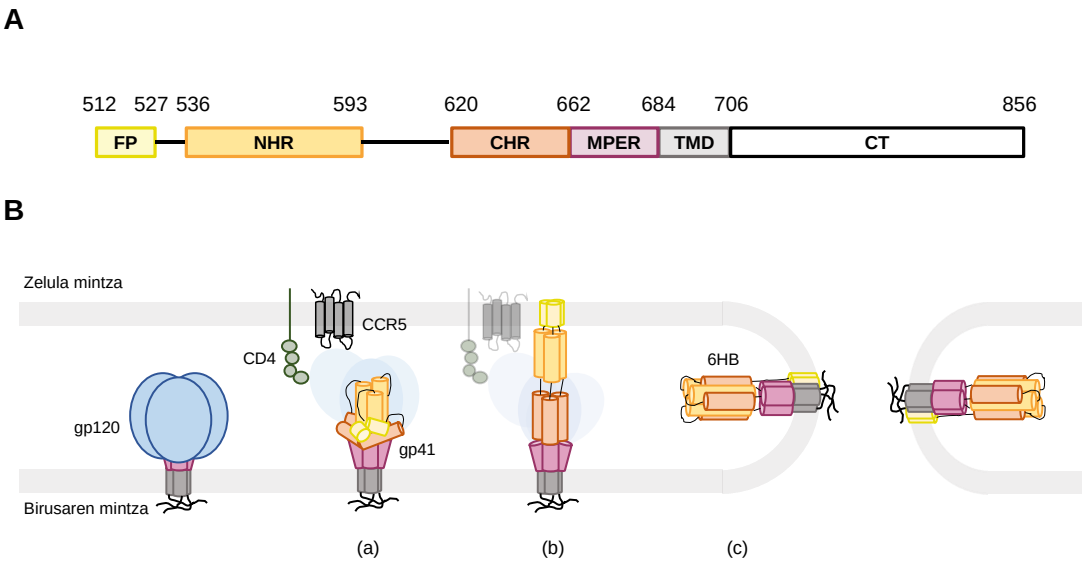

1.2. irudia: gp41 azpiunitatea birus eta zelula mintzaren arteko fusioan. (A) gp41 azpiunitatearen sekuentzia eta hau osatzen duten egitura elementu desberdinen eskema. Gp41 fusio peptido (FP) hidrofobikoaz, N eta C muturretan errepikatzen diren leuzina eta isoleuzinaz osatutako heptadez (NHR eta CHR), mintzetik gertu aurkitzen den MPER domeinuaz (ingelesetik, *Membrane Proximal External Region*), transmintz domeinuaz (TMD) eta isats zitoplasmatiko (CT) luzeaz osaturik dago. (B) GIBaren fusio prozesuaren modeloa (koloreak A-n bezala): gp120-ak CD4 hartzailearekin eta CCR5 edo CXCR4 kohartzailearekin elkarrekiten duenean (a) berrantolaketa bat jasaten du, FPa itu-zelularen mintzean txertatuz eta NHR eta CHR agerian utziz (b). Berehala, bigarren berrantolaketa batek gp41a fusio ondoko 6HB egiturara bideratuko du (c). Ondorioz, birusaren eta zelularen mintzaren nahasketa eta fusio poroaren eraketa gertatuko da.

6HB egituran, FPak (zelula mintzean txertatua) eta MPER/TMD domeinuak (TMDaren bidez birusaren mintzean ainguratua) bi mintzak elkarrengana hurbiltzen ditu (Blumenthal et al., 2012; Melikyan, 2011). Trimero bakarraren berrantolaketa prozesuan askatzen den energia askeak nahikoa izan beharko luke mintzen gainazalean ematen diren indar elektrostatiko uxagarriak gainditu eta mintzen arteko fusioa eragiteko

(Chernomordik & Kozlov, 2008), baina zenbait lanen arabera, trimero bat baino gehiagoren arteko kooperazioa ezinbestekoa da (Magnus et al., 2009). Fusio proteinek mintz bietan tokiko tolesturak sustatzen dituzte, zurtoin itxurako lehen fusio bitartekariaren eraketa bideratzeko beharrezkoa izango den energia eskaria gutxitzeko (Harrison, 2008). Ikerketa ugariren arabera, mintzaren kurbaduran estresa eta adabaki hidrofobiko txikiak eratzearen erantzuleak, batetik gp41en amino muturreko FP-a, eta bestetik MPER domeinua izango lirateke (Apellániz, Huarte, et al., 2014; Apellániz, Rujas, et al., 2014).

1.1.2. GIB-1aren gainazaleko fusio glukoproteina (Env)

GIBaren Env glukoproteina erretikulu endoplasmikoan sintetizatzen da, gp160 deituriko aitzindari bezala. Bertan, itzulpen ondoko eraldaketa ugari jasaten ditu, hala nola, disulfuro zubi kontserbakorren sorrera, N-motako glukosilazio ugari eta O-motako batzuk, eta batez ere trimeroak osatzen dituen oligomerizazioa (Land et al., 2003; van Anken et al., 2008). Glikano berriek eraldaketa gehiago jasaten dituzte Golgi aparatuan, eta furina-motako proteasa zelularrek glukoproteina trimerikoa modu ez kobalentean lotuta mantenduko duten bi azpiunitatetan ebakitzen dute, gp120 eta gp41 (Hallenberger et al., 1992). Heterodimero hauetako bakoitzaren hiru kopiek birusaren espikula heldu, monomerikoa eratzen dute. Azkenik, Env partikulak zelula ostalariaren mintzean ainguratzen dira TMDaren bidez, zelula ostalariaren mintzean proteina integral bezala.

1.1.2.1. Hiru dimentsioko egitura

GIBaren gainazalean aurkitzen den antigeno biral bakarra izanik, Env trimeroa antigorputz neutralizatzaileen itua eta txerto saiakeren itua bihurtu da. 2013. urtean, BG505 anduietik (A kladoa) eratorritako SOSIP.664 izeneko Env trimero solugarriaren lehen egiturak argitaratu ziren, X-izpien bidez (4.7 Å) eta kriomikroskopia elektronikoaz (CryoEM) (5.8 Å) eskuratuak (J. P. Julien et al., 2013; Lyumkis et al., 2013). Lehen aldiz maila-atomikoan aztertu ahal izan zen gp120ren aurkako antigorputzei loturiko Env glukoproteina izan zen. Egitura egonkor hau eskuratzeko, proteinaren sekuentzian bi eraldaketa burutu ziren: batetik, disulfuro zubi bat (SOS) sorrarazi zen gp120ren 501 eta gp41en 605 hondarren artean (Binley et al., 2000; Sanders et al., 2000); bestetik, gp41aren 559 posizioko isoleuzina prolina batez ordezkatua izan zen (IP), trimeroa desegitea ekiditeko (Sanders et al., 2002).

Lehen egitura hauek lortu zirenetik, eskuratutako Env trimeroen egituren bereizmenak hobera egin du. 2020rako, 3 Åetik beherako ebazpenarekin SOSIP egitura ugari eskuratu dira GIBaren aurkako antigorputz desberdinei (Henderson et al., 2020;

Schommers et al., 2020), edo inhibitzaile txikiei batuta (Lai et al., 2019). 2015. urtean, Kwon eta lankideek (Y. do Kwon et al., 2015) eskuratutako ligandorik gabeko trimeroaren lehen egiturak (gp120an eratutako beste disulfuro zubi batez egonkortua) antigorputzei lotutako egituretan behatutako ezaugarriak berretsi zituen. Urte bete beranduago ebatzi zen SOSIP mutaziorik gabeko bereizmen altuko lehen Env trimeroa (Lee et al., 2016): Kasu honetan, B kladoaren barnean sailkatzen den JR-LF andui basatia erabili zen, isats zitoplasmatikorik gabea eta PGT151 antigorputzari lotua. Aipatutako trimero guzti hauek egonkortasun maila altua erakutsi dute, eta egitura natiboa izan dezaketela iradoki da, antigorputz neutralizatzaileekin elkarrekiteko gaitasuna baitute, ez ordea ez-neutralizatzaileekin (Sanders et al., 2013).

Env trimeroak glikosilazio maila altua erakusten du, eta perretxiko itxura hartzen du fusio-aurreko konformazio itxian (1.3B irudia). Gp120 kate polipeptidiko bakoitza bi domeinu nagusitan tolesten da, kanpoaldekoa eta barnealdeko domeinuak deiturikoak. Bost domeinu aldakorrek (V1-V5), beste bost domeinu konstanterekin (C1-C5) tartekatzen diren eta immunitate sistemari ikusgai gelditzen diren begizta aldakorrak eratzen dituzte. V1, V2 (berdez) eta V3 (gorriz) begiztek trimeroaren egonkortze domeinua osatzen dute, mintzetik urrun gelditzen den espikularen goiko partean alboko gp120 protomeroekin elkarrekinez (1.3B irudia).

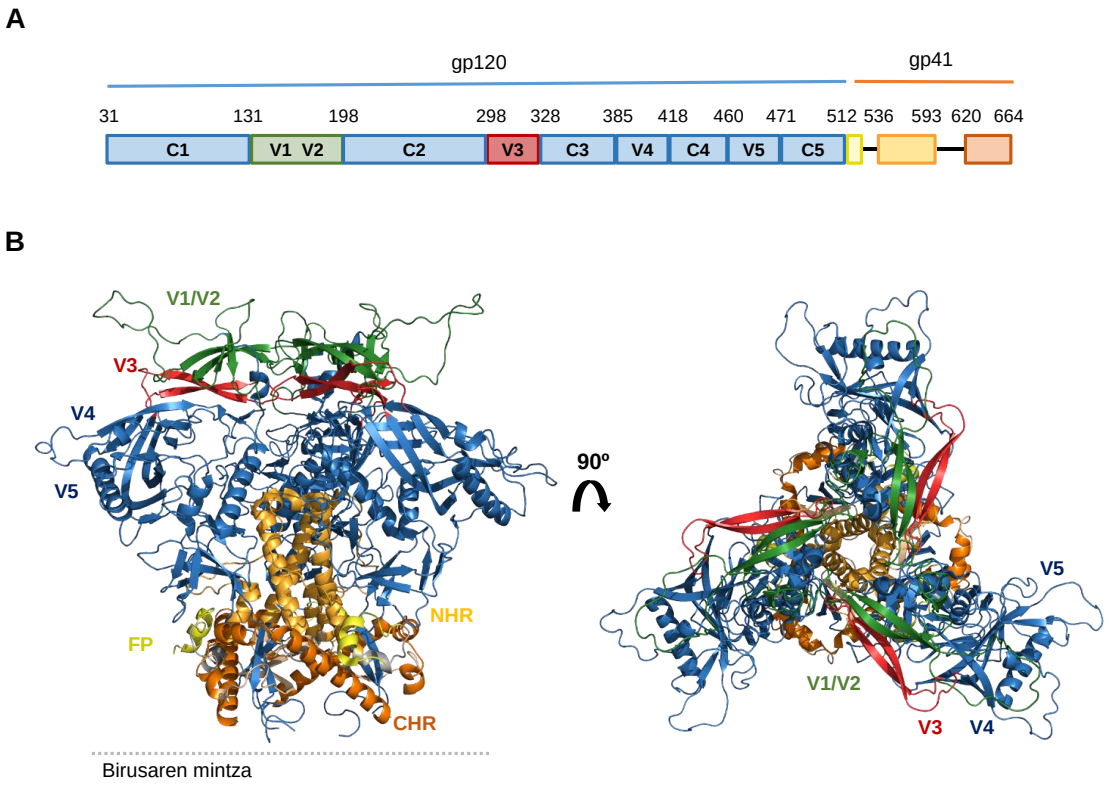

1.3. irudia: Fusio-aurreko Env glukoproteinaren hiru-dimentsioko egitura. (A) Gp120 eta gp41 azpiunitateen sekuentzien eskema. (B) Espikularen aurretiko eta goitiko bistak (PBD kodea: 5FYJ), Pymol erabiliz irudikatuak. Gp120 monomeroaren (urdinez) eta gp41en (laranjaz, 1.2. irudian erabilitako koloreekin) hiru kopiaz osatuta dago. V1-V2 (berdez) eta V3 (gorriz) begizta hiperaldakorrak nabarmenduta ageri dira.

Gp120 azpiunitatearen eta CD4 hartzailearen arteko elkarrekintza gertatzen denean, V1 eta V2 begiztek konformazio aldaketa handia jasaten dute, kohartzailearen batuketa gunea agerian utziz (Y. do Kwon et al., 2012). Gp120ren V3 begizta da CCR5 edo CXCR4 kohartzaileen espezifikotasunaren erantzule (Speck et al., 1997). Begizta honek β-lamina egitura hartzen du, eta protomero bereko V1/V2 begizten azpian kokatzen da, alboko protomeroaren N197 glikanoak estalita. Glikano hau egon ezean, trimeroaren antigorputz neutralizatzaileekiko sentikortasuna emendatzen da (Kolchinsky et al., 2001), eta aldi berean, CCR5 hartzailea adierazten duten zeluletan CD4rekiko independentea den infekzioa ahalbidetzen da. Azkenik, V4 eta V5 trimeroaren gainazaletik kanpoalderantz orientatzen dira, beste begizta aldakorrekin kontakturik egin gabe.

Fusio aurreko gp41 azpiunitate trimerikoa gp120 ainguratzen duen plataforma bat osatuz aurkitzen da, NHR helizeak erdialdean kokatzen direlarik. Bi azpiunitateen arteko elkarrekintza ez kobalenteek, batez ere hidrofobikoek, FPa disolbatzaile hidrofilikotik ezkutatuko duen poltsikoa osatzen dute (1.3B irudia). NHRaren amino muturrak gp120a

inguratzen du, eta mintzarekiko perpendikularra den *coiled coil* deituriko egitura helikoidal paraleloa osatuz jarraitzen du, trimeroaren zentroan. Ondoren, CHRak helize tolestu bat osatzen du konplexuaren kanpoaldean, mintzaren planoarekiko orientazio diagonal batean.

664. hondarrean amaitzen den SOSIP.664 trimeroak MPER domeinu hidrofobikoa falta duenez, propietate biofisiko egonkorragoak erakusten ditu, glukoproteinaren agregazioa eragotziz eta erresoluzio altuko egiturak lortzea ahalbidetuz. Zoritxarrez, hondar honetatik aurrera trimero natiboaren egitura atomikoari buruzko informazioa ez dago osaturik. Lee eta bere kideek (Lee et al., 2016) ebatzitako 10E8 antigorputzari lotutako trimeroak (8.8 Å) domeinu zitoplasmatikoa soilik falta du, baina MPER-TMDari dagokion sekuentzia mizeletan integratuta ageri bada ere, ez dago erabat ebatzita. Berriki argitaratutako lan batek erresoluzio muga hori gainditzea eta MPER-TMDaren egituraren ezaugarri batzuk identifikatzea lortu du, Env eta antigorputzen arteko konplexuak lipido bizelak erabiliz ekoiztu eta kriomikroskopiaz aztertu ostean (Rantalainen et al., 2020) (ikusi beherago).

NMR (erresonantzia magnetiko nuklearra) eta X-izpien kristalografia teknikak erabili dira gp41 azpiunitateko MPER-TMD peptidoen egitura aztertzeko, baldintza desberdinak erabiliz. GIBaren TMDa oso kontserbaturik dago, eta oligomerizazioan parte hartu ohi duen GxxxG motiboaren presentziak (Teese & Langosch, 2015) mintzaren barruan hiru monomeroen multzokatzea gertatzen dela iradokitzen du. Haatik, egitura kuaternarioari dagokionez, fusio-aurreko trimeroaren MPER-TMDaren antolaketari buruzko xehetasunek kontraesanak erakusten dituzte.

Lan gehienen arabera, espikularen transmintz domeinuak konformazio α-helikodial trimerikoa hartzen du. Oligomeroak eratzeko, amino muturrean dauden hondar hidrofobikoek *coiled-coil* motako egitura definitzen dute; karboxilo muturrean elkarrekintza polarrek trimeroa egonkortzen duten bitartean (1.4. Irudia). Zenbait taldek (Chiliveri et al., 2018; Pinto et al., 2019; Rantalainen et al., 2020) etenik gabeko helize inklinatu bat deskribatu dute. Modelo honetan, TMDa mintz osoan zehar zabalduko litzateke, MPER domeinua mintzaren gainazalean geldituko litzatekeen bitartean (1.4A irudia). Bigarren modelo baten arabera, MPER domeinua inklinaturik kokatuko litzateke mintzean, 690. hondarrean tolestu arte (Apellániz et al., 2015; Dev et al., 2016) edo 683. posizioan (1.4B Irudia) (B. Kwon et al., 2018), hortik aurrera TMDa mintzarekiko paralelo txertatuz. Azkenik, zenbait taldek bigarren hondar batean ere eteten den helizea deskribatu dute, 673 eta 674 aminoazidoen artean, hain zuzen (1.4C irudia) (Fu et al., 2018; Wang et al., 2019). Hauen arabera, MPER domeinua kurba itxi batez loturik

dauden bi helizetan banatzen da. Lehenengoa, K665-N671 hondarrek osatuko lukete, eta karboxilo muturreko helizea 683 posizioan tolestuko litzateke TMDaren *coiled-coil* egiturarekin konektatzeko.

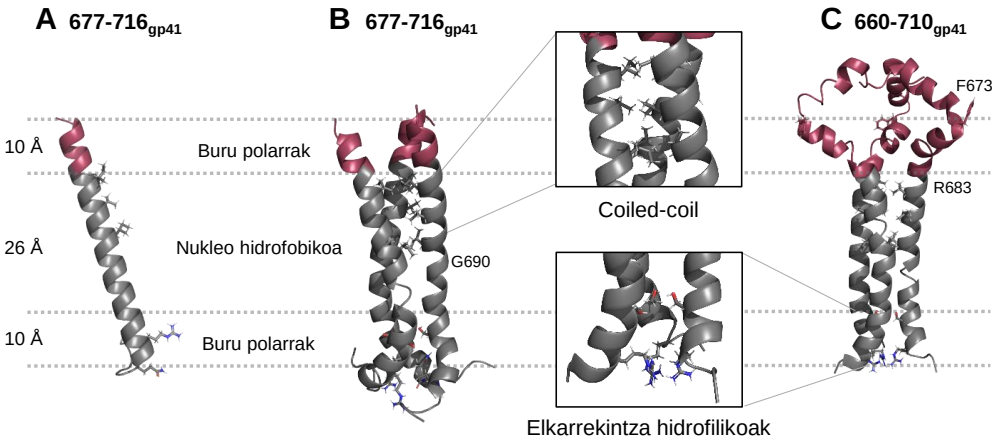

1.4. Irudia. Gp41eko MPER-TMD domeinuen hiru dimentsioko egitura. DMPC/DHPC bizeletan (puntuka irudikatuta) disolbatutako MPER-TMD domeinuen xingola bidezko irudikapena. MPER domeinuaren hondarrak (670-683 A eta B-n, edo 660-683 C--n) eta TMDrenak (684-716 A eta B-n, 684-710 C-n) granatez eta grisez koloreztatu dira, hurrenez-hurren. *Coiled-coil* hidrofobikoan eta elkarrekintza hidrofilikoetan parte hartzen duten aminoazidoak Pymol programako bastoi formatuaz irudikatu dira. PDB kodeak ondokoak dira: 6B3U (A), 5JYN (B) eta 6E8W (C).

Lan desberdinetan proposatutako modeloen aniztasun hau, posizio desberdin eta ez-natiboetan etenda dauden peptidoen erabileraren, hauen luzera desberdintasunaren edota horietako bakoitzean mintza imitatzeko erabilitako lipido motaren ondorioa izan daiteke. Bestalde, behatutako plastizitateak, eskualde honek konformazio desberdin ugaritan existitzeko duen gaitasuna islatzen du. Honek erabateko garrantzia izango du birusaren eta zelularen mintzen fusio prozesuaren etapa bakoitzean proteinak pairatzen dituen berrantolaketa ugaritan.

1.1.2.2. Env-en glikano ezkutua

Env trimeroaren protomero bakoitzak 26-30 N-glikosilazio gune ditu, eta ia denak beteta egon ohi dira. Glikanoen dentsitate handiak trimeroaren masaren %50 inguru osatzen du, espikularen bizkarrezur peptidikoa immunitate sistematik ezkutatzen duen estalki dinamikoa eratuz (Scanlan et al., 2007) (1.5. irudia).

GIBaren Env-ak N-glikano moten nahasketa aurkezten du. Batez ere manosa ugari duten glikanoak ($Man_{5-9}GlcNAc_2$) dira erretikulu endoplasmikoan itzultzen ari den kate polipeptidikoaren Asn hondarrei eransten zaizkienak. Golgi aparatuan, alabaina,

hauetako batzuk prozesatuak izango dira, $Man_3GlcNAc_2$-z osatutako muina, 2-4 adar eta azido sialikoz amaitu ahal izango diren glikano konplexuagoak eratuz (1.5. irudia). Glukosilazio gune batzuek esklusiboki manosa ugaridun motako glikanoak aurkezten dituzte, beste batzuetan konplexu motakoak soilik agertzen diren bitartean, zelula ostalariaren prozesamendu makineriak gune bakoitza desberdintzen duela nabarmenduz (Behrens et al., 2016; Go et al., 2015). Trimeroaren kanpoaldeko domeinuaren glikano dentsitateak, eta Env proteinaren berezko oligomerizazioak eragozpen esterikoak ezartzen dituzte, Golgi aparatuan glikano batzuen heltze prozesua oztopatuz. Honen eraginez, Env trimeroak giza glukoproteinetan ezohikoak diren manosa ugaridun egitura heldugabe ugari mantentzen ditu (Behrens & Crispin, 2017).

Birioietatik eratorritako gp120 azpiunitateetan “berezko manosa adabaki” bat deskribatu dute lan desberdinetan. Ezaugarri hau kontserbaturik agertzen da GIB-1en klado desberdinetan zehar, eta infekzio ziklo osoan zehar mantentzen da (Bonomelli et al., 2011). Adabaki hau N295, N332, N339, N386 eta N392 eta inguruan dauden N301 eta N411 glikanoez osaturik dago. Bestalde, N406 eta N460-N463 posizioetan glikano konplexuak aurkitu ohi dira (Cao et al., 2017).

Gp41 azpiunitateak 4-5 N-glukosilazio gune ditu, eta guztietan glikano konplexuak egon ohi dira. Batez ere hiru-lau adar izan ohi dituzte, eta fukosa eta azido sialiko molekulak izan ditzakete (Struwe et al., 2018).

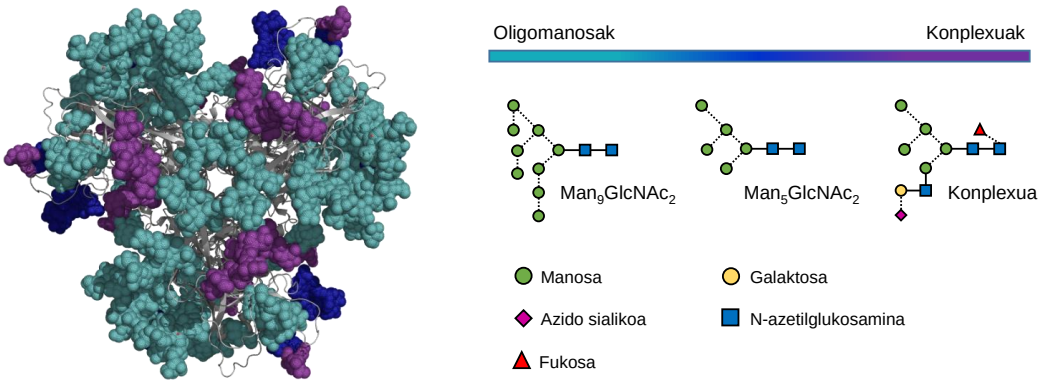

1.5. irudia: GIB-1aren espikularen glikano ezkutuaren irudikapena. SOSIP trimeroaren (PDB kodea: 5FYJ) goitiko ikuspegia. Glikanoen konplexutasuna ondoko kolore kodea jarraituz irudikatu da: Manosa ugaridunak urdin argiz, prozesamendua jasaten hasi diren erdibidekoak urdin ilunez, eta morez konplexuenak. Gutxienez glikano bakoitzaren lehen bi glukosaminak ebatzita daude, V1 eta V4 begiztak bezalako gune oso desordenatuetan izan ezik.

1.1.2.3. Env trimeroa itu dinamikoa da

Fusio-aurreko Env espikula natiboa konformazio ugaritan existitzen da, irekiera mailaren arabera desberdindu daitezkenak. Konformazio guztiz itxia da nagusia, non gp120 azpiunitateko gune zaurgarri kontserbakorrenak begizta aldakorrez estalita dauden. Gp120 protomero bakoitza CD4 hartzaile zelularrei lotzean geratzen diren berrantolaketa estrukturalek konformazio irekiago batera eramango dute trimeroa, kohartzailearen batuketa ahalbidetuz. Prozesu honetan, konformazio itxian ezkutaturik zeuden antigorputz neutralizatzaileen epitopo gehiago jarriko dira eskuragarri. Hartzailearekin elkarrekin aurretik, ordea, badirudi Env espikula konformazio itxiaren eta erlaxatuagoen artean mugitzen ari dela, “arnasketa” deritzon prozesua jarraituz (Lu et al., 2019; Munro et al., 2014) (1.6. Irudia). Molekula-indibidualetan (ingelesetik, *single-molecule*) oinarritzen den erresonantzia fluoreszentearen energia-transferentzia (snFRET) erabiliz birioietan egindako esperimentuetatik ondorioztatutako emaitzek hurrengo hiru konformazio desberdin definitu dituzte:

- 1. egoera: Birus gehienetan Env espikula metaegonkorra egoera honetan agertzen da batez ere, eta oso gutxitan egiten du jauzi gainontzeko egoeretara. antigorputz neutralizatziale gehienen lehentasunezko batuketa konformazio honetan gertatzen den arren, eta beraz, txertoen diseinurako ezinbestekoa izan arren, egoera honen 3Dko egitura ezezaguna da oraindik.

- 2. egoera: Bitartekari hau birus natiboen gainazalean modu iragankorrean soilik eskuragarri badago ere, aldrithiol-2 tratamenduak (Z. Li et al., 2020) eta antigorputz gehienen batuketak Env espikula 2. egoeran egonkortzen dute. Gainera, diseinatutako SOSIP solugarriak eta detergentea erabiliz solugarri bihurtutako Env errekonbinanteen egiturak ere 1. egoeratik 2. Egoerara desplazaturik agertzen dira. Ondorioz, orain arte eskuragarri dauden GIB-1aren Env trimeroaren ebazpen-handiko egiturak konformazio honen oso antzekoak direla sinisten da.

- 3. egoera: CD4 hartzailearekin elkarrekin ondoren sortzen da. Egoera honetan, trimeroa konformazio irekian blokeatuta dago, eta kohartzailearen batuketa guneak agerian gelditzen dira.

Protomero bakoitzak konformazioa modu independentean alda dezakenez, trimero bakarrean egoera desberdinen nahasketa ere gerta daiteke.

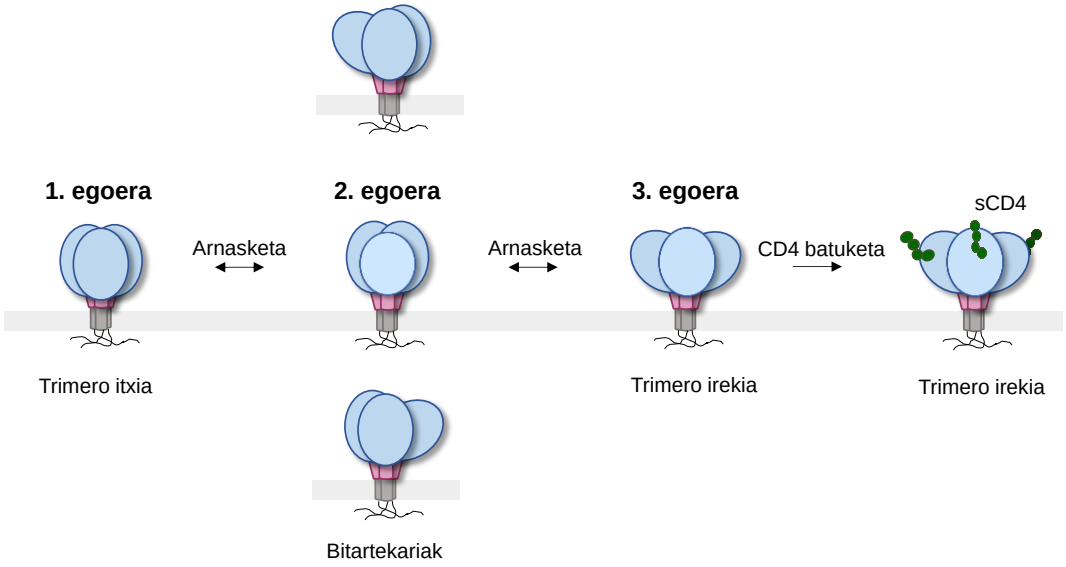

1.6. irudia. GIB-1aren Env trimeroaren konformazioen arteko kulunka. Hartzaileari lotu aurretik, Env trimeroa 1. Egoera itxiaren, konformazio apur bat irekiagoa erakusten duen bitartekarien (2. Egoera) eta 3. Egoera ireki edo erlaxatuaren artean mugitzen da. CD4ren batuketa eman ondoren, trimeroa konformazio irekian blokeatzen da, kohartzailearen batuketa-guneak agerian utziz.

1. egoeran agertzeko joera hori GIB-1 azpitalde eta anduien menpekoa dela ematen du. "*Tier 2*" edo bigarren mailako birusen ezaugarriekin bat eginez (hau da, antigorputz neutralizatzaileekiko sentikortasun baxuagoa) (Montefiori et al., 2018), JR-FL eta BG505 isolatuek (Koyanagi et al., 1987; Wu et al., 2006) 1. egoeran agertzeko joera handiagoa aurkeztu dute laborategian egokitutako NL4-3 lehenengo mailako (*Tier 1*) anduiak baino (Ma et al., 2018). 2. eta 3. egoerarantz kulunkatzeko joera, gainazalean CD4 hartzaile gutxi adierazten dituzten zelulak infektatzeko gaitasun altuari loturik egon daitekela ondorioztatua izan da; ordainetan epitopo kontserbakor gehiagoren eskuragarritasuna emendatuz, ordea.

1.1.3. Birusaren mintza

GIB-1ak zelula ostalariaren mintzetik gemazio bidez askatzean eskuratzen ditu, aldi berean, Env glukoproteinak eta birusaren bildukia osatuko duten lipidoak (Freed, 2015). GIB-1aren bildukiaren lipidoei buruzko datu goiztiarrek esfingolipido eta kolesterolez aberastutako mintza deskribatu zuten. Honek bat egin zuen birusaren mintzaren jariakortasun baxuarekin, infektatutako zelula ekoizlearenarekin alderatuz (R. C. Aloia et al., 1988; Roland C. Aloia et al., 1993).

Beranduago, 2006. urtean Brügger eta lankideek (Brügger et al., 2006) masa espektrometria erabili zuten birioietatik purifikatutako lipidoen azterketa kuantitatiboa egiteko. Lan honek, berriro ere, lipido baltsak osatu ohi dituzten kolesterola eta esfingomielina (SM) aipatu zituen osagai nagusi bezala (lipido guztien ia %50a alegia), ingurune oso antolatu bat eratuz. Teknika mikroskopiko aurreratuek birusaren mintzaren antolaketa maila altua berretsi zuten (Huarte et al., 2016). Horrez gain, birioi helduetan zelula eukarioto osasuntsuetan barneko geruzan soilik agertu ohi den fosfatidilserina (PS) ere aurkitu izan da (Carravilla et al., 2019; M. Li et al., 2014; Soares et al., 2008). Izan ere, mintz plasmatikoaren asimetria hau ATParen menpe dauden aminofosfolipido translokasek mantentzen dute, eta birusak ez du halakorik. Birusaren mintzaren konposizio kimikoak eta ezaugarri fisikoek garrantzia handia dute honen fisiologian, hauen asaldurak (zelula ostalariaren kolesterol edo esfingomielina sintesiaren inhibizioak, edo kolesterolaren estrakzioak, adibidez) birusaren fusionatzeko eta beraz infektatzeko gaitasunaren galera eragiten baitu (Carravilla & Nieva, 2018).

1.2. GIB-1aren AURKAKO ANTIGORPUTZ NEUTRALIZATZAILEAK

Env-en aurkako antigorputz neutralizatzaileak (nAb-ak) infekzioa gertatu eta zenbait astetara garatzen dira infektatutako banakoetan, baina erantzun goiztiar hau paziente bakoitzak dituen andui autologoekiko espezifikoa izan ohi da; eta ez da eraginkorra zirkulazioan dauden birus heterologoen aurka (Wei et al., 2003). Hala ere, GIB-1arekin infektatutako subjektuen %25 inguruk espektro zabalagoa duten erantzunak garatzen dituzte hurrengo hilabeteetan (Doria-Rose et al., 2009; Stamatatos et al., 2009). Antigorputz neutralizatzaile hauen agerpenak birus mutanteen sorrera gidatzen du, eboluzio prozesu partekatu bati hasiera emanez: Ostalariaren immunitate sistemak egiten duen presioak birus dibertsitate handia sorrarazten du indibiduo bakarraren baitan, eta honek, batzuetan, espektro zabaleko antigorputz neutralizatzaileen (ingelesetik, *bnAbs edo Broadly Neutralizing AntiBodies*) garapena eragin dezake (Liao et al., 2013). Antigorputz hauen bidez espektro zabala eta potentzia altua eskuratzeko, ezinbestekoa da denbora luzez etengabe antigeno biralekin kontaktuan egotea; horregatik, urteak igaro ondoren soilik sortzen dira (Burton & Mascola, 2015).

Zenbait andui neutralizatzeko gaitasuna duten antigorputzak ohikoak diren arren, pazienteen %1ak soilik dauka klado gehienen aurkako potentzia altuko aktibitatea. “Eliteko neutralizatzaile” deituriko gaixo hauek (Simek et al., 2009) sortzen dituzten antigorputzak gai dira, modu pasiboan txertatuta, primateak eta gizatiartutako saguak birusaren infekziotik babesteko (Gautam et al., 2016; Julg et al., 2017).

GIB-1arekin infektatutako gaixoen erantzun immuneen ikerkuntza bnAb ugariren isolamendurako iturri izan da. Antigorputz hauen egitura eta funtzioaren arteko erlazioaren azterketa molekularrak txerto bezala erabiliko diren immunogenoen diseinu arrazionalerako informazio baliagarria ematen du. Azken hamarkadan, zirkulazioan dauden GIB-1aren andui gehienak neutralizatzeko gai diren eta potentzia oso altua erakusten duten bnAb ugari aurkituak izan dira (Sok & Burton, 2018).

1.2.1. Giza antigorputz monoklonalen (mAb) isolamendua

GIB-1az infektatutako emaileen odol periferikoko nukleo bakarreko zelulen bahetzea da birusaren aurkako antigorputzen bilaketako lehenengo pausua. Urte askoz, B zelula lerro hilezkorretan (Köhler & Milstein, 1975; Lanzavecchia et al., 2007; Steinitz et al., 1977) eta fago-aurkezpenean oinarritutako teknologiak (Barbas et al., 1991; McCafferty et al., 1990) bezalako etekin baxuko metodologien erabilpenak antigorputzen isolamendua eta karakterizazioa mugatu du. Lehenengo teknikaren bidez, soilik odolean

aurkitzen diren B zelulen populazio batzuk bihurtzen dira hilezkor, antigorputz ugari bidean galduz. Bigarrena, berriz, cDNA liburutegien sorreran oinarritzen da. Horretarako, immunoglobulinen kate aldakorrak kodetzen dituzten RNA mezulariak B zeluletatik isolatu, alderantzizko transkripzio PCRa erabiliz cDNA bilakatu eta jarraian M13 fagoen bektorean klonatzen dira. Bakteriofagoen gainazalean adierazitako antigorputz fragmentuak antigeno-batuketa analisia erabiliz aukeratzen dira. Teknologia honen mugetako bat, ordea, soilik antigeno ezagunak dituzten antigorputzen detekzioa da, antigeno ezezagunak dituzten horiek galduz. Gainera, ekoitzitako antigorputzek ez dituzte zertan naturalki adierazitako antigorputzak islatu, kate aldakorren zorizko parekatzean oinarritzen baita.

Azken urteetan, errendimendu altuko neutralizazio saioek GIB-1arekin infektatutako gaixoen odol lagin kopuru handia aztertzea baimendu dute. Gainera, B zelulen hazkuntza metodoetan emandako hobekuntzek, besteak beste, zitokina-jariatzaileak diren zelulen bidezko aktibazioak edo zelula-indibidualetan oinarritutako antigorputzen klonazio teknikek, eta sekuentziazio teknika berriek, antigorputz monoklonalen aurkikuntza bizkortu dute.

Zelula-indibidualetan oinarritutako B linfozitoen sailkapena eta antigorputzen klonazioa, B linfozitoen berezko hartzaileen adierazpenean oinarritzen da. Markatzaile hauen aurkako antigorputz fluoreszenteak erabiliz, garapen fase desberdinetan dauden zelulak (oroimen zelulak adibidez) isolatu daitezke, fluoreszentzian oinarritzen den FACS teknika erabiliz (ingelesetik, *Flurescence-activated Cell Sorting*) (Tiller et al., 2008). Zelulen sailkapena antigeno-espezifikoa ere izan daiteke, amu bezala immunogeno desberdinak erabiliz (Scheid et al., 2009; Wu et al., 2010). Env trimero natiboak bezalako amu-proteina optimizatuen ekoizpenak aurrerapen handia ekarri zuen GIB-1aren aurkako bnAb potenteen isolamenduan. Teknika honen bidez, antigenoari batutako zelula positiboen RNA mezulariak RT-PCR bidez anplifikatu, eta B linfozito bakoitzak kodetzen duen antigorputz kateen sekuentziak determinatzen dira cDNA gisa, azkenik adierazpen bektoreetan klonatu, ekoitzi eta *in vitro* aztertzeko (1.7. irudia) (Kreer et al., 2020).

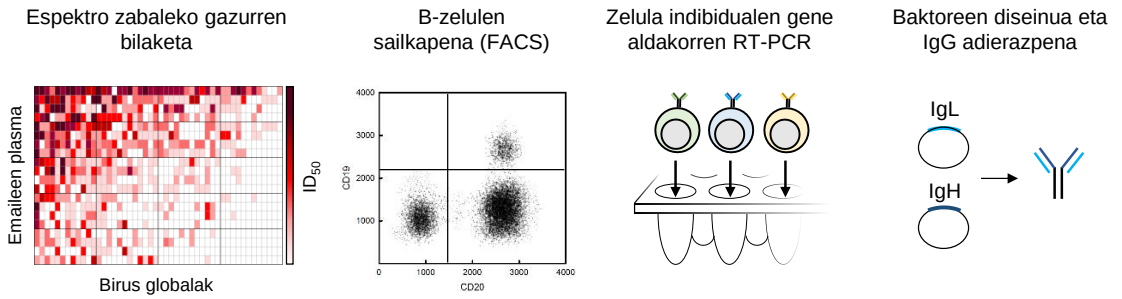

1.7. irudia. Antigorputz monoklonalen isolamendua emaileen plasmak erabiliz. GIB-1ekin infektatutako pazienteen plasma neutralizazio saio batean aztertua izaten da pseudobirus panel bat erabiliz. Lagin positiboen B zelula mota desberdinak isolatzen dira FACS erabiliz, diluitu eta zelula-indibidualen RT-PCR bidez antigorputzen bi kateak anplifikatzen dira. Azkenik, bektoreetan klonatu eta antigorputz monoklonalak adierazten dira.

1.2.2. GIB-1aren ihes mekanismoak

Env espikula birusaren gainazalean agerian aurkitzen denez, infekzioaren fase akutuan glukoproteinaren aurkako antigorputz neutralizatzaileen garapena nahiko ohikoa izaten da. Hala ere, etengabeko eboluzioa pairatzen duen trimeroak arrakasta handiz ihes egiten dio giza immunitate sistemari, eta GIB-1aren aurkako antigorputz eraginkorrak garatzea erronka zaila bilakatzen da, birusak ihes egiteko dituen aparteko mekanismoen ondorioz (Johnson & Desrosiers, 2002).

Mekanismo hauen artean, lehenik eta behin, akatsak zuzentzeko mekanismorik ez duen alderantzizko transkriptasa aurkitzen da, Env proteinaren sekuentzia erabat aldakorra bihurtzen duena, batez ere antigorputzei eskuragarri zaizkien eskualdeetan (Lee et al., 2016; Sok et al., 2014). Mundu osoan zehar aurkitzen diren GIB klado eta andui desberdinek, zein paziente bakoitzean garatzen diren bariante guztiek birusaren izugarrizko aldakortasun genetikoa agerian uzten dute.

Bigarrenik, birioiek Env espikula dentsitate baxua agertzen dute (8-14 espikula/birioi), (Zanetti et al., 2006; P. Zhu et al., 2006) antigenoen *crosslinking*-aren menpekoa den B zelulen aktibazio prozesua zailduz.

Hirugarren, Env proteina konformazio ugaritan agertzen da, erabat dinamikoa eta ezegonkorra baita. Hori dela eta, oso ohikoa da behin baino gehiagotan ez-funtzionalak diren eta antigorputz ez-neutralizatzaileen epitopo gainartzaile edo immunodominanteak agerian dituzten barianteak sortzea; hala nola, gp120ren monomeroak, gp41 soilduak edo prozesatu gabeko trimeroak, immunitate sistemaren erantzuna domeinu zaurgarrietatik desbideratuz (Moore et al., 2006).

Laugarren, ondo tolestutako trimeroetan dauden eskualde funtzionalak, oso kontserbatuak izan arren, esterikoki ezkutaturik daude. Gp120ren parte handiena konplexuaren barrualdera orientaturik dago, egitura kuaternarioak babestuta. Era berean, gp41a itu duten antigorputz gehienek ez dute Env trimeroa ezagutzen, epitopo garrantzitsuenak gp120 azpiunitatearekin elkarrekiten aurkitzen baitira, edota birusaren mintzean murgilduta.

Azkenik, aurrez deskribatu bezala, Env-en gainazala estaltzen duen glikosilazio maila altuak antigorputzek beren epitopoak ezagutzea zailtzen du. Glikanoak pazientearen zelulek sortuak direnez, ez lukete bere immunitate sistema piztu behar, eta birioia hauetaz baliatzen da eskualde kontserbatuenak ezkutatu eta nAb-en garapena eragozteko. Glikanoen dentsitate altuak eta proteina biralen hurbiltasunak, ordea, immunitate sistemarentzat arrotz bilakatzen ditu eta denbora luzez kontaktuan egon eta gero, zenbait antigorputz egokitu egin dira azukre eta peptidoak barne hartzen dituzten epitopoak ezagutzeko. Are gehiago, GIBaren aurkako antigorputz gehienek glikano hauekin kontaktuak egiten dituztenez, edo eragozten saiatzen direnez, hauen epitopoen osagai bilakatu dira (Walker et al., 2011). Modu berean, birusaren mintz lipidikotik gertu edo bertan murgilduta dauden epitopoekin elkarrekiten duten antigorputzek ezaugarri bereziak garatu dituzte beren gainazalean lipidoak egokitu edota ezagutzeko (Irimia et al., 2016, 2017).

1.2.3. Env trimeroaren eskualde zaurgarriak

Dibertsitate genetiko handiak eta birusaren ihes mekanismo ugariek immunitate sistemaren erantzuna zailtzen badute ere, birusaren dibertsitate genetiko handia eta ihes mekanismoak gainditu ondoren eskualde kontserbakor batzuen aurka garatu diren antigorputzak aurkitu dira emaile askoren gazurrean. Eskualde hauek CD4 hartzailearen batuketa gunea (CD4bs), V3 eta V1/2 begiztez eta inguruko glikanoez osatutako eskualdeak, MPER domeinua, Env-en aurpegi isila, gp41-gp120 monomeroen interfasea eta fusio peptidoa (FP) dira (1.8. irudia).

Eskualde guzti hauek ezinbesteko funtzioak betetzen dituztela dirudi. V2 eskualde apikalak, adibidez, Env trimeroaren egitura kuaternarioaren egonkortasuna mantentzen du, eta hartzailearen ezagumenduaren ondoren, kohartzailearen batuketa gunea agerian uzteko bertolesten da. V1/V2 begizten aurkako antigorputzek, PGT145 eta PGDM14000 adibidez, beren epitopo proteikoekin batera azukreak ezagutzeko ezaugarriak garatu dituzte. Kate astuneko HCDR3; begizta luze, zurrun, anionikoak erabiltzen dituzte katioiez osatutako poltsiko kontserbakorrak ezagutzeko (Lee et al., 2017; Sok et al., 2014). VRC38.01 antigorputzak (Cale et al., 2017) eskualde bera

ezagutzen du, baina albo kateen arteko elkarrekintzetan oinarritzen da glikanoz osatutako ezkutua zeharkatzeko beharrezkoa den begiztaren luzera laburtzeko.

V3-glikano gunea CCR5 kohartzailearen batuketa guneaz (Sok et al., 2016) eta inguruan dituen glikanoz osaturik dago, batez ere manosa-ugaridun adabaki kontserbakorrean parte hartzen duen N332 azukrea. PGT121, PGT128 eta 10-1074 antigorputzek ere begizta luzeak erabiltzen dituzte beren epitopoa gordetzen duen poltsiko kontserbakorrekin elkarrekiteko (J.-P. Julien et al., 2013; L. Kong et al., 2013; Pejchal et al., 2011)

CD4bs-a gp120 monomeroaren barnealdeko eta kanpoaldeko eskualdeek osatzen dute (J. P. Julien et al., 2013), eta GIBaren berezko hartzailea ezagutzeko eta lotzeko gai da. Gune hau ezagutzen duten antigorputzak dira, espezifikotasun guztien artean, espektro eta potentziari dagokionez erlazio hoberena erakusten dutenak. Normalean, hauen garapenak gainontzekoenak baino luzeago jotzen du berezko infekzioan zehar, eta hipermutazio somatiko maila altuena erakusten dute bataz beste (Scharf et al., 2015; Zhou et al., 2015). VRC07, N6 edo 1-18 (J. Huang et al., 2016; Rudicell et al., 2014; Schommers et al., 2020) bezalako antigorputz pan-neutralizatzaileen itua da.

Env trimeroaren bi monomeroek osatzen duten interfasean FP sekuentzia aurkitzen da, fusio prozesuan zelula ostalariaren mintza ainguratzeaz arduratzen dena. Horrez gain, gp160 aitzindariaren ebaketa gunea osatzen duen sekuentzia kontserbakorra ere eskualde honetan dago. PGT151 (Lee et al., 2016) eta VRC34.01 (R. Kong et al., 2016) antigorputzek fusio peptidoaren N muturra barne hartzen duten epitopo glukoproteikoak ezagutzen dituzte. 35O22 (J. Huang et al., 2014) eta 8ANC195 (Scharf et al., 2015) antigorputzek, bestalde, gp120 eta gp41 azpiunitateen interfasea ezagutzen dute, fusio aurreko konformazioan. Bi azpiunitateen aminoazido eta glikanoek parte hartzen dute hauen epitopoaren osaketan.

MPER eskualdea fusio makinariaren osagai garrantzitsuenetakoa da. 2F5 antigorputzak sekuentzia honen N muturreko konformazio desordenatua ezagutzen du (Ofek et al., 2004), 10E8, 4E10, DH511, VRC42, LN01 eta PGZL1 antigorputzen jomuga C muturreko egitura guztiz helikoidala den bitartean (Cardoso et al., 2005; J. Huang et al., 2012; Krebs et al., 2019; Pinto et al., 2019; Williams et al., 2017; Zhang et al., 2019). MPER eskualdea ezagutzen duten antigorputzak oso espektro zabala eta neurrizko potentzia izan ohi dute.

Azkenik, seigarren eskualde zaurgarri bat describatua izan zen VRC-PG05ren aurkikuntzarekin, gp120 azpiunitatearen “aurpegi isila” ezagutzen duen antigorputza (Zhou et al., 2018). SF12 antigorputzak ere (Schoofs et al., 2019) eskualde hau du

itutzat, eta osagai proteikoaz gain, N262, N295 eta N448 glikanoak ere bere epitopoaren parte dira. Bigarren antigorputz honen potentzia, espektroa eta mutazioekiko erresistentzia lehenengoarenak baino altuagoak dira.

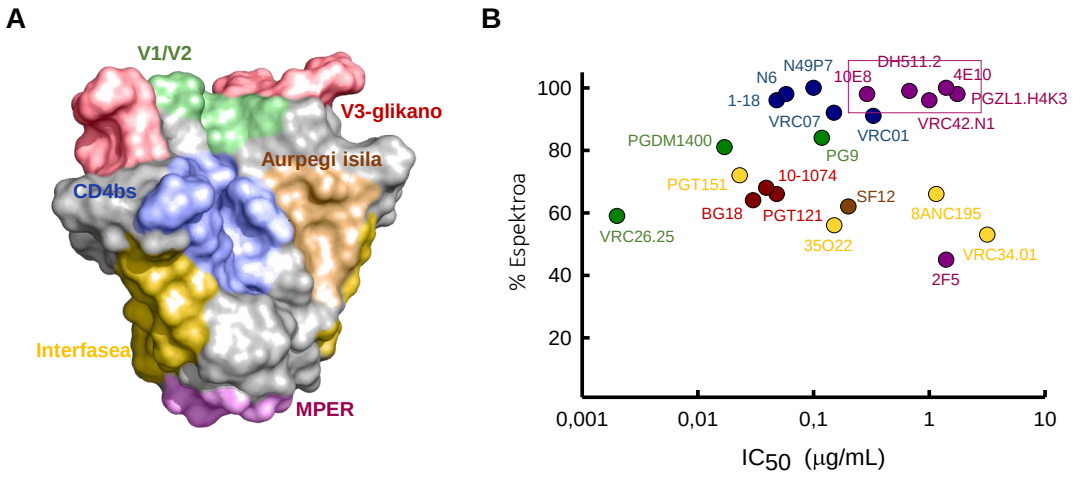

1.8. irudia: GIB-1aren Env glukoproteinaren gainazaleko bnAb-en batuketa guneak. (A) Kolore desberdinez Env-en gainazalean aurkitzen diren sei eskualde zaurgarriak irudikatu dira: CD4bs (urdinez), V3 begizta (gorriz), V1/2 begizta (berdez), MPER domeinua (morez), Env-en aurpegi isila (marroiez), eta gp41-gp120 interfasea (horiz). (B) TZM-bl zelulen saioetan oinarritutako antigorputzen potentzia (IC_{50} balioa, µg/mL-tan) eta hauen espektroaren arteko alderaketa (Neutralizazio portzentaia andui-isolatuek osatutako panel esanguratsuan). Antigorputz bakoitza A irudian ezagutzen duen eskualdearen kolorearen arabera irudikatu da. Laukian bilduta anti-MPER antigorputzak ageri dira, lan honetan aztertuak izan direnak.

Antigorputz neutralizatzaile hauetako batzuek aktibatu gabeko Env espikula ezagutzen dute ondoen (1. egoera), eta hauen batuketak espikula konformazio itxian blokeatzen dute, bere “arnasketa” eragotziz. Beste batzuek, CD4 hartzaileak eragindako aktibazioaren osteko konformazio irekian ezagutzen dute ondoen trimeroa (3. egoera), baina gai dira fusio aurreko egiturak ere ezagutzeko (Ivan et al., 2019).

1.2.4. GIB-1aren aurkako antigorputzen aparteko ezaugarriak

Giza immunoglobulinaen kate astuna (IGH), eta kappa eta lambda kate arinak kodetzen dituzten geneak hiru loci desberdinetan aurkitzen dira, bakoitza kromosoma batean (Lefranc & Lefranc, 2001). Immunoglobulinaren sekuentzia osoa domeinu konstantea kodetzen duen exon indibidual batek eta aldakor (V), aniztasun (D) (kate astunaren kasuan soilik) eta juntura (J) izeneko gene segmentuen berrantolaketaz sortutako domeinu aldakor batek osatzen dute (Tonegawa, 1983) (1.9. irudia). Immunoglobulinen eskualde aldakorrenak CDR begiztak dira; hiruna daude kate bakoitzean, *framework*

(FR) deituriko egiturazko eskualdeekin tartekatuta, eta antigorputzaren batuketa gunea osatzen dute (Chothia & Lesk, 1987).

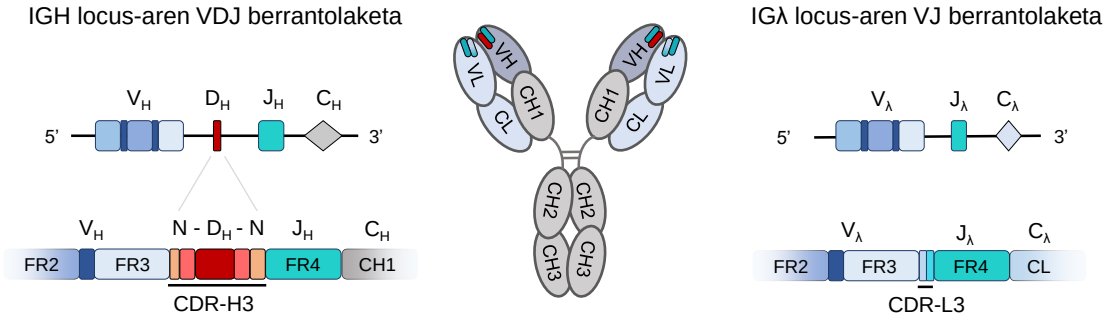

1.9.irudia. V(D)J berrantolaketaren irudikapena. IGH eta IGλ gene multzoen CDR3en eraketak irudikatuak izan dira.

V, D eta J gene segmentu indibidualen konbinazioak lerro germinalean kodeturik dagoen aldakortasuna maximizatzen badu ere, kate astuneko VDJ elkarketa prozesuan zehar ematen da immunoglobulinen aniztasunaren iturri garrantzitsuena. V_H gene segmentuak HCDR3aren amino muturra kodetzen du, D_H segmentuak bere erdialdeko sekuentzia osatuko du, eta azkenik, HCDR3aren karboxilo muturra J_H elementuan aurkitzen da (1.9. irudia). Aniztasuna mekanismo desberdinen bidez eskuratzen da: D_H segmentuak, lehenik eta behin, alderantzizko norantzan zein zuzenekoan berrantola daitezke, eta modu ebakitzeko posizioaren arabera, hiru ORF desberdinetan itzuliak izan daitezke. Berrantolaketa prozesu honetan, gainera, lerro germinalean kodeturik ez dauden N-nukleotidoak gaineratuak izan daitezke ausaz bai V eta D eta baita D eta J segmentuen artean, TdT (terminal-deoxinukleotidil transferasa) entzimaren aktibitatearen ondorioz. Prozesu honek luzera aldakorreko HCDR3 sekuentziak sorrarazten ditu, eta 10^7 VDJ lotura desberdin baino gehiago sor daitezke berrantolaketa prozesuan (Fugmann et al., 2000). HCDR3 begiztan gerta daitekeen aldakortasun somatikoa, gene segmentuen konbinaketa posible bakoitzari eta kate arina eta astunaren ausazko parekatzeari gehituz gero, banako bakoitzak sor dezaken antigorputzen errepertorioa 10^{16} immunoglobulinatik gorakoa da (Schroeder & Cavacini, 2010).

Giza B zelula *naive*tan, HCDR3 begiztek 16 hondarreko bataz-besteko luzera dute. GIB-1aren aurkako bnAb-etan, bestalde, Env trimeroan sakon eta ezkutuan dauden epitopoei lotzeko ezohiko luzera duten begiztak deskribatu dira (20-34 aminoazido) (Yu & Guan, 2014). Itu bezala V1/V2 eta V3 begiztak, gp120 eta gp41 azpiunitateen arteko interfasea edo MPER domeinua dituzten antigorputzek, adibidez, begizta oso luzeak behar dituzte

glikanoz osatutako ezkutuan edo mintz lipidikoan barneratzeko. Giza B zelulen sekuentziazio sakonaren arabera, *naive*n %3.5ak 24 hondar edo gehiagoko HCDR3ak dauzka, eta %0.43ak 28 hondarretik gorakoak (Arnaout et al., 2011; Briney et al., 2012). Beraz, proportzio altuan ez bada ere, GIB-1aren aurkako bnAb-en aitzindariak aurki daitezke giza-errepertorioan.

Konbinaketaren ondorioz lortutako hasierako aniztasun hori, B zelulen aktibazioaren ondoren emendatu egiten da, hipermutazio somatikoa (ingelesez *Somatic Hipermutation*, edo SHM) eta Fc-aren klase-aldaketa berkonbinaketa (CSR edo *Class-Switch Recombination,* ingelesetik) deituriko heltze prozesuen ondorioz (Neuberger, 2008). Antigeno jakin bat ezagutu eta T linfozito laguntzailearen koestimulazioaren ondoren, B zelula zentro germinalean (GC) sartzen da, organo linfoide periferikoetan. Hedapen klonala jasango du, zelula-zatiketa bakoitzean immunoglobulinen V, D eta J segmentuetan mutazio tasa altua jasango dutelarik, batez ere CDRtan (genoman gertatu ohi dena baino 10^5-10^6 aldiz gehiago). Prozesu honek afinitate desberdineko antigorputz kantitate handia sortzen du, eta mutazio eta antigenoek gidatutako selekzio ziklo ugariren ondoren afinitate oso altuko antigorputzak dituzten B linfozitoak eratuko dira (Rajewsky, 1996). GCtik ateratzen diren eta afinitate altuko antigeno hartzaileak dituzten B zelulak diferentziazio prozesu bat jasango dute, oroimen B zelulak edo antigorputzak jariatzen dituzten zelula plasmatikoak bilakatuz.

GIB-1arekin infektatutako banakoen kasuan, bnAb-en garapenean ematen den lehen urratsa errepertorioko B zelula-hartzaile (BCR) egokiaren aktibazioa izango litzateke, birusaren Env trimeroak eraginda. GIB-1aren eboluzio konstanteak egiten duen estimulazio kronikoaren eraginez, BCR espezifiko hauek antigeno biral berriekin kontaktuan egongo dira behin eta berriz, selekzio-mutazio ziklo etengabeak jasango dituztelarik afinitate altuko hartzaileak eskuratzeko (Breden et al., 2011). Horrela, GIB-1aren aurkako bnAb-ak infekzioa gertatu eta 3-4 urtera isolatu ohi dira gaixoetatik (Gray et al., 2011) eta SHM tasa orokorrean baino altuagoa izan ohi da (Scheid et al., 2009; Xiao et al., 2009). Antigorputzaren paratopoa osatzen duten CDRetan gertatzen dira mutazioak, baina baita normalean kontserbakorragoak diran FR eskualdeetan ere (Klein, Diskin, et al., 2013). GIBaren kontrako immunoglobulina hauen heltze prozesu luze eta konplexuarekin bat, hipermutazio somatikoari insertzio eta delezioak (indel-ak) gaineratu behar zaizkio, gehienetan neutralizazio gaitasun zabala eskuratzeko ezinbestekoak direnak (Kepler et al., 2014).

Birus honen aurka sortzen diren bnAb-etako batzuek poli- edota auto-erreaktibitatea erakutsi dezakete. Antigorputz polierreaktiboek itxuraz zerikusirik ez duten antigeno edo

autoantigeno bat baino gehiago ezagutzen dituzte. Autoerreaktiboek, berriz, autoantigeno bat edo batzuk batzen dituzten modu espezifikoan. CD4bs (VRC01 adibidez) edo V3-glikanoa ezagutzen duten antigorputzen artean, batzuek autoerreaktibitate maila baxua erakutsi izan dute, baina ezaugarri hau batez ere anti-MPER antigorputzetako batzuei lotua izan da (4E10 eta 2F5 bnAb-ak, besteak beste, karga negatiboa duten zenbait lipido propiori lotzen zaizkie), (Finney & Kelsoe, 2018) baina ez guztiei (10E8 edo DH511.2) (J. Huang et al., 2012; Williams et al., 2017). Autoantigorputzen ezaugarrien garapena ez da ezinbestekoa GIB-1aren aurkako espektro zabaleko antigorputzak eskuratzeko; zenbaitetan, ordea, espektro zabalari lotuta agertu ohi da. Geneen berrantolaketatik espektro zabala eskuratu arte aztertua izan diren bnAb batzuen garapenean, azken ezaugarri hau autoerreaktibitateari loturik agertu da (Liao et al., 2013), eta gauza bera gertatu da espektroa zabaltzeko ingeniaritza genetikoz eraldatutako bnAb batzuen kasuan. Adibide hauek espektro zabala eta potentzia altua eskuratze aldera ematen den heltze prozesua polierreaktibitatea ekiditeko beharrari estuki lotuta doala berresten dute.

1.2.4.1. bnAb-en aurkikuntzaren eragina txertoaren garapenean

“Egituran oinarritutako” txertoa eskuratzeko saiakeren porrotak eta azken urteetan aurkitutako aparteko ezaugarriak dituzten antigorputzen behaketak, “generazio-berriko” txertoen garapena ikertzera eraman ditu birus honekin lanean diharduten zientzialariak. Txerto hauek, immunizazio desberdinez baliatuz, infekzio naturalean garatu daitezkeen antigorputzen sorrera erreproduzitzea dute helburu. Prozedurak diseinatzeko, bnAb-en garapena eragiten duten faktoreak (ostalariarenak eta birusarenak) sakonki ezagutzea ezinbestekoa da.

Horrela, gero eta talde gehiago ari dira bnAb ezagunak ekoizten dituzten B zelulen ontogeniaren azterketan lanean, eta garapen urrats bakoitza bideratzen duten Env trimeroaren aldaerak identifikatzen saiatzen dira (Bonsignori et al., 2011; Doria-Rose et al., 2014; Liao et al., 2013). Garapena bideratzen ari diren antigenoaren bitartekari garrantzitsuenak ezagutzeaz gain, garatzen ari den antigorputzaren leinuko bitartekari zein aitzindariak (lerro germinalean kodetzen diren aldaerak, “mutatu gabeko arbaso komuna” edo UCA) isolatzea (edo inferitzea) eta karakterizatzea ezinbestekoa da txerto hauek diseinatzeko. Zenbait kasutan, bnAb batzuen UCA gai da Env-en aldaera goiztiarrak batu zein neutralizatzeko (Rantalainen et al., 2018). Beste askotan, ordea, ez dute neutralizatzeko gaitasunik, eta ez dira gai Env molekularen aldaera gehienak ezagutzeko (Ota et al., 2012; Xiao et al., 2009). BnAb hauen garapena azaltzeko ideia desberdinak proposatu dira: batetik, gaur egun erabiltzen diren saioetan detektaezina

izan arren, UCA hauen afinitatea nahikoa izan daiteke BCRen seinalizazioa aktibatzeko *in vivo*; bestetik, erantzun hauek beste patogeno batzuen aurkako erantzunetatik eratorriak izan daitezke.

SHM maila altua, indel-ak eta CDR begizta luzeak dituzten antigorputzak txertaketa bidez sortzea erronka zaila da. Dena den, giza immunoglobulinetan ohikoagoak diren ezaugarriak dituzten birusaren aurkako bnAb berrien aurkikuntzak, eta indibiduo desberdinen antigorputzen garapen bidezidorretan behatutako antzekotasunek GIBaren aurkako txerto prebentibo eta eraginkor baten garapenaren ametsa hauspotu dute (Doria-Rose & Landais, 2019).

1.2.5. BnAb-ak GIBaren infekzioaren prebentzioan eta profilaxian

GIB-1aren aurkako bnAb ahaltsuak proposatuak izan dira, lehenengoaren aurkikuntzatik, infekzioaren prebentzio, tratamendu eta baita sendaketarako ere, “jo eta erahil” (ingelesetik, *kick and kill*) protokoloaren baitan (Pace & Frater, 2019). Ahalmen neutralizatzaileaz gain, GIB-1aren aurkako antigorputzek zelula infektatuak garbi ditzakete Fc-aren menpeko erantzun immunearen bitartez (Igarashi et al., 1999), baita zelularteko transmisioa inhibitu ere (Malbec et al., 2013). Horrez gain, gazurrean duten erdibizitza luzeak, aldeko segurtasun profilak eta ostalariaren immunitate sistemarekin elkarrekiteko duten gaitasunak immunoterapian erabiltzeko hautagai interesgarriak bihurtu ditu.

1985az geroztik, 100 inguru dira klinikan erabiltzeko onartuak izan diren antigorputz monoklonalak (mAb-ak) edota hauen eratorriak. mAb-ak gero eta ohikoagoak bihurtzen ari dira zenbait minbiziren eta gaixotasun immuneen tratamenduan. Gaixotasun infekziosoen tratamenduan, bestalde, ez dira oso ohikoak oraindik. GIB-1 infekzio multierresistenteen aurka onartutako lehen antigorputz monoklonala Ibalizumab, CD4 hartzailea batzen duen antigorputza izan zen (Emu et al., 2018). Antigorputz monoklonal terapeutikoak gero eta indar gehiago hartzen ari dira GIBaren aurkako borrokan, eta dagoeneko zenbaitek gizakietan egindako saio klinikoetan arrakasta erakutsi dute. (ikusi: https://clinicaltrials.gov/ct2/home).

GIB-1arekin infektatutako pazienteekin egindako lehen saio klinikoak CD4 batuketa gunearen aurkako 3BNC117 eta VRC01, eta V3 begizta ezagutzen duen 10-1074 antigorputzekin burutu dira (Caskey et al., 2015, 2017; K. H. Mayer et al., 2017; Scheid et al., 2016). Antigorputz hauen administrazioa orokorrean segurua eta ondo toleratua izan da egundaino burututako saioetan. 20-30 mg/kg-ko dosien infusioaren ondoren,

antigorputz neutralizatzaileak 8-16 astez mantendu ziren pazienteen odolean, 10 µg/mL baino kontzentrazio altuagotan.

Hiru antigorputz hauetako bakoitzaren 30-40 mg/kg karga biral altuko indibiduoetan txertatzeak karga biralaren berehalako jaitsiera eragin zuen, eta pazienteek biremia maila baxutan mantendu zuten 28 egunez (Caskey et al., 2019). 4 asteren buruan, ordea, berragertze birala eman zen orokorrean, batez ere 10-1074 antigorputzaren kasuan, bariante erresistenteen hautespen azkarra eragin baitzuten. Erresistentzien agerpen honek antigorputzen monoterapiak izan ditzaken mugak nabarmentzen ditu, eta hau eragozteko espezifizitate desberdineko bnAb desberdinen konbinaketen beharra iradokitzen du.

Hori berretsiz, 3BNC117 eta 10-1074 antigorputzen konbinaketa eraginkorra suertatu zen birusaren karga birala oso maila baxutan mantentzeko. Gainera, bi antigorputzen konbinaketak profil farmakozinetiko egokia eta segurtasun maila ona aurkeztu zuen elkarrekin erabiltzean. Biremia aktibodun zazpi pazienterekin egindako saioan, karga birala ia desagerrarazteaz gain, hiru hilabetez maila baxuan mantentzea lortu zen (Bar-On et al., 2018). Konbinaketa bera birusa kontrolaturik zuten gaixoekin probatu zen, zeinak antigorputzen hiru dosi jaso zituzten terapia antiretrobirala utzi ondoko 0, 3 eta 6. asteetan (Mendoza et al., 2018). Guztien karga birala detekzio mailatik behera jaitsi eta horrela mantendu zen azken dosia jaso ondoren 21 astez, eta pazienteetako bik hala jarraitu zuten azterketak iraun zituen 30 asteetan. Bi ikerketetan ez zen erresistentzia bikoitza garatu zuen aldaera biralik aurkitu.

PGDM1400, PGT121, N6 eta 10E8v4 (Ikusi 3.3 kapitulua) GIB-1aren aurkako antigorputz neutralizatzaileekin ere 1. fasean dauden entsegu klinikoak egiten ari dira dagoeneko.

1.2.6. BnAb-en ingeniaritza genetikoa

GIB-1aren aurkako antigorputz terapeutikoen funtzio biologikoak ingeniaritza genetikoa erabiliz optimizatu daitezke (Igawa et al., 2011)

1.2.6.1. Neutralizazio potentzia

Antigorputzen ezaugarri desiragarrienetako bat potentzia altua da, infekzioa inhibitzeko gaitasuna zenbat eta altuagoa izan, orduan eta baxuagoa baita terapian erabili beharreko dosia. Antigorputzen Fab domeinuaren ingeniaritza arrazionalak edota egituran oinarritutako diseinuak Env glukoproteinarekiko afinitatearen hobekuntza ekar dezake, bere potentzia emendatuz.

VRC07-523 antigorputza adibidez, VRC01 antigorputzaren kate astuna, potentzia altuagoa duen NIH45-46ren eskualde homologoarekin aldatuz lortu zen (Diskin et al., 2011). Beste lan batean, 10E8 antigorputzaren potentzia 5 bider emendatzea lortu zen, Env trimeroarekin egiten dituen elkarrekintza semi-espezifikoen optimizazioaz baliatuz, bere espektro zabalean eragin gabe (Y. D. Kwon et al., 2018).

1.2.6.2. Solugarritasuna edota egonkortasuna

G Immunoglobulinen solugarritasuna orokorrean altua bada ere (>100 mg/mL), GIB-1aren aurkako zenbait antigorputzek solugarritasun baxua aurkezten dute. Adibidez, espektro oso zabaleko 10E8 anti-MPER antigorputzaren fabrikazioa asko zailtzen du ezaugarri honek. Biologia estrukturala erabili zen, aldaera somatikoen optimizazioarekin batera 10E8aren solugarritasuna emendatzeko, ezinbestekoak ez diren adabaki hidrofobikoak identifikatu eta atzera lerro germinalean zehaztutako hondar hidrofilikoekin ordezkatuz (Kwon et al., 2016). 10E8v4 deituriko amaierako produktuak solugarritasun altua erakusteaz gain, antigorputz parentalaren potentzia eta espektro zabala mantentzen ditu.

1.2.6.3. Funtzio efektorea

Antigorputzek betetzen dituzten funtzio antibiralen artean, Fc eskualdeaz baliatuz burutzen dituzten funtzio efektoreak aurkitzen dira; konplementuaren menpeko funtzio zitotoxikoa (ingelesetik *CDC, Complement dependent cytotoxicity*) batetik, C1q errekrutatuz, edota antigorputzen menpeko zitotoxizitate zelularra (ingelesetik ADCC, *Antibody dependent celullar cytotoxicity*) edo fagozitosia (ingelesetik *ADP, Antibody dependent phagocytosis*) FcγR hartzaileen bidez. Funtzio hauek birioi askeen zein infektatutako zelulen aurkakoak izan daitezke (Burton, 2002).

FcγR eta C1q-ekin elkarrekiteko *hinge* (edo “giltzarri”) eskualdeko eta honen alboko CH_2 aminoazidoak erabiltzen dituzte antigorputzek. IgG azpitaldeen artean, IgG1 eta IgG3k konplementuaren erreklutamendua egokiago burutzen dute IgG2 eta IgG4ak baino (Tao et al., 1993). Horrez gain, IgG2 eta IgG4ek ADCC eragiteko gaitasun mugatua aurkezten dute (Brezski et al., 2014). Hori dela eta, azpitaldeen arteko trukea edo Fc-aren ingeniaritza genetikoa erabili daitezke GIB-1aren aurkako funtzio efektorea emendatu zein murrizteko.

GIB-1aren aurkako tratamenduan ADCC efektore funtzioa benetan interesgarria suertatu da, mota honetako erantzunak gaixotasunaren progresio geldoagoekin lotu izan baitira (Wren et al., 2013). Saguekin egindako esperimentuek eta gizakiekin egindako

saio klinikoen datuen modelizazioek FcγR hartzaileen rola nabarmentzen dute bnAb-ek eragindako onura terapeutikoen atzean. Gainera, biremiaren kontrola azkarragoa eta denboran luzeagoa izan zen FcγR hartzailearen batuketa hobetzeko Fc-a mutaturik zuten 3BNC117 IgG1 antigorputza jaso zuten animalietan (Bournazos et al., 2014).

1.2.6.4. Erdi-bizitza seroan

Antigorputzen erdi-bizitza luzatzeak, pazienteen odolean antigorputz maila eraginkorra mantentzeko eman beharreko dosi kopurua gutxitzea ahalbidetzen du. Honek, aldi berean, albo-ondorioen eta kostuen murrizketa dakar. Antigorputz baten erdi-bizitza Fc eskualdea ingeniaritza genetikoaren bidez mutatuz modula daiteke, antigenoaren batuketari eta Fc eskualdeak betetzen dituen gainontzeko funtzioei eragin gabe. CH_2 eta CH_3 domeinuetan egindako zenbait mutaziok, M428L/N434S (LS) (Zalevsky et al., 2010) eta M252Y/S254T/T256E (YTE) (Robbie et al., 2013) besteak beste, FcRn hartzailearekiko afinitatea emendatzen dute. FcRn hartzaile birziklagarriak antigorputzen *in vivo* erdi-bizitzaren erregulazioan parte hartzen du (Kang & Jung, 2019). Horrela, LS mutazioa saio klinikoetan aurrera egin duten GIB-1aren kontrako antigorputz neutralizatzaile ugaritan integratua izan da (Gautam et al., 2016; Ko et al., 2014).

1.2.6.5. Immunoglobulina multiespezifikoak

Aldi berean bi epitopo desberdin edo gehiago ezagutzeak bi abantaila nagusi ditu: birus erresistenteak agertzeko aukera murrizten du, immunoglobulinaren espektroa zabaltzearekin batera. Egungo teknologia berriek antigorputz biespezifiko edo triespezifikoen ekoizpena ahalbidetzen dute, zeinak antigorputz konbinaketen edo "antigorputz *cocktail"*-en alternatiba gisa aurkeztuak izan diren. Antigopurtz biespezifiko batzuk dagoeneko onartuak eta erabiliak izan dira agente terapeutiko bezala kartzinoma, leuzemia zein hemofilia bezalako gaixotasunen aurka (Burges et al., 2007; Jen et al., 2019; Mahlangu, 2018), GIB-1a bezalako agente infekziosoen kontra ere immunoglobulina multiespezifikoen erabilerari ateak irekiz.

GIB-1aren aurka *in vitro* saiotan emaitza itxaropentsuak erakutsi dituzten antigorputz biespezifiko eta triespezifikoek, birusaren aurkako aktibitatearen hobekuntza frogatu dute animalia modelotan ere. Antigorputz biespezifiko desberdinak ekoitziak izan dira: Env trimeroaren bi eskualde zaurgarri ezagutzen dituzten antigorputzak konbinatuz alde batetik, hala nola, VRC07 eta PG9-16, edo 3BNC117 eta 10-1074 (Bournazos et al., 2016), edo GIB-1aren aurkako antigorputz bat CD4 hartzailea itu duen ibalizumab (iMab) antigorputzarekin elkartuz bestetik (Y. Huang et al., 2016). Konbinaketa guztiek espektro

zabalagoa aurkeztu dute. Hauez gain, VRC01, PGT121 eta 10E8 antigorputzen espezifitateak konbinatuz sortutako antigorputz triespezifikoak potentzia oso altua eta ia andui guztiak neutralizatzeko gaitasuna biltzen ditu (Xu et al., 2017). Antigorputz hauetako batzuekin dagoeneko saio klinikoak egiten ari dira.

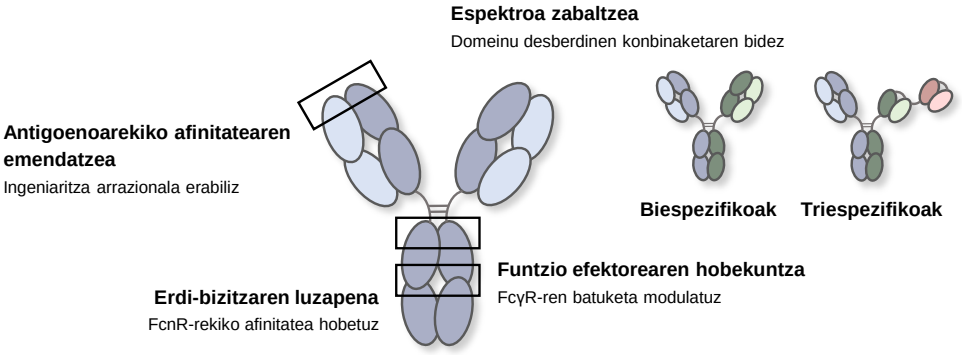

1.10. Irudia. bnAb-en eraginkortasuna emendatzeko antigorputzen ingeniaritza. Antigeno-batuketa, espektroa, funtzio efektoreak edota erdi-bizitza hobetzeko aukera desberdinak marraztu dira. Kolore bakoitzak espefzifikotasun desberdina irudikatzen du, eta laukiek mutazio eskualdeak erakusten dituzte. (Grobben et al., 2019) artikulutik egokitua.

1.3. ESPEKTRO ZABALEKO ANTI-MPER ANTIGORPUTZAK

GIB-1en MPER domeinua gp41 azpiunitateko ektodomeinuaren C muturreko azken 24 aminoazidoek osatzen dute. Hondar aromatikoz aberastuta dagoen eskualde honek gp41 ektodomeinua eta transmintz eskualdea lotzen ditu (Salzwedel et al., 1999). MPER oso kontserbaturik dago GIB-1en isolatu desberdinen artean, ezinbesteko zeregina burutzen baitu birusaren eta zelularen mintzen arteko fusio prozesuan (Muñoz-Barroso et al., 1999). Aurrez aipatu bezala, MPER antigorputz ugariren itua da: hauetako batzuek N muturrak osatzen duen azpieskualdea dute helburu eta ez dute oso espektro zabala aurkezten (2F5, Z13e1, m66.6 eta 2H10 VHHa (edo *nanobody*-a (Lutje Hulsik et al., 2013); gainontzekoak, berriz, C muturra ezagutzen dute ,GIB-1en aurkako bnAb guztien artean espektrorik zabalena erakutsiz (4E10, 10E8, DH511.2, VRC42, LN01 and PGZL1) (1.1. Taula). Ezaugarri hauek guztiek MPER domeinua GIB-1en aurkako txerto baten itu egokia bilakatzen dute.

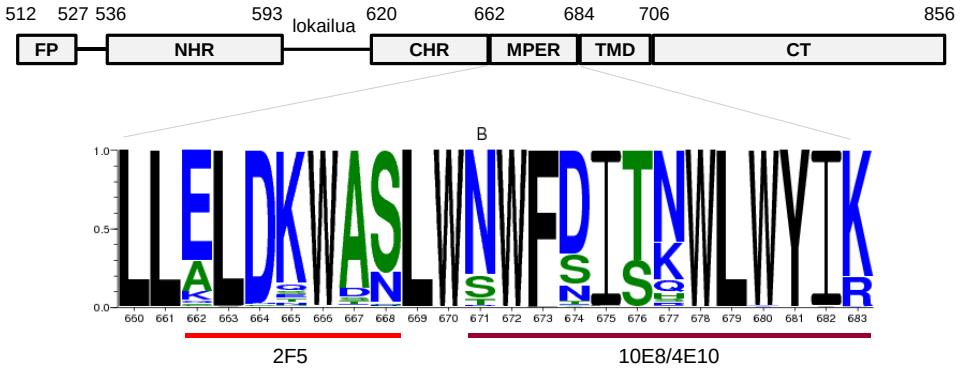

1.11. Irudia. MPER sekuentziaren kontserbakortasuna. Los Alamos Laborategi Nazionaleko GIB sekuentzien datu-basean eskuragarri dauden GIB/SHIVcpz azpitalde guztien genomak kontuan hartzen dituen WebLogo bidezko MPER sekuentziaren kontserbakortasunaren irudikapena. Sinboloen altuerak aminoazido bakoitzak posizio jakin horretan agertzeko duen maiztasun erlatiboa erakusten du. Koloreak: Hidrofilikoak (urdinez), neutroak (berdez) eta hidrofobikoak (beltzez). 2F5 eta 4E10/10E8 antigorputzen epitopoak gorriz eta morez azpimarraturik daude, hurrenez hurren.

Eskualde honek birioi natiboetan hartzen duen egitura eta antolaketa ez dago oso argi, aurrez aipatu bezala, trimeroaren ezaugarri bereziak direla eta (B. Chen & Chou, 2017; Ward & Wilson, 2015). NMR bidez baldintza ezberdinetan aztertua izan denean (Apellániz et al., 2015; Reardon et al., 2014; Schibli et al., 2001; Serrano et al., 2014; Sun et al., 2008) MPER peptidoak egitura helikoidala aurkeztu du detergente mizeletan. X-izpien bidezko kristalografia erabiliz antigorputz-peptido konplexuak aztertu direnean, eskualdearen C muturrak helize itxura mantentzen duela ikusi da (J. Huang et al., 2012;

Krebs et al., 2019; Pinto et al., 2019; Williams et al., 2017; Zhang et al., 2019; Zwick et al., 2001) (1. 12. Irudia). N muturrak, bestalde, egitura destolestuago bat erakusten du, ez helikoidala (Ofek et al., 2004), fusio prozesuan zehar MPER eskualdeak duen elastizitate konformazionala agerian utziz.

Anti-MPER antigorputz gehienak gp41 azpiunitatearen fusio prozesuko bitartekariak ezagutzeko gai dira (Cardoso et al., 2005). Hala ere, hauetako batzuk, 4E10, DH511.2 eta 10E8 besteak beste, fusio-aurreko trimeroari batu eta neutralizatzeko gaitasuna dute (Carravilla et al., 2019; Williams et al., 2017), fusioa hasi aurretik MPER eskualdea birusaren mintzean murgilduta aurkitzen den arren. Beraz, nahiz eta eskuragarritasun baxua izan, anti-MPER antigorputzak gai dira beren epitopoa ingurune lipidiko batean ezagutzeko, N muturreko hondarrak altxatuz edota trimeroaren “arnasketa” prozesuan zehar eskualde hau modu iragankorrean agerian gelditzen denean.

Env-en ektodomeinuak ere eragozpen esterikoek ezartzen dizkie antigorputz hauei, MPER eskualdearen ezagumendua oztopatuz (Lee et al., 2016) (1.13A. Irudia). Irisgarritasun arazoei aurre egiteko, anti-MPER bnAb-ek ezaugarri estruktural berezi batzuk garatuz eboluzionatu dute, mintz ingurunean euren epitopoa ezagutu eta blokeatzeko gaitasuna ematen dietenak.

1.1. Taula: Anti-MPER antigorputz neutralizatzaileak. Antigorputzen potentzia (IC_{50} balioak) eta neutralizatzeko gai diren anduien portzentaia; gene erabilera eta hipermutazio somatikoen (SHM) kopurua; eta HCDR3ren luzera eta poli/auto-erreaktibitatea.

	Ab ID	Espektroa / IC50 (ug/mL)	V geneak / SHM	Auto/Poli erreakt.	HCDR3 luzera	Erreferentziak
N-MPER	**2F5**	%58 / 1.4	VH2-5 / %12.1 Vκ1-13 / %11.8	Bai	24	(Buchacher et al., 1994)
	M66.6	%24 / 13.04	VH5-51 / %10.6 Vκ1-39 / %10.6	Bai	21	(Z. Zhu et al., 2011)
	Z13e1	%16 / 26.8	VH4-59 / %17 Vλ3-11 / %3.5	Bai	19	(Zwick et al., 2001)
C-MPER	**4E10**	%99 / 1.76	VH1-69 / %6.8 Vκ3-20 / %4.7	Bai	20	(Zwick et al., 2001)
	VRC42.01	%96 / 4.7	VH1-69 / %11 Vκ3-20 / %6	Bai	15	(Krebs et al., 2019)
	PGZL1	%84 / 6.11	VH1-69 / %20.9 Vκ3-20 / %12.6	Bai	15	(Zhang et al., 2019)
	10E8	%98 / 0.35	VH3-15 / %19.4 Vλ3-19 / %14.2	Ez	22	(J. Huang et al., 2012)
	DH511.2	%99 / 0.67	VH3-15 / %17.6 Vκ1-39 / %14	Ez	23	(Williams et al., 2017)
	LN01	%92 / 1.1	VH4-39 / %28 Vκ1-39 / %27	Ez	20	(Pinto et al., 2019)

MPER eskualdea ezagutzen duten antigorputzen ezaugarri nagusietako bat, epitopoari batu ondoren birusaren mintz lipidikoarekin elkarrekiten duen HCDR3 begizta luze ta hidrofobikoa da (Krebs et al., 2019; Pinto et al., 2019; Sánchez-Martínez et al., 2006; Scherer et al., 2010; Williams et al., 2017; Zhang et al., 2019) (1.12. Irudia). HCDR3 begizta hauen hondar hidrofobiko batzuk kanpoalderantz orientatzen dira, eta mintzerantz banatzeko joera aurkezten dute. Hondar hauen ordezkapenak antigorputz hauek lipidoei batzeko duten gaitasuna mugatzen du, mintzik gabeko kontestuan epitopoaren batuketari eragin gabe baina beren neutralizazio potentzia txikituz (J. Chen et al., 2014; J.-P. Julien et al., 2010; Rujas et al., 2015, 2016). Birusaren mintzarekin gertatzen den elkarrekintzak, beraz, berebiziko garrantzia dauka anti-MPER antigorputzen neutralizazio mekanismo molekularrean, antigorputz batetik bestera honen ekarpena desberdina izan daitekeen arren.

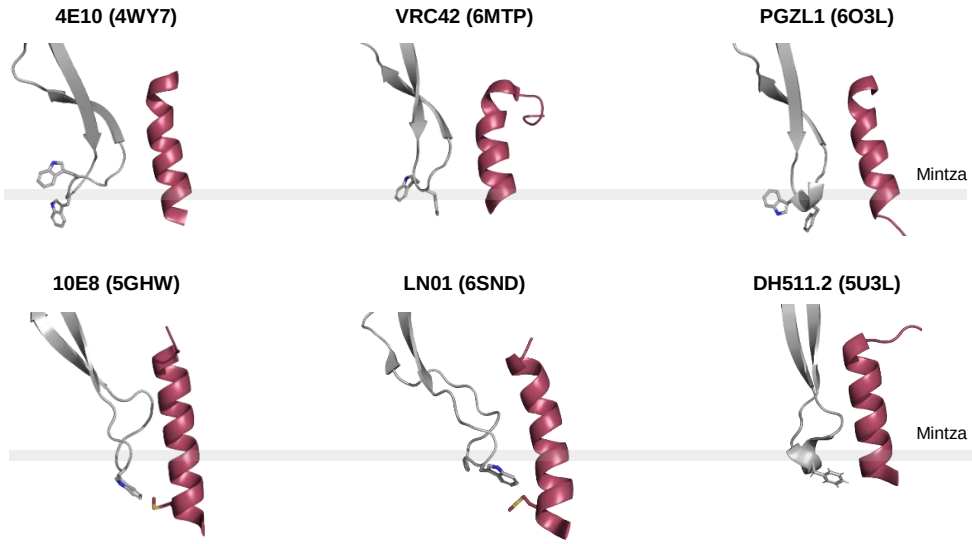

1.12. irudia. Anti-C-MPER bnAb desberdinen HCDR3 begiztek eta MPER eskualdetik eratorritako peptidoek osatutako konplexuen kristal egiturak. Neutralizaziorako ezinbestekoak diren HCDR3 begiztetako hondar aromatikoak grisez irudikatu dira. Birusaren mintza lerro gris baten bidez irudikatua izan da, MPER peptidoak magentaz, eta peptido luzea duten 10E8 eta LN01 konplexuetan (669-689) M687 hondarra ere irudikatua izan da.

1.3.1. Mintz birala anti-MPER bnAb-en epitopoaren osagaia da

Anti-MPER antigorputzek birusaren mintzarekin egiten dituzten elkarrekintza osagarriak beren neutralizazio potentzia emendatzeko erabiltzen dituzte. Elkarrekintza hauek neutralizazio prozesuan duten efektuari buruz, bi mekanismo proposatu dira. Batetik, 2F5 eta 4E10 antigorputzen eta gp41-lipido konplexuaren arteko batuketa bi pausutako prozesu sekuentzial gisa deskribatua izan da: Aurrena, antigorputza lipidoari lotuko

litzateke, horrela iragankorki agerian dagoen MPER eskualdea ezagutzea erraztuz (Alam et al., 2009). Bestetik, mintz birala bigarren batuketa gune gisa erabiliko luke antigorputzak, abidezia handituz (heteroligazioa) (Klein, Mouquet, et al., 2013). Deskribatu direnen anti-MPER antigorputzen artean, ordea, gutxi dira mintz biluziekin erreakzionatzeko gai, batik bat karga negatibodun fosfolipidoekin. 2F5, 4E10, VRC42.N1 eta PGZL1 bnAb-ek (Alam et al., 2007; Haynes et al., 2005; Krebs et al., 2019; Zhang et al., 2019) gp41eko epitopoaren ausentzian mintzekiko polierreaktibitatea erakutsi dute, 10E8, LN01 eta DH511.2 bnAb-ek ez bezala. Datu deigarria da, hain zuzen 10E8, LN01 eta DH511.2 baitira aurreneko taldearekin alderatuz neutralizazio potentzia altuena erakusten dutenak (1.8. Irudia, 1.1. Taula). Guztien artean, 10E8 da potenteena.

Kristalografia erabiliz lortutako datuek lipidoekin elkarrekiteko edo hauei egokitzeko “poltsikoak” deskribatu dituzte anti-MPER antigorputzetan (Irimia et al., 2016, 2017; Krebs et al., 2019; Pinto et al., 2019; Zhang et al., 2019), zeinak gai diren mintz birala osatzen duten fosfolipidoen buru polarrekin elkarrekintza ez-espezifikoak ezartzeko (Carravilla et al., 2020). Anti-MPER bnAb guztiek, beraz, epitopoaren ezagumenduan zehar lipidoen buru polarrak egokitzeko gai den gainazal bat duten komunean (1.13B Irudia), baita espontaneoki mintzei batzeko gaitasunik ez dutenak ere. Egiturari buruzko datu hauek erabiliz, gainera, Fab-MPER-mintza konplexuaren modelo estrukturalak ondorioztatu ahal izan dira, horrela MPER helizeak, lipidoek eta Env-en ektodomeinuko zenbait kontaktuk osatutako epitopo kuaternario osoak definituz (Rantalainen et al., 2020). Modelo hauetan, MPER eskualdea orientazio ia perpendikular batekin txertatuko litzateke mintzean (Irimia et al., 2017; Rujas et al., 2016). 10E8, DH511 eta LN01 antigorputz neutralizatzaileek antzeko hurbilketa-angelua erabiliko lukete beren epitopoari batzeko (Pinto et al., 2019), potentzia baxuagoa aurkezten duten 4E10 eta hurbileko VRC42.04 barianteak angelu desberdina erabiltzen duten bitartean (Krebs et al., 2019), neutralizazio potentziaren eta hurbilketa-angeluaren arteko erlazio bat iradokiz.

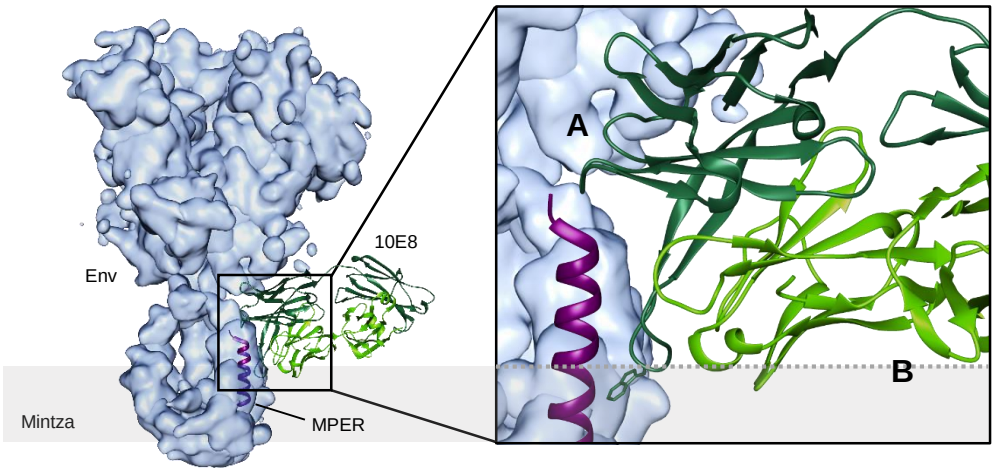

1.13. 10E8 bnAb-aren eta Env trimero natiboan MPER epitopoaren arteko elkarrekintza. Ezkerrean: 10E8 Fab-a (PDB code: 5SY8) Env trimerikoan (EMDB-3308) egokitu da. Eskuinean: antigorputzak bi gainazal garatu ditu mintzean txertatutako bere epitopoaren ezagumenduan trimeroaren ektodomeinuak (A) eta birusaren mintzak (B) ezartzen dituzten oztopoei egokitzeko.

Orain arte identifikatu diren anti-MPER antigorputzen artean, seik kate astuna edo arina kodetzen dituzten geneak partekatzen dituzte (1.1. Taula), paziente desberdinetatik eratorriak izan arren, ezagumendu molekularrari dagoekion arazo berberaren aurrean irtenbide konbergenteak bilatu dituztela aditzera emanez. Horrez gain, gazur poliklonaletan ere anti-MPER antigorputz espezifikoak detektatu izanak (Doria-Rose et al., 2017; J. Huang et al., 2012) ere MPER eskualdeari zuzendutako erantzun immune arrakastatsua ez dela zertan ohiz kanpokoa izan iradokitzen du. Antigorputz hauen eta mintzean txertatutako euren epitopoaren arteko ezagumendua eta neutralizazio potentziaren garapena gidatzen duten mekanismo molekularrak ulertzea ezinbestekoa da anti-MPER-gisako antigorputzak sorraraziko lituzkeen txerto bat lortzeko. Ez hori bakarrik, hauen funtziorako kritikoak diren ezaugarri estrukturalak deskribatzea ere garrantzia handikoa litzateke antigorputz hauetan oinarri hartuta GIB infekzioaren aurkako agente immunoterapeutiko prebentibo zein profilaktikoak diseinatzeko orduan.

1.4. HELBURU NAGUSIAK

Birusaren mintza, anti-MPER antigorputzen epitopo kuaternarioaren partaide bezala definitua izan dena, antigorputz hauen portaera funtzionala emendatzeko (afinitate altuagoa lortzeko, abidezia hobetzeko) itu egokia da. Tesi honen helburu nagusia espezifitate eta potentzia altuko fusio-inhibitzaile merkeak eskuratzea izan da: i) anti-MPER espektro zabaleko antigorputz errekonbinanteak plataforma gisa erabiliz, eta ii) beren antigenoaren ezagumendua ahalbidetzeko mintzaren interfasearekin elkarrekiten duten antigorputzak optimizateko ingeniaritza genetiko arrazionalaz baliatuz.

1.4.1. Helburu espezifikoak

- Bakteriak erabiliz genetikoki eraldatutako, potentzia altuagoko antigorputz errekonbinanteak ekoiztea, MPER epitopoari batzearekin batera mintzarekin elkarrekiten duten hondarrak manipulatuz.

- Anti-MPER antigorputz errekonbinanteen aktibitate antibirala emendatzea, birusaren mintzarekin kontaktuan dauden, edo hau egokitzen duten gainazaletan konposatu aromatikoak erantsiz.

- Antigorputz biespezifikoak diseinatu eta zelula ugaztunak erabiliz ekoiztea, anti-MPER antigorputzak eta birusaren lipidoekin espezifikoki elkarrekiteko gai diren domeinuak konbinatuz.

2. Kapitulua

TEKNIKA ESPERIMENTALAK

2. TEKNIKA ESPERIMENTALAK

Kapitulu honetan tesian zehar erabilitako teknika esperimental nagusiak deskribatzen dira. 3. kapituluan metodologia sakonago azalduko da.

2.1. PROTEINEN ADIERAZPENA, PURIFIKAZIOA ETA MARKAKETA

Intereseko proteina bat biokimikoki karakterizatzeko ezinbestekoa da lehenik eta behin kantitate handitan ekoiztea. Zelulak edota beren makineria oso erabiliak izan dira proteina birkonbinanteak adierazteko plataforma gisa (Kaur et al., 2018). Proteinen ekoizpen prozesuan bakterien erabilerak zenbait abantaila aurkezten ditu; kostu baxua, hazkuntza zinetika azkarra eta etekin altua adibidez. Baditu zenbait muga ordea, besteak beste, disulfuro zubiak edota bestelako itzulpen ondoko eraldaketak burutzeko gaitasun eza.

2.1.1. Adierazpena eta purifikazioa bakteria zeluletan

Bakteria baten zitoplasmak ingurune erreduzitzailea erakusten du baldintza fisiologikoetan, disulfuro zubi egonkorren eraketa eragotziz (Bessette et al., 1999). Horregatik, jariatutako proteinen toleste prozesua bakterien periplasman gertatzen da, non baldintza oxidatiboak bermatzen diren. Bertan daude DsbA eta DsbC deituriko entzima oxidatzaileak: Lehenengoak disulfuro zubien eraketa katalizatzen du, bigarrena, berriz, isomerasa aktibitateaz baliatzen da proteinen toleste natiboa bermatzeko (Collet & Bardwell, 2002).

T7 SHuffle ingeniaritza genetikoa erabiliz sortutako *E. coli*-ren anduia (Lobstein et al., 2012) bere zitoplasman disulfuro zubien eraketa baimentzeko moldatuta dago. Hori lortzeko, *thioerredoxin* erreduktasa (*trxB*) eta *glutathion* erreduktasa (*gor*) entzimetan mutazioak eragin zaizkio, eta AhpC peroxidasa entzima, disulfuro zubiak erreduzitzeko gai den AhpC* erreduktasa bilakatua izan da (Ritz et al., 2001). Azken aldaketa honek ohiko oxidoerreduktasen ibilbide metabolikoak trunkatzearen ondorioz zelulan eragindako hazkuntza arazoak konpontzen ditu. Azkenik, DsbC entzima gehitu zaio bakteria hauen genomari. Isomerasa honen adierazpen konstitutiboak intereseko proteinen toleste egokia bermatzen du.

T7 SHuffle anduia erabili da tesi honetan zehar anti-MPER antigeno-batze atalak (antigen-binding fragments edo Fab) ekoizteko.

Fab-a antigorputz batean antigenoa batzen duen zatiari deritzo, eta disulfuro zubiz egonkortutako kate arin (ingelesetik, *light chain* edo LC) eta kate astun (ingelesetik, *heavy chain* edo HC) batez osatuta dago. Bi kateek domeinu konstante eta aldakor bana dute (V_L eta C_L kate arinean, eta V_H and C_{H1} kate astunean), eta azken hau da antigorputza eta antigenoaren arteko espezifikotasunaren eta afinitatearen erantzulea. Antigenoaren ezagumendua antigorputzen sekuentzian agertzen diren CDR izeneko hiru eskualde hiperaldakorrei esker ematen da batez ere.

pColaDuet plasmidoa erabili da T7 SHuffle zelulak transformatzeko (2.1A irudia). Plasmido honek ezaugarri berezi bat dauka: T7 sustatzaile (promotore) bakar baten menpe dauden bi Klonaziorako Gune Anizkoitz (MCS, *Multiple Cloning Site*) ditu, berauetan klonatutako bi kateak ratio berean adieraziko direla bermatuz. MCS1an antigorputzaren kate astunaren Fab sekuentzia txertatu da, N muturrean histidina isatsarekin, eta MCS2an antigorputzaren kate arina. Ekoiztutako mutante guztiak zuzendutako mutagenesiaren bidez sortuak izan dira KOD-Plus mutagenesi Kita erabiliz (Toyobo, Osaka, Japonia).

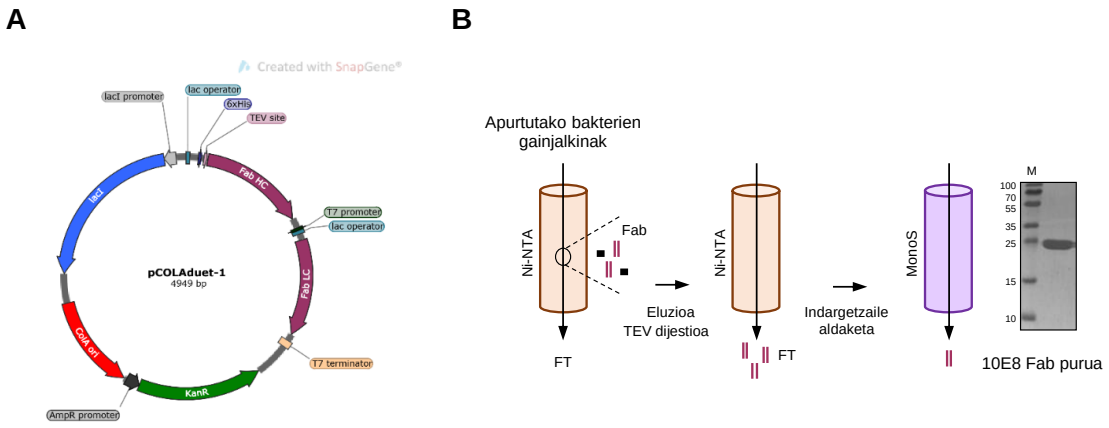

2.1. irudia. Fab-en adierazpena eta purifikazioa bakterietan. (A) pColaDUET-1 plasmidoa: bektore honek bi MCS kodetzen ditu, bakoitza T7 sustatzaile baten ondoren kokatua, aldi berean bi gene desberdinen adierazpena ahalbidetuz. Horrez gain lac operoia, erribosomen batuketa gunea (rbs), ColA erreplikoia eta kanamizinaren erresistentzia genea kodetzen ditu. (B) Fab purifikaziorako urratsak: gau osoz 18 gradutara induzitu ondoren, zelulak apurtu, zentrifugatu, gainjalkinak Ni-NTA zutabean kargatu eta eluituak izan dira, eta TEV proteasa erabiliz gau osoz dijerituak. Ni-NTA bigarren afinitate kromatografia burutu ondoren (His-isatsadun TEV bereizteko), ioi trukeko kromatografiaz Fab puruak eskuratzen dira. Purutasuna SDS-PAGE erabiliz berretsia izan da.

Proteina birkonbinanteen adierazpena gau osoz (16 orduz) induzitu da, bakterien dentsitate optikoa (OD) 0.8ra iritsi ondoren 0.4 mM isopropil-D-tiogalaktopiranosido (IPTG) gehituz. Zelulak 8000 xg-tara zentrifugatu dira ondoren, eta jalkinak bersuspenditzeko 50 mM HEPES (pH 7.5), 500 mM NaCl, 35 mM imidazol, DNasa (Sigma Aldrich, St Louis, MO) eta proteasa inhibitzaileak (Roche, Madrid, Espainia) dituen indargetzailea erabili da. Avestin Emulsiflex C5 homogeneizatzailea erabili da zelulak apurtzeko, eta zelula hondarrak zentrifugazioz bereiztu dira, gainjalkina nikelezko afinitate zutabean (Ni-NTA, GE Healthcare) txertatu aurretik. Histidina isatsaz markatutako proteinak 500 mM imidazol dituen indargetzailea erabiliz berreskuratu dira, kontzentratu, Tobacco etch birusaren (TEV) proteasarekin nahastu eta 50 mM NaH_2PO_4 (pH 8.0), 300 mM NaCl, 1 mM DTT, eta 0.3 mM EDTA dituen soluzioan dializatzen utzi dira gau osoz.

Behin histidina isatsa ebakita, Fab-ak bigarren Ni-NTA afinitate zutabe bat erabiliz bereiztu dira gainontzeko proteina eta TEV proteasatik. Jarraian, berriro kontzentratu eta indargetzailea aldatu zaie (20 mM NaAc pH 5.6, %10 glizerol) ioi trukeko kromatografiaren bidez (MonoS) purifikatzen jarraitu aurretik. Itsatsitako proteina berreskuratzeko KCl gradiente bat erabili da, eta proteina puruak SDS-PAGE erabiliz berretsi dira. Fab-ak 4 ºC-tan eta 10 mM NaH_2PO_4 (pH 7.5), 150 mM NaCl eta %10 glizerola dituen indargetzailean kontserbatu dira (2.1B irudia).

2.1.2. Adierazpena eta purifikazioa zelula ugaztunetan

Bakterietan zenbait giza proteina adierazteko ingeniaritza genetikoa erabili den arren, hauetako batzuk modu egokian tolestu eta ekoizteko beharrezko diren itzulpen ondoko zenbait eraldaketen konplexutasunak zelula ugaztunen erabilera eskatzen du. Azken urteetan, ugaztun zeluletan oinarritutako adierazpen sistemen erabilerak gora egin du (Hunter et al., 2019).

293F (Vink et al., 2014) 293 Giza Enbrioiaren Giltzurrun (*Human Embryonic Kidney* 293 edo HEK293) zeluletatik eratorritako lerroa da. Gazurrik gabeko medioan hazkuntza azkarra bermatzen dute, eta transfekzio etekin eta proteina ekoizpen altua (Gibco, 2014). Tesi honetan HEK 293F zelulak erabili dira IgG osoak eta anti-gp120 Fab fragmentuak adierazteko. Kate astun eta arinak pHLsec bektore banatan klonatu dira horretarako, AgeI eta KpnI (Aricescu et al., 2006) errestrikzio entzimak erabiliz (2.2A irudia).

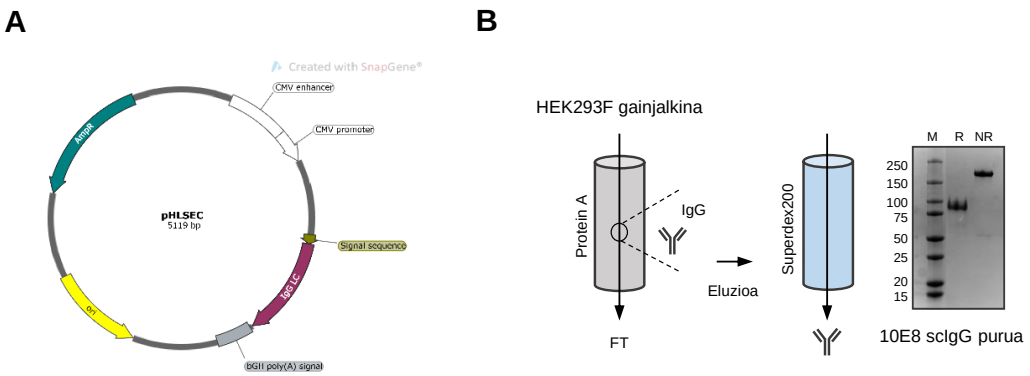

2.2. irudia: IgGen adierazpena eta purifikazioa ugaztunen zelulak erabiliz. (A) pHLsec plasmidoa: kopia-ugaridun pHLsec bektorea, ampizilinarekiko (AMP) erresistentzia eta CMV sustatzailea kodetzen dituena, erabili da ugaztun zelulen transfekzio iragankorra burutzeko. Ig kate bakoitza plasmido banatan klonatua izan zen, eta zelulak hauen kontzentrazio ekimolarrekin kotransfektatu dira. (B) IgG purifikaziorako urratsak: HEK293F zelulak transfektatu ondoren, proteinak 5-7 egunez adierazten dira. Denbora hau igarota, zelulak zentrifugatu eta gainjalkinak Ni-NTA edo A proteinadun zutabetan kargatuak izan dira. Eluitu ondoren gel iragazpenezko kromatografiaren bidez lagin homogeneoak eskuratu eta SDS-PAGE erabiliz purutasun maila aztertu da.

Ig kate bakoitza kodetzen duen plasmido bana erabili dira HEK293F zelulak (eta 0.8×10^6 zelula/ml-ko dentsitatean) transfektatzeko. FectoPRO transfekzio erreaktiboa (Polyplus Transfections) erabili da horretarako, 1:1 (DNA:FectoPRO) ratioan. Proteinen dierazpena 5-7 egunetan zehar eman da 37º C, %8 CO_2 eta 125 rpm-tako irabiaketa baldintzak bermatzen dituen Multitron Pro shaker (Infors HT) inkubatzailean.

Purifikatzen hasteko, zelulak zentrifugatu (6000 xg-tan 15 minutuz) eta gainjalkinak 0.22 µm poro tamaina duten filtroetan (EMD Millipore) zehar pasa dira, dagokien afinitate zutabean txertatu aurretik: KappaSelect, LamdaSelect (kappa edo lamda kate arina duten Fab-entzat) edo ProteinA (IgG osoen kasuan) (GE Healthcare). 100 mM glizinadun (pH 2.2) indargetzailea erabili da zutabeari batutako proteina berreskuratzeko, 1M Tris-HCl (pH 9)rekin berehala neutralizatuz. Kontzentratu ondoren, 10mM NaH_2PO_4 (pH 7.5), 150 mM NaCl indargetzailean orekatutako gel iragazpenezko kromatografia erabiliz (Superdex 200, GE Healthcare) eskuratu dira proteina puruak (2.2B).

2.1.3. Zuzendutako proteina markaketa

Ekoiztutako proteinen zuzendutako markaketa fluoreszentea edota konjugazio kimikoa aurrera eramateko, zisteina aminoazidoak erreduzitzeko eta disulfuro zubiak eratzeko duen gaitasuna baliatu da.

Haloazetiloek eta maleimida taldeak zisteinetan aurkitzen diren sulfidril taldeekin erreakzionatu dezakete pH fisiologikoetan. Prozesu honetan, aminoazidoaren sulfuro atomoak (SH taldea) iodoa (edo beste elementu halogenatu bat) ordezkatuko du ordezkapen nukleofilikoaren bidez, tioeter lotura egonkor bat sortuz (Thermo Fisher web orrialdea).

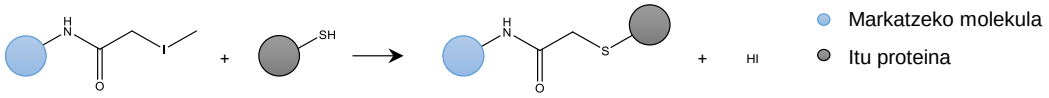

2.3. irudia. Iodoazetiloaren erreakzio eskema. Borobil urdinak markatzeko erabiliko den molekula irudikatzen du, iodoazetil talde batekin funtzionalizatua. Zisteina aske bat (eta honi dagokion sulfidril talde funtzionala) daraman interesko proteina borobil grisarekin irudikatua izan da.

Lehenik eta behin, posizio jakin bateko aminoazidoa zisteina batez ordezkatuz mutanteak sortu dira zuzendutako mutagenesia erabiliz. Hauek ekoiztu ondoren, 30 minutuz inkubatu dira 1mM Ditiotreitol (DTT)-rekin, disulfuro zubiak eratzen ari ez diren zisteinak erreduziteko. Proteina eta agente erreduzitzailea banatzeko indargetzaile aldaketa burutu da PD-10 zutabe bat (GE Healthcare) erabiliz. Berehala, markatzeko erabili den molekula fluoreszentea edo 3. kapituluan erabilitako konposatu aromatikoetako bat (maleimida edo iodoazetamidaz funtzionalizatuta) gehitu zaio, eta gau osoz inkubatu da 37 ºC-tan. Azkenik, lagina zentrifugatu (14.000 xg-tan 5 minutuz), eta konjugatu gabeko molekula kentzeko berriz ere PD-10 zutabe batean zehar pasa da. Markaketaren etekina aztertzeko fluoreszentzia neurketa zein masa espektrometria (*Matrix-assisted laser desorption/ionization-time-of-flight* edo MALDI-TOF) erabili dira.

2.1.4. Masa espektrometria

Masa espektrometriaz egindako neurketan Ibon Ilorok burutu ditu CICBiogunen (Derio), antigorputzen eta molekula aromatikoen arteko konjugazioaren etekina aztertzeko. Neurketak hasi aurretik, Fab lagin guztiei gatza erauzi zaie ZipTip® C4 mikrozutabeak (Milipore) (2 µL-ko laginak) eta SA indargetzailearen (azido sinapinikoa, 10 mg/mL azetonitriko:azido trifluoroazetiko-tan %0.1 [70:30]) 0.5 µL erabiliz. Laginak 384 putzutxoko *Ground Steel* plaketan (Bruker Daltonics) jarri eta masa determinatzeko Autoflex III MALDI-TOF espektrometroa (Bruker Daltonics) erabili da. Espektrometroa kalibratzeko Proteinen Kalibraziorako Nahasketa Estandarra (I) (Bruker Daltonics) erabili da, laginen masa-tarte berdinean. Datu bilketa eta espektroen analisiak flexAnalysis 3.0 softwarea erabiliz egin dira (Bruker Daltonics).

2.2. PROTEINEN ARTEKO ELKARREKINTZAK

2.2.1. ELISA zuzena

ELISA (ingelesetik, E*nzyme Linked Immunosorbent Assay*) antigorputz batek oinarri solido batean inmobilizatutako epitopoa ezagutzeko duen gaitasunean oinarritutako teknika immunologikoa da, eta erreakzio kolorimetriko baten bidez neurtzen da. Tesi honetan, ekoiztutako antigorputzen funtzionaltasuna frogatzeko erabili da, lehen teknika gisa, baita antigeno desberdinen aurrean duten polierreaktibotasuna aztertzeko eta saguetatik erauzitako gazurrean antigorputz espezifikoak detektatzeko ere. Horretarako, GIBaren gp41 azpinunitateko MPER sekuentziatik eratorritako peptidoak, autoantigeno desberdinak edota liposomak erabili dira antigeno bezala.

96 putzuko plakak (Corning Inc., Corning, NY) MPER domeinuan oinarritutako peptidoarekin (1.37 µM) edota liposomekin (0.5 mM) inkubatu dira gau osoan zehar giro tenperaturan. Garbiketa indargetzailearekin (PBS+%0,05 Tween 20) itsatsi gabeko peptidoa kendu ondoren, batuketa inespezifikoak ekiditeko, putzuak %3-ra behi-gazur albumina (BSA, ingelesetik *Bovine Serum Albumin*) duen 300 µL PBS-z (Phosphate Buffered Saline) blokeatu dira giro tenperaturan bi orduz inkubatuz. Ondoren Fab-en (edo saguen gazurraren) diluzio seriatuak (100 µL) erantsi dira (PBS, %1 BSA, %0,02 Tween-20 indargetzailean) eta ordubetez inkubatu dira giro tenperaturan. Fosfatasa alkalinoa entzima duen giza immunoglobulinak ezagutzen dituen antigorputz sekundarioa (SIGMA-Aldrich) (1:1000) gaineratu eta 50 minutuko inkubazioa bukatuta, 4-nitrofenil fosfato disodio gatz hexahidratoa gehitu da, fosfatasa alkalinoarekin erreakzionatuz produktu kromogeniko bat ematen duena. 30 minuturen ondoren, erreakzioa NaOH 3M erabiliz geldiarazi eta erreakzioaren produktua 405 nm-ko absorbantzia neurtuz kuantifikatu da Bio-Tek Sinergy HT plaka irakurgailu batean (Bio-TEK Instruments Inc., VT, USA).

2.2.2. Biogeruzen interferometria (BLI)

Biogeruzen interferometria markaketarik behar ez duen teknika optiko analitikoa da, biomolekulen artean ematen diren elkarrekintzak neurtzen dituena. Bi gainazaletan gertatzen den argi zuriaren interferentzia patroia aztertzen du: Lehen geruza inmobilizatutako proteina jakin batek sentsore biologiko baten gainean osatzen duena litzateke, eta bigarrena, erreferentzia gisa erabiliko den gainazal bat. Teknika honek ligandoaren (sentsore biologikoan inmobilizatuta) eta analito solugarriaren arteko elkarrekintza denbora errealean neurtzen du.

Biosentsorearen gainazalean inmobilizatuta dagoen ligandoaren eta analitoaren arteko batuketak gainazal molekularraren lodiera handitzen du, gero eta molekula gehiago lotu ahala. Espektroaren patroia aldatzen joango da gainazalaren lodiera optikoaren funtzioan, eta aldaketa hau detektoreak jasotzen du. Seinalea sensograma batean irudikatua izango da azkenik, uhin luzera aldaketa bezala (nm-ko desplazamendua). Elkarrekintza molekularrari buruzko informazioa eskuratu daitezke plataforma honen bidez; bai elkarrekintzaren afinitate konstanteak eta baita molekulen kuantifikazio espezifikoa ere. Horretarako, datuak analizatzeko softwarea erabili da (Kumarasawamy & Tobias, 2015).

Tesi honetan erabilitako zenbait antigorputzen eta beren epitopoen arteko elkarrekintzaren batuketa afinitateak aztertzeko BLI erabili da tesi honetan, Octet RED96 BLI sistema (Pall ForteBio) erabiliz. Ni-NTA sentsore biologikoak erabili dira, aurrez zinetika indargetzailean (PBS, pH 7.4, 0.002% Tween, 0.01% BSA) hidratatuak izan direnak. MPER-his ligandoa erabili da, 10 µL/mL-ko kontzentrazioan, 60 segunduz eta 1000 rpm-tan sentsoreak kargatzeko. Ondoren, sentsore hauek zinetika indargetzaileaz betetako putzutxoetan busti dira 60 segunduz, eta jarraian antigorputzen diluzio seriatuak (500 nM-tik 62.5 nM-era) dituzten putzutxoetan murgildu dira. 180 segundu irauten dituen asoziazio fase honen ondoren, beste 180 segunduz zinetika indargetzailedun putzutxoetan busti dira sentsoreak, disoziazio fasean. Batuketaren analisia egiteko Octet softwarea erabili da, 1:1 egokitze modeloetan oinarrituta.

2.3. TEKNIKA ESTRUKTURALAK

2.3.1. Dikroismo zirkularreko espektroskopia (CD)

Dikroismo zirkularra biomolekulen egitura sekundarioa (Urrutiko UB) eta tertziarioa (gertuko UB) zehazteko teknika sentikorrenetako bat da. Aldi berean, konformazio aldaketak eta egonkortasuna neurtzeko ere erabili daiteke (Fasman, 1996). Teknika honen abantaila nagusiak molekula kantitate txikiaren erabilera eta datuen analisi erraza dira.

Dikroismo zirkularra argiaren absortzioan oinarritzen den espektroskopia teknika bat da. Kromoforo batek ingurune asimetriko batean modu zirkularrean ezkerralderantz eta eskuinalderantz polarizatutako argia xurgatzean ematen diren desberdintasunak neurtzen ditu. Proteina batean agertzen diren kromoforo ohikoenak N terminala eta aminoazido aromatikoen albo kateak dira. Absortzioaren ondorioz gertatzen diren trantsizio elektronikoak uhin luzera eta intentsitate desberdina izango dute, elektroiek

espazioan duten kokapenaren arabera, eta honek egituraren inguruko informazioa emango digu.

Jasko J-810 espektropolarimetroa erabili da tesi honetan dikroismo zirkularreko neurketak egiteko, zeinaren ohiko kalibraketa prozedurak (1S)-(+)-10-azido kanforsulfonikoa eta amonio gatza erabiliz egin diren. Fab-en neurketak 25 ºC-tan, 5 µM-ko kontzentrazioan eta %10 glizerola duen PBStan egin dira. Datuak 1 nm-ko banda zabalerekin (100 nm/min abiaduran) jaso dira, eta horretarako 1 mm-ko luzera duen kuartzozko zelda erabili da. Guztira bost neurketa erabili dira bataz-besteko balioak lortzeko.

2.4. MINTZ EREDUEN SISTEMAK

Mintz biologikoak batez ere molekula anfipatikoz (fosfolipidoak, esfingolipidoak edo esterolak), proteinez eta karbohidratoz osatutako antolaketak dira. Mintz hauek bi geruzek osatzen dituzte, eta organismo batean barnealdea eta kanpoaldea definitu eta bereizteaz gain, prozesu fisiologiko gehienetan modu aktiboan parte hartzen dute (Watson, 2015). Mintz biologikoen antolaketa eta funtzioa aztertzeko modelo artifizialak erabili izan dira.

2.4.1. Liposomen (lipido besikulen) ekoizpena

Liposoma bat bi geruzaz osatutako egitura lipidikoa da, barnealdean soluzio urtsu bat enkapsulatzen duena. Egitura hauek modu espontaneoan sortzen dira zilindro itxurako molekula lipidikoak soluzio urtsuetan diluitzen direnean, eta tratamenduaren arabera, lamela bakarreko edo ugariko (*mutilamellar vesicles* edo MLV) bigeruzak izan daitezke.

Tesi lan honetan, MLVtan oinarritutako formazio metodoa erabili da liposomak ekoizteko: bai lamela bakarreko besikula handiak (*large unilamellar vesicles* edo LUVak) eta baita lamela bakarreko besikula erraldoiak (*giant unilamellar vesicles*, edo GUV).

Intereseko lipido kantitatea (espezie bakarra edo nahasketa) udare itxurako kristalezko tutuan nahastu da lehenengo, fase organikoan eta nitrogeno gasaren fluxua erabiliz lehortu, huts ponpan ordubetez sartu aurretik (disoluzio organikoaren traza guztiak kentzeko). Eskuratutako lipido geruza H_2Oz saturatuta dagoen nitrogeno gasaren fluxuaz hidratatu da ordu erdiz burbuilatzailea erabiliz, eta aukeratutako lipidoen trantsizio tenperaturaren gainetik dagokion soluzio urtsuarekin inkubatu ondoren MLVak eskuratu dira.

GIBak infektatutako zelula ostalariaren mintzetik eskuratzen du bere lipido bildukia (Sundquist & Kräusslich, 2012). Birusaren lipidoak isolatuz eta masa espektrometria erabiliz, mintzaren konposaketa zehatza argitaratu zuten lehen aldiz 2006an (Brügger et al., 2006). Hauek oinarri hartuta, birusaren mintza imitatzen duten bi lipido nahasketa erabili dira tesi honetan zehar: Alde batetik, VL-2 (*virus-like*-2) besikulak, 2-dioleoil-*sn*-glizero-3-fosfatidilkolina (DOPC), 1,2-dioleoil-*sn*-glizero-3-fosfatidiletanolamina (DOPE), 1,2-dioleoil-*sn*-glizero-3-fosfatidilserina (DOPS), arraultza esfingomielina (SM) eta kolesterolaz (Chol) osatuta (14:16:7:16:47 mol ratioan). VL-3 nahasketak 1-palmitoil-2-oleoil fosfolipidoak (POPC; POPE; POPS) ditu fosfolipido saturatu gabeen ordez, eta birusaren mintzean existitzen den paketatze mailaren antza handiagoa dauka (Huarte et al., 2016).

2.4.1.1. Lamela bakarreko besikula erraldoiak

Lamela bakarreko besikula erraldoiak edo GUVak erreminta interesgarriak dira, beren tamaina handia dela eta (5-100 µm inguru, zelula baten tamainarekin alderagarriak) mikroskopio optiko baten bidez aztertu daitezkelako, baita GUV bakarreko domeinu desberdinak ere. Birusaren konposaketa lipidikoa islatzen duten besikula erraldoi hauek erabili dira ekoiztutako fab birkonbinanteek mintzak batzeko duten gaitasuna aztertzeko, mikroskopia fluoreszente aurreratua erabiliz.

Berezko puztea (*spontaneous swelling*) metodologia (Shnyrova et al., 2013) erabili da GUVak eskuratzeko. Lamela anitzeko besikulak ekoiztu dira aurrena eta ondoren, hauetako 20 µL hartu eta 40 µm-ko diametroa duten silikazko mikroesferen (*bead*-ak) 5 µL-rekin nahastu dira politetrafluoroetilenozko gainazal batean. Nahasketa homogeneizatu ondoren 2-3 µL-tako tantatxotan bereiztu eta huts ponpan lehortu da ordubetez. Lipido-*bead* lehorrak pipeta baten punta erabiliz jaso eta A indargetzailea duen (5mM HEPES, pH 7.4, sakarosa 3g/L) beste punta batean murgildu dira. Indargetzaile hau besikulen barnealdean egongo da hauek eratzen direnean. Bost minutuz ur lurrunez asetutako ontzi batean jarri da lipido-*bead* nahasketadun punta hau, eta hidratazioaren ondorioz sortutako besikulak B indargetzaileaz (5mM HEPES, pH 7.4) betetako behaketa platertxora pasa dira. GUVen barneko soluzioaren dentsitatea kanpoko soluzioarena baina altuagoa izanik, besikulak platertxoaren azpian pilatuko dira.

2.4.1.2. Lamela bakarreko besikula handiak

Lamela bakarreko besikula handiek (LUV) 100-1000 nm inguruko diametroa izan dezakete, eta lipidoen portaera ikertzeko sistema modelo erabiliena dira. Aukeratutako

osagai lipidikoak modu homogeneoan banatzen dira bi geruzetan, eta tokiko kurbadura ia zerokoa da. LUVak MLVen estrusio mekanikoaren bidez eratu ohi dira (L. Mayer, 1986). 10 aldiz izoztu eta desizozten dira aurrez eratutako MLVak, eta ondoren, beste 10 aldiz 100 nm-ko nanoporoak dituzten polikarbonatozko filtroetatik pasarazten dira, bigeruza bakarreko 100 nm-ko besikulak eskuratzeko.

Lan honetan, MPER peptidoa txertatuta duten liposomak eta liposoma biluziak GIBaren mintza bailiran erabili dira, eta ekoiztutako Fab-ek haiekin elkarrekiteko duten gaitasuna aztertu da bai flotazio saioen bidez, eta baita espektroskopia fluoreszentea erabiliz ere.

2.4.2. Lipido kontzentrazioaren determinazioa

Eratutako liposomen amaierako kontzentrazioa zehazteko fosforo ez-organikoaren kuantifikazioa erabili da. Prozedura hau Fiskek garatu zuen 1925ean (Fiske, 1925) eta Bartlett (Bartlett, 1958) eta Böttcherek (Böttcher et al., 1961) moldatu zuten beranduago. Fosfolipidoen hidrolisian oinarritzen da Fiskeren teknika: fosfato taldea aske gelditu ondoren erreaktibo desberdinekin elkarrekin ahal izango du, haserako kontzentrazioaren menpekoa izango den produktu koloredun bat emanez.

LUVen lagin txiki bat hartu (50 nmol fosforodun lipido inguru dituena), eta horrez gain, 0, 25, 50, 75 eta 100 nmol fosforodun indargetzailez betetako zuzen patroi bat prestatzen da, beranduago kalibrazio kurba bezala erabiliko dena. Lagin guztiak 500 µL azido perklorikorekin (%70) nahastu, tutuak irabiatu eta 205 ºC-tan dagoen plakan utzi dira 45 minutuz fosfolipidoen hidrolisia gerta dadin.

Laginak hoztu ondoren, amonio heptamolibdatoan oinarritutako soluzioaren 4 mL eta 500 µL azido askorbiko gehitu zaizkie. Fosfato taldeek molibdatoarekin erreakzionatuko dute, eta azido askorbikoarekin gero, produktu horixka bat sorraraziz. Bost minutuz irakin ondoren, laginek kolore urdinerantz joko dute hasierako fosforo kantitatearen arabera. 812 nm-tan neurtzen da laginen absorbantzia, eta zuzen patroiaz baliatuz liposomen kontzentrazioa kalkula daiteke.

2.4.3. Sakarosa gradiente bidezko liposomen flotazioa

Besikulen flotazio saioa proteinen eta LUVen arteko elkarrekintza neurtzeko erabiltzen da. Proteinak eta LUVak inkubatu ondoren sakarosa gradientean egindako flotazioak lipidoei batutako eta batu gabeko proteinak bereizten ditu. Tesi honetan ondoko prozedura jarraitu da saio hauek egiteko: 100 µL-tako laginean rodaminadun liposomak (1.5 mM) eta intereseko fab-ak (150 nM) nahastu dira, eta sakarosadun soluzioa gehitu zaio, 300 µL-tan 1.4 M-ko kontzentraziora egokitu arte. Segidan 0.8 M (400 µL) eta 0.5

M-eko (300 µL) sakarosa geruzak gehitu dira gainean. Gradiente hau 436.000 xg-tan zentrifugatu da hiru orduz TLA 120.2 errotore bat erabiliz (Beckman Coulter, Brea CA, USA), eta 250 µL tako frakzioak berreskuratu dira. Tutuetan itsatsita gelditu den materiala eramateko %1 SDS bero erabili da, eta honekin bostgarren frakzio bat jaso da. Fab-en presentzia Western-blot (WB) teknika erabiliz antzeman da, liposomen frakzioak, berriz, rodaminaren fluoreszentzian oinarrituz zehaztu dira.

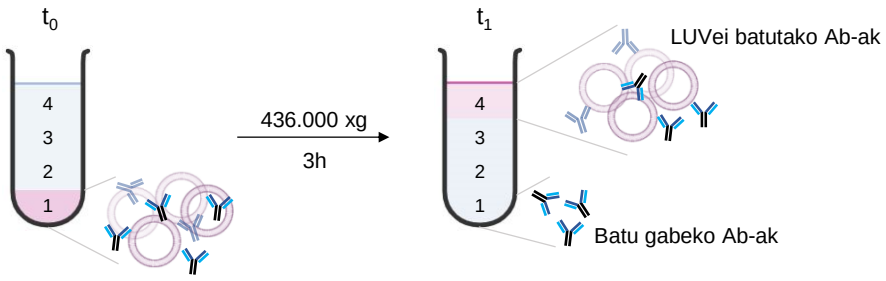

2.4. irudia. Besikulen flotazio saioaren irudikapen eskematikoa. Liposomak antigorputzekin inkubatzen dira, eta sakarosa gradiente bat aplikatzean espezieak dentsitatearen arabera 4 frakziotan banatzen dira. Liposomak goiko frakzioan berreskuratzen dira (4. frakzioa), eta batuketa gertatu bada, Fab-ak ere bertan egongo dira. 1, 2 eta SDS frakzioetan flotatu ez duen material dentsoak egongo dira (batu gabeko proteina kasu).

2.5. FLUORESZENTZIAN OINARRITUTAKO ESPEKTROSKOPIA

Lotura kobalente batean dauden elektroiak energia baxueneko mailan aurkitzen dira oinarrizko egoeran (S_o). Fotoi baten absortzioaren ondoren, orbital jakin batean dagoen elektroiak energia altuagoko orbital batera egingo du salto, kitzikapen egoerara pasatuko delarik (S_1). Prozesu honi kitzikapena deritzo.

Molekulak berehala askatzen du energia ingurunera, berriz ere energia baxueneko S_o egoerara itzuliz. Energia modu ez erradioaktiboetan askatu izan ohi da, batez ere beroa bezala. Kasu batzuetan, ordea, energia argi moduan aska daiteke, fluoreszentzia deritzon fenomenoaren bitartez (Croney et al., 2001).

Proteinetan, hauen berezko fluoreszentziaren erantzule diren zenbait aminoazido aromatiko aurkitzen dira, triptofanoa (Trp) adibidez. Aminoazido honek emiti dezakeen fluoreszentzia inguruko medioaren araberakoa da, kitzikapenak irauten duen denboran bere ingurunearekin elkarrekiten baitu. Ingurune polar batean, esaterako, π elektroiak kitzikatu eta energia maila altuago batera jauzi egitean, beren dipolo momentua handiagotu egiten da. Horrela, disolbatzaile polarraren eta triptofanoaren molekulen

arteko elkarrekintza estuagoa izango da, eta kitzikapen egoeraren energia maila jaisten da. Oinarrizko eta kitzikapen egoeraren arteko energia desberdintasun txikiagoa izango da egonkortze honen ondorio zuzena, eta hau fluoreszentziaren igorpenean islatuko da: ingurune polarrean, igorpena uhin luzera luzeagotara desplazatzen da (gorrirantz).

Aminoazido aromatikoen ezaugarri hau proteinen domeinuek ingurune polar zein apolarrekiko duten lehentasunaren ikerketan erabil daiteke. Besteak beste, erreminta interesgarria da proteinen eta lipidoen arteko elkarrekintzak aztertzeko (Ladokhin et al., 2000), triptofanoaren igorpen fluoreszentearen intentsitatean eta desplazamenduak ematen duen informazioaz baliatuz. Triptofanoak nahiko ugariak dira proteinen sekuentzian, ordea, eta erabilera hau apur bat mugatzen dute.

2.5.1. NBD zundan oinarrituatko espektroskopia bidezko titulaketa

7-nitrobenz2-oxa-1,3-diazol-4-yl (NBD) zundak, triptofanoak bezala, fluoreszentzia intentsitate baxua aurkezten du uretan, eta altua disolbatzaile organikotan (Fery-Forgues et al., 1993). Zuzendutako aldaketa kimikoa erabiliz, iodoazetamida-NBD (IA-NBD) zunda proteinen hondar zehatzekin ordezkatu daiteke, eta honek antigorputzak inguratzen dituen medioari buruzko informazioa lortzea ahalbidetzen du. Zundaren ezaugarri hau anti-MPER antigorputzen eta birusaren mintzaren arteko elkarrekintzak aztertzeko erabili da tesi honetan.

VL-2 eta VL-3 lipido konposaketak ekoiztu dira titulaketak egiteko. MPER peptidoa mintzetara gehitu den kasuetan, erabilitako nahasketa kolesterolik gabe prestatu da, izan ere, peptido hauek aktibitate fusogenikoa erakusten dute kolesterol ugari duten lipido nahasketetan (Apellániz, Rujas, et al., 2014). Beraz, kasu hauetan erabilitako konposaketa hurrengoa izan da: DOPC:DOPE:DOPS:SM (27:29:14:30 mol ratioan).

Espektroskopia esperimentuak egiteko 8100 Aminco-Bowman lumineszentzia espektrofotometroa (Spectronic Instruments, Rochester, NY) erabili da. Neurketak 25 ºC-tan egin dira, PBS indargetzailean, eta 470 nm-ko uhin luzeraz kitzikatu ondoren, fluoreszentzia igorpena 500-600 nm artean jaso da. Datuak egokitzeko, lagin bakoitzari dagokion molekula fluoreszenterik gabeko laginen espektroak kendu zaizkio. Banaketa kurbak lortzeko, NBDz markatutako antigorputzak lipido kontzentrazio desberdinekin titulatu dira. Datu hauek erabiliz frakzio molarren banaketa koefizienteak eskuratu dira, K_x, balio esperimentalak ondoko funtzio hiperbolikora (1) doituz:

$$\frac{F}{F_0} = 1 + \frac{[(F_{max}/F_0) - 1][L]}{K + [L]}$$

[L] eskuragarri dagoen lipido kontzentrazioa izango da, eta K, batutako proteina frakzioa 0.5 denean eskuragarri dagoen lipido kontzentrazioa. Horrela, K_x= [W]/K izango da, [W] ur kontzentrazio molarra izanik. Ur ingurunetik mintzera ematen den banaketan behatutako energia librearen aldaketa hurrengo ekuazioa erabiliz kalkulatu da (2):

$$\Delta G_{obs} = -RT + lnK_x$$

R gas idealen konstantea eta T tenperatura izanik.

Horrez gain, teknika espektroskopikoak erabili dira Fus-4 molekula aromatikoaz markatutako antigorputzek lipidoei lotzeko duten joera neurtzeko. Pirenoaren igorpen intentsitatea askoz altuagoa da ingurune apolarretan, 340 nm-ko uhin luzeraz kitzikatu ondoren. 0.5 µM fab edo fus-4 askea erabiliz, igorpen espektroak 360-600 nm-tako tartean jaso dira lipido kontzentrazio desberdinetan, denboran zehar egindako neurketak egiteko 200 µM VL liposoma erabili diren bitartean. Aurrez aipatu bezala, lagin bakoitzari dagokion molekula fluoreszenterik gabeko laginen espektroak kendu zaizkio datuak egokitzeko.

2.6. FLUORESZENTZIAN OINARRITUTAKO MIKROSKOPIA AURRERATUA

Mikroskopia fluoreszentea interesko laginen handipen eta kontraste handiko irudiak eskuratzeko tresna erabilgarria da. Ohiko epifluoreszentzia mikroskopio batean argi iturri gisa lanpara bat erabiltzen da. Argia objektiboaren aurretik aurkitzen den kitzikapen filtro batean zehar pasarazten da uhin luzera bat aukeratuz. Objektibo berdinak igorritako fluoreszentzia jasotzen duenez, detektagailura iritsi aurretik filtro dikroiko baten bidez kitzikapen argitik bereizten da.

2.6.1. Mikroskopia konfokala

Mikroskopia konfokalaren bidez foku-plano baten bereizmen handiko irudiak eskuratzen dira. Hori lortzeko, detektagailura iritsi aurretik fokutik kanpo gelditzen den argia baztertzen du, igorpen ibilbidean kokatutako irekidura optiko baten bidez. Foku-planoaren gaineko zein azpiko planoetatik datorren argia, beraz, ez da jasotzen, eta honek eragin zuzena du irudiaren kontrastean. Gainera, argi iturri gisa erabiltzen den lanpara laser batekin ordezkatuz fokoaren bolumena asko txikitzen da. Detektagailuak argi forman jasotako informazioa seinale elektrikoa bilakatzen du, irudi digital bat eraikitzeko erabiliko diren pixeletara itzuliz (Dean, 2001).

Lan honetan, Abberior Star Red (KK114) molekula fluoreszentearekin markatutako antigorputzen eta VL2 konposaketa duten GUVen arteko elkarrekintza antzemateko Leica TCS SP5 II mikroskopio konfokala erabili da (Leica Microsystems GmbH, Wetzlar, Alemania). Laurdan edo NBD zundekin markatutako GUVak eratu, behaketa platertxoetan (MatTek) jarri eta bertara 0,25 µM fab gehitu dira. Besikulak 340 nm-ko uhin luzeraz kitzikatu dira, 63x handipena duen ur-murgiltze objektibo bat erabiliz (irekidura optikoa = 1.2), eta igorpena 435 ± 20 nm-tan jasoz 512x512 pixeleko irudiak lortu dira. KK114 zunda daramaten Fab-en igorpena 775 ± 125 nm-tan jaso da, HeNe laser batekin 633 nm-tan kitzikatu ondoren.

2.7. BIOLOGIA ZELULARRA

2.7.1. Zelulen infekzio eta neutralizazio saioak

Anti-MPER antigorputzak GIBaren infekzioa blokeatzeko gai dira, birusaren mintzaren eta zelula ostalariaren mintz plasmatikoaren arteko fusioa blokeatuz. Tesian zehar ekoiztutako antigorputzen eta antigorputz frakzioen infekzioa blokeatzeko gaitasuna zehazteko neutralizazio saio estandarrak (Montefiori, 2009) eta laborategian bertan prestatutako sarrera biralaren blokeoan oinarritzen diren saioak erabili dira (2.5. irudia). Bi saioetan, antigorputz kontzentrazio zehatzekin inkubatu ondoren birus andui desberdinek CD4 eta CCR5 hartzaileak adierazten dituzten TZM-bl zelulak infektatzeko gaitasuna zehaztu da.

2.7.1.1. Pseudobirusen ekoizpena

HEK293 Giza Enbrioiaren Giltzurrun (*Human Embryonic Kidney* 293) zeluletatik eratorritako hazkuntza lerroa da. 293T zelula lerroak hurrengo aldaera aurkezten du: SV40 T antigenoa dauka, eta SV40 jatorria, transfektatutako plasmidoen kromosomaz kanpoko erreplikazioa baimentzen duena. Zelula lerro hau 37 ºC-tan eta %5 CO_2 kontzentrazioarekin mantendu da %10 behi fetuaren gazurrez, aminoazido ez esentzialez (1:100), sodio pirubatoz (1:100) eta penizilina/estreptomizina antibiotikoez (1:100) osatutako *Dulbecco's Modified Eagle's Medium* izeneko hazkuntza medioan.

Pseudobirusak (PsV) ekoizteko, HEK293T zelulak GIB andui desberdinen Env genea kodetzen duen plasmido batekin transfektatu dira kaltzio fosfatoaren metodoa erabiliz: pHXB2-env, PVO.4 (AIDS Research and Reference Reagent Program, Division of AIDS, NIAID, NIH), edo JR-CSF (Jamie K. Scottek emana). Plasmido hauetako bakoitza pWPXL-GFP eta pCMV8.91 (Patricia Villacek (CSIC) emana) bektoreekin batera

transfektatua izan da, hurrenez-hurren GFP zunda (zelula ostalariaren genoman txertatuko diren LTR eta Ψ sekuentziekin) eta Env-ik gabeko GIB-1en genoma kodetzen dutenak. Azken honek LTR eta Ψ sekuentziak falta ditu, eta horrez gain, Vpu, Vpr eta Vif gene biralek mutazioak dituzte infektatzeko gaitasuna duten ondorengoen eraketa eragozteko.

Plasmidoak transfektatu eta 18 ordutara, hazkuntza medioa aldatu da, gazurrik gabeko Optimem-Glutamax II (Invitrogen Ltd, Paisley, UK) gehituz. 48 ordu beranduago partikula biralak jaso, 0.45 µm-ko porodun filtrotatik (Millex® HV, Millipore NV, Brusela, Belgika) pasarazi eta sakarosa gradientean egindako ultrazentrifugazioz kontzentrau dira. -80º C-tan gordetzen dira, PBS indargetzailetan.

Pseudobirusen infekzio gaitasuna TZM-bl zelulak (AIDS Research and Reference Reagent Program, Division of AIDS, NIAID, NIH) erabiliz neurtu da. Aurrez JC53-bl (13 klona) deitua, TZM-bl HeLa zelula lerrotik eratorritako lerroa da, T_h linfozitoen CD4 eta CCR5 hartzaileak modu egonkorrean adierazten dituena. Zelula hauek mantentzeko HEK293T zelulen mantentze protokolo bera erabili da.

Ekoiztutako pseudobirusen diluzio seriatuak TZM-bl zelulekin inkubatu dira, infekzio maila zehazteko. Neurketa 72 ordu beranduago burutzen da, GFP adierazten duten zelulak zenbatuz BD FACSCalibur Fluxu zitometroa (Becton Dickinson Immunocytometry Systems, Mountain View, CA) erabiliz.

2.7.1.2. Neutralizazio saioa

Antigorputzen neutralizazio potentzia determinatzeko txanda bakarreko TZM-bl zelulen infekzio saioak erabili dira. Horretarako, antigorputz laginen kontzentrazio seriatuak 96 putzutxoko plaketan prestatu dira, eta ordu t'erdiz 37 ºC-tan inkubatu %10-15eko infekzio gaitasuna duen Psv dosiarekin. Berehala, 11000 TZM-bl zelula gehitu dira putzu bakoitzean, 30 µg/mL DEAE-dextranoz (Sigma-Aldrich, St-Louis, MO) osatutako medioan. Antigorputzen neutralizazio gaitasuna 72 orduren ondoren determinatzen da fluxu zitometria erabiliz. Antigorputz bakoitzak infekzioaren %50a blokeatzeko beharrezkoa den kontzentrazioa (IC_{50} balioa) zehazteko, neutralizazio portzentaia vs antigorputzen kontzentrazioa alderatuz eraikitako grafikoak erabili dira.

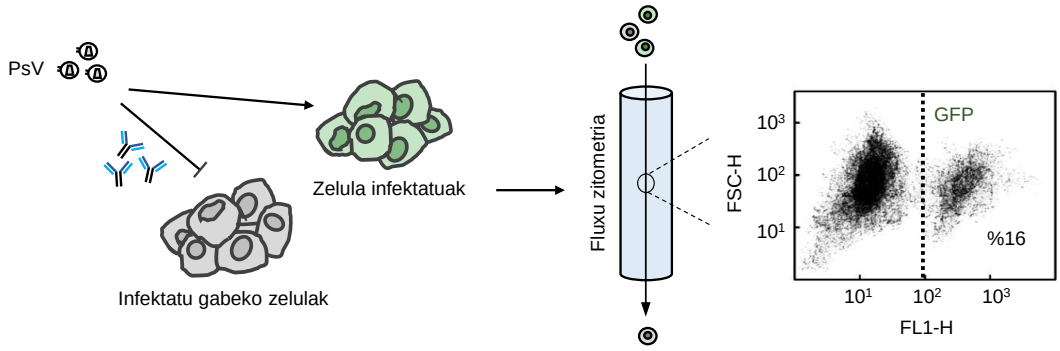

2.5. irudia. GFP zundaren fluoreszentzian oinarritutako neutralizazio saioa. Env adierazten duten PsVak TZM-bl zelulekin inkubatuak izan dira GIBaren aurkako antigorputzen presentzian, edo hauek gabe, eta infekzio prozesua inhibitzeko gaitasuna fluxu zitometria erabiliz determinatua izan da, GFP adierazpenean oinarrituz.

2.7.2. Bideragarritasun saioa

Tesi honetan erabilitako hazkuntza lerroak konposatu desberdinak dituzten antigorputzekin inkubatuak izan dira. Hauek zelulentzat kaltegarriak izan ez direla ziurtatzeko, zelulen bideragarritasun saioak burutu dira. Hildako zelulen portzentaia determinatzeko erabiltzen diren ohiko metodologietako bat mintz plasmatikoaren osotasunaren galeran oinarritzen da (Riss et al., 2019). CytoTox 96® *Non-Radioactive Cytotoxicity Assay* (Promega) kitak kuantitatiboki neurtzen du laktato deshidrogenasaren (LDH) presentzia hazkuntza medioan. Entzima hau zelulen zitosoloean aurkitzen da, baina mediora askatzen da zelula mintzak apurtu edo poroak eratuz gero.

Proba-laginen diluzio desberdinak aurrez putzutxo bakoitzean plakeatutako 11.000 TZM-bl zelulekin inkubatu dira, Opti-MEM hazkuntza medioaren (Thermo Fisher) 200 µL-tan. Lau ordu igaro eta gero, mediora askatutako LDH kontzentrazioa neurtzeko 30 minutuko erreakzio kolorimetriko bat jarraitu da. Gainjalkinei tetrazolio gatza (INT) erreaktiboa duen substratu bat gehitzen zaie, eta LDH entzimaren presentzian, kolore gorriko formazan produktua eskuratuko da. 490 nm-tan neurtu da putzutxo bakoitzaren absorbantzia, plaka irakurgailua (Bio-TEK Instruments Inc., VT, USA) erabiliz. Kontrol negatiboaz (konposaturik gabe inkubatutako zelulak) eta positiboaz (%100eko zelula lisia eragiten duen detergenteaz tratatutako zelulak) baliatuz datuen normalizazioa burutu da.

2.7.3. HEp-2 zelulen immunofluoreszentzia saioa

Giza-epitelioaren zelula lerroak (Giza laringeko epitelioko minbizi zelula lerroa edo HEp-2, adibidez) nukleoaren aurkako antigorputzen (ingelesetik, *anti-nuclear antibody* edo

ANA) detekzioan eta GIBaren ikerketa esparruan konkretuki, antigorputz autoerreaktiboen bilaketan oso erabiliak izan dira (Buchner et al., 2014; Haynes et al., 2005). Kit moduan komertzializatu ohi dira HEp-2 zelulak, eta mikroskopioan behatzeko porta batean fixaturik saltzen dira. Zelula hauek substratu sentikor gisa erabili dira polierreaktibitate patroien identifikazioa ahalbidetzeko.

Tesi honetan, GIB-1an negatibo diren HEp-2 (VIRGO ANA/HEp-2) zelulak erabili dira, immunofluoreszentzia ez-zuzenaren bidez antigorputz desberdinek hauei batzeko duten gaitasuna aztertzeko. Horretarako, 50 µg/mL-tan zeuden Fab-en 10 µL erabili dira test bakoitzean, saltzailearen protokoloari jarraiki. Fluoreszeina isothiozianatoari (FITC) batutako anti-giza Fab-ak (Jackson) erabili dira antigorputz sekundario bezala. Porten irudiak Leica TCS SP5 II mikroskopio konfokala erabiliz lortu dira (Leica Microsystems GmbH, Wetzlar, Alemania).

2.8. ANIMALIA MODELOEKIN (SAGUAK) EGINDAKO SAIOAK

Tesi honetan ekoitzitako zenbait IgGren PK/PDak aztertzeko Balb/c saguak erabili dira. *In vivo* prozedura guztiak Europar Zuzendaritzak ezarritako 2010/63/EU erregulazioa jarraituz burutu dira, The Art of Discoveryn (TAD) berrkusitako IACUC (ingelesetik, *Institutional Animal Care and Use Committee*) protokoloak jarraituz eta bertako beterinario baten presentzian. Antigorputzen txertaketa intrabenosoa eta erauzitako gazurraren tratamendua saguen manipulaziorako akreditaziodun TADeko laborategi teknikariak egin ditu. 20-21 gramoko Balb/c sagu emeak lau saguz osatutako bost taldetan banatuak izan dira, eta taldeko sagu bakoitzari 10E8 IgGaren edo honen eratorrietako baten 100 µg administratu zaizkio.

2.8.1. Antigorputzen bioeskuragarritasuna saguetan

Saguei antigorputzak eman ondoko 0, 2, 5, 8, 15, 22 eta 29 egunetan atera zitzaien odola, astean erauzitako odol kopurua 100 µL baino baxuagoa izanik. Gazurra giro tenperaturan egindako 45 minutuko inkubazioaren eta 200 xg-tan egindako 10 minutuko zentrifugazioaren ondoren isolatua eta ondoren aztertua izan da. Laginak -80 ºC-tan gordeak izan dira, ELISA bidez aztertua izan arte sagu bakoitzaren odolean giza-antigorputz espezifikoen maila zehazteko. 10E8 antigorputzaren kantitate zehatza ezagutzeko, gazurrarekin nahastutako antigorputz errekonbinante purifikatuak ere gaineratu dira ELISA putzutxotan. Hemendik eskuratutako kurba estandarretatik saguen seroetan dagoen antigorputz kontzentrazio zehatza kalkulatu daiteke.

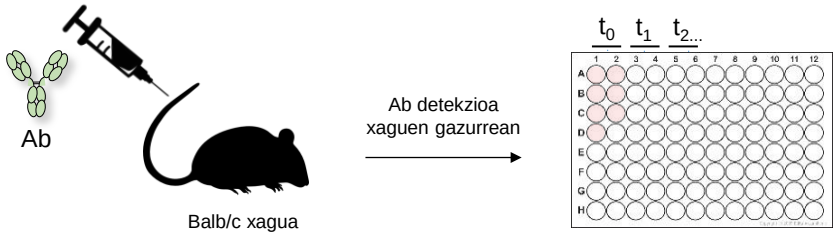

2.6. Irudia. Antigorputzen bioeskuragarritasunaren analisiaren eskema. Balb/c sagu modeloetan txertatu dira antigorputzak. Hurrengo 0, 2, 5, 8, 15, 22 eta 29. Egunetan odola atera eta gazurra isolatu ondoren, ELISAk erabili dira giza antigorputzen detekziorako.

2.8.2. Medikamenduaen aurkako antigorputzen detekzioa

MAb-ak proteina terapeutikoa seguruak eta ez-toxikoak kontsideratuak izan dira. Hala ere, behin eta berriro administratuz gero, medikamenduaren aurkako antigorputzen garapena eragin dezakete (ADA, ingelesetik *anti-drug antibody)*. Antigorputz hauek medikamenduarekin elkarrekin dezakete, edo hau neutralizatu bere eraginkortasuna mugatuz (de Groot & Scott, 2007). Balb/c saguen odolean ADA presentzia detektatzeko ELISAk erabili dira. Horretarako, sagu bakoitzak jasotako antigorputzaren 0.5 µM plakeatu dira gau osoz, BSArekin blokeatu eta putzutxoak ordubetez inkubatuak izan dira saguen gazurraren diluzioekin. Saguen Fc-en aurkako antigorputz sekundarioa (AP-ri batua) (Sigma-Aldrich) erabili da detekziorako.

Chapter 3.1

RESULTS: ANTIBODY OPTIMIZATION BY CONVENTIONAL MUTAGENESIS

3. RESULTS

3.1. ANTIBODY OPTIMIZATION BY CONVENTIONAL MUTAGENESIS:

FUNCTIONAL OPTIMIZATION OF ANTI-MPER ANTIBODY 10E8 BY PROMOTING MEMBRANE INTERACTIONS

Abstract

Antibodies 4E10 and 10E8 target similar helical epitopes in the membrane-proximal external region (MPER) and transmembrane domain (TMD) of the envelope glycoprotein (Env) subunit gp41, and are among the broadest known neutralizing antibodies against HIV-1. Accordingly, these antibodies and their mechanisms of action provide timely models in the development of effective vaccines and immunotherapies. Both antibodies exhibit unusual adaptations to attain specific, high-affinity binding to the MPER at the membrane interface. Reversing charge of basic paratope surfaces (from net positive to net negative) reportedly abolished electrostatic interactions between the antibodies and the membrane and lowered the neutralization potency of 4E10 and 10E8. Here, it is hypothesized that by increasing the net positive charge in similar polar surface-patches the neutralization potency of these antibodies may be enhanced. With 4E10, increasing positive charge at this paratope surface strengthened an electrostatic interaction between antibody and lipid bilayers during recognition of the MPER-TMD, but did not affect its neutralizing activity. In contrast, a similar approach enabled 10E8 to interact spontaneously with membranes; notably, the modified 10E8 neutralized with significantly greater potency. Binding analyses indicated that the optimized 10E8 bound with higher affinity to the epitope peptide anchored in lipid bilayers, and to Env spikes on virions. Overall, these data provide a proof-of-principle for rational optimization of anti-MPER antibody 10E8 via manipulation of its membrane interaction, and the possibility of combining different interactions to attain that goal. They also emphasize the crucial role played by the viral membrane in the antigenicity of the MPER-TMD of HIV-1.

3.1.1. Introduction

Antibodies 4E10 or 10E8 engage with a conserved epitope on the membrane-proximal external region (MPER) of the gp41 subunit of envelope glycoprotein (Cerutti et al., 2017; Irimia et al., 2016, 2017; Jeong Hyun Lee et al., 2016; Rujas et al., 2016) resulting in one of the broadest levels of HIV-1 neutralization reported to date (Binley et al., 2004; Burton & Hangartner, 2016; J. Huang et al., 2012; Zwick et al., 2001). Antibodies against this vulnerable site also mediate neutralization breadth and potency of sera from certain infected individuals (Burton & Hangartner, 2016; J. Huang et al., 2012; Jacob et al., 2015). Despite reported similarities in the epitope binding profile, 10E8 displays higher neutralization potency than 4E10, and, if any, very limited polyreactivity by comparison (J. Huang et al., 2012; Kim et al., 2014). These advantageous features have put the focus on 10E8 as a suitable template on which to base vaccine design (Kwong & Mascola, 2012; Montero et al., 2008; Zwick, 2005) and rational development of immunotherapeutic agents (Asokan et al., 2015; Barbian et al., 2015; Y. do Kwon et al., 2016; Pegu et al., 2014; van Gils & Sanders, 2014; L. Xu et al., 2017).

The antigen responsible for eliciting 4E10/10E8-like antibodies and the molecular mechanism underlying effective MPER recognition are not totally understood. Recently published structural data suggest that the MPER and its connection to the gp41 trasmembrane domain (TMD) are organized as a continuous, straight helix that emerges obliquely from the HIV membrane plane (Apellániz et al., 2015; Irimia et al., 2016, 2017; Pinto et al., 2019; Rantalainen et al., 2020; Rujas et al., 2016). The ability to access the helical MPER epitope at the viral membrane interface thus appears to support the neutralizing activity of 4E10 and 10E8 (Irimia et al., 2016; Rujas et al., 2016). Structural adaptations sustain effective interactions with the lipid bilayer surrounding the viral particle: i) a long heavy-chain complementarity determining region 3 (HCDR3) loop decorated at the apex with hydrophobic-at-interface aromatic residues strictly required for function (J. Huang et al., 2012; Rujas et al., 2016; Rujas, Insausti, et al., 2017; Scherer et al., 2010); and ii) a flat surface at the paratope that establishes favorable interactions with the viral membrane interface (Irimia et al., 2016, 2017; Rujas, Caaveiro, et al., 2017).

Recent studies have suggested that the association of 4E10/10E8 with membranes might be driven by electrostatic interactions between basic residues on the surface of the paratope, and anionic phospholipids (Irimia et al., 2016, 2017; Rujas, Caaveiro, et al., 2017). In particular, the crystal structures of complexes between 4E10 Fab and anionic short phospholipids reveal contacts between paratope and membrane surfaces

upon MPER epitope binding (Irimia et al., 2016). This possibility received further support from experiments that measured water-membrane partitioning, which demonstrated that electrostatic forces were beneficial for binding of the antibody to the membrane-anchored MPER peptide and for neutralization potency (Rujas, Caaveiro, et al., 2017). In contrast, 10E8 did not partition spontaneously into lipid bilayers under equivalent experimental conditions (Rujas, Caaveiro, et al., 2017) (see also below). Nonetheless, recent cryo-EM and x-ray crystallography studies reveal that the 10E8 paratope surface may establish favorable contacts with the viral membrane interface (Irimia et al., 2017; Jeong Hyun Lee et al., 2016; Rantalainen et al., 2020; Rujas et al., 2016).

The relevance of electrostatic interactions with the membrane was inferred from the deleterious effects caused by mutations to negatively charged residues at the paratope surface (Irimia et al., 2017; Rujas, Caaveiro, et al., 2017). Here, the opposite approach was followed; to optimize function of 4E10 and 10E8 by enhancing the net positive charge of their paratopes. The strength of antibody-membrane interactions was determined using liposome-flotation assays (a physical separation method). This standard method was complemented with fluorescence-based assays, namely, confocal microscopy of Giant Unilamellar Vesicles (GUVs) and spectroscopic titration assays (water-membrane partitioning in intact systems). In addition, whether the strength of antibody-membrane interactions was associated with neutralization potency was investigated. The data demonstrate that neutralization function of the 10E8 antibody can be optimized by manipulation of antibody-membrane interactions, and that several manipulations can be combined for that purpose. Interestingly, the observations emphasize that preservation of interactions with the membrane are likely crucial to the functional antibody-antigen binding surface, and therefore highly relevant for inducing effective anti-MPER B-cell responses. Finally, in a more general sense, they suggest a possible pathway for improving the potency of antibodies targeting membrane-displayed epitopes.

3.1.2. Materials and methods

3.1.2.1. Materials

The peptides used in this study were synthesized in the C-terminal carboxamide form by solid-phase methods using Fmoc chemistry, purified by reverse phase high-pressure liquid chromatography (HPLC), and characterized by MALDI-TOF (purity >95%). Peptides were routinely dissolved in DMSO and their concentration determined by the bicinchoninic acid microassay (BCA) (Pierce, Rockford, IL, USA) or by their absorbance

at 280 nm. Goat anti-human IgG-Fab antibody was purchased from Sigma (St. Louis, MO). Secondary antibody conjugated to horseradish peroxidase (HRP), mouse anti-goat IgG-HRP and rabbit anti-human IgG-HRP were purchased from Santa Cruz (Heidelberg, Germany), while goat anti-human-Fc-HRP and Fluorescein isothiocyanate (FITC)-conjugated goat anti-human secondary antibodies was from Jackson ImmunoResearch. The fluorescent probes 6-dodecanoyl-2-dimethylaminonaphthalene (Laurdan) and 4-Chloro-7-Nitrobenz-2-Oxa-1,3-Diazole (NBD) were obtained from Molecular Probes (Eugene, OR, USA). Abberior Star RED (KK114) was obtained from Abberior (Göttingen, Germany). Lipids DOPC, DOPE, DOPS, SM, Chol and 1,2-dioleoyl-sn-glycerol-3-phosphoethanolamine-N-(lissamine rhodamine B sulfonyl) (Rho-PE) were purchased from Avanti Polar Lipids (Alabaster, Alabama).

3.1.2.2. Expression, purification and labeling of Fabs

The sequences of 4E10 or 10E8 were cloned in the plasmid pColaDuet and expressed in *Escherichia coli* T7-shuffle strain (as described in section 2.1.1.), and labeled following the instructions in 2.1.3. In brief, a cysteine substituted Fab derivative ($W100b_{HC}C$) was first generated by site-directed mutagenesis, expressed, purified and finally modified after o-n incubation with a sulfhydryl-specific IA derivative of NBD. This procedure results in the conservative replacement of the Trp indole ring by the similarly bicyclic nitrobenzoxadiazole ring, which makes comparable changes in polarity scored by the NBD label. For confocal microscopy experiments, the fluorescence probe KK114 was introduced in vitro at position $C216_{HC}$ according to the same procedure as the one used for the NBD probe. In both cases, conjugation was monitored by emission of fluorescence.

3.1.2.3. ELISA to assess antigen binding

96-well plates were coated o/n at room temperature (RT) with 100 µL/well of MPER derived peptide KKK-^{671}N<u>WF</u>DITNWLWYIKLFIMIVGGLV^{693}-KK (1.37 µM). A peptide with alanine mutations of the two underlined critical residues in the epitope was used as negative control. After 2 hour well blocking with 3 % (w/v) BSA, serial dilutions of the fabs (starting in 1 µg/mL for 4E10 Fab, and in 10 µg/mL in the case of the 10E8) were incubated 1 hour at RT. Bound fabs were detected with an alkaline phosphatase-conjugated goat anti-human immunoglobulin. The reaction was measured by absorbance at a wavelength of 405 nm in a Synergy HT microplate reader.

3.1.2.4. Lipid vesicle production

LUVs made of the VL2 lipid mixture (DOPC, Chol, SM, DOPE and DOPS in a molar ratio of 14:46:17:16:7 (Rujas, Insausti, et al., 2017)) were produced following as described in 2.4.1.2.. Briefly, lipid suspensions were subjected to 10 freeze-thaw cycles prior to extrusion 10 times through 2 stacked polycarbonate membranes with a nominal pore-size of 0.1 µm. GUVs with the same composition were produced by spontaneous swelling following procedures described in 2.4.1.1. (Rujas, Caaveiro, et al., 2017; Shepard et al., 1998). For preparation of peptide-containing vesicles, lipids (0.125 mg of the VL lipid mixture) and peptides were mixed at the desired peptide-to-lipid molar ratio in CHCl3:CH3OH (9:1) prior to desiccation for 1 h to remove the organic solvent. Dried silica beads covered with lipid-peptide mixtures were collected and transferred to a 7.5 g/L sucrose buffer to induce spontaneous swelling of GUVs, which were transferred to the observation dish.

3.1.2.5. Vesicle flotation assays

The partition of the antibody into membranes was examined by vesicle flotation experiments in sucrose gradients following the method described by Yethon et al (Shepard et al., 1998) and in 2.4.3. In brief, 100 µl of LUVs of various compositions and labeled with the lipid rhodamine-PE were adjusted to a sucrose concentration of 1.4 M in a final volume of 300 µl, and subsequently deposited of a stepwise gradient composed of successive solutions containing 0.8 M (400 µl) and 0.5 M sucrose (300 µl). The gradient was centrifuged at 436,000 × g for 3 h and, four fractions each of 250 µl were collected. The material adhered to the centrifugation tubes was obtained by washing the tubes with 250 µl of a solution of 1% (w/v) SDS at 100 °C.

3.1.2.6. Confocal microscopy

Images were acquired on a Leica TCS SP5 II microscope as described previously at section 2.6.1. Laurdan-stained GUVs were excited at 340 nm, and emission was imaged at 435 ± 20 nm. The KK114-labeled Fab fragments were excited at 633 nm by using an HeNe laser, and emission was imaged at 775 ± 125 nm.

3.1.2.7. Spectroscopic titration

Partitioning curves were computed from the fractional changes in emitted NBD fluorescence when 150 nM NBD-labeled Fab was titrated with increasing lipid concentrations. VL-2 and DOPC:DOPS compositions were used to prepare bare liposomes. For peptide-containing experiments (1.7 μM of the MPER derived peptide KKK-^{671}NWFDITNWLWYIKLFIMIVGGLV^{693}-KK), DOPC:DOPE:DOPS:SM (27:29:14:30 mole ratio) LUVs were prepared. The mole fraction partition coefficients, Kx, and the observed free energy of water-membrane partitioning were following the equations showed in section 2.5.1. For the estimation of the electrical potential at the membrane surface (ψ_0) as a function of the PS content, the following equation was used:

$$\psi_0 = \left[\frac{2kT}{ze}\right] arc\sinh[A\sigma/(c)^{\frac{1}{2}}]$$

where c is the number of ions per volume and σ is the surface charge density (Heuck et al., 2000). To calculate the latter parameter, a surface area per phospholipid of 69.5 Å^2 was considered, and net charges of 0 and -1 were assigned to DOPC and DOPS, respectively.

3.1.2.8. Pseudovirus production and neutralization assays

HXB2 (Tier-1), JRCSF (Tier-2) and PVO.4 (Tier-3) PsVs were used to perform cell-entry assays. For that, HIV-1 PsVs were produced by transfection of human kidney HEK293T as previously described in 2.7.1.1. HIV entry was determined by using a single-cycle neutralization assay with CD4+, CXCR4+, CCR5+ TZM-bl cells as target following 2.7.1.2. protocol. Antibodies were added to virus in cell culture medium (DMEM supplemented with 10% FBS, 1 mM sodium pyrubate and MEM non-essential amino acid solution, 100 U/ml penicillin, and 100 μg/mL streptomycin), and the mixture was incubated for 1 h at 37°C prior to addition to target cells. Infection levels after 72 hours were inferred from the number of GFP-positive cells as determined by flow cytometry.

3.1.3. Results

3.1.3.1. Design of the 3R mutations

To generate antibodies 4E10 and 10E8 that interact more effectively with lipid bilayers, 3 basic residues (3R mutations) were introduced into the corresponding Fabs at strategic positions in which side-chains are exposed to solvent (Figures 3.1.1A, B). These triple

substitutions (G27R/S30R/S74R and S30R/N52R/S67R in the Fabs 4E10 and 10E8, respectively) resulted in an increased positive charge at the surface patches predicted to contact the viral membrane interface (Irimia et al., 2016, 2017; Rujas et al., 2016) (Figures 3.1.2A,B).

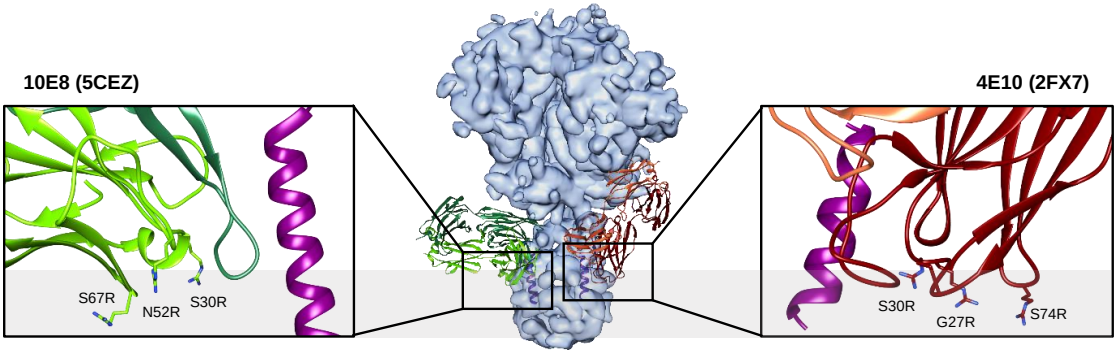

Figure 3.1.1. Structure-based selection of residues in 4E10 and 10E8 predicted to lay close to the viral mebrane. The 10E8 fab (PDB: 5CEZ) and the 4E10 fab (PDB: 2FX7) in complex with the epitope helix (magenta) were docked onto the Env trimer bound to 10E8 (EMDB code: EMD-3312) and positioned in contact with the lipid bilayer. In the squares, close-up views of the fabs displaying the selected mutations.

None of these changes altered binding to epitope peptide, as judged from the comparable patterns of specific binding observed for mutant and parental Fabs in ELISA (Figures 3.1.2A,B).

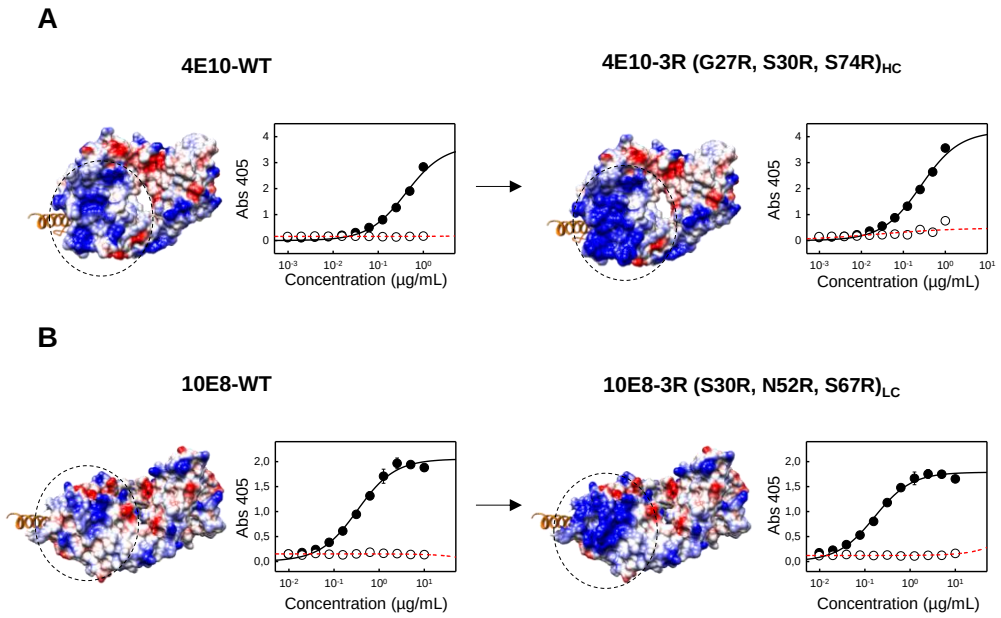

Figure 3.1.2: Design of 4E10 (A) and 10E8 (B) mutants with 3 Arg residues exposed on the paratope
Surface density charge representation of wild-type 4E10 (PDB entry code: 2FX7) and 10E8 (PDB entry code: 5GHW) Fabs and their triple mutants. Negative and positive surface electrostatic potentials are colored in red and blue, respectively. The triple substitutions G27R/S30R/S74R or S30R/N52R/S67R were introduced in the heavy and light chains of the Fabs 4E10 or 10E8, respectively. Encircled patches are predicted to establish contact with the membrane interface upon engagement with MPER epitope. The epitope peptide MPER(664-690) (PDB entry code: 5GHW) is modeled in the structures as an orange helix.. Fab binding to epitope peptide MPER(671-693) (black line) and to a control epitope peptide that contains the crucial residues 672WF673 substituted by Ala (red dotted line) was measured in a ELISA.

Thus, the membrane-binding characteristics and biological function of the resulting Fab mutants 4E10-3R and 10E8-3R were next studied, in comparison with those of the parental specimens 4E10-WT and 10E8-WT.

3.1.3.2. Effect of the 3R mutations on 4E10 water-membrane partitioning

Flotation experiments were used to establish the effect of the 3R mutations on Fab 4E10 partitioning from water into virus-like (VL) vesicles (Figure 3.1.3A). Whereas a fraction of the Fab 4E10-WT was recovered in pellets (i.e., non-floating fraction), recovery of all input antibody co-floating with vesicles, suggested an improved capacity of 4E10-3R for spontaneous partitioning into membranes. Membrane-binding assays using fluorescently labeled Fabs confirmed the same behavior in intact systems (i.e., without physical separation of the vesicle-bound specimens, Figures 3.1.3B,C). Moreover, confocal microscopy of GUVs showed stronger staining of the lipid bilayer by the KK114-4E10-3R mutant, in comparison to KK114-4E10-WT (Figure 3.1.3B). A similar pattern was observed in titration experiments using Fabs labeled with the molecular sensor NBD

(Figure 3.1.3C). Both the observed shift of the emission maximum wavelength and the increase of the fluorescence intensity were of larger amplitude with NBD-4E10-3R, revealing a stronger tendency to associate spontaneously with VL membranes in comparison to 4E10-WT.

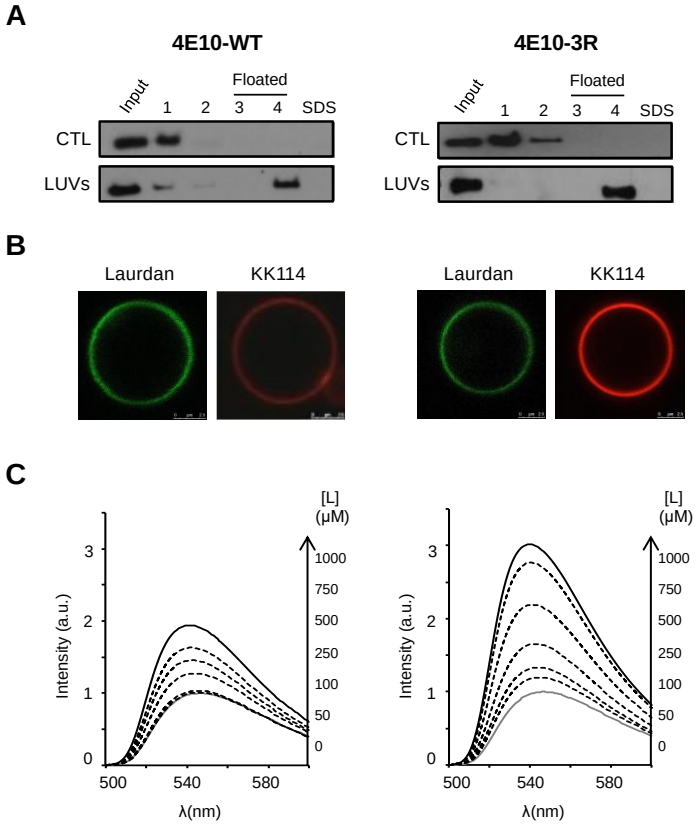

Figure 3.1.3: Partitioning of the Fabs 4E10-WT and 4E10-3R into membranes. (A) Membrane partitioning as measured by flotation assay using VL vesicles. After centrifugation in a sucrose gradient the sample was divided into four different fractions based on their different densities, and the presence of Fab probed by Western blot. VL LUVs were monitored by the presence of Rho-PE (not shown) and found in the third and fourth fractions (i.e., floated fractions). An additional fraction employing SDS was collected to recover the material attached to the surface of the tube. The CTL and LUV panels correspond to a samples centrifuged in the absence or presence of VL vesicles, respectively. (B) Partitioning of KK114-Fabs into VL GUVs. Micrographs display confocal images of VL GUVs at the equatorial plane. The lipid bilayer was labeled with Laurdan, and bound antibody imaged following fluorescence emission of KK114. The micrographs of both samples were rendered with equal contrast and brightness to best appreciate the difference in emission intensity. (C) Fluorescence emission spectra of Fabs labeled with the dye NBD. Emission spectra were measured in solution (gray solid line) or in the presence of increasing concentrations of VL vesicles (black solid and dotted lines) as indicated.

To assess the relative contribution of electrostatic interactions to the observed differences in partitioning of the Fabs, titration experiments were performed in vesicles combining DOPC and DOPS lipids at different mole ratios (Arbuzova et al., 1997, 2000) (Figure 3.1.4). The K_x values calculated for the partitioning of NBD-4E10-WT and NBD-

4E10-3R Fabs into vesicles containing 50% of the negatively charged lipid DOPS (Figure 3.1.4A), were $0.54 \cdot 10^6$ and $0.46 \cdot 10^7$ respectively, consistent with the more favorable electrostatic interaction of the latter antibody (Figure 3.1.4B). Furthermore, the similar dependence (parallel plots) observed for the partitioning free energies (ΔG_{obs}) on the surface potential (Ψ_0) calculated using Equations [2] and [3], respectively (McLaughlin, 1989; White & Wimley, 1999), suggested an additive effect of the charged Arg residues to the interaction (Figure 3.1.4C).

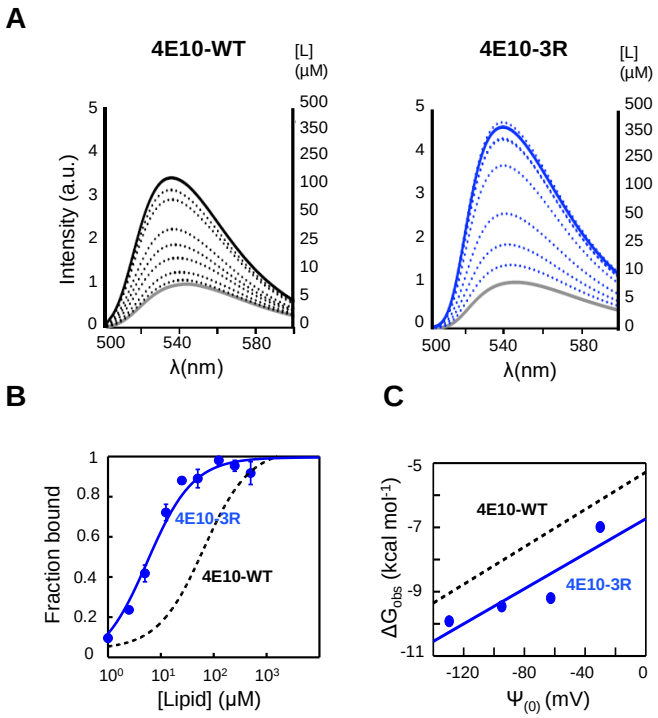

Figure 3.1.4: Binding of 4E10-WT (black traces and symbols) and 4E10-3R (blue traces and symbols) to PC:PS LUVs monitored by changes in NBD fluorescence. (A) Titration of NBD-labeled Fab with increasing concentrations of liposomes as indicated. (B) Plots of the fraction of Fab bound as a function of the concentration of lipid accessible (half the total lipid concentration). The molar fraction partition coefficients, K_x, were calculated from the best fit of Equation [1] to the data (curves). Each symbol on the plot represents an average of three independent experiments (±S.D. if larger than symbol). (C) Plots of the free energy of partitioning versus the membrane-surface potential in the previous lipid vesicles, estimated according to Equations [2] and [3], respectively.

3.1.3.3. Effects of the 3R mutations on 4E10 antiviral activity

Having determined that the 3R mutations increased 4E10 binding to lipid vesicles, we tested their effect on neutralizing activity. The 3R mutation did not improve 4E10 neutralization relative to 4E10-WT against any of the PsVs tested (Figure 3.1.5). Thus,

while introduction of the 3R residues increased the binding of 4E10 to membranes (Figures 3.1.3 and 3.1.4), neutralization was barely altered (Figure 3.1.5).

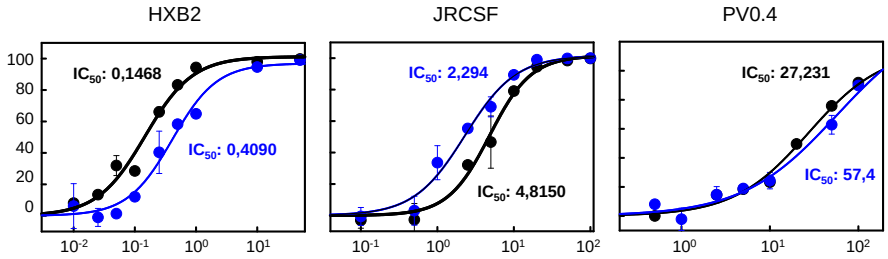

Figure 3.1.5: Neutralization of HIV-1 by 4E10-3R. 4E10-WT and 3R mutant Fabs were tested in a neutralization assay using TZM-bl target cells and three HIV-1 isolates: HXB2 (Tier 1), JRCSF (Tier 2) and PV0.4 (Tier 3). In all the cases, IC_{50} values were similar for both antibodies.

3.1.3.4. Effects of 3R mutations on 10E8 water-membrane partitioning

Consistent with published observations, Fab 10E8-WT did not interact appreciably with VL membranes in any of the assays that monitored water-membrane partitioning (Figure 3.1.6A-C, left panels). In sharp contrast, under comparable experimental conditions, 10E8-3R was found co-floating with vesicles after sucrose centrifugation (Figure 3.1.6A, right). Moreover, its fluorescently labeled derivative KK114-10E8-3R stained the bilayer upon incubation with GUVs (Figure 3.1.6B, right), and the fluorescence of the Fab NBD-10E8-3R was increased in intensity and was blue-shifted upon titration with VL LUVs (Figure 3.1.6C, right).

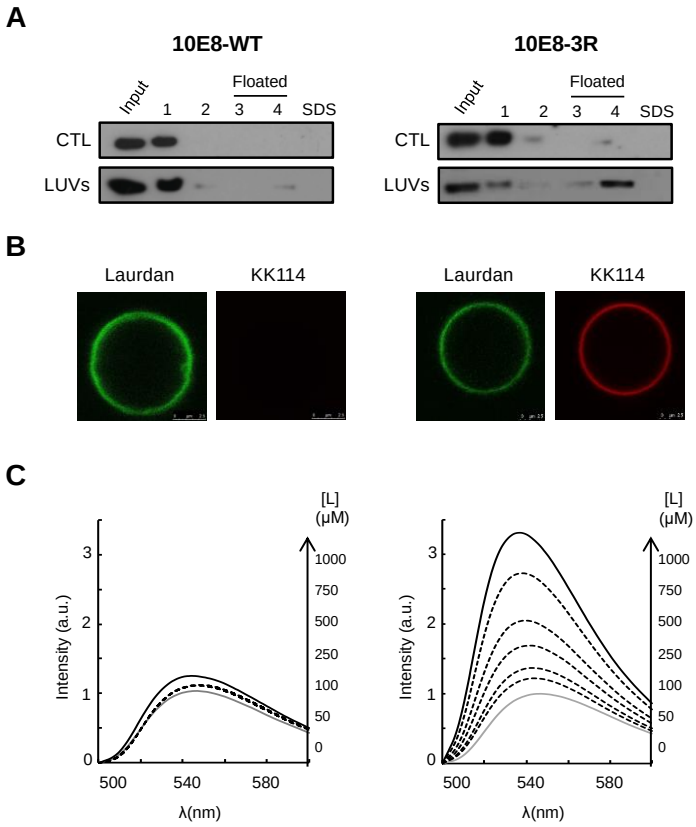

Figure 3.1.6: Partitioning of the Fabs 10E8-WT and 10E8-3R into membranes. The same methodologies described in Figure 3.1.3 have been followed in flotation (A), confocal microscopy (B) and NBD titration experiments (C).

The increased partitioning of the Fab 10E8-3R into DOPC:DOPS lipid bilayers that contained increasing amounts of anionic phospholipid was further consistent with interactions being driven by electrostatic forces (Figure 3.1.7). Thus, 10E8-3R followed a membrane-binding pattern that resembled a peripheral membrane interaction, as has been described previously for the Fab 4E10-WT (Rujas, Caaveiro, et al., 2017).

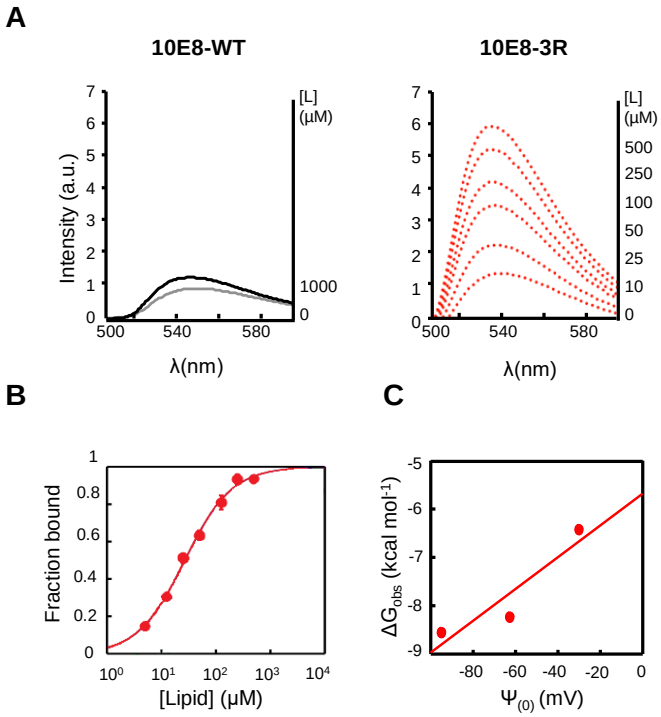

Figure 3.1.7: Binding of 10E8-WT (black traces and symbols) and 10E8-3R (red traces and symbols) to DOPC:DOPS LUVs monitored by changes in NBD fluorescence. (A) Titration of NBD-labeled Fab with increasing concentrations of liposomes as indicated in the panels. (B) Plot of the fraction of Fab 10E8-3R bound as a function of the concentration of lipid accessible. (C) Plot of the free energy of partitioning versus the membrane-surface potential. Conditions otherwise as in the previous Figure 3.1.4.

It has been shown that 10E8 neutralizing activity correlates with its capacity for epitope recognition in a membrane environment (Rujas et al., 2016). Therefore, we sought to establish whether 10E8-3R bore an improved epitope binding function (Figure 3.1.8). Indeed, binding in the membrane milieu resulted in increased fluorescence intensity and a blue shift of the maximum emission wavelength that is consistent with more efficient recognition of MPER peptide by 10E8 (Figure 3.1.8A, left). The enhanced association of NBD-labeled 10E8-3R with peptide-vesicle complexes in comparison with empty liposomes can be deduced from their water-membrane partitioning constant values of $0.24 \cdot 10^7$ and $0.11 \cdot 10^6$, respectively. Furthermore, in comparison with the parental antibody, the optimized mutant bound with a higher apparent affinity to GUV membranes decorated with epitope-peptide, as inferred from the more intense staining of GUVs by the Fab KK114-10E8-3R (Figure 3.1.8B).

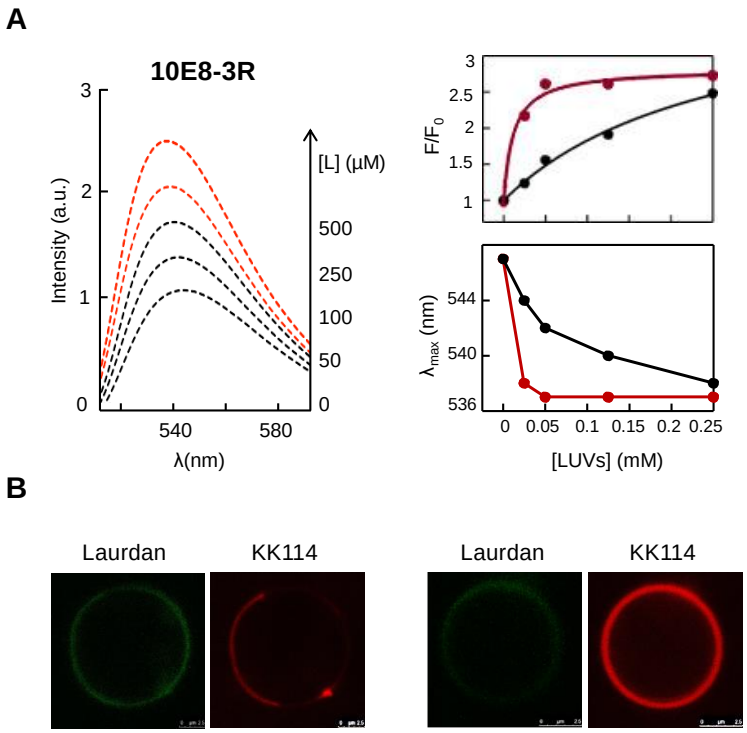

Figure 3.1.8: Effect of enhanced electrostatic interactions on epitope recognition at the membrane surface. (A) Left: Changes of NBD-10E8-3R fluorescence emission spectra in the presence of increasing concentrations of VL vesicles without cholesterol as indicated, were measured in the absence (black solid and dotted lines) or in the presence of 1.7 μM of $MPER_{(671-693)}$ peptide inserted in the membrane (red solid and dotted lines). Right: Increase in fractional emission and the position of the maximum of fluorescence emission wavelength in the previous samples (top and bottom panels, respectively). The initial value of fluorescence (F_0) was determined from the maximum intensity of the labeled Fab in the presence of empty vesicles. Each data point corresponds to the average of three titrations (± SD) as the ones displayed in the previous panel. (B) Partitioning of KK114-labeled Fabs 10E8-WT and 10E8-3R into VL GUVs containing attached epitope peptide MPER(671-693). Conditions otherwise as in previous Figure 3.1.3.

3.1.3.5. Effects of the 3R mutations on 10E8 antiviral activity

To determine the biological effects of the 3R mutations we compared Fabs 10E8-WT and 10E8-3R in neutralization assays (Figure 3.1.9).

10E8-3R was notably more potent against the three PsVs relative to 10E8-WT (with an average 5-fold decrease in IC_{50}; table 3.1.1). The improvement differed from a strain to other, suggesting that the effect is somewhat isolate dependent.

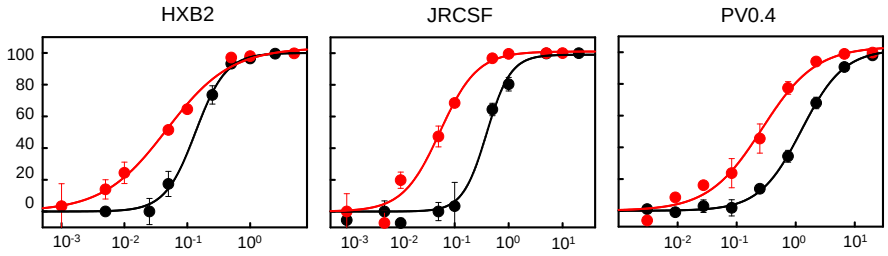

Figure 3.1.9: Neutralization of HIV-1 by 10E8-3R. 10E8-WT and 10E8-3R Fabs were tested in a neutralization assay using TZM-bl target cells and three HIV-1 isolates: HXB2 (Tier 1), JRCSF (Tier 2) and PV0.4 (Tier 3). In all the cases, the mutant antibody showed improved potency.

Table 3.1.1: Neutralization of HIV-1 by 10E8-WT and the 3R variant.

Virus	Tier	IC_{50} value (µg/mL)		Fold change
		10E8-WT	10E8-3R	
HXB2	1	0.135	0.047	2.87
JRCSF	2	0.392	0.053	7.39
PV0.4	3	1.25	027	4.63

3.1.3.6. Complementary functional effects of 3R mutations on engineered 10E8 antibodies

Similarly to peripheral proteins, antiMPER bnAbs can combine electrostatic and hydrophobic interactions to ensure spontaneous association with the membrane interface (Rujas, Caaveiro, et al., 2017; Rujas et al., 2016). It has been reported that an increase of the HCDR3 hydrophobicity by introduction of the H.S100cF mutation improved 10E8 potency ~5 to 10-fold (Y. do Kwon et al., 2018). Thus, the effect of adding the 3R mutation was also determined in a Fab already improved by the H.S100cF mutation (Figure 3.1.10A). The H.S100cF mutation did not alter the epitope peptide binding profile in ELISA, (Figure 3.1.10B). Following the predicted trends, separately, each mutation, 3R and H.S100cF, increased the potency of the Fab in our cell entry inhibition assays (Figure 3.1.10C and Table 3.1.2). However, the combination of the 3R and S100cF mutations resulted in a more robust potentiation (> 10-fold) of the Fab's antiviral activity.

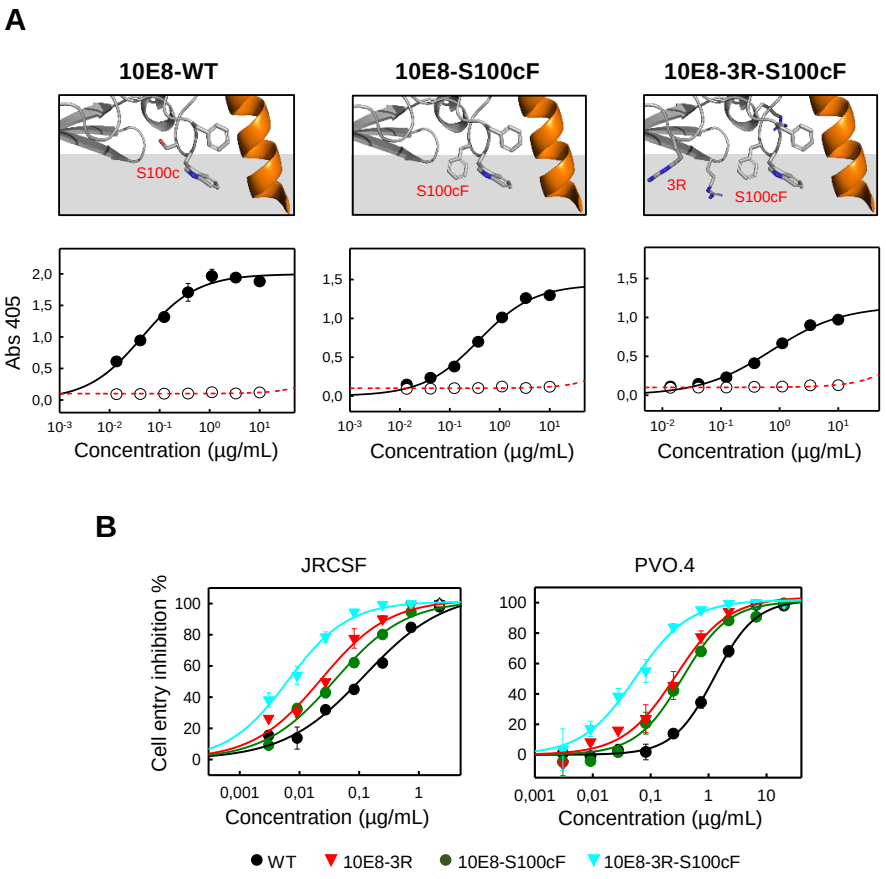

Figure 3.1.10: Effects of combining 3R and S100cF mutations on epitope binding, and antiviral activity of 10E8. (A) Top: Location of the combined mutations in the 10E8 paratope and adjacent areas. Side chains of key aminoacids are shown as ribbon, and MPER peptide is depicted in orange. Bottom: ELISA binding curves for 10E8 Fabs with CpreTM and Cala MPER sequences. (B) Cell-entry inhibition curves for 10E8 Fabs against JRCSF (tier-2) and PVO (tier-3) HIV-1 pseudoviruses.

The rescue by the 3R mutation of the loss of activity of a poorly-active variant bearing the H.W100bG mutation was next tested (Figure 3.1.11A). In this case, the mutation removes the side-chain of the Trp residue at the tip of the HCDR3, thereby reducing its hydrophobicity, and interfering with the antiviral activity of 10E8 (Carravilla et al., 2019; Rujas et al., 2016) (see also next chapter). Incorporation of the 3R or S100cF substitutions to the H.W100bG did not ameliorate the defective binding of this Fab variant to epitope-peptide in ELISA (Figure 3.1.11A). Interestingly, these mutations were able to partially rescue the antiviral function of the Fab mutated at the tip of the HCDR3 loop (Figure 3.1.11B).

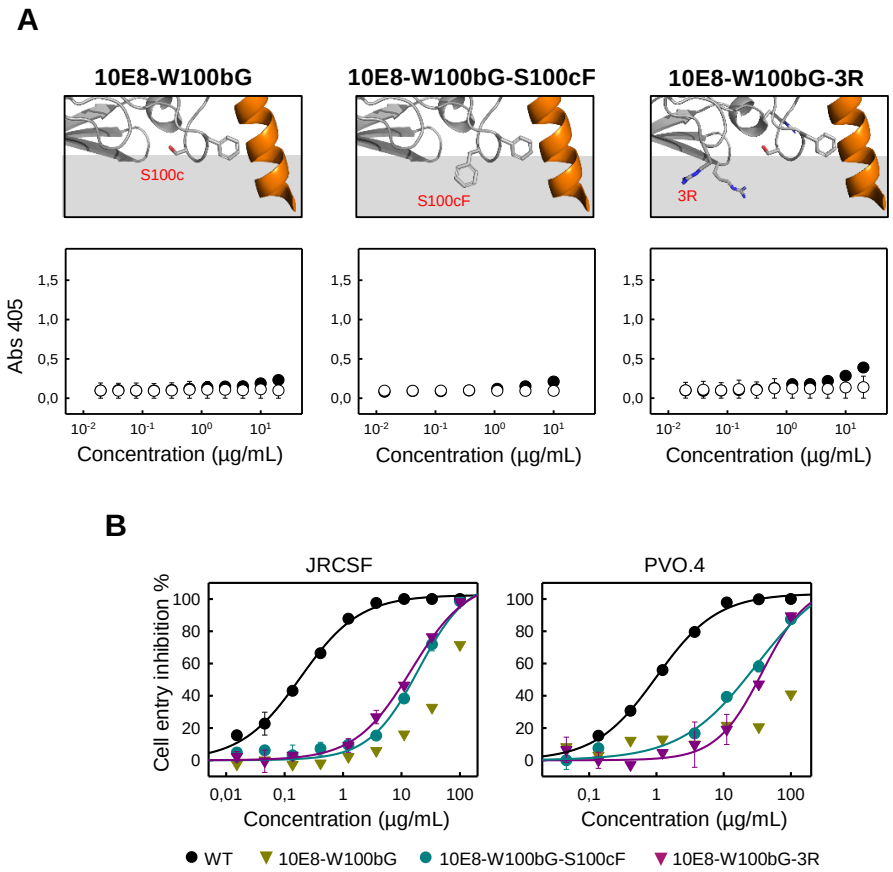

Figure 3.1.11: Functional complementation of W100bG deleterious mutation by 3R or S100cF. Mutation location and epitope binding (A), and antiviral activity of 10E8 (B) as in the previous Figure 3.1.10.

Table 3.1.2: Neutralization of HIV-1 by 10E8-WT and the new variants:

Antibody ID	IC_{50} (µg/mL)	Fold-increase	IC_{50} (µg/mL)	Fold-increase
	JRCSF - Tier 2		**PVO - Tier 3**	
WT	0.131	N/A	1.257	N/A
W100bG	>50	N/A	>50	N/A
S100cF	0.038	3.49	0.323	3.89
W100bG + S100cF	19.63	N/A	31.2	N/A
3R	0.022	5.98	0.251	5.01
3R + S100cF	0.010	13.64	0.068	18.49
3R + W100bG	14.76	N/A	37.52	N/A

Finally, to ascertain whether the H.S100cF mutation indeed conferred to 10E8 the ability to spontaneously associate with membranes, this Fab mutant was compared with 10E8-3R in GUV-based assays (Figure 3.1.12). Contrary to the expectations, the H.S100cF mutation did not promote partitioning of the Fab 10E8 into membranes, and even appeared to reduce the signal in membranes of the 10E8-3R mutant in GUV membranes.

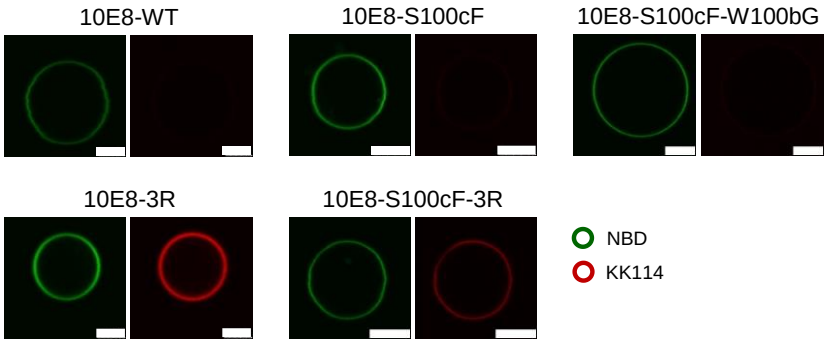

Figure 3.1.12: Effects of combining 3R and S100cF mutations on the Fab capacity to associate with GUV membranes. The plots display aGUV binding assay, where vesicles are visualized as green circles (NBD-DOPE), and presence or absence Fab binding was qualitatively inferred from the intensity of red color around the GUVs (KK114-Fab). Scale Bar is 2.5 µm for 10E8-WT, 10E8-3R and 10E8-S100cF-W100bG, and 5 µm for 10E8-S100cF and 10E8-S100cF-3R.

3.1.4. Discussion

The isolation of numerous highly potent bNAbs in the past decade has facilitated the study of effective humoral responses elicited during HIV-1 infection (Burton & Hangartner, 2016; Kwong & Mascola, 2012). The knowledge gained has stimulated current proposals for rational vaccine development (Burton, 2017; Haynes & Mascola, 2017; Kwong, 2017). At the same time, the isolated bNAbs have inspired the rational design of biologics expected to prevent and treat HIV infection (F. Klein, Mouquet, et al., 2013; West et al., 2014). Indeed, passive administration of engineered versions of bNAbs has been shown to prevent HIV infection in cells, animal models and humans (Barouch et al., 2013; Gruell & Klein, 2018; Halper-Stromberg et al., 2014).

In this context, the potency and breadth of neutralization by 10E8 as well as its effectiveness at conferring cross protection *in vivo* in primate models(Barbian et al., 2015; J. Huang et al., 2012; Pegu et al., 2014; van Gils & Sanders, 2014), makes it potentially useful for therapeutic developments. Two complementary strategies have been followed to overcome potential limitations of 10E8 for pharmacological use, namely: i) optimization of function and stability through mutagenesis (Y. do Kwon et al., 2016), and ii) promotion of polyvalence by antibody engineering (Montefiori, 2016). Following the latter strategy, recently published works describe development of antibodies that simultaneously interact with 2 (bivalent) or 3 (trivalent) independent Env determinants, which contained the antigen binding block of 10E8 as a basic component (Asokan et al., 2015; Y. Huang et al., 2016; L. Xu et al., 2017).

In this chapter, following strategy (i) it has been explored the possibility that the function of anti-MPER antibodies can be upgraded by promoting their interaction with membranes. Both selected antibodies, 4E10 and 10E8, engage with one surface of the MPER helix stuck into the viral membrane interface. This molecular organization defines a membrane-interacting surface at their paratopes. As emphasized by recent structural studies, interaction of MPER antibodies with the viral membrane could be driven by favorable electrostatic interactions (Irimia et al., 2016, 2017; Jeong Hyun Lee et al., 2016; Rujas et al., 2016), a possibility that has been formally demonstrated in the case of 4E10 antibody (Rujas, Caaveiro, et al., 2017). This chapter specifically inquired: (i) whether 4E10-membrane interactions can be further intensified and what are the consequences for the neutralization potency of this antibody; (ii) whether manipulation of the membrane-contacting surface of 10E8 would enable spontaneous interaction with membranes, and what the effects of this property might be on its biological function; and (iii) whether electrostatic and hydrophobic interactions can be combined to enhance 10E8 function.

The surface of 4E10 predicted to interact with the membrane surface exposes several basic residues (Irimia et al., 2016; Rujas, Caaveiro, et al., 2017). In this work, we demonstrated that binding of 4E10 to VL vesicles (LUVs and GUVs) can be enhanced by introduction of 3 additional Arg residues, which supports the hypothesis that the paratope surface inferred from structural data actually establishes contact with membranes (Irimia et al., 2016). However, these effects neither translated into better, nor worse neutralization activity.

In contrast to 4E10, the 10E8 antibody displays higher potency (Burton & Hangartner, 2016) but does not partition spontaneously into bare VL lipid bilayers (Rujas, Caaveiro, et al., 2017). The introduction of Arg residues at positions predicted to establish contact with the viral membrane interface (Irimia et al., 2017; Rujas et al., 2016), enabled the Fab 10E8 to interact spontaneously with lipid bilayers. This change also results in a more potent neutralizing activity. Notably, the improvement in 10E8 function correlated with an enhancement in binding affinity of the MPER epitope peptide in a membrane environment.

The data also demonstrate that, contrary to the 4E10 antibody, with 10E8 there is room for functional improvement by engineering the membrane-interacting surface of the paratope. In line with that idea, the addition of the 3R mutation to a Fab formerly optimized by increasing hydrophobicity at the H.S100cF position (Y. do Kwon et al., 2018), improved potency relative to WT and both individual mutants. This observation

suggests that combining individual beneficial mutations can be a viable path for improvement of antibody function.

However, contrary to the assumption, the improvement in potency from combining the mutations 3R/H.S100cF does not appear to correlate with stronger Fab-membrane interactions. The H.S100cF mutation did not promote 10E8 binding to GUVs, and even decreased membrane affinity when combined with the 3R mutation, which suggests that its effect on membrane interactions is weak or deleterious. Although the mechanism by which the H.S100cF mutation exerts its action remains unclear, the results from both the ELISA and the cell-entry inhibition assay imply that it cannot functionally replace the H.W100b residue. The double H.W100bG/H.S100cF mutant was incapable of binding to peptide, and it did not significantly inhibit cell entry at low concentrations. These observations further support that the H.W100b residue is necessary for 10E8 function (Rujas et al., 2016). Collectively, these evidences suggest that H.S100cF only improves 10E8 function when its epitope is presented in the context of the Env trimer. Future work will be required to test this hypothesis.

In conclusion, the observations in this chapter favor the idea that electrostatic interactions with the lipid bilayer are the consequence of structural adaptations undergone by anti-MPER antibodies to enable functional binding to the Env antigen in the membrane milieu (Irimia et al., 2016, 2017; Jeong Hyun Lee et al., 2016; Rujas, Caaveiro, et al., 2017; Rujas et al., 2016; Rujas, Insausti, et al., 2017). If this idea is correct, vaccines targeting the MPER epitope should elicit antibodies that approximate if not reproduce cognate membrane interactions.

Chapter 3.2

RESULTS: ANTIBODY OPTIMIZATION BY AROMATIC GRAFTING (I)

3.2. ANTIBODY OPTIMIZATION BY AROMATIC GRAFTING I:

AFFINITY FOR THE MEMBRANE INTERFACE UNDERPINS POTENCY OF HIV ANTIBODIES

Abstract

The contribution of membrane interfacial interactions to the functionality of antibodies that recognize membrane-embedded immunotherapeutic targets is currently unclear. Here, it is shown the possibility of optimizing broadly neutralizing anti-HIV antibodies by grafting aromatic residues at protein sites contacting the viral membrane, but distant from the epitope-binding pocket. The anti-viral activity of antibody 10E8 was significantly strengthened (by more than two orders of magnitude) via single-site chemical modification with synthetic aromatic acetamides. Upon conjugation, these aromatic compounds promote the partition of the antibody to the viral membrane where a neutralizing epitope of the Env glycoprotein is located. Antibody potentiation, demonstrated in cell-entry inhibition assays, is accompanied by an increase in affinity for the native antigen in virions. Site-selective chemical modification also improved a second antibody, 4E10, arising from a different lineage. In this antibody, chemical modification of a distant single site complemented the ablation of the heavy-chain complementarity determining region 3 (HCDR3) loop apex, resulting in the functional recovery of a fully inactive version. These observations support the harnessing of interfacial affinity through chemical modification to optimize Abs targeting membrane-proximal epitopes.

3.2.1. Introduction

Chemical modification of proteins is a method widely used to engineer proteins and to elucidate their function in the cell (Isenegger & Davis, 2020; Krall et al., 2016; Sakamoto & Hamachi, 2019). In antibodies, chemical modifications are generally introduced to link the protein to a second molecule for further functionalization, such as in antibody-drug conjugates, or to label the protein for analytical purposes. Using these and other approaches, a large collection of engineered antibodies is being developed for diagnostic and as therapeutic tools for the treatment and prevention of viral infections (Marasco & Sui, 2007; Walker & Burton, 2018). The case of broadly neutralizing antibodies (bnAbs) against the human immunodeficiency virus (HIV) can be considered a paradigm for the field (Ahmad et al., 2017; Caskey et al., 2019). Following the implementation of single B cell antibody cloning and high-throughput neutralization assays, the catalog of anti-HIV bnAbs available for therapeutic intervention has been progressively expanding in the last decade (F. Klein, Mouquet, et al., 2013; Sok & Burton, 2018). Characterization of these bnAbs revealed the distribution of several conserved neutralizing epitopes on the HIV surface antigen, the Env glycoprotein, that have served to guide the rational design of HIV vaccines. In addition, bnAbs are becoming attractive therapeutic tools against HIV due to their potent antiviral activity observed in challenge studies in animal models, together with their ability to reduce viremia when therapeutically infused in HIV infected patients (Baba et al., 2000; Caskey et al., 2019; Hessell et al., 2009; F. Klein et al., 2012; Lynch et al., 2015).

Among the anti-HIV bnAbs isolated so far, those targeting the C-terminus of the membrane-proximal external region (C-MPER) of the transmembrane gp41 Env subunit, consistently display the broadest levels of viral neutralization, being capable of blocking infection by the large majority of circulating HIV-1 strains and isolates tested (J. Huang et al., 2012; Krebs et al., 2019; Pinto et al., 2019; Sok & Burton, 2018; Stiegler et al., 2001; Williams et al., 2017). Passive administration of 10E8, the most potent antibody of this class, provides protection against infection in animal models (Pegu et al., 2014), also when incorporated in bi- and tri-specific antibodies as a cross-reactive binding-block component (Asokan et al., 2015; Y. Huang et al., 2016; Khan et al., 2018; Steinhardt et al., 2018; L. Xu et al., 2017). Despite its promising therapeutic profile, 10E8 still displays inhibitory concentrations (IC_{50}) about two orders of magnitude lower than those measured for the most potent bnAbs more recently isolated, and some of them already under clinical development (Caskey et al., 2019; Sok & Burton, 2018). Because of its very broad neutralization capacity, 10E8 represents an excellent candidate for functional optimization (increase in potency) by protein engineering.

Cumulative evidence suggests that engagement of Env by C-MPER bnAbs entails not only specific/high-affinity binding to the MPER peptide sequence, but also semi-specific interactions with a surface comprising regions of both the Env spike and the viral membrane interface (Irimia et al., 2016, 2017; Jeong Hyun Lee et al., 2016; Rujas et al., 2016). Recent work published by others and our laboratory have also demonstrated that the potency of 10E8 can be improved about 10-fold by mutating residues that enhance interactions with the membrane (Y. do Kwon et al., 2018; Rujas et al., 2018). Some of these residues belong to the paratope area in contact with membrane interface (Carravilla et al., 2019; Rujas et al., 2018). Furthermore, super-resolution microscopy studies of intact virions have revealed that the affinity of these optimized antibodies for native Env increased (Carravilla et al., 2019). Therefore, MPER-mediated neutralization depends, in addition to antigen recognition, on favorable antibody-membrane interactions.

This chapter reports that the modification with selected compounds at specific positions of the paratope increases the anti-viral potency of bnAb 10E8 by about two orders of magnitude, both in cell-entry inhibition and standardized neutralization assays. Mechanistically, the optimization of the antibody correlates with an increase in affinity for the native, integral membrane Env antigen in virions. The same approach and principles were applied to the 4E10 antibody. In this case, a fully inactive version of 4E10 could be functionally recovered via a single chemical modification. In conclusion, chemical engineering using aromatic grafting could provide a general route to improve the functionality of antibodies recognizing epitopes that are located at membrane interfaces.

3.2.2. Materials and methods

3.2.2.1. Materials

The peptides used in the affinity studies were synthesized as described in 3.1.2.1. The secondary Abberior Star 580 probe was obtained from Abberior (Göttingen, Germany). The chemical compounds were obtained by two different ways: 2-Iodo-N-phenylacetamide (Lin1) and 2-Iodo-N-pyren-1-ylacetamide (Fus4) were commercially available and obtained from Ark Pharm (Arlington Heights, IL, USA) and Molecular Probes (Eugene, OR, USA), respectively. Compounds Lin2, Lin3, and Fus2 were synthesized by A. Ojida (Department of Chemical Biology, School of Pharmaceutical Sciences, Kyushu University, Fukuoka, Japan).

The rest of the plasmids, probes and antibodies were obtained as indicated in 3.1.2.1.

3.2.2.2. Production and site-specific chemical modification of Fabs

Experimental procedures described in 3.1.2.2 were followed for the mutation, expression, purification and fluorescence labeling of Fab-s. Mutant Fabs bearing Cys residues at defined positions were subsequently modified with sulfhydryl-specific iodoacetamide derivatives of the aromatic compounds listed in Figure 3.2.2. Conjugation was monitored by matrix-assisted laser desorption/ionization (MALDI) mass spectrometry (Figure 3.2.3).

3.2.2.3. Characterization of Fabs

Binding to the epitope of produced fabs was detected by ELISA, following the methodology described in 3.1.2.3.

VL vesicles were obtained as indicated in 3.1.2.4, to test lipid binding by spectroscopic fluorescence. Fluorescence emission spectra of NBD were obtained by fixing the excitation wavelength at 470 nm, as described in 3.1.2.7. Briefly, fluorescence intensity was measured after NBD-labeled Fabs (0.5 μM) were incubated with MPER derived peptide (KKK-^{671}NWFDITNWLWYIKLFIMIVGGLV^{693}-KK. 1.7 μM) containing LUVs (DOPC:DOPE:DOPS:SM in 27:29:14:30 mole ratio, 250 μM).

3.2.2.4. Mass spectrometry

MALDI-TOF measurements were performed as described in chapter 2.1.4. Briefly, Fabs were desalted and arrayed onto a Ground Steel massive 384 target plate. Mass determinations were accomplished using a MALDI, tandem time-of-flight (TOF/TOF) spectrometer Autoflex III (Bruker Daltonics). Data acquisition and analysis were performed using flexAnalysis 3.0 software (Bruker Daltonics).

3.2.2.5. Thermostability assays

Melting (T_m) and aggregation (T_{agg}) transition temperatures of the WT Fabs and its chemically-modified variants were measured using a UNit system (Unchained Labs). T_m and T_{agg} values were obtained by measuring the barycentric mean fluorescence and the temperature at which the static light scattering at a 266 nm increased to 50% with respect to baseline, respectively. Samples were concentrated to 1.0 mg/mL and subjected to a thermal ramp from 25 to 95°C with 1°C increments. The average and the standard error of 2 independent measurements were calculated using the UNit analysis software.

3.2.2.6. Virus production and cell-entry assays

Screening for effective chemical compounds was carried out using neutralization-resistant JRCSF (Tier-2) and PVO.4 (Tier-3) PsVs in cell-entry assays (Bobardt et al., 2008). HIV-1 PsVs were produced by transfection of human kidney HEK293T as previously described in 2.7.1.1. HIV entry was determined after incubation of PsVs with TZM-bl cells following 2.7.1.2. protocol. Infection levels after 72 hours were inferred from the number of GFP-positive cells as determined by flow cytometry.

3.2.2.7. STED microscopy measurements

STED microscopy measurements were performed as described in 2.6.2. Briefly, Anti-MPER Fabs (25 ng/µL) were incubated for 1h in blocking buffer and revealed upon incubation with anti-human Abberior STAR RED (KK114) conjugated antibody before STED analysis. Imaging was performed on a STED microscope based on a modified Abberior Instrument RESOLFT QUAD-P super-resolution microscope (Abberior Instruments GmbH). Resolution was typically around 40 nm. Emitted photons were recorded line by line in STED microscopy mode, and Vpr.eGFP was next imaged in confocal mode to determine the location of HIV-1 virions. Image analysis was performed using Python scripting language and custom written functions, based on a previously developed program (Carravilla et al., 2019; Galiani et al., 2016).

3.2.3. Results

3.2.3.1. Strategy to optimize 10E8 by chemical modification with aromatic compounds

The first aim was to identify and validate potential regions within 10E8 for modification. The elements of 10E8 that stabilize lateral binding to its epitope at the viral membrane interface are the HCDR3 loop, which acts as a membrane anchor displaying at its tip an hydrophobic-at-interface Trp residue; and a paratope region adjacent to the HCDR3 that interacts with the periphery of the viral membrane (J. Huang et al., 2012; Irimia et al., 2017; Jeong Hyun Lee et al., 2016; Rujas et al., 2016). The specific positions subjected to modification were the surface-exposed residue H.W100b at HCDR3 and residue L.S65 at the membrane-associating paratope area, as structure-based analyses suggested that they insert to some degree into the membrane interface upon binding to the epitope (Figure 3.2.1). To carry out the chemical modification, 10E8 Fab was first engineered to contain a single Cys residue at each position (H.W100bC and L.S65C mutants).

Interaction of the selected residues with the membrane upon binding to the epitope was probed by conjugation of the introduced Cys residues with the fluorescent polarity-sensitive probe NBD. The fluorescence emission of these two labeled mutants increased significantly in the presence of proteoliposomes, in contrast to the absence of change of signal when the Fab was modified at a site expected to remain distant from the membrane (Figure 3.2.1, left spectra).

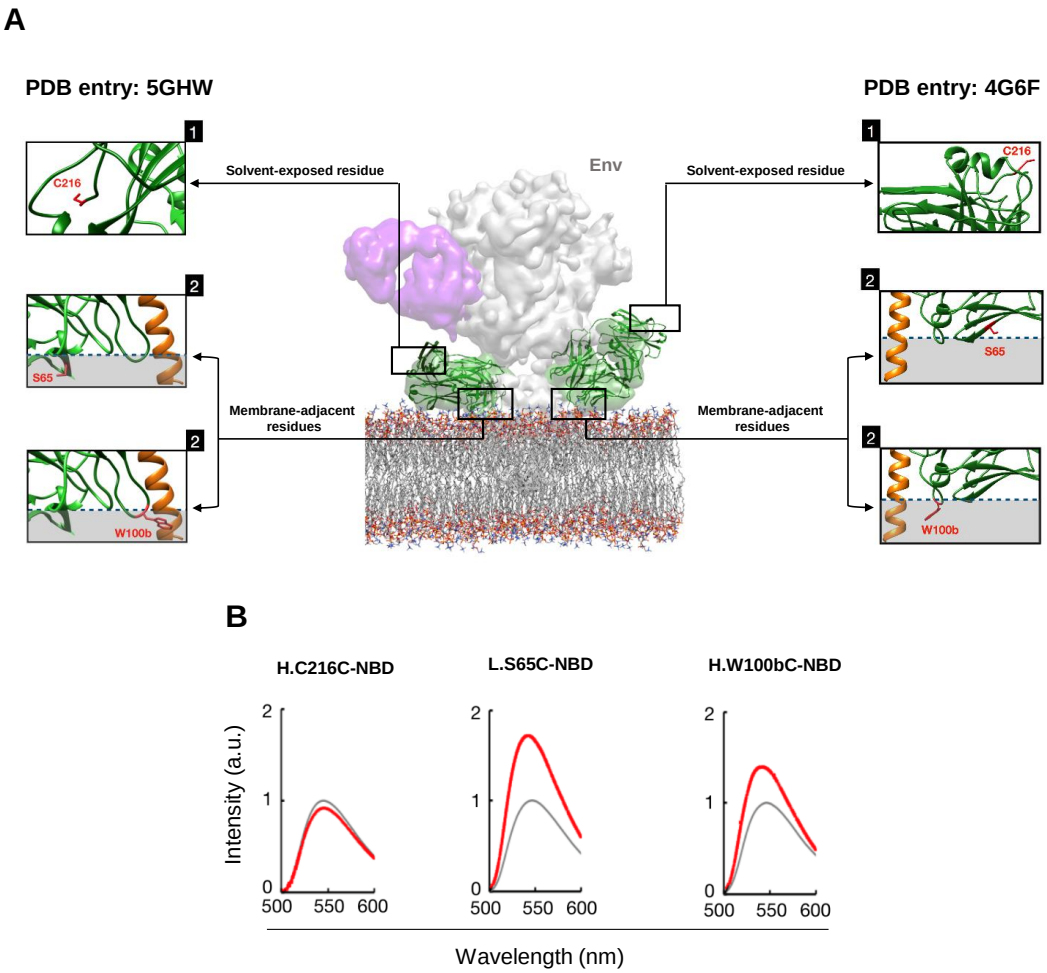

Figure 3.2.1: Structure-based selection of Ab 10E8 residues predicted to establish contact with the viral membrane interface. (A) Two Fab molecules (green) in complex with the epitope helix (orange) were docked onto the Env trimer bound to 10E8 (EMDB code: EMD-3312) and positioned in contact with the lipid bilayer. PDB IDs shown in the panel correspond to the atomic structures used for the fitting into the Fab 10E8 contours. The contour in magenta corresponds to Fab PGT-151 used to stabilize the Env trimer. Panels on the left are close-up views of the selected positions L.S65 and H.W100b in each copy of the Fab 10E8. (B) Fluorescence spectra of Fabs conjugated to NBD at those positions. Spectra measured in solution (gray traces) and upon incubation with liposomes containing epitope-peptide inserted (red traces) are shown. NBD label added at the remote residue H.C216 was used as a negative control.

Next, it was sought to optimize 10E8 interactions with the viral membrane through chemical modification with aromatic compounds. Even though aromatic compounds could increase the affinity of protein surfaces for the membrane interface, not all aromatic compounds have the same properties. For example, when considering aromatic residues, the side chain of Phe partitions with similar efficacy into the interface and the hydrocarbon core region, whereas for Trp, the interaction with the membrane interface is energetically more favorable compared with its immersion into the hydrophobic core (Andersen & Koeppe, 2008; McDonald & Fleming, 2016). In view of these differences, two different classes of synthetic aromatic compounds were selected to improve the functionality of Fab 10E8 through site-selective chemical modification (Figure 3.2.2). For a first evaluation, a series of phenyl-based linear compounds was selected, designated as Lin1, Lin2 and Lin3, which, depending on their length, might differentially contribute to the peripheral membrane interaction. And second, the effects of conjugating Fabs to polycyclic aromatic compounds, similar in size (naphthyl group, Fus2), or bulkier (pyrenyl group, Fus4) than that of the indole group of Trp, were also tested. The quadrupole moments of these compounds augmented with the number of fused rings, presumably benefiting their interaction with the complex environment of the membrane interface (Andersen & Koeppe, 2008; McDonald & Fleming, 2016).

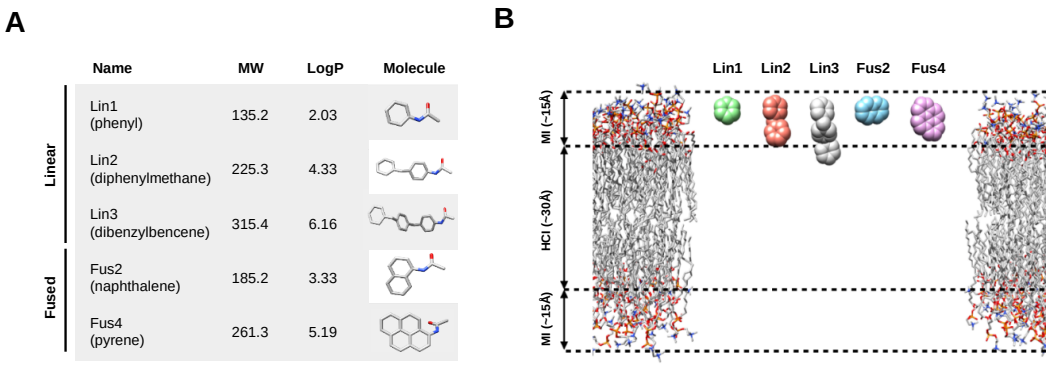

Figure 3.2.2: Synthetic aromatic compounds selected for the chemical modification of the antibody. (A) Basic properties and structural formulae of the synthetic aromatic compounds Lin1, Lin2, Lin3, Fus2 and Fus4. (B) Space-filling models of the aromatic moieties of compounds Lin1, Lin2, Lin3, Fus2 and Fus4 used for chemical modification. For size comparison the moieties are shown together with a lipid bilayer made of 1-palmitoyl-2-oleoyl-sn-glycero-3-phosphocholine (POPC). The approximate ranges of the interface (MI) and hydrocarbon core (HC) regions are indicated. All molecules displayed in the view were rendered to the same scale using 'Chimera' (Pettersen et al., 2004).

Chemical modification of the Fab at the positions selected were obtained by treating the Fab portion of the antibody with iodoacetamide synthetic derivatives. The modification was verified for the most hydrophobic and bulkier compounds of each series, i.e., Lin3

and Fus4, by mass spectrometry (Figure 3.2.3). These modifications did not appreciably affect the thermostability of the Fabs (Figure 3.2.4A,B), or the secondary structure of the antibody (Figure 3.2.4D), nor their ability to recognize the epitope (Figure 3.2.4C).

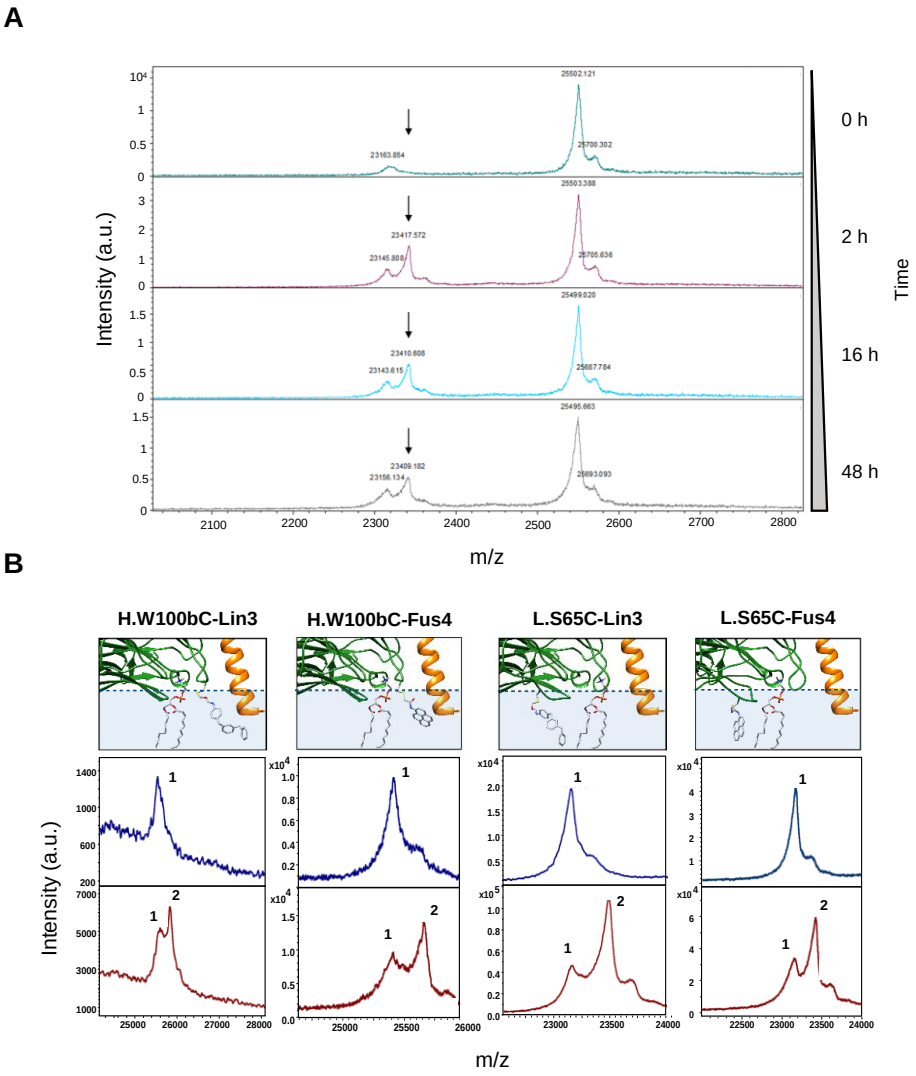

Figure 3.2.3: Chemical conjugation followed by mass spectrometry. (a) Time course of chemical modification. The Fab L.S65C of 10E8 was modified with Fus4. The mass increase of the light chain was monitored by MALDI-TOF for 48 hrs. The incorporation of Fus4 appeared to reach its maximum after two hours. **(b)** Labeling of membrane-contacting Fab positions modified with Lin3 or Fus4. The top panels depict the position of the modification. The bottom panels show the MALDI-TOF m/z plot before and after the modification, respectively.

A time course of the chemical modification was performed to stablish the effect of the incubation time in antibody modification yield. Incubation of fus4 with L.S65C mutant of the 10E8 over time was followed by MALDI-TOF, and incorporation reached its maximum after two hours (Figure 3.2.3).

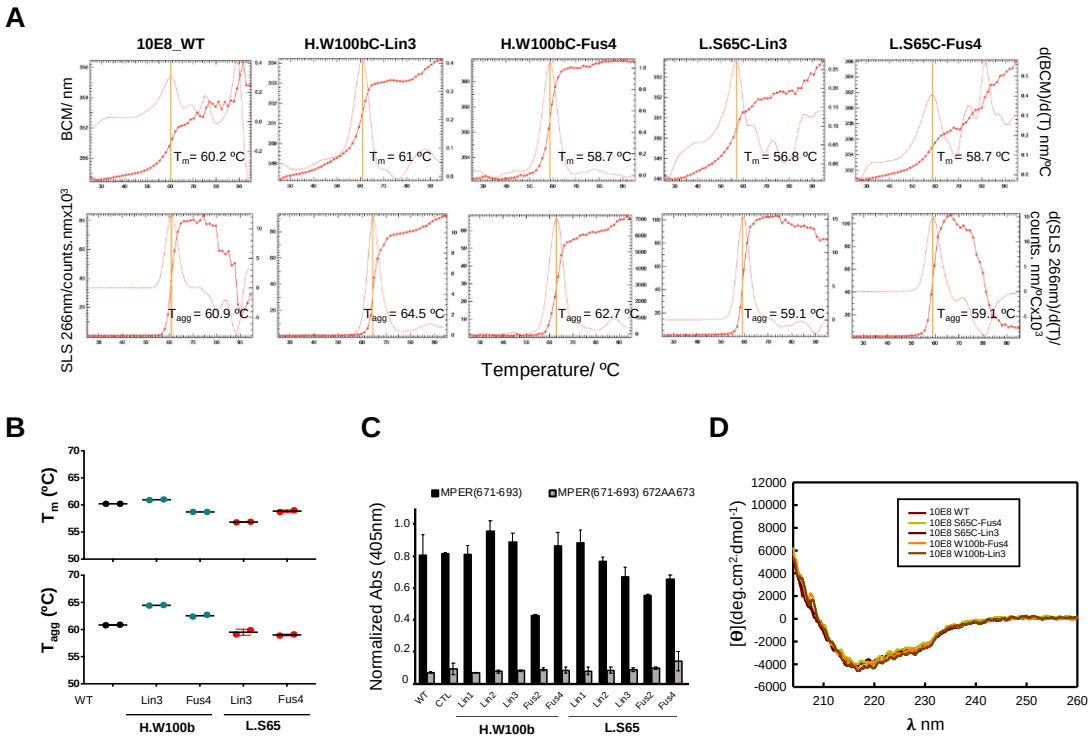

Figure 3.2.4: Thermostability and functionality of the chemically-modified Fab 10E8. (A) Thermostability. BCM (top panels) and SLS (bottom panels). Thermal transition temperatures (TM and Tagg) are indicated with yellow lines. (B) Thermal stability data (duplicates) employing the unfolding temperature (Tm, top panel) and aggregation temperature (Tagg, bottom panel) inferred from the previous experiments. (C) Binding to the epitope peptide MPER by ELISA performed in duplicate wells (values represent means ±SD). Black and gray bars correspond to native sequence and an inactive variant (double Ala mutant), respectively. (D) Circular dichroism spectra of WT Fab, and variants L.S65C and H.W100bC modified each with Fus4 or Lin3.

3.2.3.2. Aromatic grafting enhances 10E8 anti-viral potency.

A functional screening was next performed by measuring the antiviral activity of the chemically modified Fabs against two neutralization-resistant HIV-1 PsVs bearing Env JRCSF (Tier-2) or PVO.4 (Tier-3) (Figures. 3.2.5 and 3.2.6).

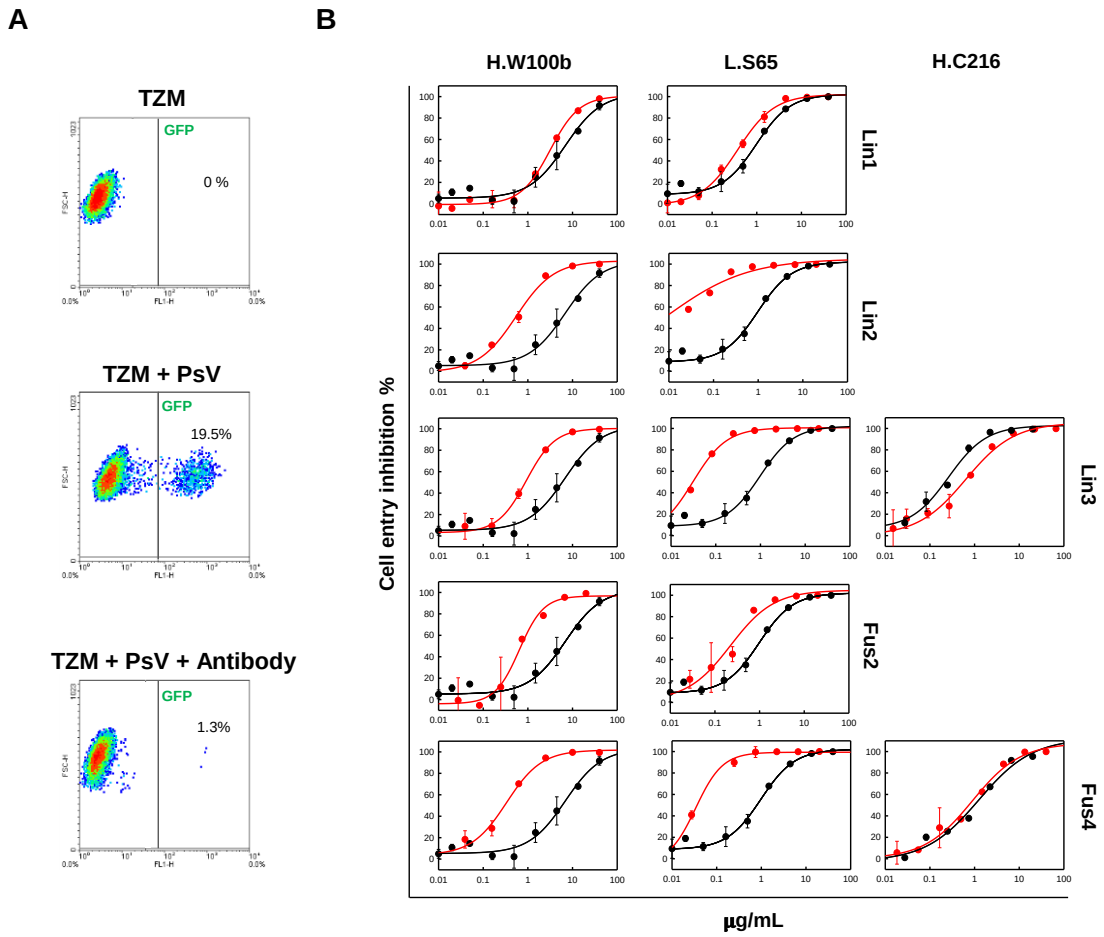

Figure 3.2.5: Effects of labelling the selected 10E8 Cys residues as seen in the cell-entry inhibition assay. (A) Cytometric determination of host cells expressing the GFP gene that was transduced by Env PsVs JRCSF, and inhibition of the process by incubation with HIV Abs. (B) Titration of Fab Cys mutants before modification (black traces and symbols) and after modification with aromatic compounds (red traces and symbols). From top to bottom, the modification introduced was Lin1, Lin2, Lin3, Fus2, and Fus4. Fab variants L.S65C and H.W100bC were modified with aromatic compounds. Fabs modified with Lin3 or with Fus4 at position H.C216 predicted to remain far from membrane (Figure 3.2.1) were used as negative controls. Experimental values correspond to mean (±SD) from two replicate wells.

Some of the compounds induced a dramatic increase in potency, as determined by the abrupt reduction of the IC_{50} values with respect to the wildtype (WT) Fab (Figure 3.2.6). The modification with the linear compounds Lin1, Lin2 and Lin3 (Figure 3.2.6A, black traces) at L.S65C significantly increased the potency of 10E8. The modifications with the longest compounds Lin2 or Lin3 were the most effective (ca. 20-30-fold more potent). In contrast, the effect of the modification at H.W100bC of the HCDR3 was more complex to analyze. The modification with the shortest and longest compounds, Lin1 and Lin3, decreased the potency of the antibody. Meanwhile, the modification with Lin2, of intermediate length, enhanced the potency of the Fab, but only to a small degree. The smaller and heterogeneous effect of the modification at the tip of HCDR3 compared to

that at the membrane-associating paratope area may reflect a greater sensitivity of the antibody when being modified in the epitope recognition loop (Rujas et al., 2016).

The potency of the antibody modified at position L.S65C was greatly influenced by the size of the fused ring (Figure 3.2.6A, red traces). Incorporation of Fus2 or the natural residue Trp (its indole side-chain has similar aromaticity characteristics to that of Fus2, but different structure) at position L.S65C had just minor potentiation effect. Remarkably, modification with the bulkier compound Fus4 resulted in a dramatic increase (roughly 80-100-fold) of the potency of the antibody (Figure 3.2.6B).

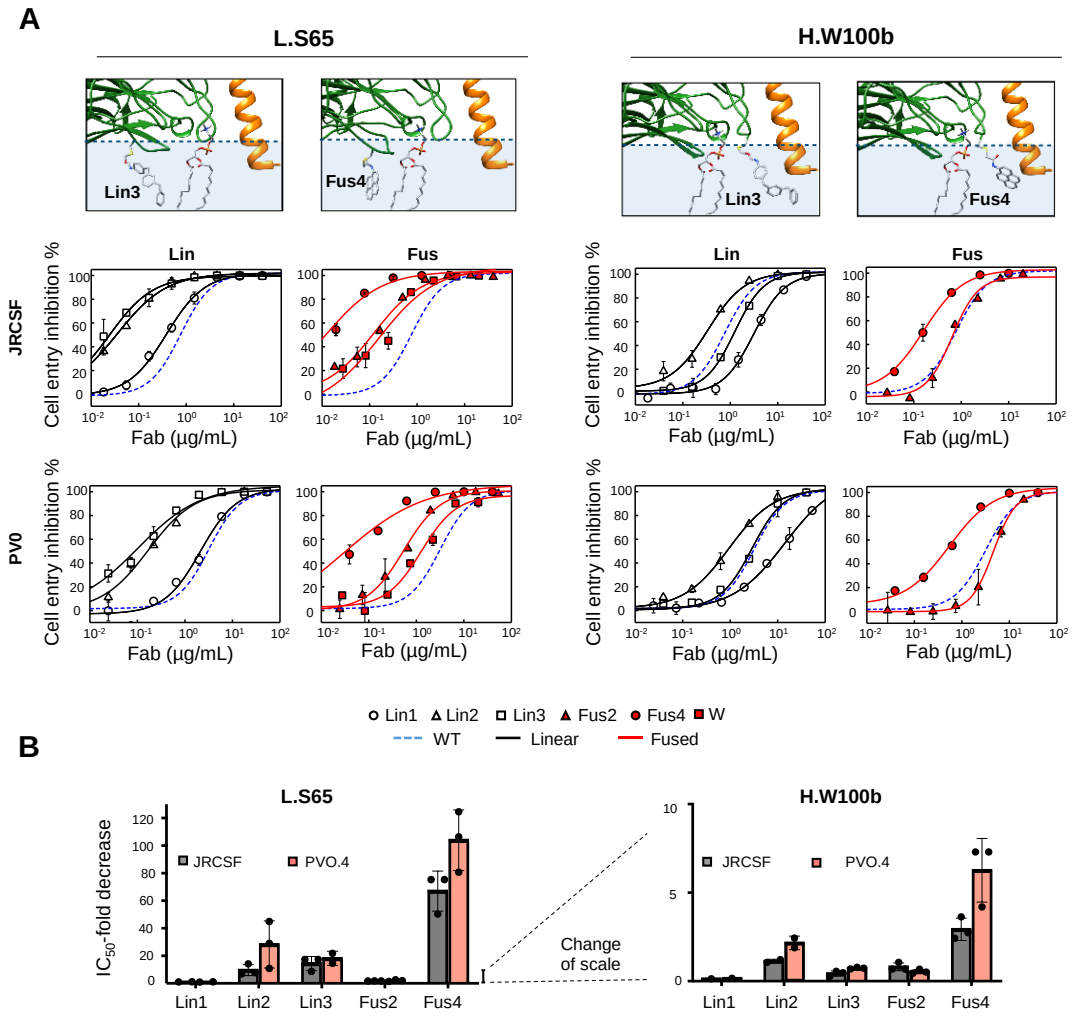

Figure 3.2.6: Effect of site-specific chemical modification with aromatics on the anti-viral activity of Fab 10E8. (A) Cell-entry inhibition assays against JRCSF (Tier-2) and PVO.4 (Tier-3) PsVs comparing unmodified WT Fab with Fabs modified with the synthetic aromatic compounds. The top panels depict the position of the modifications with Lin3 or Fus4. In the dose-response curves bellow, the dotted blue lines follow the activity of the WT Ab. Modifications of the linear and fused series are shown in black and red solid lines, respectively. Empty circles, triangles and squares correspond to Lin1, Lin2, Lin3, respectively. Data for Fus2, Fus4 and Trp are shown with red-filled circles, triangles and squares, respectively, and correspond to mean values (±SD) from two replicate wells in a representative experiment. (B) Increases in potency over the WT Ab (mean IC_{50} fold decrease ±SD), as determined from cell-entry inhibition data, are shown as a function of the position and the compound used for chemical modification. IC_{50} values were interpolated from dose-response curves obtained from three independent experiments as those shown in panel A.

These results indicate that synthetic compounds can enhance the functional performance of antibodies beyond that attainable by mutation with an equivalent natural amino acid. In the case of residue H.W100b, the increase in potency achieved by modification with Fus4 is less marked, but still significant (ca. 5-fold), specially taking into account the proximity of this residue to the key region recognizing the peptide epitope and its environment, and the fact that the substituted Trp residue is itself a large aromatic residue. The modification of the same position with Fus2 mostly recapitulated the activity

of the WT Fab, underscoring the idea that the nature of the compound is relevant to the level of Ab optimization.

These results thus identified unnatural aromatic compounds Lin2, Lin3 and Fus4 as enhancers of 10E8 anti-viral activity, especially when placed at the membrane-proximal paratope region (Figure 3.2.6B). Moreover, the chemical modification with Fus4 led to an extremely potent Ab 10E8.

3.2.3.3. Aromatic grafting stimulates Fab binding to the integral membrane antigen but does not promote spontaneous partitioning into virus-like membranes

To gain insights into the molecular basis explaining the antiviral potentiation of 10E8, the effects of chemical modification with Fus4 on the antigen-binding function of the Ab were next determined (Figure 3.2.7). Quantitative super-resolution fluorescence stimulated emission depletion (STED) microscopy was employed to establish whether grafting Fus4 affects the binding of the antibody to native Env in intact virions, as previously reported (Carravilla et al., 2019). When characterizing the interaction of bnAbs with HIV particles, STED microscopy provides mechanistic information at two levels (Carravilla et al., 2019). First, by detecting the fluorescent foci over the virion surface, one can determine the number of Env clusters recognized by the Abs. Thus, this technique has the potential to monitor off-target Ab interactions that might occur with membrane areas devoid of antigen. And second, emission intensity analyses on the virion images allow the quantitative comparison of affinities towards the integral membrane-antigen of modified vs. unmodified Abs. Due to the linear nature of STED the number of photons emitted is proportional to the number of fluorescent molecules.

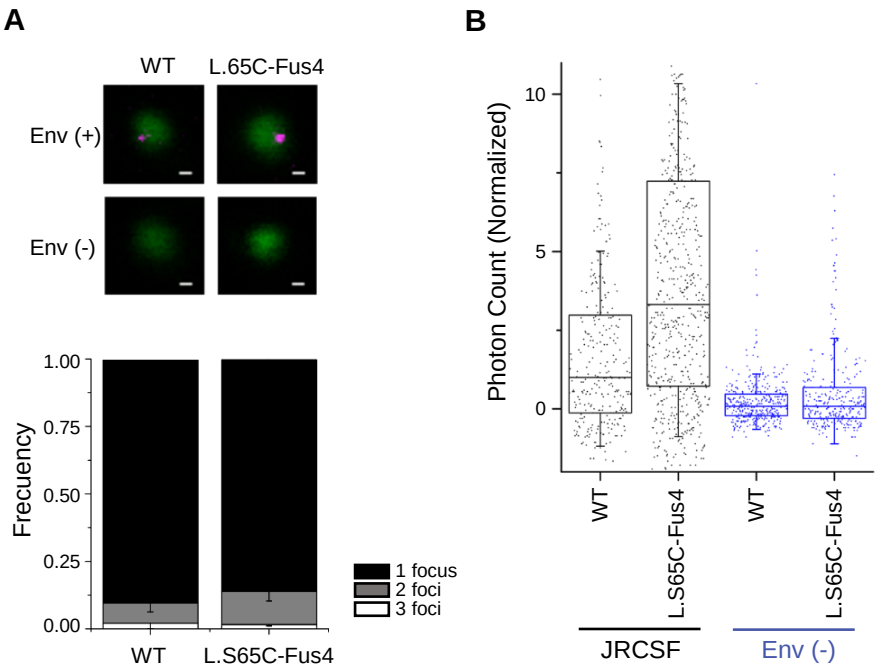

Figure 3.2.7: Binding of chemically-modified Fab to the integral membrane Env antigen. (A) Top: Representative images of the binding of antibodies by STED microscopy (KK114, STED modus, magenta) in the presence of Env JRCSF or Env(-) HIV-1 virions (Vpr.GFP, confocal modus, green). Scale bars are 100 nm. Bottom: distribution of the number of antibody foci detected per individual Env JRCSF virions. (B) Emission intensity of individual WT and 10E8 L.S65C-Fus4 Ab foci on Env JR-CSF (black) and Env(-) (blue) HIV-1 virions as determined from the STED microscopy images (from left to right, n=282, 629, 369 and 315). The intensity was normalized to that of 10E8 wt after background signal subtraction. Results are shown in box-plots (center line, median; box, IQR; whiskers SD).

Figure 3.2.7A displays micrographs of individual eGFP-labeled viral particles incubated with WT or chemically-modified L.S65C-Fus4 (top panels). Binding to Env on the viral particles was visualized using a secondary dye-labeled antibody. In this setting, the antibody/Env complexes were visualized in the super-resolved STED microscopy mode (magenta), whereas the eGFP signal was recorded in conventional confocal mode to identify the individual viral particles (green). Analysis of the punctate pattern revealed the number of antibodies/Env foci per virus, whose distribution was similar for WT and L.S65C-Fus4, demonstrating similar engagement with clustered Env (Figure 3.2.7A, upper panels). In the absence of Env (Env(-) particles), the modified antibody did not engage with the viral membrane as evidenced by the lack of antibody signal (Figure 3.2.7A, middle panels). Analysis of the signal intensity in every individual virion revealed an increased binding to Env for L.S65C-Fus4 compared to the WT antibody. In contrast, the signal on the Env(-) particles was undistinguishable from the background signal (Figure 3.2.7B).

The absence of Ab signal in particles devoid of Env reveals an important mechanistic aspect, i.e. that the chemical modification does not promote spontaneous partitioning of the Ab into the bare viral membrane. This conclusion was further supported by experiments employing VL model vesicles, which confirmed that Fus4 can spontaneously insert into membranes in the free form, but not appreciably as part of the Fab-Fus4 conjugate (Figure 3.2.8). Thus, even if Fus4 was by itself capable to partition into VL membranes experimentally, the small modification of the Fab (<1% of the total mass) does not confer the capacity for spontaneous insertion into the viral membrane to the Ab-Fus4 conjugate. Thus, Fus4 effects on 10E8 function appear to operate during or after the specific recognition of the Env epitope by the paratope elements.

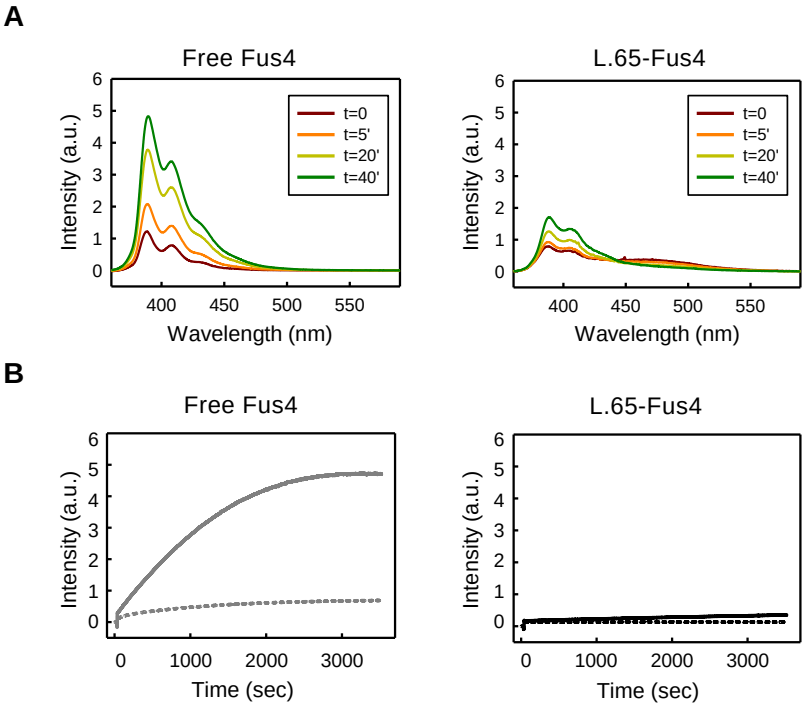

Figure 3.2.8: Interactions with membranes of Fab-conjugated Fus4. (A) Interactions with membranes of free and Fab-conjugated Fus4. Changes in fluorescence emission spectra of compound Fus4 dissolved in buffer (left) or after conjugation with Fab10E8 (right) that occur upon incubation with VL vesicles. Fus4 and lipid concentrations were 0.5 and 200 mM, respectively. (B) Fus4 fluorescence emission (385 nm) was recorded as a function of time in the presence or absence of VL vesicles (solid and slashed traces, respectively). Changes occurring to the free compound are compared to those of the Fab-Fus4 conjugate (gray and black traces, respectively). Conditions otherwise as in the previous panel.

3.2.3.4. Mechanistic insights and specificity of the potentiation effect

To gain insights into the specificity and mechanism underlying the increase in Ab potency after site-selective chemical modification, the effects of the most potent compound Fus4 were next explored in a variety of experimental conditions. To rule out potential site-dependent interactions not mediated by membrane, the effects of Fus4 placed at different positions on the 10E8 surface that accommodates the viral membrane were first determined (Figure 3.2.9A,B). The selected positions L.S30, L.N52, and L.S65 were all distant from the MPER epitope (alpha-carbons at 14, 18 and 22 Å from the epitope, respectively). As a control for no-interaction with the membrane, the effect of Fus4 was also tested linked to the C-terminal residue H.C216, which is predicted to remain exposed to the aqueous solution upon engagement with the MPER epitope. These positions were modified with the Fus4 one by one and the activities of the resulting chemically-modified variants compared in cell-entry inhibition assays (Figure 3.2.9B). As expected from the absence of membrane insertion, modification with Fus4 at residue H.C216 had no effect on the activity of the Ab. For the rest of the positions, L.S30, L.N52 and L.S65, the observed functional improvements were comparable to each other, suggesting that a particular location of the chemical modification at the membrane-accommodating area is not important to improve the anti-viral function of 10E8.

Chemical conjugation with Fus4 was also efficient in the context of a paratope that has been altered by classical site-directed mutagenesis to reduce the activity of 10E8 (Figure 3.2.9C). The mutation H.W100bG removes the side-chain of the Trp residue at the tip of the HCDR3, producing a substantial reduction of the antiviral activity of 10E8 (Carravilla et al., 2019; Rujas et al., 2016). Thus, cell-entry assays were performed to establish whether adding Fus4 at a distant site through chemical conjugation could rescue functionally the mutation at the tip of the HCDR3 loop. As shown in panel 38D, Fus4 linked at L.S65C position also increased the activity of the deficient H.W100bG mutant.

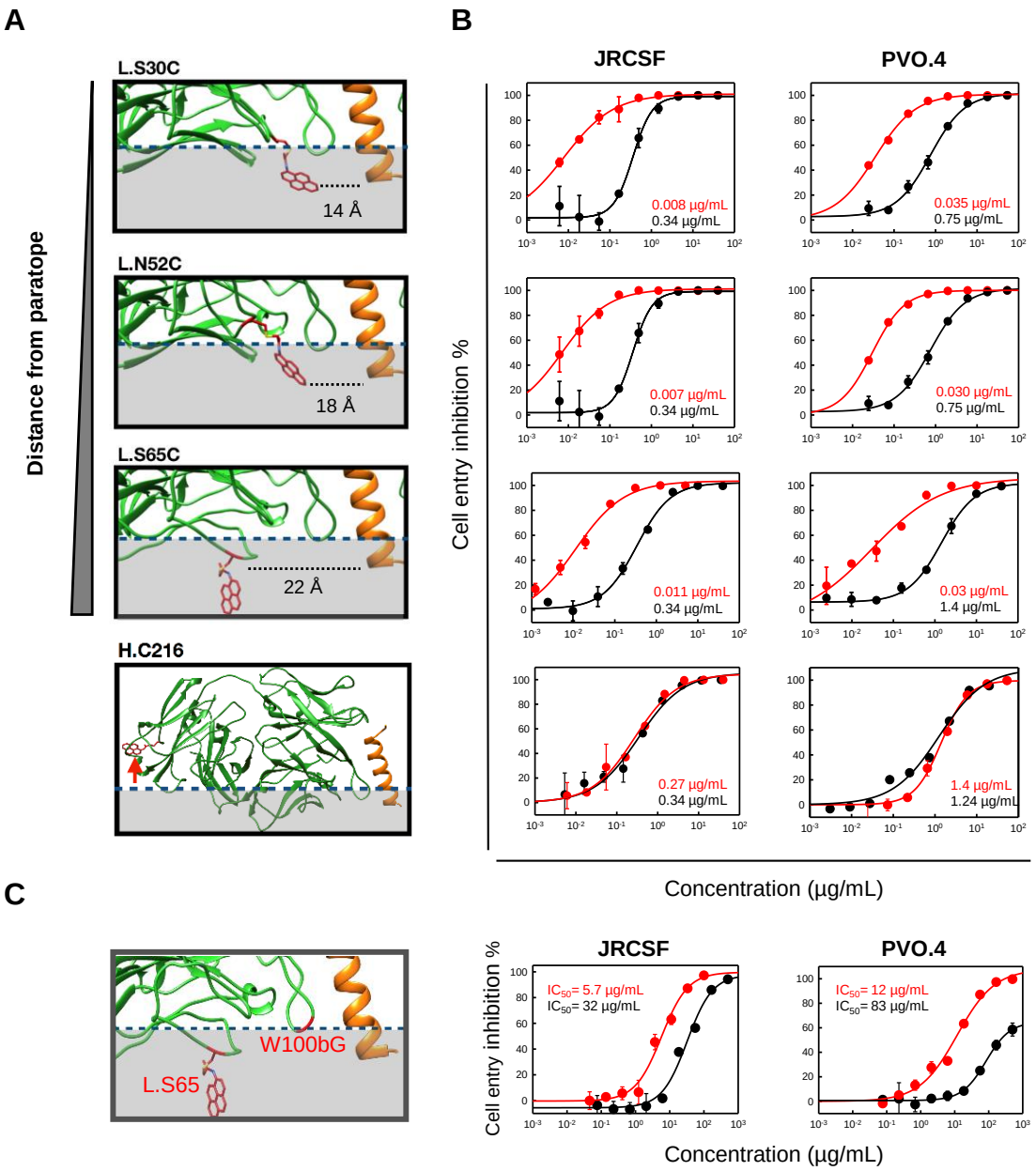

Figure 3.2.9: Effects of Fus4 conjugated at different membrane-proximal sites. (A) Lateral views displaying the positions of the residues chemically-modified with Fus4 (residues depicted in red) and the bound epitope-peptide (helix depicted in orange). Distances to the Cα-s of modified Fab residues were calculated from that of Lys683 at the bound helical epitope. The bottom panel displays the position of H.216C used as negative control for Fab-membrane interaction. (B) Comparison of the antiviral activities of 10E8 Fabs modified with Fus4 at the different membrane-proximal positions indicated in the previous panels. The left and right panels correspond to the entry inhibition assay using JRCSF and PVO.4 strains, respectively. Solid black and red lines (and symbols) correspond to unmodified and chemically-modified antibody, respectively. Otherwise, same conditions as in Figure 3.2.6A. (C) Effects of L.S65C-Fus4 modification on the Ab carrying the deleterious H.W100G mutation. Symbols and lines are defined as in panel (B).

The effect of attaching Fus4 to Abs already manipulated to increase their potency was also investigated (Figure 3.2.10). The effect of the chemical modification is not additive, since the incorporation of a second molecule of Fus4 within the membrane-proximal Ab

region did not result in greater neutralization potency (Figures 3.2.10A,B). However, the attachment of Fus4 to the membrane accommodating surface of an electrostatically-optimized antibody (3R mutant, described in chapter 3.1 (Rujas et al., 2018)) resulted in a modest potentiation of less extent than that observed after modification of the WT antibody (Figure 3.2.10C-E). Notably, the combination of the 3R triple mutant with the Fus4-based chemical modification, rescued completely the loss of activity of the poorly-active variant bearing the H.W100bG mutation at the epitope-binding site.

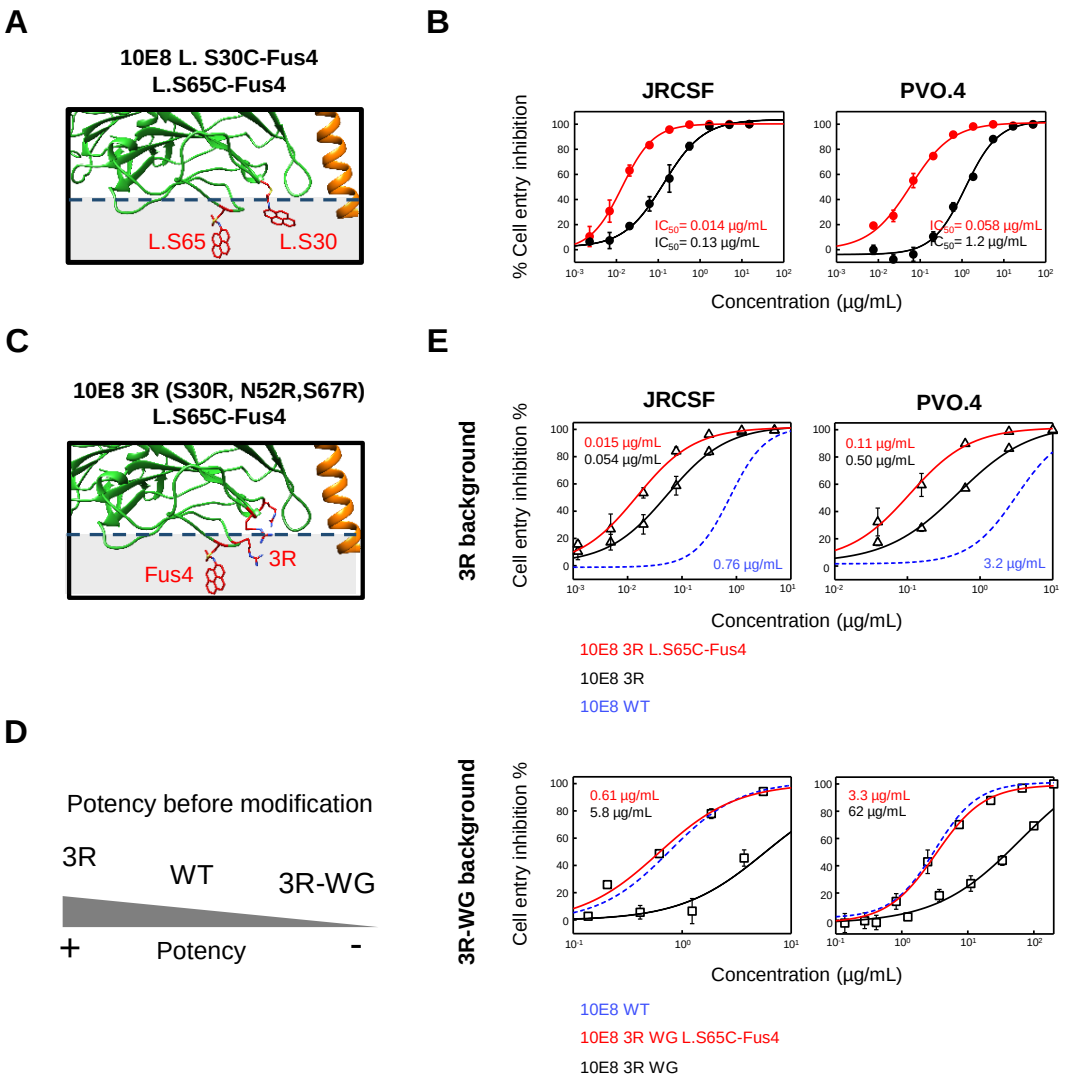

Figure 3.2.10. Effect of chemical modification on previously optimized Abs. (A) Depiction of the double-modified Ab. (B) The left and right panels correspond to the entry inhibition assay using JRCSF and PVO.4 strains, respectively. Solid black and red lines (and symbols) correspond to WT and Ab modified at two sites, respectively. (C) Relative position of the modification introduced in the membrane-proximal area of the paratope with respect to the triple-mutation 3R. (D) Scheme describing the relative potency of the Abs prior to modification. (E) Cell entry inhibition of Abs of two different background modified with Fus4. Red and black lines correspond to modified and unmodified Ab. Blue dotted lines correspond to unmodified Ab. IC_{50} values for each plot as indicated in the panels. Otherwise, conditions as in Figure 3.2.9.

Together, these observations highlight a significant flexibility to introduce chemical modifications at various positions of the membrane-proximal region of 10E8, but also the difficulty to attain additive effects by combining modifications at multiple sites. Notably, they also suggest that chemical modification can functionally complement a deleterious mutation introduced at the distant epitope-binding site.

3.2.3.5. Successful modification of a second antibody

Finally, to prove the effectiveness of functional optimization with Fus4 in the context of a paratope arranged differently, the effects induced by grafting this compound in an Ab arising from a different lineage were examined. Although less potent, the HIV antibody 4E10 also embodies a surface that accommodates the viral membrane in Fab-epitope complexes, which in this case is composed by heavy-chain residues (Irimia et al., 2016; Rujas, Caaveiro, et al., 2017) (Figure 3.2.11A). A chemically-modified version of 4E10 was prepared following an analogous approach to that of antibody 10E8, by mutating residue H.S28 to Cys (Figure 3.2.11B).

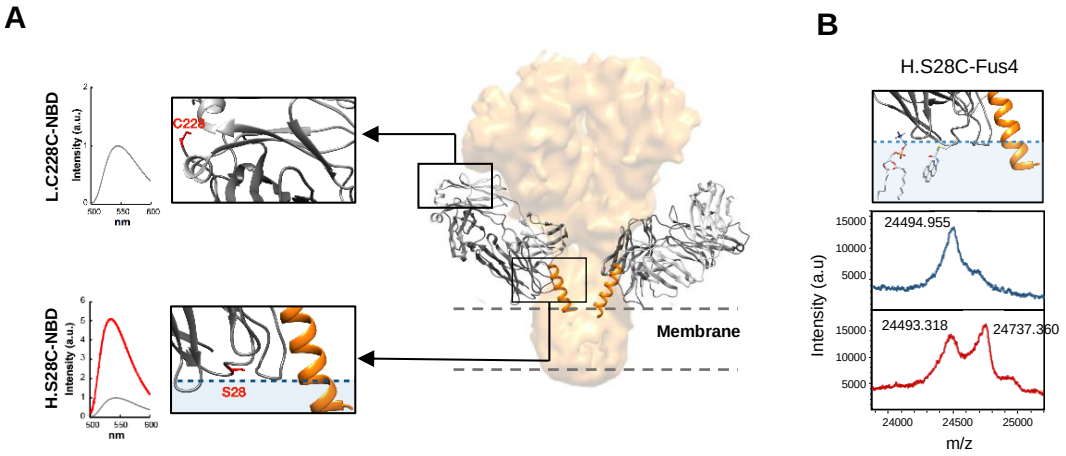

Figure 3.2.11: Fus4 modification of the membrane-proximal area in a second antibody. (A) Structural model of Fab 4E10 interacting with the Env complex. Fab was chemically modified at positions H.S28 or H.C228 which are predicted to interact with the membrane or remain solvent-exposed, respectively, upon engagement with MPER epitope. The interaction between Fab labeled with NBD and proteoliposomes was monitored by fluorescence. (B) MALDI-TOF m/z plot before and after the modification, respectively.

The 4E10 H.S28C-Fus4 conjugate was proven to retain the functional binding to MPER epitope peptide in ELISA (Figure 3.2.12A) and not to lose thermal stability (Figures 3.2.12B,C). Despite the different docking angle of 4E10 to MPER and the distinct

residues accommodating to the membrane surface with respect to 10E8, modification with Fus4 also enhanced the antiviral potency of 4E10 largely (Figure 3.2.12D).

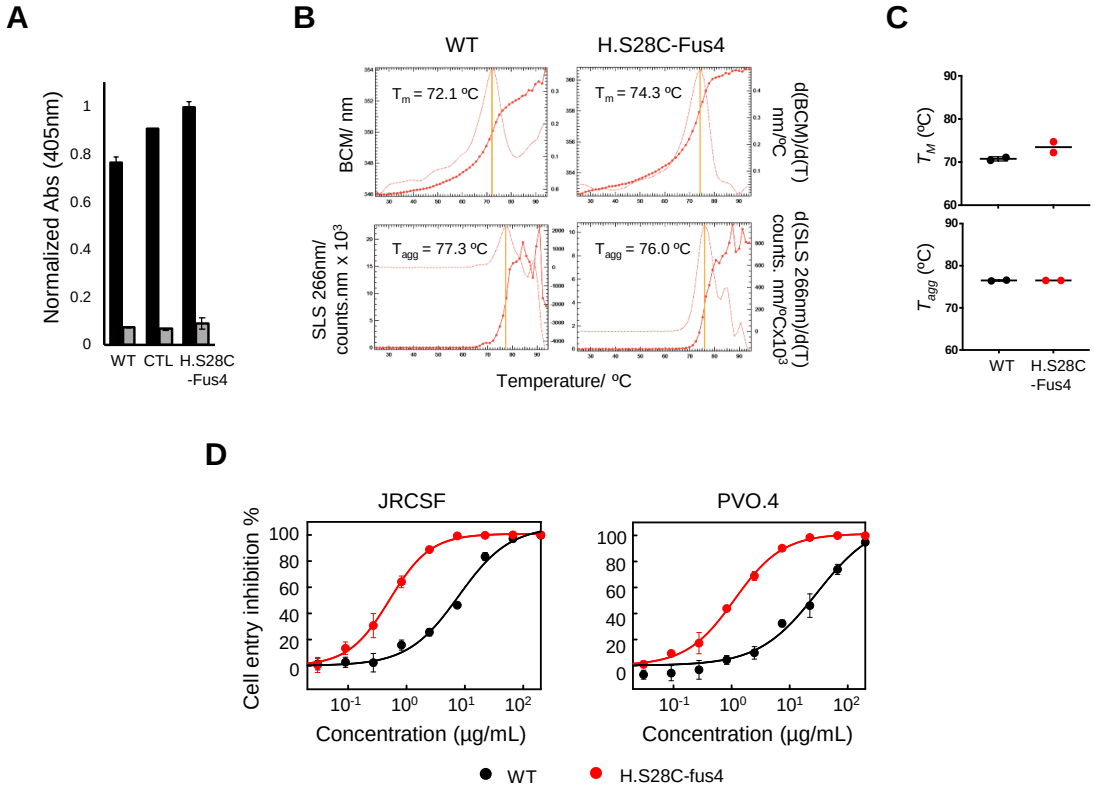

Figure 3.2.12: Effects of Fus4 modification of the membrane-proximal area in 4E10 Ab. (A) Binding to the epitope MPER peptide by ELISA. Black and gray bars correspond to native MPER and an inactive variant (double Ala mutant), respectively. (B) Thermostability. BCM (top panels) and SLS (bottom panels). (C) Thermal stability data (duplicates) employing the unfolding temperature (Tm, top panel) and aggregation temperature (Tagg, bottom panel) inferred from the previous experiments. (D) Anti-viral activities of the Fab 4E10. Red traces and symbols correspond to the chemically modified H.S28C mutant.

The effects of site-selective modification with Fus4 were next explored with a 4E10 variant totally inactivated through mutagenesis (Figure 3.2.13). The substitution of the hydrophobic HCDR3 loop apex sequence W_{H100}-G_{H100A}-W_{H100B}-L_{H100C} with a Ser-Gly dipeptide (Figure 3.2.13A) was described to generate an inactive form of the Ab 4E10, designated as 4E10 ΔLoop (Rujas et al., 2015). This variant does not bind to native Env (Carravilla et al., 2019) (see also Figure 3.2.14, below), and therefore lacks anti-viral activity at concentrations ≤ 200 µg/mL. Chemical modification with Fus4 was also attained after introducing Cys at position H.S28 (Figure 3.2.13B), and proven not to affect the thermal stability of the ΔLoop Fab (Figure 3.2.13C). Strikingly, the functional recovery of the ΔLoop variant occurred when Fus4 was attached at the Fab surface that

accommodates the viral membrane (Figure 3.2.13D). Thus, conjugation to Fus4 yielded a Fab ΔLoop with an antiviral activity in the range of that of the 4E10 WT.

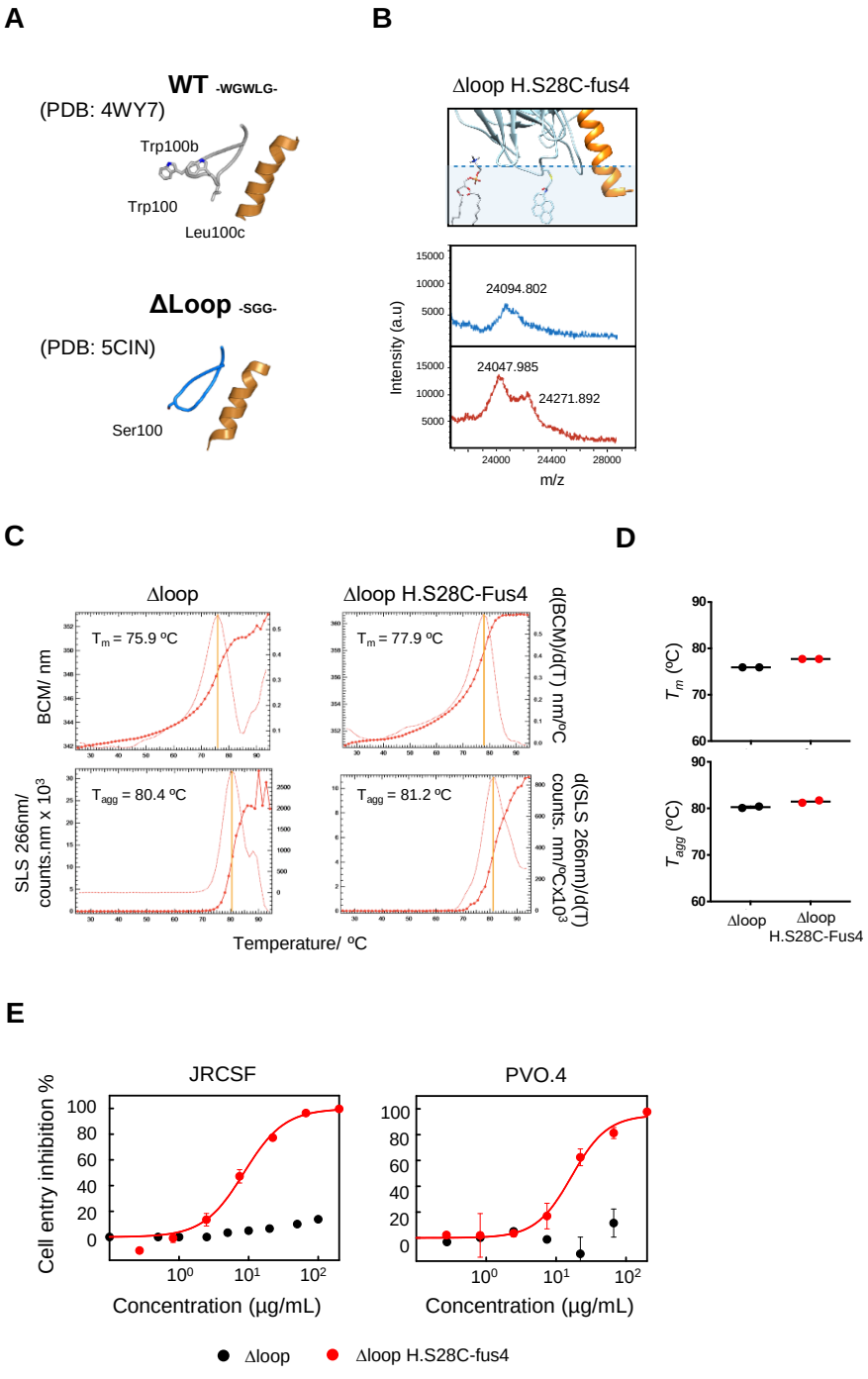

Figure 3.2.13: Effects of Fus4 modification of the membrane-proximal area in an inactivated 4E10 variant. (A) Schematics of Fab 4E10 and its H3-CDR apex-deleted variant, called Δloop. (B) MALDI-TOF m/z plot before and after the chemical modification at position H.S28, respectively. (C) Thermostability. BCM (top panels) and SLS (bottom panels). (D) Thermal stability data (duplicates) employing the unfolding temperature (Tm, top panel) and aggregation temperature (Tagg, bottom panel) inferred from the previous experiments. (E) Anti-viral activities of the Fab 4E10 Δloop. Red traces and symbols correspond to the chemically modified H.S28C mutant. Otherwise, conditions as in Figure 3.2.9.

Next, it was investigated if antibody optimization with Fus4 was also correlated with an increased binding of 4E10 to native Env by using STED microscopy (Figure 3.2.14). Similarly to the results presented in Figure 3.2.7A for the modification of 10E8, STED microscopy data for 4E10 displayed individual puncta of antibody-Env complexes (Figure 3.2.14A), whose intensity analysis confirmed that the functional improvement induced by site-specific modification with Fus4 correlated with an increase in binding to native Env on virions (Figure 3.2.14B). Furthermore, the functionally restored, chemically modified ΔLoop variant, showed levels of Env binding comparable to those measured for the WT 4E10 (Figures 3.2.14A,B). Here again, signal on the Env (-) particles was only background like. Overall, these results suggest that chemical modification constitutes a procedure, not only to improve, but also to confer functional capacities to anti-MPER bnAbs.

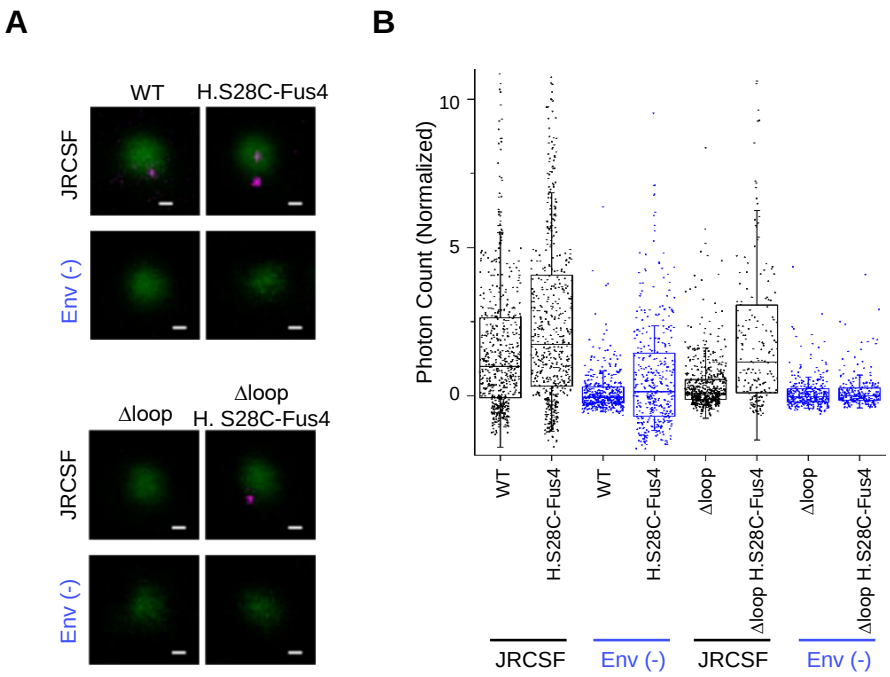

Figure 3.2.14: Binding of chemically-modified 4E10 and 4E10 Δloop to the integral membrane Env antigen. (A) Representative images of the binding of antibodies by STED microscopy (KK114, STED modus, magenta) in the presence of Env JRCSF or Env(-) HIV-1 virions (Vpr.GFP, confocal modus, green). Scale bars are 100 nm. (B) Emission intensity of individual 4E10 WT and Δloop (and H.S28C-Fus4 of each fab) Ab foci on Env JR-CSF (black) and Env(-) (blue) HIV-1 virions as determined from the STED microscopy images. The intensity was normalized to that of 4E10 WT after background signal subtraction. Results are shown in box-plots (center line, median; box, IQR; whiskers SD).

3.2.4. Discussion

Approaches to Ab optimization, including those applied to HIV bnAbs, are generally based on (and limited by) modifications with function-enhancing natural amino acid residues. In this work, we sought to optimize the anti-viral function of a relevant HIV-1 bnAb with site-specific chemical modification using rationally designed synthetic molecules (Krall et al., 2016), thus unconstrained by the availability of proteinogenic amino acid residues. The selection and design of those molecules was carried out on the basis of recent structure-function studies showing the stabilizing role of interactions at the membrane interface for the formation of the antibody-antigen complex (Irimia et al., 2017; Y. do Kwon et al., 2018; Jeong Hyun Lee et al., 2016; Rujas et al., 2016, 2018), and under the assumption that any gain in antibody function produced by strengthening non-covalent interactions with the lipid bilayer cannot be counteracted by viral scape mechanisms (Melikyan, 2010; st. Vincent et al., 2010). Inspired by the White and Wimley model of interaction at membrane interfaces (White et al., 2001; White & Wimley, 1999; Wimley & White, 1996), aromatic compounds were employed to enhance the membrane interactions hoping to increase the antiviral potency of the antibody. Indeed, it was successfully showed that chemical modification with two different classes of synthetic compounds, at rationally designated sites, dramatically increased the potency of the bnAb 10E8, an HIV Ab with therapeutic potential.

The modification approaches described herein involve the addition, at single positions, of synthetic molecules ≤ 300 Da. The extent of the resulting modification is very small in comparison to the size of the antibody, and yet their effect on function can be remarkable. In agreement with the tenet of the White and Wimley model, the modified antibody bearing the compound with the greatest tendency to interact with the membrane interface resulted in the greatest antiviral potency. The application of this procedure to optimize a second antibody was demonstrated with anti-HIV-1 bnAb 4E10, which was modified by analogous strategy and principles. Notably, the efficacy of this approach is such that it did not only improve the potency of the WT antibody by chemical modification with Fus4, but also rescued a completely inactive variant (termed ΔLoop) to WT-like neutralization levels. Together, these observations suggest new approaches for improving function of moderately potent 10E8-like Abs.

Chapter 3.3

RESULTS: ANTIBODY OPTIMIZATION BY AROMATIC GRAFTING (II)

3.3. ANTIBODY OPTIMIZATION BY AROMATIC GRAFTING II:

EFFECTS OF SITE-SELECTIVE CHEMICAL MODIFICATION ON THE BIOLOGICAL PROPERTIES OF THE HIV ANTIBODY 10E8

Abstract

Engineered variants of broadly-neutralizing antibodies (bnAbs) have shown efficacy in passive immunotherapy of HIV-1 infection. The preceding chapter 3.2 introduced 'aromatic grafting' as a possible pathway for the optimization of MPER-targeting bnAbs. In this chapter, the Fab 10E8 was modified at its membrane-proximal surface with Lin3 and Fus4, the most efficient compounds described therein. The biological properties of the resulting conjugates LC.S65C-Lin3 and LC.S65C-Fus4, including their autoreactivity and pharmacokinetics (PK) profiles, were compared. Even though previous screening efforts based on cell-entry inhibition assays demonstrated that Fus4 was slightly superior at enhancing 10E8 antiviral activity *in vitro*, both modified Fabs displayed comparable staining profiles in Hep-2 cell-based immunofluorescence assays, and none of them bound to autoantigens in ELISA. Chemical modification with Lin3 or Fus4 also enhanced the antiviral activity of the IgG version of the antibody 10E8. However, after intravenous infusion in mice, the decay in the serum concentration of the IgG chemically-modified with Fus4 was faster than that of the IgG-Lin3 conjugate, and both chemical conjugates were less stable than the unmodified variant. Importantly, none of the chemically-modified antibodies was cytotoxic in culture, or induced adverse effects in mice. Moreover, the IgG-Lin3 conjugate induced lower levels of anti-drug antibodies than the IgG-Fus4 conjugate. The results in this chapter underscore the requirement of additional cycles of protein and/or chemical engineering to sustain the *in vivo* application of the 'aromatic grafting' procedure.

3.3.1. Introduction

In the previous chapter a novel strategy was proposed to improve the function of the HIV Ab 10E8: grafting of synthetic aromatic compounds onto the surface that accommodates the viral membrane upon formation of the 10E8-Env complex (Rantalainen et al., 2020; Rujas et al., 2016). Conjugation with the compounds did not appear to promote the spontaneous association of the Fab 10E8 with membranes, and thus it was inferred that the observed improvements in binding and antiviral activity, was consequence of stronger interactions with membranes that probably occurred concomitantly, or shortly after, the specific recognition the native antigen ensued (Carravilla et al., 2019).

Nonetheless, the risk that the chemically-modified antibodies will bind non-specifically to any entity with a membrane in complex biological matrices still persists. These potential off-target effects might increase the required effective concentrations and enhance the toxicity of Ab-compound conjugates *in vivo*. Therefore, in this chapter several studies have been conducted to address the polyspecific autoreactivity, toxicity and *in vivo* clearance of 10E8 conjugated to Fus4 or Lin3.

The assays demonstrated that the 10E8 variants improved by chemical conjugation with the synthetic compounds were reactive with HEp-2 cells, yet more efficient than the parental version in blocking HIV infection *in vitro*. Moreover, they were not cytotoxic for the target cells and did not provoke adverse effects when administered intravenously to mice. Overall, these data underscore the necessity of engineering both, the chemical compounds and the Fabs, to achieve better efficacy *in vivo*, while reducing off-target effects.

3.3.2. Materials and methods

3.3.2.1. Materials

Goat anti-mouse-AP antibody was purchased from Sigma (St. Louis, MO). The plasmid encoding the 10E8v4 was kindly provided by Jean-Philippe Julien (The Hospital for the Sick Children, Toronto). The rest of the plasmids, lipids, peptides, probes, antibodies and chemical compounds used in this chapter were obtained as indicated in 3.1.2.1 and 3.2.2.1.

3.3.2.2. Animal studies

All *in vivo* procedures were carried out in compliance with European Directive 2010/63/EU, under The Art of Discovery (TAD) reviewed IACUC protocols and under the

supervision of a site attending veterinarian. BALB/c female mice were divided into five groups containing four mice per group, and the mice in each group were administered intravenously (i.v.) 100 µg of 10E8, 10E8 L.65-fus4, 10E8v4, 10E8v4 L.65-Lin3 or 10E8v4 L.65-Fus4 antibodies in a volume of administration of 300 µL of PBS. No adverse effects were observed in the animals studied.

3.3.2.3. Assessment of mAb clearance in mice

Blood was drawn from all animals at 0, 2, 5, 8, 15, 22 and 29 days after antibody administration, and manipulated as described in 2.8.1. Antibody levels were determined in each sample by ELISA, as previously described in 2.2.1. Briefly, plates were coated with 1.37 µM/well of MPER peptide o-n, washed, blocked with BSA and incubated with mouse serum for 2 h at RT. Purified antibodies in PBS for the standard curves were also added to the wells. An anti-human-AP was used to detect bound antibodies.

To estimate the amount of 10E8 present in the sera of each mice, an initial binding analysis was performed using the MPER peptide and a peptide with alanine mutations of the two underlined critical residues, NFxAA. Dilutions to use in the ELISAs (from 1:20 to 1:200) were determined based on detection range of the technique (Fig 43A). Antibody concentrations in sera were calculated using the equations obtained from the standard curves (an example is shown in Fig 43B).

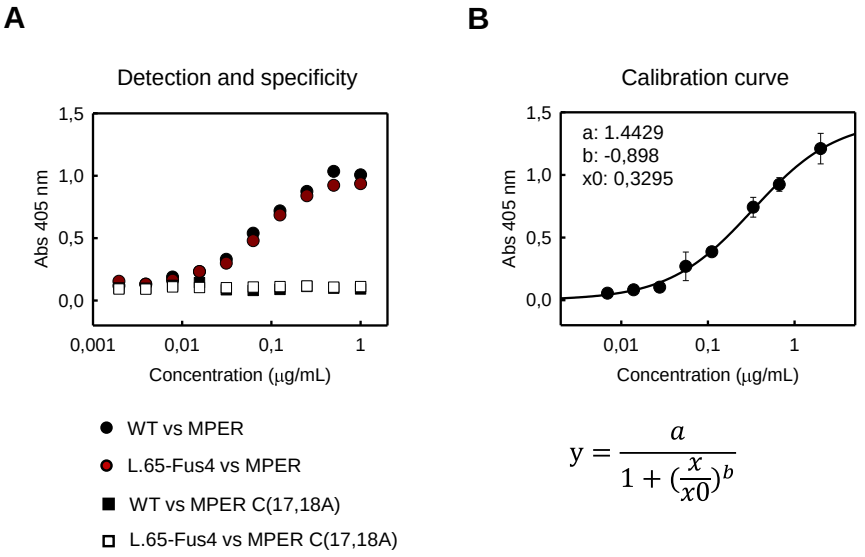

Figure 3.3.1. Determination of antibody concentration in mice sera. (A) MPER peptide and an alanine mutant were used to specifically detect 10E8 and modified antibodies mixed with pre-immune mice serum. (B) An example of one of the standard curves and the equation to calculate antibody amount in each sample. Values were fitted to a sigmoidal equation.

3.3.2.4. Screening for anti-drug antibodies (ADA)

ELISAs were also performed to determine the presence of ADA in mice sera. Besides, a booster dose was administered at week 4, and blood was also collected and analyzed 7 and 14 days after second Ab infusion. Briefly, 10E8v4, 10E8v4 L.65-Lin3 or 10E8v4 L.65-Fus4 antibodies were plated o-n at 0.5 µg/well. ELISA wells were blocked with BSA, and mouse serum was incubated for 1 h at RT. ADA-s were detected by an anti-mouse-AP.

3.3.2.5. Production and site-specific chemical modification of Abs

Experimental procedures described in 3.1.2.2 were followed for the mutation, expression, purification and chemical conjugation of Fabs. For the expression of 10E8 IgGs, HEK293-F cells were transfected with FP, and after 5-7 days supernatants were collected and antibodies were purified using affinity chromatography and SEC, as described in 2.1.2. Mutants bearing Cys residues at defined positions were subsequently modified with sulfhydryl-specific iodoacetamide derivatives of the aromatic compounds fus-4 and lin-3. Conjugation was monitored by matrix-assisted laser desorption/ionization (MALDI) mass spectrometry as described before (3.2.2.4).

3.3.2.6. HEp-2 cell immunofluorescence assay.

Fabs were tested for the ability to stain HIV-1 negative human epithelial HEp-2 (VIRGO ANA/HEp-2) cells on glass slides by indirect immunofluorescence microscopy, as described in 2.7.3. 50 µg/mL of each antibody were used, and fluorescein isothiocyanate (FITC)-conjugated goat anti-human Fab (Jackson) was used as the secondary probe. Slides were observed on a Leica TCS SP5 II confocal microscope (Leica Microsystems GmbH, Wetzlar, Germany).

3.3.2.7. Lipid binding assays

VL vesicles were obtained as indicated in 3.1.2.4, to test lipid binding by vesicle flotation assays. Fab binding to POPC, VL-2 or VL-3 naked liposomes was assessed following instructions in 3.1.2.5.

3.3.2.8. ELISA to assess polyreactivity

Antibody polyreactivity was also assessed by ELISA, following the steps explained in previous chapters. In this particular case,the WT antibody and the modified antibodies

were tested against the following plated antigens: 10 nM of Chol, DOPS, POPC, DOPE (in methanol) were plated and left to evaporate overnight at 4°C. In addition, 500 ng/mL of dsDNA and BSA were also diluted in PBS and plated o-n. Binding to the antigens after 1 hour of antibody-incubation was detected with an anti-human-AP secondary Ab.

3.3.2.9. Citotoxicity assay

The CytoTox 96® Non-Radioactive Cytotoxicity Assay (Promega) was used to test the cytotoxicity of conjugated antibodies, as described in 2.7.2. Briefly, serial dilutions of the fabs were incubated with 11.000 TZM-bl cells/well, and after 4 hour incubation, released LDH in culture supernatants was measured with a 30-minute coupled enzymatic assay. Absorbance data were collected at 490nm using a standard 96-well plate reader. The cytolitic Fragaceatoxin C (FraC) was used as positive control.

3.3.2.10. Virus production and cell-entry assays

HIV-1 PsVs were produced by transfection of human kidney HEK293T using the calcium phosphate method, as previously described in 2.7.1.1. HIV entry in host cells was determined after incubation of PsVs with TZM-bl cells following previously described 2.7.1.2. protocol. Infection levels after 72 hours were inferred from the reduction in the number of GFP-positive cells as determined by flow cytometry.

3.3.3. Results

3.3.3.1. Polyreactivity of 10E8 Fabs conjugated to Lin3 or Fus4

To test the effects of chemical modification on 10E8 polyspecificity, the WT Fab was compared with the chemical conjugates in HEp-2 assays and ELISA (Figure 3.3.2). Indirect immunofluorescence assays based on HEp-2 cells is becoming the standard procedure in the field to estimate the polyspecific autoreactivity of HIV therapeutic antibodies (Haynes et al., 2005). Both, natural and engineered variants of the bnAb 10E8 have been analyzed by this means, and estimated to be not reactive or poorly reactive with HEp-2 cells (J. Huang et al., 2012; Y. do Kwon et al., 2016; Rujas et al., 2018). Conjugation with either Fus4 or Lin3 appeared to enhance HEp-2 cell staining, consistent with an increase in the nonspecific binding of the antibody 10E8 (Figure 3.3.2A).

The HEp-2 cells provided by the manufacturer, are permeabilized and fixed onto slides (Dellavance & Andrade, 2019). The immunofluorescence assay is primarily designed for the clinical detection of antinuclear antibodies (ANA test), such as those found in the serum of subjects suffering autoimmune diseases. Accordingly, up to 29 different patterns have been observed, which include staining of nuclear and cytoplasmic

structures, and linked to particular diseases (Dellavance & Andrade, 2019). Interestingly, none of the described patterns seemed to fit neatly with the increase in cell fluorescence labeling observed for samples incubated with the chemically modified antibodies. Compared to the positive control sample provided by the manufacturer, or the 4E10 3R mutant (defined in Chapter 3.1 above), which labeled cell nuclei, the Lin3 and Fus4 conjugates did not clearly bind to any defined subcellular domain, but instead increased the fluorescence signal nonspecifically.

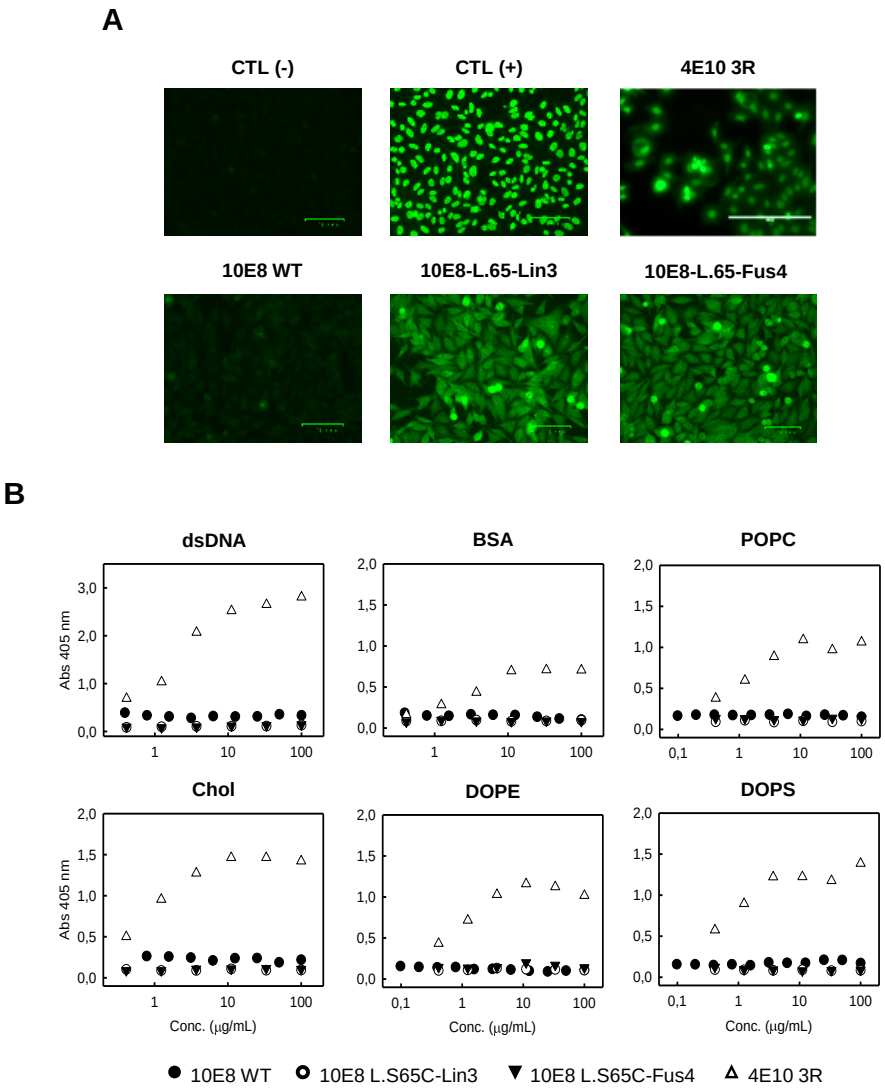

Figure 3.3.2. Autoreactivity of chemically-modified Fab 10E8. (A) Immunofluorescence assay based on Hep-2 cells. Fabs were tested at 50 µg/mL, together with the positive and negative controls provided by the diagnostic kit. (B) ELISA binding against various antigens. dsDNA; BSA, POPC, Chol, DOPE, and DOPS. In both panels, the Fab 4E10-3R was used as a positive control for a polyreactive anti-MPER antibody (see previous chapter 3.1).

Polyreactivity of the Fab 10E8 and its chemical conjugates was subsequently compared with that of 4E10-3R in standard ELISA against double-strand DNA, BSA and various lipids (Fig 3.3.2B). Significant binding to those antigens was only observed for the 4E10-3R mutant.

3.3.3.2. Interaction with lipid vesicles of 10E8 Fabs conjugated to Lin3 or Fus4

To ascertain the absence of reactivity with lipids in a system that mimicked more closely the physiological conditions in living tissues and cells, lipid bilayers were reproduced in vesicles, and binding of Fab-compound conjugates to these membrane model systems assayed in co-flotation experiments (see for a description of the assay Figure 17 in chapter 2.4.3. and Figure 3.1.3 in the previous chapter 3.1).

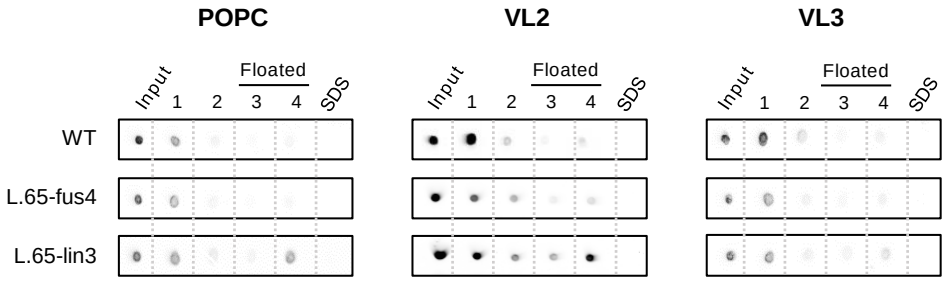

Figure 3.3.3. Membrane interactions of chemically-modified Fab 10E8 in a model system. Partitioning of Fab 10E8 and its derivatives into LUVs of different compositions was evaluated in flotation experiments. The presence of Fab in the different fractions was probed by Dot-blot. Fabs associated to vesicles were found in the third and fourth fractions (i.e., floated fractions). An additional fraction, employing SDS, was collected to recover the material attached to the tube surface. POPC, VL2 (DOPC:DOPE:DOPS:SM:Chol (14:16:7:16:47)) and VL3 (POPC:POPE:POPS:SM:Chol (14:16:7:16:47)) LUV compositions were chosen.

As shown in the data displayed in Figure 3.3.3, 10E8-Lin3 appeared to co-float with vesicles based on the single phospholipid POPC, and with VL2 vesicles, based on a virus-like mixture containing phospholipids with unsaturated acyl chains (Huarte et al., 2016). Interestingly, none of the Fabs co-floated efficiently with VL3 vesicles made of a lipid mixture that closely simulates the level of lipid packing existing in the HIV envelope (Huarte et al., 2016).

3.3.3.3. Cytotoxicity of 10E8 Fabs conjugated to Lin3 or Fus4

Next, the possible cytotoxic activities of the chemically-modified Fab versions were explored under the conditions used to measure antiviral activity (cell-entry inhibition assays). Figure 3.3.4A compares the antiviral activity of the chemically-modified Fabs

against HIV-1 pseudoviruses (PsVs) bearing Env JRCSF (Tier-2) or Env PVO.4 (Tier-3), which display decreasing sensitivity to 10E8. Consistent with the results in the previous chapter, conjugation with Fus4 or Lin3 induced enhancements of 10E8 potency, reflected by the reduction of the IC50 values with respect to the wild-type (WT) Fab. However, the differences in potency observed for the chemically-modified Fabs still reflected the resistance to neutralization of the particular Env pseudotype, i.e., similarly to the WT, both, 10E8-Fus4 and 10E8-Lin3 neutralized less potently PVO.4 than JRCSF PsVs. This observation appears to rule out a direct cytotoxic activity of the Fabs against the host cells, which would make them incompetent for PsV entry at a given dose regardless the pseudotype used in the assay.

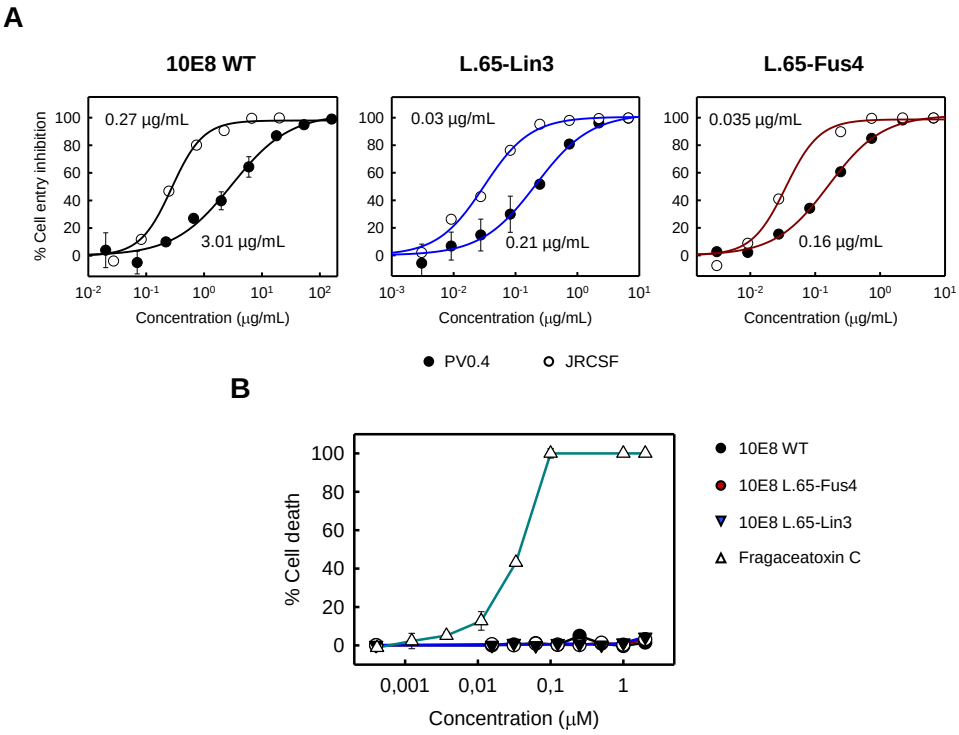

Figure 3.3.4. Antiviral activity in the absence of cytotoxic effects against the target cells. (A) Cell-entry inhibition assays to establish the decrease in antiviral activity of the Fabs against Tier-3 PVO4, in comparison with that against Tier-2 JRCSF pseudoviruses. The decrease in potency (IC_{50} fold increase) was of the same range in the parental and chemically-modified Fabs (insets). (B) Absence of toxicity induced by chemically-modified Fab on TZM-bl host cells. The CytoTox 96, Non-Radioactive Cytotoxicity Assay (Promega) was carried out following the instructions of the manufacturer. The cytolytic toxin Fragaceatoxin C was used as positive control.

To further rule out direct cytolytic effects against the host cell line TZM-bl, standard cytotoxicity assays were carried out using the Fab-compound conjugates (Figure 3.3.4B). In contrast to the marked effect induced by the cytolytic toxin Fragaceatoxin C,

used as a positive control, the 10E8 Fabs did not exert any appreciable effect, not even when incubated with the target cells at doses >1 µM (ca. >50 µg/mL).

3.3.3.4. Effects of chemical labeling on the antiviral activity and *in vivo* clearance of the IgG 10E8

Due to their higher stability in serum and the effector functions they can carry out, IgG-s are the antibody versions of choice for therapeutic approaches (Elgundi et al., 2017). Thus, in order to test effects of chemical modification, the eukaryotic cell production of the IgG 10E8 was set up in the laboratory (Figure 3.3.5A). The antiviral activity of the IgG 10E8 produced at home was comparable to that of a specimen obtained from the AIDS Research and Reference Reagent Program repository (data not shown). Chemical modification with Fus4 after introduction of the Cys residue at position LC.S65, rendered a 10E8 IgG with enhanced antiviral potency (Figure 3.3.5B). The 10E8 IgG and its chemically-modified variant were then compared in PK assays in the sera of Balb/c mice (Figure 3.3.5C). The amount of IgG for injection was selected to attain initial blood doses in the range of 50-100 µg mL-1 (Table 1). To estimate the amount of 10E8 present in the sera of mice at different times after injection, ELISAs were set up using an MPER epitope peptide immobilized in the plates. Additionally, a variant containing the double substitution NWxAA was used as a negative control for specific binding (See below “Material and Methods”, Figure 3.3.1A). Calibration curves were then produced for each IgG version tested (see an example below Figure 3.3.1B).

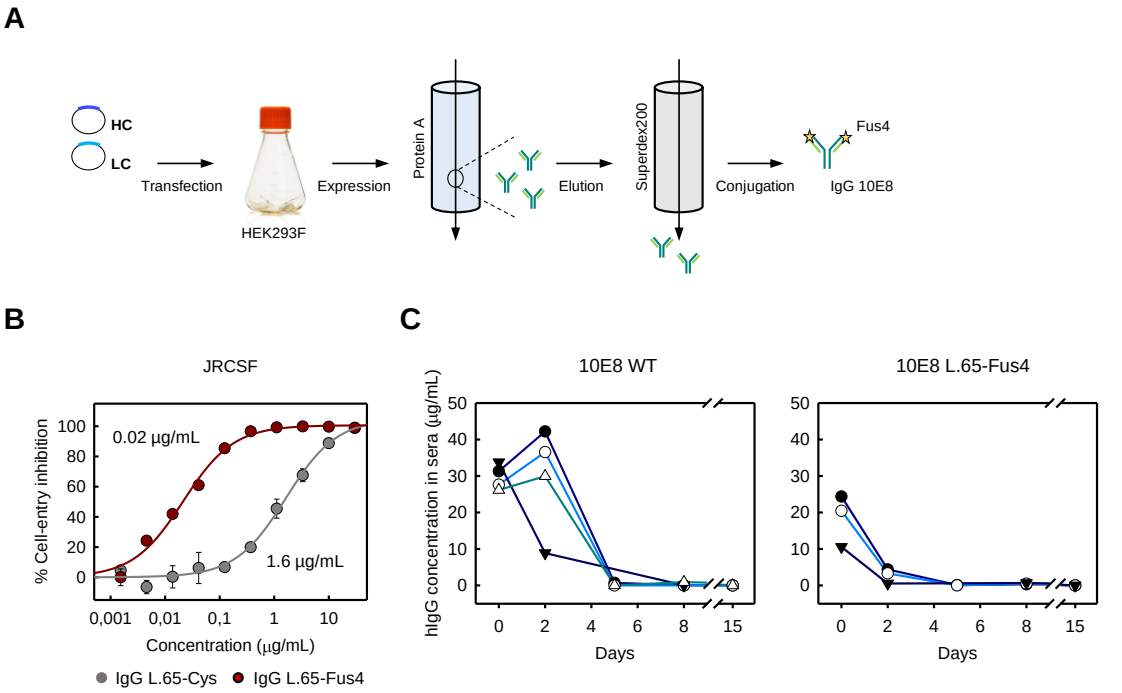

Figure 3.3.5. In vivo studies of IgG 10E8 chemically modified with synthetic aromatic compounds. (A) Diagram illustrating the production of the IgG 10E8 conjugated to Fus4. (B) Cell entry inhibition assays to demonstrate the efficacy of the conjugation procedure. (C) mAb clearance in mice. The parental and the chemically-modified IgG were intravenously administered to Balc/c female mice (Table 1) and serum collected after 10 min (day 0). Decay of specific anti-MPER reactivity in sera collected at different time-points was followed in epitope-peptide ELISA, performed as described in Materials and Methods. Each symbol represents an individual mouse. No adverse effects were observed in mice during the time course of the experiment, nor after 6 months after of subsequent surveillance.

Figure 3.3.5C displays plots illustrating the IgG concentration versus time profile after intravenous administration of a drug dose of ca. 100 µg mL^{-1} of IgG 10E8 (see Table 4). Following a similar pattern to that described for the availability of the IgG 10E8 intraperitoneally administered to mice (Y. do Kwon et al., 2016), the initial amounts of antibody 10E8 detected in serum were in the order of one third of the administered amount (Figure 3.3.5C, left panel). Moreover, 10E8 IgG was almost undetectable on day 5 after injection. Even lower doses were initially detected and faster decays observed in the case of the IgG chemically-modified with Fus4 (Figure 3.3.5C, right panel). These observations may reflect an intrinsically low stability of the IgG 10E8 *in vivo,* as previously discussed by other authors (Y. do Kwon et al., 2016). Furthermore, the low stability in sera appeared to be exacerbated upon chemical modification with Fus4.

Table 3.1. Determination of IgG concentration in mice sera versus times after injection.

IgG ID	IC50 (nM)		Mouse	Sample conc. (ug/mL)	Injected vol. (uL)	Initial conc. in sera (ug/mL)
	JRCSF	PV0.4				
10E8v1	3,08	16,62	1	230	420	31,30
			2	230	420	27,60
			3	230	420	33,76
			4	230	260	26,15
10E8v1 L.65-fus4	0,14	0,42	5	230	440	24,38
			6	230	440	20,45
			7	230	150	10,56
				-	-	-
10E8v4	4.70	22.9	9	240	420	62,79
			10	240	420	65,60
			11	240	420	80,41
			12	240	400	59,83
10E8v4 L.65-fus4	0.41	1.06	13	240	420	43,09
			14	240	420	51,43
			15	240	420	43,31
			16	240	270	32,92
10E8v4 L.65-Lin3	0,47	2,02	17	250	400	35,92
			18	250	400	41,78
			19	250	400	34,35
			20	250	400	28,32

Given the poor performance of the WT IgG in the previous experiments, an optimized version that incorporated several stabilizing mutations, IgG 10E8v.4, was additionally produced in the laboratory (Figure 3.3.6A). Following the pattern of the WT variant, chemical modification with Fus4 or Lin3 also augmented the antiviral potency of the more stable v.4 of the IgG (Figure 3.3.6B).

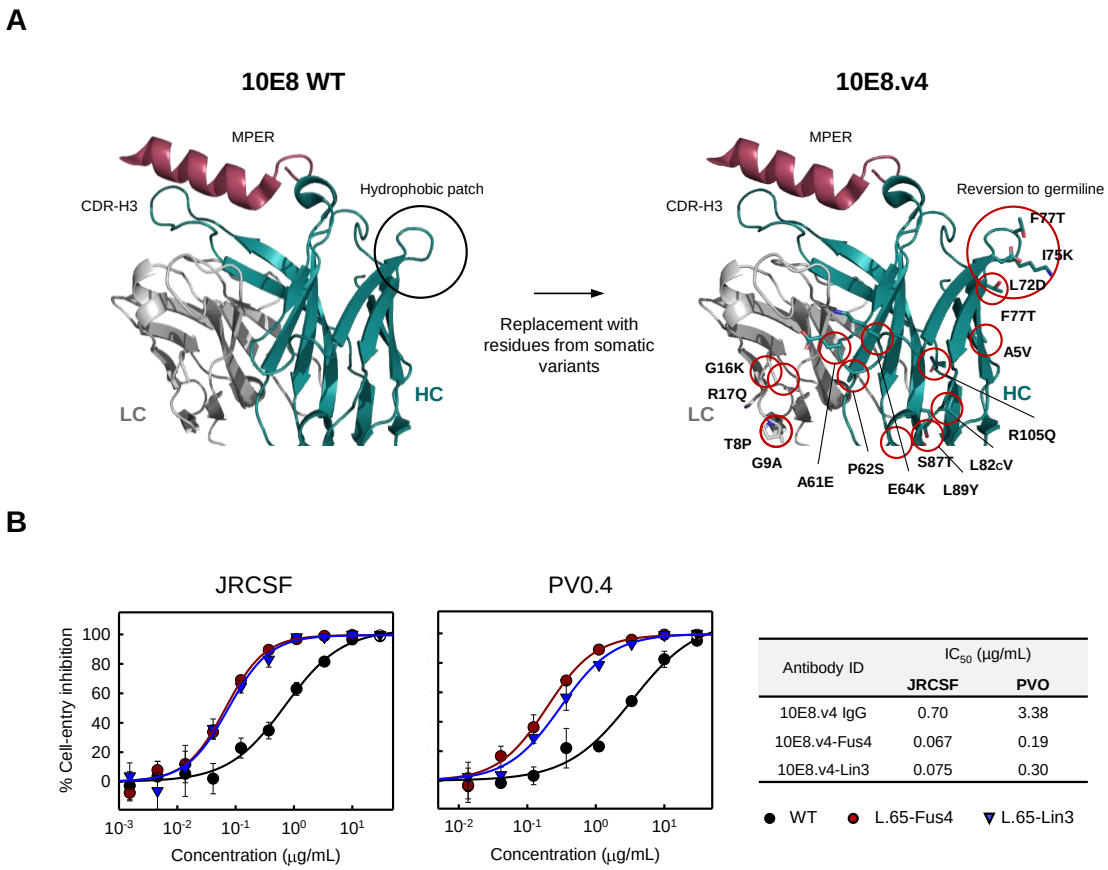

Antibody ID	IC_{50} (μg/mL)	
	JRCSF	PVO
10E8.v4 IgG	0.70	3.38
10E8.v4-Fus4	0.067	0.19
10E8.v4-Lin3	0.075	0.30

Figure 3.3.6. Chemical modification of the IgG variant 10E8v.4 incorporating several stabilizing mutations. (A) Structure of the Fab 10E8 illustrating the residues substituted to produce the IgG v.4. (B) Cell entry inhibition assays comparing IgG 10E8 v.4 and its variants chemically modified with Lin3 or Fus4.

Subsequent PK analyses in mice revealed higher initial serum concentrations of IgG 10E8v.4 compared to those of the parental version and slower clearance (Figure 3.3.7A, left panel), also following the pattern described in the literature (Y. do Kwon et al., 2016). Chemical modification accelerated the clearance in serum concentration, an effect that was more evident in the case of the Fus4 compound (Figure 3.3.7A, right panel). Interestingly, the IgG 10E8v.4 modified with Lin3 (Figure 3.3.7A, mid panel) displayed an intermediate behavior between that of the unmodified variant and the one modified with Fus4. Specifically, concentrations of the Lin3 conjugate in the range of 10 μg mL^{-1} were still detectable on day 5 post-injection, whereas after 2 days, the Fus4 conjugates were already below the 5 μg mL^{-1} levels.

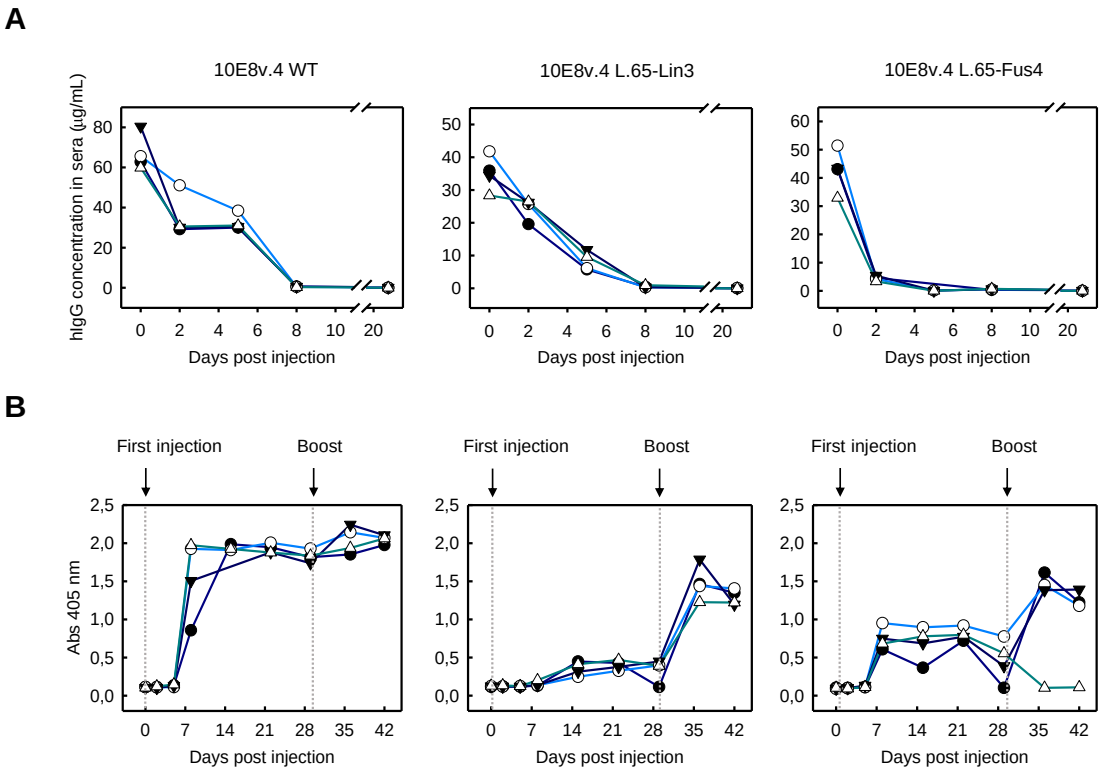

Figure 3.3.7. Pharmacokinetic and Anti-Drug Antibody studies of the IgG 10E8v.4 variant. (A) Pharmacokinetic analyses performed in Balc/c female mice (Table 4). The parental IgG 10E8v.4, and its Lin3 and Fus4 conjugates were administered i.v., and the serum concentration of anti-MPER ab determined at multiple time points, as described in the previous Figure 3.3.5B. (B) ADA response observed during the study. The levels in serum of anti-human Abs was determined by ELISA using an anti-mouse-AP (Sigma) antibody. Each symbol represents an individual mouse. No adverse effects were observed in mice during the time course of the experiment, nor after 6 months of subsequent surveillance.

The levels of ADA measured in serum appeared to partially explain the drops in the IgG concentration of the different variants (Figure 3.3.7B). The parental version of IgG 10E8v4 induced an ADA response, which was evident on day 8 after injection and coincident with its disappearance from serum. By comparison, the Lin3 conjugate induced an attenuated response, consistent with the comparatively lower levels of IgG 10E8 measured in the mice sera. Interestingly, the Fus4 conjugate induced a more pronounced response than the one induced by Lin3, even when its serum levels were almost undetectable on day 5 post-injection. The ADA response was confirmed in all three cases by the response elicited after a booster dose administered at week 4.

3.3.4. Discussion

In the previous chapter, the promotion of favorable interactions with the membrane interface was introduced as a procedure for potentiating the molecular recognition of this class of epitopes. This potentiation effect was achieved through chemical modification of

membrane-proximal surfaces of the antibody with synthetic aromatic compound. However, the necessity to bind non-specifically membranes to gain access to the epitope originates a prospective problem for the application of this approach, in the context of complex biological matrices such as living tissues. In this chapter, several biological properties of the 10E8 conjugates LC.S65C-Fus4 and LC.S65C-Lin3 have been compared *in vitro* (cell cultures) and *in vivo* (mouse model).

Despite the slightly better performance shown by the Fab labeled with Fus-4 in the neutralization assays described in the previous chapter, both, LC.S65C-Fus4 and LC.S65C-Lin3, displayed diffuse labeling patterns in the Hep-2 cell assay, consistent with their capacity to associate nonspecifically, but not preferentially, with components of the permeabilized cells. ELISA using immobilized specimens discarded cross-reactivity with specific lipids, whereas flotation experiments revealed certain degree of direct association with membranes, a tendency that was more evident in the case of the Lin3 conjugate. Thus, this behavior seems to reflect a certain tendency to associate with hydrophobic surfaces and insert into lipid bilayers bearing a low degree of lipid packaging, but not to react specifically with lipid autoantigens, as would be the case of autoantibodies associated with antiphospholipid syndrome or other autoimmune diseases. These potential membrane interactions were nevertheless not toxic for the target cells of the HIV, nor interfered with the elevated antiviral activity of the chemically-modified Ab evaluated *in vitro*.

Chemical modification also endowed the IgG versions of the 10E8 antibody with higher potency. In therapeutic setups, the efficacy of several anti-HIV IgGs has been related to their concentration in blood (Sok & Burton, 2018). Therefore, concentrations of the IgG 10E8 were monitored upon intravenous injection. As highlighted by a recent comparative analysis, the minimal Ab concentrations required in serum to provide protection against SHIV challenge in macaques are about 200-fold higher than the mean neutralization IC_{50} values determined *in vitro* (Sok & Burton, 2018). A recent clinical trial also revealed that concentrations in serum that prevented viral rebound by Abs 3BNC117 and 10-1074 (≥ 10 μg/mL), were ca. 100-200-fold higher than their neutralization IC_{50} values (Caskey et al., 2017; Mendoza et al., 2018). Thus, it has been argued that neutralization potency values inferred from standard assays based on PsVs and TZM-bl cells are highly predictive for protection *in vivo* (Sok & Burton, 2018).

Neutralization assays in this chapter provided IC_{50} values for the chemically-modified 10E8 IgGs in the order 0.05 μg/mL against the standard tier-2 JRCSF isolate (Figs 4B and 5B). This implies that a desirable goal for the potential use of these Abs as

therapeutic agents would be to reach a sustained IgG concentration of ca. 5-10 µg/mL in serum. Although intravenous injection did not cause apparent adverse effects in mice, the clearance of human IgG-s varied with the type of chemical modification. The serum levels of the IgG conjugated to Fus4 diminished faster than those of the parental unmodified variant or those of the IgG conjugated to Lin3. Thus, it seems that Fus4 conjugates would stick nonspecifically more readily to structures present in a complex biological matrix like an intravascular space, or those present in the routes of trafficking through the liver and other tissues. Surprisingly, despite its lower levels in serum, the ADA elicited by the Fus4 conjugate was higher than that elicited by the Lin3 conjugate.

Although useful for initial, comparative analyses of the effects of chemical modification on the half-lives, ADA production and toxicity, conventional mice are not adequate models to obtain relevant information about the stability in human serum of each IgG, due to two reasons. First, as documented in this chapter, the adaptive immune system of mice recognizes human Abs and generates an anti-human IgG ADA response, which neutralize them by days 7-8 after injection. Second, the half-lives of IgG-s in mammals are conditioned by the FcRn moieties, which mediate their recycling and avoid lysosomal degradation. Differences between mouse and human FcRn-s also result in a faster clearance of human IgG-s in the sera of mice. To address these limitations, the next step should be to analyze the behavior of WT and modified IgG-s *in vivo* using humanized mice as the animal model (Jiménez-Díaz et al., 2009).

In summary, the results described in this chapter caution that the chemical structure of the compound can unexpectedly condition the behavior of the IgG conjugate *in vivo*. Therefore, future clinical use of these antibodies will require previous chemical and/or protein engineering cycles, seeking to promote functional efficacy, while reducing possible off-target effects. In this sense, the preliminary observations point to linear compounds such as Lin3, as candidates more suitable for further development than the compounds based on membered rings.

Chapter 3.4

RESULTS: IMPROVEMENT OF ANTI-MPER ANTIBODY AVIDITY THROUGH THE PROMOTION OF SPECIFIC INTERACTIONS WITH VIRAL LIPIDS

3.4. IMPROVEMENT OF ANTI-MPER ANTIBODY AVIDITY THROUGH THE PROMOTION OF SPECIFIC INTERACTIONS WITH VIRAL LIPIDS

GENERATION OF BISPECIFIC COMPLEXES COMBINING ANTI-MPER Fab-s WITH PHOPHATIDYLSERINE-BINDING DOMAINS AND PRELIMINARY FUNCTIONAL ASSESMENTS

Abstract

Due to their high potency, breadth and the capacity to limit viral escape, the generation of multivalent molecules targeting the HIV-1 Env spike has become a pursued goal, some of these complexes having already entered clinical trials. As enveloped virions and infected cells, but not healthy cells, expose phosphatidylserine (PS) in the outer leaflet of the membrane, at least in theory, PS-binding domains can be used to target them specifically. With the aim of enhancing the avidity of anti-MPER antibodies and, thus, increase their neutralization potency, in this chapter 4E10 and 10E8 Fab-s have been combined with PS-binding moieties. Two bispecific formats have been designed to test this concept. On the one hand, complete single-chain (sc)IgGs have been produced adding a Bavituximab Fab to a 4E10 or a 10E8 Fab. On the other hand, taking advantage of the knobs-into-holes methodology, T-cell Immunoglobulin mucin (TIM) ectodomains have been combined with the anti-MPER Fabs. The new bispecific MPER-PS antibodies were correctly expressed and purified, but only combinations containing TIM domains interacted with both MPER and PS antigens. Moreover, although these constructs presented both functional arms, anti-MPER/TIM combinations did not appear to improve consistently the neutralization potency of the Fab-s 10E8 or 4E10 acting individually. Therefore, although conceptually feasible, the preliminary results included in this chapter failed to confirm in all instances the PS recognition-mediated improvement of anti-MPER antibodies.

3.4.1. Introduction

The HIV envelope glycoprotein (Env), which mediates binding and entry into the host cell, is targeted by bnAbs that recognize at least six conserved regions (Sok & Burton, 2018). The use of these bnAbs is being explored as passively administered therapeutic and preventative agents, and combinations of them have been proposed to optimize their potency, breadth and limit the emergence of viral resistance. Multivalent molecules as bi- or trispecific antibodies targeting more than one vulnerability site have become a desirable goal due to their exceptional potency and breadth (Steinhardt et al., 2018; L. Xu et al., 2017). Moreover, combination of different specificities in a single molecule increases antibody avidity and simplifies treatment regimens. BnAbs targeting the C-MPER have been included in various multivalent formats (Padte et al., 2018) owing to their high breadth (Sok & Burton, 2018).

The Env spike, the only exposed viral antigen, is expressed in low density on the surface of the virion (J. S. Klein et al., 2009; P. Zhu et al., 2006), and therefore, the ability of multispecific antibodies to bind to the spike in a multivalent fashion is very limited. However, anti-C-MPER antibodies entail semi-specific interactions with the viral membrane interface (Irimia et al., 2016, 2017; Rujas et al., 2016), opening up the possibility of enhancing their avidity by combining them with lipid targeting domains in a multivalent format.

Given the fact that the virion acquires the lipid envelope from the plasma membrane of the infected cell, the viral membrane has been thought to be inert for the immune system. However, the viral membrane is enriched in some lipids: phospahtidylserine (PS), for instance, which is normally accumulated in the plasma membrane internal leaflet, facing the intracellular medium (Seigneuret & Devaux, 1984; Williamson & Schlegel, 1994) and becomes exposed on the outer membrane surface on enveloped virions and infected cells (Carravilla et al., 2019; M. Li et al., 2014). Thus, the presence of accessible PS molecules seems to be a conserved feature among all HIV-1 isolates, becoming a potential target for antiviral candidates against enveloped viruses. Moreover, anti-PS immunotherapy is also a growing field in the treatment against cancer, as various biochemical pathways associated with apoptosis induce PS externalization in the tumor microenvironment (Zwaal et al., 2005).

Bavituximab is a chimeric monoclonal antibody consisting of murine VH and Vκ chains linked to human IgG1 constant domains. It binds with high affinity to PS after forming a complex with its actual antigen, the serum cofactor β2GP1 (Soares et al., 2008). Clinical trials showed that the treatment with bavituximab of patients co-infected with hepatitis C

and HIV was safe and reduced virus load in the blood (J Slim, MS Sulkowski, 2011). This mAb has also demonstrated the capacity to bind other infected cells and virions in vitro, including Ebola virus (Dowall et al., 2013). Finally, clinical trials evaluating the antibody as monotherapy and in various combination regimens in patients with multiple tumor types have shown promising results of activity and an acceptable safety profile (Belzile et al., 2018).

Some immune cells also express receptors that directly bind PS, participating in immune regulatory activity, and they play critical roles in viral infections. T cell/transmembrane, immunoglobulin, and mucin (TIM) family receptors are type I transmembrane proteins: They present a variable Ig-like (IgV) domain extending from the plasma membrane in their N-terminus, a glycosylated mucin domain, a single transmembrane domain and a cytosolic C-terminal tail that mediates intracellular signaling (Freeman et al., 2010). Despite sequence variations, the IgV regions of all TIM proteins contain a conserved PS binding site (DeKruyff et al., 2010; Santiago et al., 2007). Interestingly, TIM-family proteins have shown the ability to inhibit HIV-1 release, reducing viral production and replication (M. Li et al., 2014).

In this last chapter of results, the concept of simultaneous engagement of multiple sites within a spike was expanded to include antibodies that concurrently target MPER and the phospholipid PS. The design of bi-valent molecules was sought to increase the avidity for HIV-1 of anti C-MPER antibodies 10E8 and 4E10. Two different formats based on PS binding proteins were used: On the one hand, a bispecific antibody that combines 10E8.v4 and Bavituximab was produced, co-transfecting single-chain-IgG genes (with a linker between the LC and the HC) of each parental Ab. On the other hand, using a knobs-into-holes Fc heterodimerization strategy (Atwell et al., 1997; Ridgway et al., 1996) anti-MPER/TIM bispecific molecules have been produced. TIM ectodomain-Fc constructs were generated and transfected together with the HC and the LC of 10E8 or 4E10 anti-MPER antibodies. The results showed that bispecific antibodies were correctly expressed and purified; however, the construct 10E8.v4/Bavituximab lacked the ability to bind PS. Moreover, although they presented two functional arms, the preliminary results of neutralization assays suggest that anti-MPER/TIM combinations do not consistently improve potency of the individual Fabs 10E8 or 4E10.

3.4.2. Material and methods

3.4.2.1. Materials

The scIgG containing pcDNA plasmids were purchased from GeneArt, while pK and pCMV plasmids were kindly provided by Jose M. Casasnovas (Centro Nacional de Biotecnología, CSIC). Protein A-HRP secondary antibody was purchased from Sigma-Aldrich. The rest of the plasmids, probes and antibodies were obtained as indicated in 3.1.2.1 and 3.2.2.1.

3.4.2.2. Construct design

Two strategies were followed in this chapter to generate bispecific antibodies. 10E8.v4/Bavituximab antibody, was produced by the co-expression of two scIgG chains. Here, the LC and the HC of each antibody were cloned in the same pcDNA plasmid, with a SG linker between them. The linker contained a Streptavidin (Strep) affinity tag in the case of 10E8.v4, and a His tag for Bavituximab, allowing the selection of the bispecific antibody from its parental versions during the purification.

Fc heterodimerization was differently promoted in the anti-MPER/TIM species by creating “knobs-in-holes” mutations in the C_H3 domain, which is a prerequisite to assemble two half antibodies with different specificity. For that, three independent plasmids were designed: First, VH-CH_1 domains of the anti-MPER antibodies were cloned in a pCMV plasmid containing the signal peptide (SP) and the IgG1-Fc wearing the “knob” mutations (Y349C and T366W). The ectodomain of human-TIM-1 (hT1) or murine-TIM-1 (mT1) was cloned in a pEF-derived plasmid, containing the SP and the IgG1-Fc wearing the “hole” mutations (T366S, L368A, Y407V and E365C). Finally, the LC-s of the correspondent anti-MPER antibodies were cloned in a third plasmid, derived from a SP containing pK.

3.4.2.3. Protein expression and purification

The plasmids were co-transfected into HEK293-F cells using a 1:1 ratio of DNA:FectoPRO (FP), as described in 2.1.2, at a cell density of 0.8×10^6 cells/ml and incubated at 37 °C, 125 rpm, 8% CO2. 5–7 days later, cells were harvested and supernatants were filtered with a 0.22 µm membrane. Supernatants containing anti-MPER/TIM species were first loaded in a HiTrap Protein A High Performance column (SigmaAldrich) affinity column (GE Healthcare) using an AKTA Start chromatography system (GE Healthcare). The column was washed with 20 mM Tris (pH 8.0) 150 mM

NaCl buffer and eluted with 100 mM glycine (pH 2.2). Eluted fractions were neutralized with 1 M Tris-HCl pH 9.0. In contrast, supernatants containing 10E8.v4/Bavituximab, were passed through a StrepTrap HP column and eluted with 20 mM Tris (pH 8.0) 150mM NaCl 1mM EDTA 2.5mM desthiobiotin. Next, protein-containing fractions were loaded in a HisTrap Ni-NTA column (GE Healthcare), and eluted with an increasing gradient of imidazole (up to 500 mM). Finally, fractions containing antibody were concentrated and loaded on a Superdex 200 Increase SEC (GE Healthcare) previously equilibrated in 20 mM Tris pH 8.0, 150 mM NaCl buffer to achieve size homogeneity. The purifying strategy will be further explained below, in 3.4.3.1.

3.4.2.4. ELISA to assess antigen binding

96-well plates were coated o/n at room temperature (RT) with 100 µL/well of MPER derived peptide KKK-^{671}NWFDITNWLWYIKLFIMIVGGLV^{693}-KK (1.37 µM), or 50 µM PS LUV-s, which were produced as described in previous chapters. After 2 hour well blocking with 3 % (w/v) BSA, antibodies or supernatants were incubated 1 hour at RT (In the case of Bavituximab containing constructs the buffer was supplemented with 10% of sera, and in the case of TIM containing constructs, with 2.5 mM $CaCl_2$). Bound species were detected with an AP-conjugated goat anti-human immunoglobulin. The reaction was measured by absorbance at a wavelength of 405 nm in a Synergy HT microplate reader.

3.4.2.5. Dot-blot

Decreasing amounts of PC:PS (10:1) LUV-s were spotted onto Hybond C nitrocellulose (GE Healthcare). The nitrocellulose was then blocked with 5% fat-free milk in PBS (Blocking Buffer) for 2 h and incubated for 1 more hour with antibodies (1 µg/ml) in Blocking Buffer supplemented with 10% of sera at RT. The membranes were washed 3 times, 10 min each with PBS. Filters were developed using HRP-conjugated protein A.

3.4.2.6. Bio-Layer Interferometry (BLI)

The binding affinities of 10E8.v4 and 10E8.v4/Bavituximab to their His-tagged epitope was measured by BLI. Ni-NTA biosensors were hydrated in kinetics buffer (PBS, pH 7.4, 0.002% Tween, 0.01% BSA) and loaded with 10 µg/mL MPER-His for 60 s at 1000 rpm. Biosensors were then transferred into wells containing 1× kinetics buffer to baseline for 60 s before being transferred into wells containing a serial dilution of the antibody starting at 500 nM and decreasing to 15.6 nM. The 180 s association phase was subsequently

followed by a 180 s dissociation step in kinetics buffer. Analysis was performed using the Octet software, with a 1:1 fit model.

3.4.2.7. Neutralization assays

PsV particles were produced as described in 2.7.1.1. Briefly, cells were co-transfected with the vectors pWPXL-GFP, pCMV8.91 and PVO.4 or JR-CSF Env-clone by the calcium phosphate method. Neutralization potency was calculated after incubation of PsV with TZM-bl cells in presence of serial concentrations of the antibody. Infection level was inferred after 72 hours from the number of GFP-positive cells.

3.4.3. Results

3.4.3.1. Strategy to produce bispecific species

As described before, two different methods were followed to generate bispecific anti-MPER/anti-PS antibodies.

Co-expression of two scIgG genes was used to produce 10E8.v4/Bavituximab bispecific antibodies. In this format, a linker connects both Ig genes during protein expression, allowing the correct pairing of the respective LC with its cognate HC. In addition, the linker encodes an affinity tag (His-tag or Strep-tag), and facilitates the double selection: antibodies formed by two identic arms are discarded during the purification process due to their inability to bind one of the affinity columns (Figure 1A and 1B). Purified bispecific scIgG, together with the parental scIgG-s were loaded in a SDS-PAGE (Figure 1C).

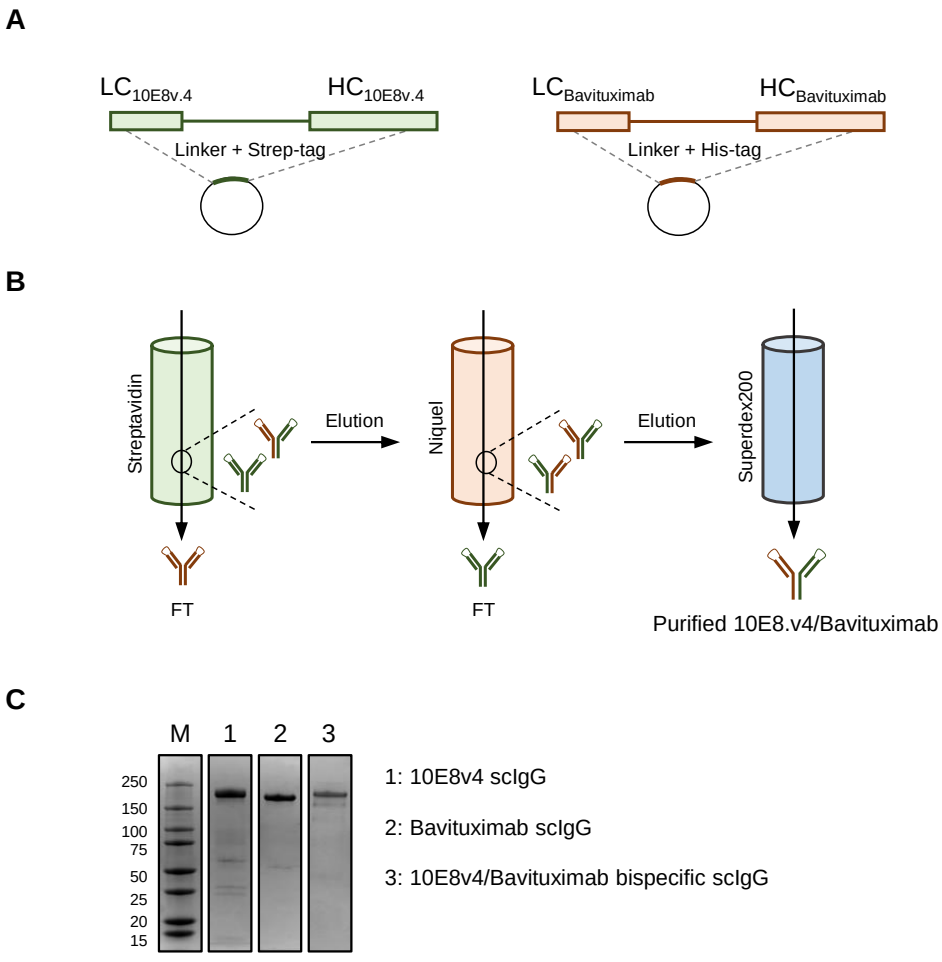

Figure 3.4.1. Bispecific antibody production by the expression of scIgG-s. (A) 10E8.4/Bavituximab expression plasmids: 10E8.v4 scIgG gene (in green) and Bavituximab scIgG gene (orange) are shown. (B) Bispecific antibody purification: The first step was the streptavidin affinity column, where Bavituximab homodimers were discarded. The second step, the Niquel column, discarded 10E8.v4 homodimers, Finally, bispecific Ab containing fractions were loaded in a Superdex200 to achieve size homogeneity. (C) Purified scIgG-s in a SDS-PAGE, loaded in non-reducting conditions.

The second approach took advantage of the “knobs-into-holes” methodology. This strategy involves engineering C_H3 domains to create either a “knob” or a “hole” in each HC to promote heterodimerization. The arm encoding the Fc-linked TIM ectodomain, wearing the “hole” substitutions T366S, L368A, Y407V and E365C, formed dimers with the arm encoding the HC of the anti-MPER (10E8 or 4E10) antibody, with “knob” Y349C and T366W mutations. At the same time, the anti-MPER LC, expressed from a third plasmid, was associated with its corresponding V_H-C_H1 domain (Figure 3A).

Anti-MPER antibodies used in this format were 4E10 and 10E8, which bind the same epitope but differ in their neutralization potency and their ability to directly interact with some phospholipids. The PS binding arm of the bispecific antibody was also constructed

using two TIM orthologs, human-TIM-1 (hT1) and mouse-TIM-1 (mT1), giving raise to different bispecific combinations that differ from each other in the mucin domain length. This domain, that extends the IgV domain from the cell surface and it is crucial for ligand binding, is almost twice longer in the human variant (Figure 3.4.2.) (Wilker et al., 2007).

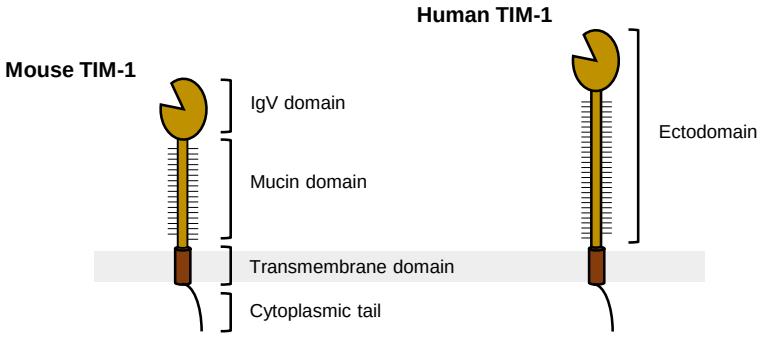

Figure 3.4.2. Schematic representation of TIM proteins. A IgV domain, a glycosylated mucin domain, a transmembrane domain and a cytoplasmic tail compose the TIM protein. In this work, the ectodomain of both mT1 and mT1 have been used to produce antibodies with two specificities.

In this case, purification was performed using a protein A affinity column (Figure 3.4.3B), which binds the Fc of the antibody. LC dimers were discarded, and the only correctly assembled antibody-like protein, bispecific anti-MPER/TIM, was selected. Finally, burified bispecific antibodies and the WT IgG-s were loaded in a SDS-PAGE (Figure 3.4.3C).

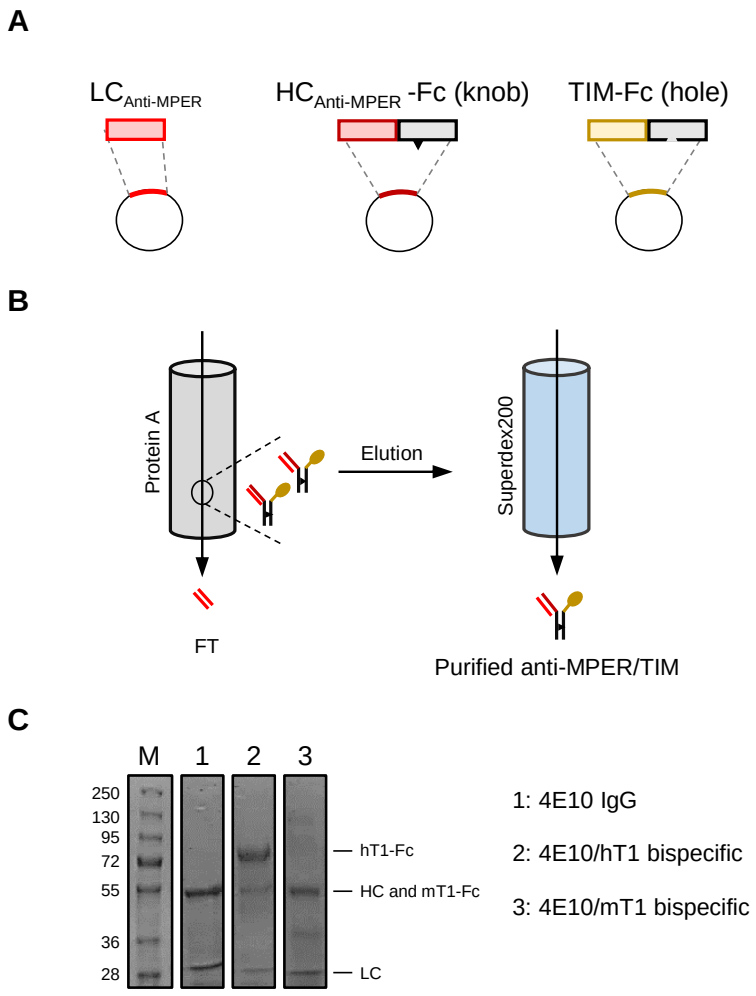

Figure 3.4.3. Bispecific antibody production by Knobes-into-holes technology. (A) Bispecific Ab Anti-MPER/TIM expression plasmids: Anti-MPER LC gene (in red), anti-MPER.v4 HC, gene (V_H-C_H1 domain in dark red and C_H2-C_H3 domains in black) and TIM-Fc gene (TIM ectodomain in yellow and C_H2-C_H3 domains in black) are depicted. (B) Bispecific antibody purification: Protein A column retained the only well assembled Fc wearing protein. Next, bispecific Ab containing fractions were loaded in a Superdex200 to achieve size homogeneity. (C) Purified antibodies in a SDS-PAGE, loaded under reducing conditions.

3.4.3.2. Bispecific antibodies bind MPER peptide

Correct expression does not imply the correct functionality of both antigen interacting paratopes in each bispecific antibody. To confirm their dual specificity, binding activity of the anti-MPER arm to its MPER epitope was initially characterized by two different techniques. For 10E8.v4/Bavituximab scIgG, the ability of the 10E8.v4 moiety to recognize the MPER epitope was measured by Bio-Layer Interferometry (BLI) (Figure 4). Binding signal demonstrated the correct assembly of the anti-MPER arm of the bispecific antibody. Binding to the immobilized peptide was also measured for the parental antibodies and as expected, only 10E8.v4 antibody interacted with the MPER

peptide. Moreover, the parental antibody doubled the signal observed for the bispecific, in accordance with the number of Fab present in each construct.

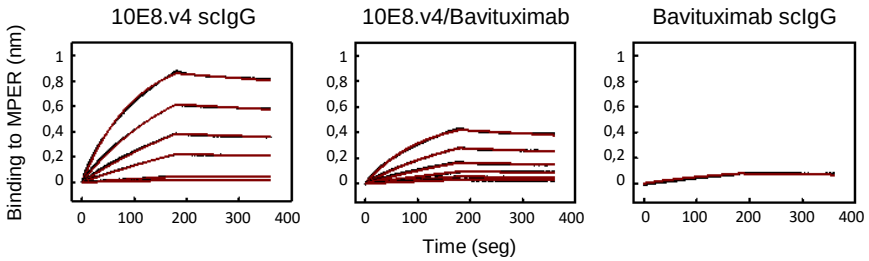

Figure 3.4.4. Binding of 10E8.v4/Bavituximab to immobilized MPER by BLI. 10E8.v4 and the bispecific antibody bound the MPER while Bavituximab did not interact with the immobilized peptide. 10E8.v4, which has two MPER-binding domains, recognizes the peptide with higher affinity than the bispecific antibody.

To confirm the binding ability of the 4E10 and 10E8 moieties present in each anti-MPER/TIM formats, ELISAs were set up using an MPER epitope peptide immobilized in the plates. Additionally, a variant containing the double substitution NWxAA was used as a negative control for specific binding (Figure 3.4.5).

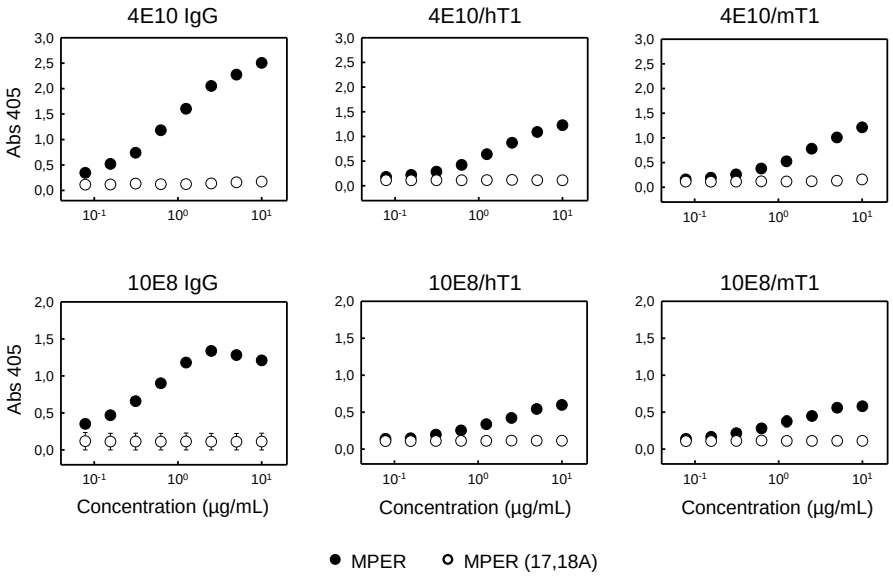

Figure 5. Binding of different anti-MPER/TIM variants to MPER petide by ELISA. 4E10, 10E8, and bispeficic versions combined with mT1 and hT1 interacted with the MPER peptide but not with its alanine mutant in ELISA.

The results confirmed that the anti-MPER moieties incorporated in both produced bispecific formats specifically recognized the MPER sequence, and, consequently, were correctly folded.

3.4.3.3. Anti-MPER/TIM antibodies but not 10E8v.4/Bavituximab retain the ability to bind PS

Next, the specificity of the second arm of the bispecific antibodies was tested by analyzing PS binding. Although the parental antibody Bavituximab effectively bound to PC:PS (10:1) LUV-s in ELISA plates in presence of FBS, bi-specific 10E8v.4/Bavituximab antibody did not (Figure 3.4.6A).

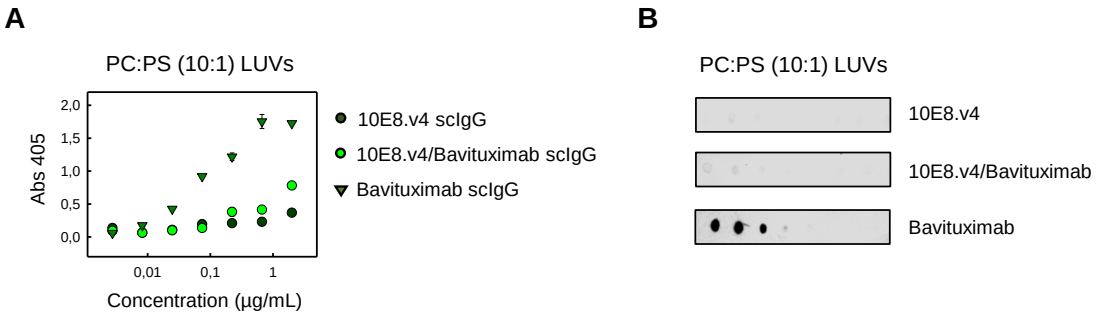

Figure 3.4.6. Binding of Bavituximab-containing bispecific antibodies to PC:PS LUVs. Binding of the IgG 10E8v.4/Bavituximab and its parental antibodies was tested against 0.5 mM of PS cotaining LUVs by ELISA (A) and Dot-blot (where a serial dilutions of LUVs were dotted) (B). Only Bavituximab IgG interacted with high affinity with the phospholipids.

In contrast, 4E10/hT1, 4E10/mT1 and 10E8/mT1 and 10E8/hT1 (not shown) interacted with PS in ELISA, while the signal of the 4E10 and 10E8 antibodies was residual (Figure 7). In the particular case of 4E10, a modest binding to PS can be observed, in agreement with the autoreactivity profile described for this antibody.

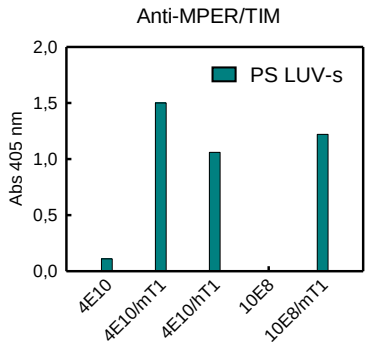

Figure 3.4.7. Binding of TIM-containg bispecific antibodies to LUVs containging PS. Binding of 4E10/hT1, 4E10/mT1 and 10E8/mT1, and parental antibodies 10E8 and 4E10 to PS in ELISA plates.

3.4.3.4. Bispecific antibodies do not enhance consistently the anti-viral potency of parental Fabs

Attending to the previous results, further use of the bispecific 10E8v.4/Bavituximab was discarded, and a functional screening measuring antiviral activity against two HIV-1 PsV-s, JRCSF (Tier-2) and PV0.4 (Tier-3), focused on the 4E10/hT1, 4E10/mT1, 10E8/mT1 and 10E8/hT1 bispecifics. Figure 8 displays results of cell-entry inhibition assays comparing the TIM/anti-MPER bispecifics and their parental antibodies, Fabs and IgGs.

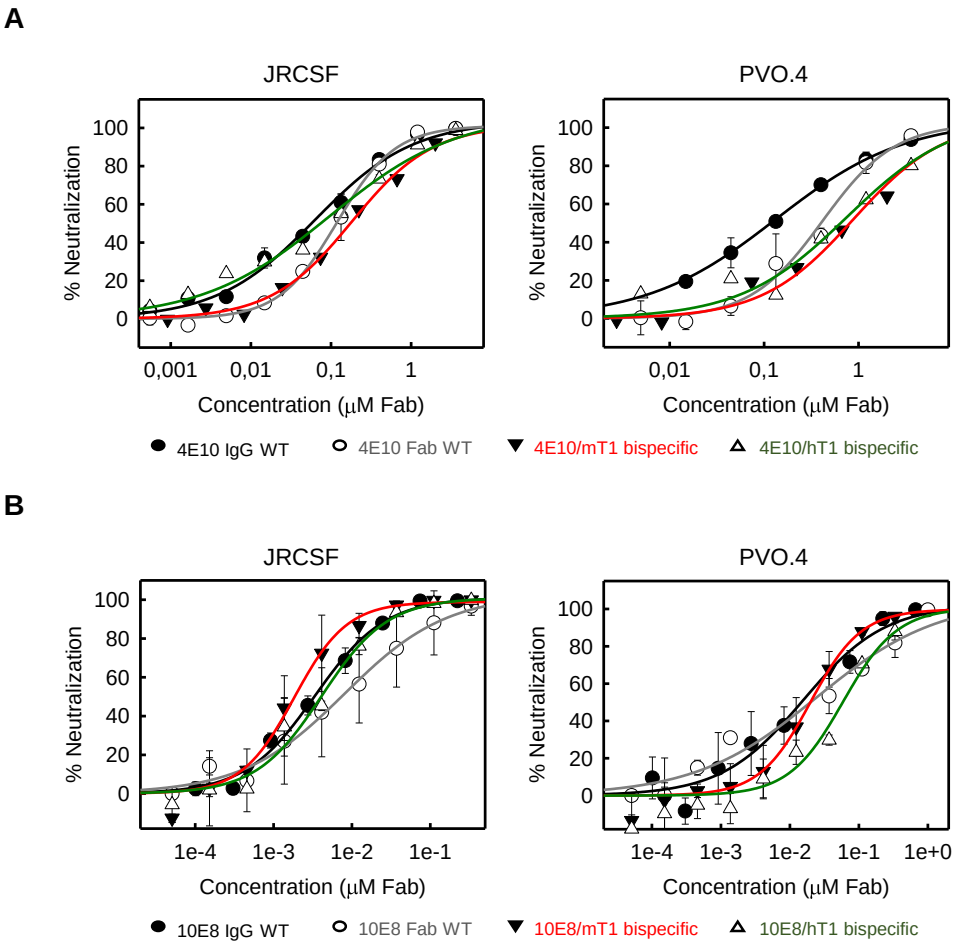

Figure 3.4.8. Cell-entry inhibition by parental and anti-MPER/TIM bispecific antibodies. A. Cell-entry inhibition assays against JRCSF (Tier-2) and PVO.4 (Tier-3) PsVs comparing unmodified WT 10E8 Fab (monovalent) and 10E8 IgG (bivalent) with bispecific antibodies 4E10/hT1 and 4E10/mT1. B. Same for 10E8 antibodies. Experimental values (means ± SD of 2 determinations) were adjusted to sigmoidal curves and IC_{50} and IC_{90} values calculated by interpolation.

A significant enhancement of potency with respect to the Fab, was only observed for the 10E8/mT1 bispecific. For the rest of the conditions, no significant differences were observed in the IC_{50} or IC_{90} values measured for bispecific antibodies or anti-MPER Fabs (Tables 3.4.1 and 3.4.2).

Table 3.4.1: Cell-entry inhibition of HIV-1 by 4E10-WT and the bispecific antibodies.

Antibody ID	**JRCSF (Tier - 2)**		**PVO (Tier - 3)**	
	IC_{50} (nM)	IC_{90} (nM)	IC_{50} (nM)	IC_{90} (nM)
4E10 IgG	55.2	996.9	113.3	2761.9
4E10 Fab	115.7	696.4	393.5	2532.9
4E10/mT1	171.4	2076.6	783	7880.6
4E10/hT1	69	2457.3	621.6	7979.5

Table 3.4.2: Cell-entry inhibition of HIV-1 by 10E8-WT and the bispecific antibodies.

Antibody ID	**JRCSF (Tier - 2)**		**PVO (Tier - 3)**	
	IC_{50} (nM)	IC_{90} (nM)	IC_{50} (nM)	IC_{90} (nM)
10E8 IgG	3.4	33.5	15.6	252.1
10E8 Fab	8	22.3	24.3	547.2
10E8/mT1	1.8	10.5	19.8	124.3
10E8/hT1	4.1	34.6	59	419.9

3.4.4. Discussion

Targeting multiple epitopes with a single molecule have shown to improve potency and breadth of HIV targeting antibodies. In recent years, many multispecific antibodies have been developed (Padte et al., 2018). Those molecules include bispecific and trispecific designs targeting, on the one hand, more than one vulnerability site within the Env (Asokan et al., 2015; Bournazos et al., 2016) or, in the other hand, one vulnerability Env site and the main receptor (CD4) or co-receptor (CCR5 or CXCR4 of the HIV (Y. Huang et al., 2016).

In this chapter, the ability of anti-MPER antibodies to recognize their epitope in the proximity of the membrane was further exploited to increase their potency. Thus, it was inferred that promoting favorable interactions with the membrane through a second PS-binding moiety could increase the potency of these antibodies by improving their avidity and pre-concentrating them near to their epitope. Accordingly, two bispecific antibodies containing an anti-MPER and an anti-PS specificity were engineered.

The first lipid-binding domain to be integrated in the bispecific design was selected after searching for anti-PS antibodies that had been already tested in clinical trials. The chimeric antibody Bavituximab has shown promising results in different cancer therapies (Burton & Hangartner, 2016; Burton & Mascola, 2015; F. Klein, Mouquet, et al., 2013; Kwong & Mascola, 2012) and against some enveloped viruses (Burton & Hangartner, 2016; Burton & Mascola, 2015; F. Klein, Mouquet, et al., 2013; Kwong & Mascola, 2012); however, it requires prior binding to the serum protein β2GP1 for effective interaction with PS. The function of the antibody, thus, might be conditioned by the clearance kinetics of this protein from serum. Moreover, β2GP1 intervention could increase the distance of the bispecific construct from the viral envelope, which is a factor possibly limiting avidity since the second Fab of the bispecific molecule targets a membrane-embedded epitope.

10E8v.4/Bavituximab was correctly expressed and purified, and its 10E8.v4 arm kept MPER-binding ability as observed by BLI. The other arm, nevertheless, failed to recognize PS containing liposomes in presence of β2GP1 containing sera. The parental scIgG Bavituximab, in contrast, did recognize these LUVs, confirming that bivalent binding to β2GP1 is mandatory to create a high-affinity PS binding complex (Figure 3.4.9) (Belzile et al., 2018).

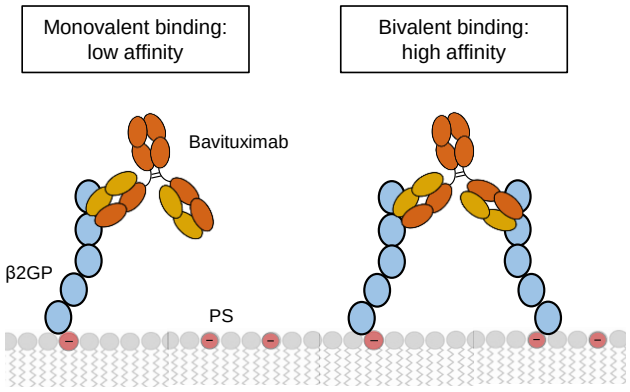

Figure 3.4.9. PS binding mechanism of Bavituximab-β2GP1 complex. Bavituximab (in orange) binds β2GP1 (in blue) with low affinity (left). High PS exposure promotes the interaction of the antibody with two β2GP1 molecules to form a high avidity complex (right). Figure adapted from (Belzile et al., 2018).

In an alternative approach, the orthologue receptors mT1 and hT1 were chosen as specialized domains for binding to the PS exposed on the HIV-1 envelope. As one of their differences lies on the mucin domain length, critical for the simultaneous binding of the two arms within the bispecific antibody, we designed four variants combining 4E10 and 10E8 anti-MPER antibodies with mT1 and hT1.

4E10/hT1, 4E10/mT1, 10E8/mT1 and 10E8/hT1 were constructed in a second bispecific format, based on “knobs into holes” technology, to avoid the formation of monovalent antibody-like molecules. After protein expression, all of them showed binding activity against MPER peptide and PS containing liposomes, confirming their correct assembly. However, cell-entry inhibition assays were not conclusive in confirming that addition of PS specificity conferred higher neutralization potency to MPER Fabs.

Contrary to the expectations, only the 10E8/mT1 construct showed improved potency in comparison with the parental Ab. For the rest of 10E8 and 4E10 bispecific antibodies, IC_{50} values were similar to those obtained for the WT Fabs (monovalent binding) and slightly higher than those obtained for the IgG (bivalent binding) in both JRCSF and

PV0.4 strains. One option to explain the lack of effect is that simultaneous binding of the two antigens is not happening in the PsV context due to differences in length and/or flexibility of the arms composing the bispecific construct. Thus, additional engineering steps could help to overcome this problem: modification of the length of the PS binding arm could be done by engineering the mucin domain of the TIM, or replacing it with a IgG CH1 domain). Besides, once bound, the distance of the membrane-binding domain with respect to the MPER binding site could also be critical. The results obtained in this chapter suggest that pre-concentration of the anti-MPER Ab near the envelope appears to have no effect in the cell entry inhibition capacity. In contrast, the potency is enhanced when membrane-binding forces are located close to the paratope, as demonstrated in 3.1 and 3.2 chapters.

4. Kapitulua

EZTABAIDA OROKORRA ETA ONDORIOAK

4. EZTABAIDA OROKORRA

Ingeniaritza genetikoa erabiliz eraldatuatko antigorputzak infekzio biralen detekzio, tratamendu edota prebentzio terapien zein diagnostiko erreminten garapenean protagonista bilakatu dira (Marasco & Sui, 2007; Walker & Burton, 2016). GIBak eragindako infekzioaren kasuan, Ab-ek molekula txikien aurrean dituzten abantailek (hau da, erdibizitza luzea gazurrean, espezifitate altua, toxizitate intrintseko murritza eta infektatutako zelulak deusezteko ostalariaren immunitiate sistemarekin elkarrekiteko gaitasuna) espektro zabala eta neutralizazio potentzia altua duten bnAb-ak terapia antierretrobiral tradizionalaren osagarri bezala, eta kasu batzuetan ordezko bezala, erabili daitezkela iradokitzen du (Klein, Mouquet, et al., 2013; Sok & Burton, 2018).

Azken hamarkadan B zelula indibidualetan oinarritutako antigorputzen klonazio teknikek eta etekin altuko neutralizazio saioek izandako aurrerapenen ondorioz, GIBaren aurkako bnAb erabilgarrien katalogoa etengabe zabaltzen ari da (Burton & Hangartner, 2016; Burton & Mascola, 2015; Klein, Mouquet, et al., 2013; Kwong & Mascola, 2012). Espezifitate desberdineko bnAb-en aurkikuntzak Env trimeroaren ektodomoeinuko gainazalean aurkitzen diren epitopo kontserbakorren irudi orokor bat eraikitzea ahalbidetu du (Burton & Mascola, 2015; Klein, Mouquet, et al., 2013; Kwong & Mascola, 2012; Sok & Burton, 2018). Hauen artean, gp41 azpiunitateko MPER domeinuaren C muturreko epitopo kontserbakorra (lan honetan C-MPER deitua) itu dutenak dira GIBaren neutralizazio espektro zabalena erakusten dutenak (J. Huang et al., 2012; Kwong & Mascola, 2012; Sok & Burton, 2018; Stiegler et al., 2001; Williams et al., 2017). Hau da, C-MPERen aurkako antigorputzek zirkulazioan dauden GIB-1en andui eta isolatu gehienen infekzioa blokeatzeko gaitasuna dute eta horregatik, pan-neutralizatzaileak kontsideratzen dira (Kwong & Mascola, 2012). 4E10 eta 10E8 dira mota honetako bnAb-en artean, bai estruturalki eta bai funtzionalki hobekien deskribatuak izan direnak (Huang et al., 2012; Irimia et al., 2016, 2017; Kim et al., 2014; Y. do Kwon et al., 2016; Lee et al., 2016; Rujas et al., 2015, 2016; Stiegler et al., 2001; Zwick et al., 2001), eta PhD tesi lan honen protagonistak.

4E10 eta 10E8 bnAb-ek GIBaren aurkako antigorputzen artean espektro zabalena erakusteaz gain, beste ezaugarri berezi bat dute: tximinoak eta gorilak infektatzen dituen immunoeskasiaren birusa edo SHIVa (ingelesetik, *simian/human immunodeficiency virus*) neutralizatzeko gaitasuna (Barbian et al., 2015). Ezaugarri hauek 4E10 bnAb-a immunoterapia pasiboan erabiltzeko aukera aztertzen zuten lan goiztiarrak bultzatu

zituzten. *In vivo* egindako lanek, 4E10 Ab-ak makakoak SHIVaren infekzioatik babesteko gaitasuna berretsi zuten (Ferrantelli et al., 2003; Hessel et al., 2010); 1. faseko eta 2. faseko saio klinikoek, berriz, Ab-aren dosi altuak gizakientzat seguruak eta ongi toleratuak izan zirela egiaztatu zuten (Armbruster et al., 2004; Joos et al., 2006; Mehandru et al., 2007; Verkoczy & Diaz, 2014). Lan hauek, ordea, 4E10ak, 2F5 eta 2G12 antigorputzekin konbinatuta, infektatutako pazienteetan terapia antirretrobirala eten ondoren birusaren berragerraldia ekiditeko gaitasunik ez zuela frogatu zuten (Mehandru et al., 2007; Trkola et al., 2005). Lehenengo belaunaldiko anti-MPER antigorputz hauen eraginkortasun apala arrazoitzeko, gazurrean aurkezten zuten kontzentrazio baxuaren eta potentzia apalaren inguruan eztabaidatu zen (Manrique et al., 2007; Mendoza et al., 2018). Hain zuzen, neutralizazio saio estandarretan 4E10aren bataz-besteko IC_{50} balioak 2-5 μg/mL-ko kontzentrazioen artean mugitzen dira, egun deskribatuak izan diren, eta saio klinikotan dauden antigorputz potenteenekin alderatuz gero 1000 aldiz ahulagoak (Sok & Burton, 2018).

10E8 bigarren belaunaldiko antigorputz potenteagoen artean aurkitzen da, eta bere bataz-besteko IC_{50} balioak 4E10arenak baino 10 aldiz baxuagoak dira (0.1-0.5 μg/mL) (J. Huang et al., 2012; Sok & Burton, 2018). Antigorputz honek, modu pasiboan administratuta, animalia modeloak babesteko gaitasuna erakutsi du lan desberdinetan (Pegu et al., 2014), batez ere antigorputz bi- eta triespezifikoen osagai gisa (Asokan et al., 2015; Huang et al., 2016; Khan et al., 2018; Steinhardt et al., 2018; Xu et al., 2017). Ingeniaritzaz egonkortutako 10E8aren aldaera bat eta CD4 hartzailearen aurkako Ibalizumab antigorputza konbinatzen dituen $10E8_{v2.0}$/iMab molekula biespezifikoaren kasuan, aktibitate antibiral emendatua aurkeztu du *in vivo* (Huang et al., 2016). $10E8_{v2.0}$/iMab formatuak, gainera, beste bnAb eta antigorputz biespezifikoek baina gaitasun handiagoa erakutsi du Saharaz hegoaldeko Afrikan nagusiak diren (Wagh et al., 2018) GIB-1aren A, C eta D azpitaldeen infekzioa prebenitzeko. VRC01/PGDM1400-10E8v4 Ab-en konbinaziotik sortutako molekula triespezifikoaren (SAR441236 izendatua) inguruan eskuratutako emaitzek, bestetik, antigorputz parentalek bakarka zein konbinazioan erakusten dutena baino espektro-potentzia zabalagoa aurkeztu dute (Xu et al., 2017).

Neutralizazio saio estandarrek, haatik, 10E8 antigorputzaren potentzia gaur arte deskribatutako GIB-1aren aurkako bnAb potenteena baina 100 aldiz baxuagoa dela determinatu dute (Sok & Burton, 2018). Zenbat eta potentzia altuagoa izan, orduan eta baxuagoa da banakoa babesteko (profilaxia) (Pegu et al., 2014; Sok & Burton, 2018), zein infektatutako pazienteetan agerraldiak eragozteko (tratamendua) (Mendoza et al., 2018) beharrezkoa den gazurreko antigorputz kontzentrazioa; horregatik,

immunoterapia pasiboan erabili ahal izateko, bere espektro zabala baldintzatu gabe 10E8 antigorputzaren aktibitate antibirala hobetzea helburu desiragarria bilaktu da.

Gaur egun GIB-1aren aurkako bnAb-en potentzia emendatzeko erabiltzen diren estrategiak antigenoarekiko afinitatearen hobekuntzan oinarritzen dira, horretarako diseinu arrazionala (egiturak eskuragarri badaude) edo gainazaleko matrizearen bahetzea (Diskin et al., 2011; Y. do Kwon et al., 2018; Liu et al., 2019; E. Rujas et al., 2018) baliatuz. PhD tesi honetan funtzioa ementzatzeko burututako ahaleginek berriki argitaratutako anti-MPER bnAb-en egitura eta funtzioa erlazionatzen dituzten lan desberdinetan hartu dute funtsa. Hauen arabera, mintzaren interfasearekin egiten dituzteen elkarrekintzek Ab-Env konplexua egonkortzen dute (Irimia et al., 2017; Kwon et al., 2018; Lee et al., 2016; Rantalainen et al., 2020; Rujas et al., 2016, 2018). Informazio honekin, afinitate altuko batuketa-gunetik urrun dauden gainazalen eta mintz biralaren arteko elkarrekintzak indartuz, eta perfil poliespezifikoa asko baldintzatu gabe, anti-MPER bnAb-ak potentziatzea posible dela proposatua da. Gainera, birusaren mintzaz baliatuz lortutako funtzioaren edozein hobekuntza ez litzateke honen ihes-mekanismoen bidez indargabetua izango, birioiek zelula ostalaritik eskuratzen baitute (Freed, 2015). Lan honetan, beraz, birusen mintzetan eragiten duten espektro zabaleko zenbait antibiralen kasuan bezala, bildukia itu egoki eta batez ere, aldagaitz gisa kontsideratua izan da.

4.1 irudiak PhD tesi lan honetan anti-MPER antigorputzen eta mintzen arteko elkarrezkintzak indartzeko jarraitu diren estrategiak laburbiltzen ditu, idazki honen hirugarren kapituluko azpiataletan deskribatuak izan direnak:

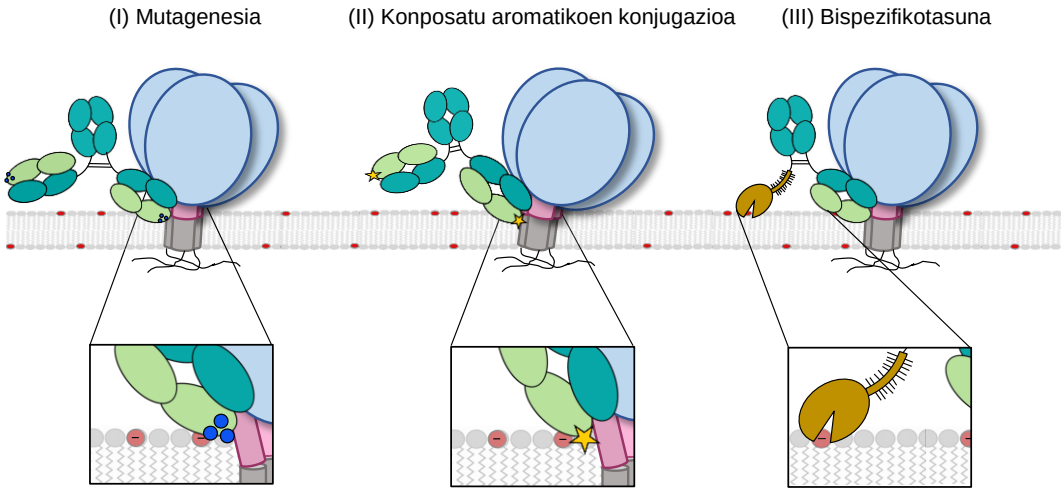

4.1 Iirudia. Tesi honetan anti-MPER antigorputzak optimizatzeko erabilitako estrategia desberdinak. Anti-MPER antigorputzak mutagenesis konbentzionala erabiliz (I), zuzendutako konposatu aromatikoen konjugazioaren bidez (II) eta espezifitate desberdineko bigarren batuketa-bloke bat erantsiz (III) eraldatuak izan dira tesi lan honetan, beren funtzio biologikoa emendatzeko asmoz. MPER kolore arrosazi irudikatu da, antigorputzaren kateak berde argiz (LC) eta ilunez (HC), eta TIM hartzailearen ektodomeinua horiz.

I) 3.1 kapituluan mutagenesi tradizionala erabili da birusaren mintza egokitzeko Fab-ek erabiltzen duten gainazalean Arg hondarrak gehitzeko. Ordezkapen honen helburua gainazal hauen karga neto positiboa handitzea izan da, honen bidez birusaren bildukiarekin elkarrekintza elektrostatikoak sustatzeko; izan ere, birusaren mintzaren kanpoaldeak karga neto negatiboa erakusten du, PS fosfolipido anionikoaren eraginez (Carravilla et al., 2019). Estrategia honi jarraiki, 10E8-3R eta 4E10-3R Fab-ak ekoiztuak izan dira, zeinak PSdun mintzetan banatzeko joera handiagoa erakutsi duten. Bi mutante berrien artean, lehenengoak soilik aurkeztu du aktibitate antibiralaren hobekuntza (hau da, neutralizazio saioetan lortutako bataz-besteko IC_{50} balioak antigorputz basatiarenak baino 5-10 aldiz baxuagoak izan dira). Ez hori bakarrik, 3R mutazioak HC.S100cF ordezkapenarekin konbinatuz, oraindik potentzia altuagoa duen 10E8 antigorputza eskuratu da (basatia baina 20 aldiz hobea neutralizazio saioetan). 3R ordezkapenak, bestalde, ez du 4E10-3R antigorputzaren neutralizazio aktibitatea emendatu.

Mintzarekiko elkarrekintzak indartzeak, beraz, ez du 4E10 antigorputzaren potentzian eraginik. Aurkikuntza hau, anti-MPER antigorputzen neutralizazio mekanismoaren lehen pausu bezala mintzaren batuketa ezinbestekoa dela defendatzen duen hipotesiaren (Chen et al., 2014) aurka doa. Horrez gain, hiru saio desberdin eta osagarriren bidez 10E8 Fab-ak (4E10 eta 4E10-3R baino potenteagoa) espontaneoki mintzekin elkarrekiten ez duela berretsi izanak, antigorputz hauek epitopoari batu aurretik birusaren mintzean pilatzeak neutralizazio mekanismoan bestelako eraginik ez duenaren ideia indartzen du. Era berean, HC.S100cF ordezkapenak 10E8

antigorputzaren HCDR3 begiztaren hidrofobizitatea eta neutralizazio potentzia handitzen baditu ere (Kwon et al., 2018), ez du mintzetan espontaneoki txertatzeko antigorputzaren joera emendatzen.

Horrela, 3.1 kapituluan aurkeztutako emaitzak, orokorrean anti-MPER antigorputzek beren neutralizazio mekanismoaren barruan mintz biralarekin elkarrekiten dutela babesten badute ere, ez datoz bat zenbait lanek proposatutako “bi pausuko” modeloarekin, zeinak anti-MPER antigorputzak lehenik eta behin mintz biralari eta ondoren Env antigenoari batzen direla babesten duen (Alam et al., 2009; J. Chen et al., 2014; Haynes et al., 2010). Eskuratutako datuek Ab eta mintzaren arteko elkarrekintzak Env trimerari batu ondoren, edota batzearekin batera gertatzen direla proposatzen dute. Mintzarekiko batuketak Env-Ab konplexua egonkortuko luke, antigorputzaren potentziaren emendioa afinitate altuko elkarrekintzari lotuz. Bestetik, 4E10aren eta mintzaren arteko elkarrekintza elektrostatikoak murrizteak antigorputzaren neutralizazio potentzia apaltzen duenez (Rujas et al., 2017), baina indartzeak, aldiz, bere funtzionaltasunean eraginik ez duenez, badirudi 4E10 basatiaren kasuan elkarrekintza elektrostatikoek neutralizazio mekanismoan duten eraginak goia jo duela.

II) 3.2 eta 3.3 kapituluek anti-MPER antigorputzak optimizatzeko metodologia berri bat proposatzen dute, proteinak osatzen dituzten aminoazido naturalen katalogoaren mugak gainditzen dituena: zuzendutako konjugazio kimikoaz baliatuz, arazoia erabiliz diseinatu eta aukeratutako molekula sintetikoen eransketa (Krall et al., 2016) (4.1 irudia). Orain arte argitaratutako lanetan, konposatuei lotutako antigorputzek, batetik, gainean daramaten konposatu zitotoxikoari espezifikotasuna ematea (farmako-Ab konjugatuak), edota agente terapeutikoen *in vivo* immunogenizitatea murriztea (polietilen glikolari lotutako Ab-ak, adibidez) (Elgundi et al, 2017) izan dute helburu. Lan honetan erabilitako molekula sintetikoak, ordea, MPER epitopoari batu ondoren mintz biralarekin kontaktuan gelditzen den Fab-aren gainazaleko interfasearekiko hidrofobizitatea handitzeko diseinatuak izan dira.

Lipido bigeruzaren interfasea kimikoki askotarikoa da, eta berezitasun gisa, polaritate gradiente maldatsu bat erakusten du: hau da, fosfolipidoetan aurkitzen diren ur molekulen eta atomo polarren dentsitatea murriztuz doa hidrokarbonoz osatutako nukleora hurbildu ahala (White et al., 2001; White & Wimley, 1999). Wimley eta Whitek hondar aromatikoen albo-kateak interfase honetarantz banatzen direla frogatu zuten (interfasearekiko hidrofobikoak bezala sailaktuak izan ziren) (White & Wimbley, 1999). Ezagumendu hau eta aurretik egindako froga esperimentalak kontuan hartuta, bi kapitulu hauetan aurkeztutako estrategia berriaren bidez C-MPER antigorputzen

potentziaren optimizazioa bilatu da, mintzaren interfasearekin kontaktuan dauden antigorputzaren gainazalak kimikoki eraldatuz. Diseinatutako konposatu aromatikoen bidez, antigorputzen eta birusaren bildukiaren arteko elkarrekintzak egonkortu nahi izan dira.

3.2 kapituluan azaldutako emaitzek, metodologia berri hau erabiliz 10E8 eta 4E10 antigorputzen antigeno batuketa gaitasuna eta aktibitate antibirala bezalako funtzio biologikoak modu esanguratsuan hobetuak izan daitezkela frogatzen dute. Bataz besteko IC_{50} balioak 100 adliz txikiagoak izan dira eraldatutako antigorputz batzuen kasuan, eta beraz, asko hurbiltzen dira gaur egun terapian erabiltzeko aukeratuak izan diren GIB-1aren aurkako bnAb potenteenen balioetara. Orokorrean, antigorptuzen zuzendutako konjugazio kimikoa bi arlo desberdinetan izan daiteke aplikagarria.

Batetik, hurbilketa hau mintzean txertatutako Env antigenoaren eta antigorputzen arteko egitura-funtzio erlazioaren ikerketan izan daiteke baliagarria: anti-MPER antigorputzek mintzak osatzen duen ingurune hidrofobikoan epitoparen ezagumendu molekularra ahalbidetzeko jasandako egokitzapenak ulertzeko erabil daiteke (4.2A Irudia). Konposatu aromatikoen posizioaren araberako efektua, antigorputzak mintzaren interfasearekiko hartzen duen orientazio egokia definitzeko baliatu daiteke; eta antigorputzaren eta MPER helikoidalaren arteko batuketan geometria mesedegarriena definitzeko aukera emango luke. Analisi hau mintzean txertatutako epitopoak ezagutzen dituen edozein antigorputzetara zabaldu daiteke, baita Ab-antigeno egiturari buruzko informazio eskuragarririk ez dagoenean ere. L.S65 posizioan eraldatutako 10E8aren kasu partikularrean, baliteke lortutako aldeko antolaketa hau fusio-aurreko Env trimeroaren egoera konformazionaletako batekiko osagarria izatea (Carravilla et al., 2019; Munro et al., 2014). Are gehiago, behatutako potentzia altuak, optimizatutako 10E8aren batuketak nolabait Env glukoproteinak mintz biralarekiko haserako makurdura modu eraginkorragoan eragin dezakela, edota trimeroa mintzetik bereizita egonkortzeko gaitasun handiagoa duela iradokitzen du, modu honetan Ab-aren k_{off} balioa murriztuz.

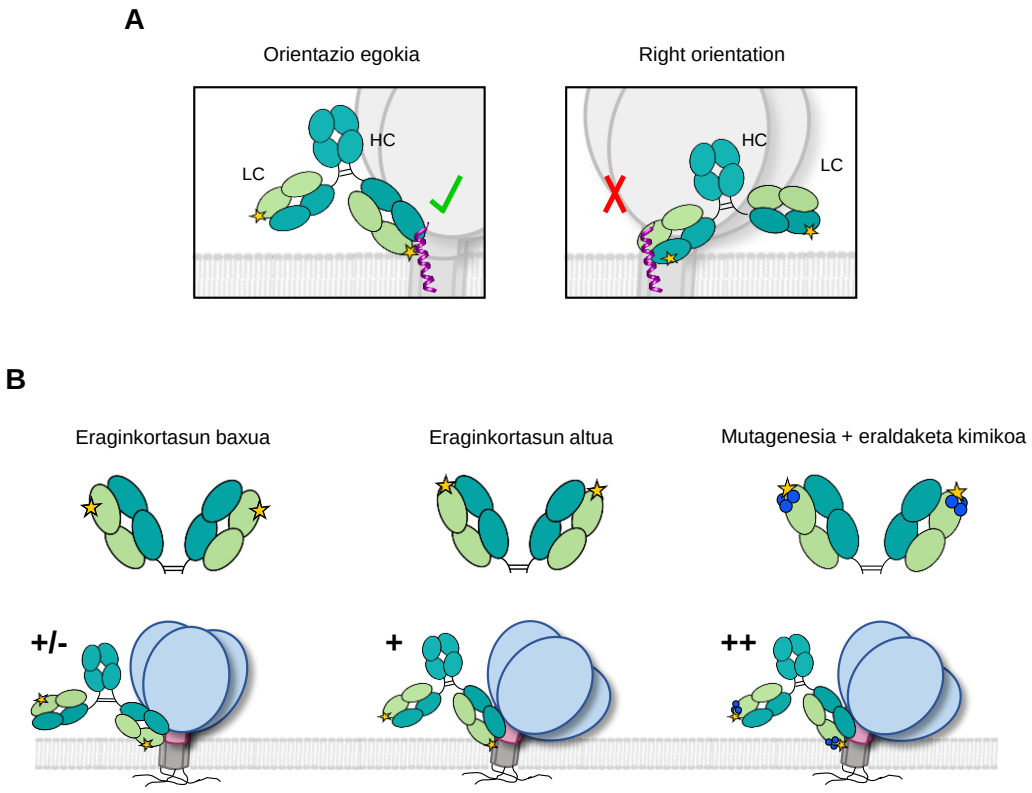

4.2 Irudia. Antigorputzen zuzendutako eraldaketa kimikoaren aplikazioak. (A) Ab-en potentzia hurbilketa-angeluaren araberakoa denez, konposatu aromatikoen eransketa mintzetan murgilduta dauden epitopoak ezagutzen dituzten antigorputzen orientazioa ondorioztatzeko erreminta gisa erabil daiteke. (B) Ezagumendu honek, halaber, ingeniaritza genetikoa erabiliz antigorputzen funtzioak hobetzeko ingeniaritza aukera ematen du: Posizio egokiak aukeratzea, adibidez, erabakigarria izan daiteke potentziaren emendioan. Gainera, eraldaketa kimikoa mutagenesi tradizioanalarekin ere konbina daiteke.

Bestalde, behin antigorputzak mintzarekiko hartuko luken orientazio egokiena determinatu ondoren, Ab hauen bertsio optimizatuen diseinu arrazionalari ekitea posible da (4.2B Irudia). Mintzarekin kontaktuan dauden antigorputzaren eskualde desberdinak eraldatu daitezke adibidez, eta funtzio biologikoan eraginik duten frogatu. Posizio desberdinetan egindako eraldaketak mutagenesi bidez burututako ordezkapenekin ere konbinatu daitezke. Azkenik, hurbilketa honekin jarraituz, izaera eta egitura desberdineko konposatu kimikoak diseinatzea ere posible da (4.3 Irudia). Adibide bat llan honetan deskribatutako konposatu aromatikoak talde funtzional kargatuekin konbinatzea izan daiteke, molekula adarkatuak sortuz. Hala eta guztiz ere, terapian erabiltzea aintzakotzat hartu aurretik, sortutako antigorputz bakoitzaren ezaugarri biologikoak definitzea ezinbestekoa izango da.

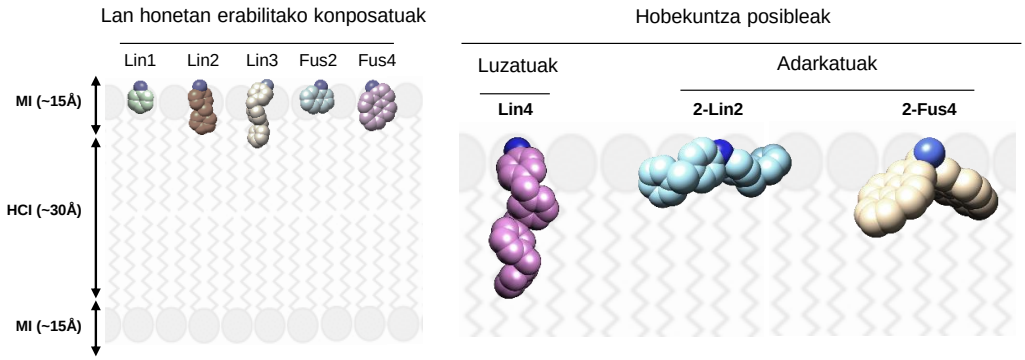

4.3 Irudia. Ezkerretan, tesi lan honetan aukeratutako konposatu sintetikoak. Eskuinetan, etorkizunean erabiliak izan daitezken molekula kimikoetako batzuk.

.3 kapituluan kimikoki eraldaktutako 10E8 antigorputzen (perfil terapeutiko interesgarriena duena) ezaugarri biologikoak aztertuak izan dira. Emaitzek optimizatutako antigorputz bakoitzaren polierreaktibitatea, toxizitatea eta bioeskuragarritasuna erabilitako eraldaketa kimiko konkretuaren menpekoa izan daitekela iradokitzen dute, konsposatu bakoitzaren egitura eta ezaugarri fisiko-kimikoak soilik aztertuz ondorioztatzeko zaila. Zentzu honetan, terapian erabiltzeko garrantzitsua izango da antigorputz berriek PK/PD perfil egokiak aurkeztea, eta beraz, molekula berrien diseinuan kontuan hartzeko ezinbesteko ezaugarria izango da.

III) 3.4 kapituluak fosfolipidoen ezagumendu espezifikoaren erabileraren aukera aztertzen du gainetik, anti-MPER antigorputzen abidezia, eta horrekin batera potentzia, emendatzeko erreminta gisa (4.1 irudia). Hasierako emaitzek anti-MPER Fab-ak eta PS-batuketa domeinuak konbinatuz molekula biespezifikoak sortzea posible dela baieztatu badute ere, esperimentu gehiagoren beharra nabarmentzen da ondorio esanguratsuak atera ahal izateko. Zehatzago, batuketa bloke bakoitzaren portaera karakterizatu beharko litzateke PsVen edo hau imitatzen duten peptido-liposoma modeloak erabiliz. Horrez gain, epitopoari lotzeko gaitasuna murriztua duten mutanteekin eraikitako konbinaketek batuketa bloke bakoitzak elkarrekintzan duen ekarpena definitzea ahalbidetuko lukete.

- **ONDORIOA**

Mintz proteina integralak antigorputzetan oinarritutako terapien garapenean ohiko itua bilakatu dira (Elgundi et al., 2017). Multzo honetan transmintz domienu ugari eta ektodomeinu txikiak dituzten proteinak aurki daitezke, tumoreekin erlazionatutako antigenoak adibidez (CD20 edo CD37 tetraspaninak) (Hendriks et al., 2017); ioi-kanalen familia desberdinak (Hutchings et al., 2019) edota G-proteinei akoplatutako hartzaileak (Hutchings et al., 2017). Kasu guztietan, mintzaren hurbiltasunak afinitate edo potentzia altuko antigorputzen ekoizpena zailtzen du, izan ere, hauen aurka deskribatuak izan diren antigorputz terapeutiko gehienek mintz ingurunean txertatutako edota honen gainazalean etzanda aurkitzen diren epitopoak ezagutzen baitituzte. (Flyak et al., 2018; Hutchings et al., 2017; C. Klein et al., 2013; Jun Ho Lee et al., 2014; Pahuja et al., 2018; S. Z. Xu et al., 2005). Horrez gain, mintzetik gertu aurkitzen diren epitopo biralak ez dira soilik GIBaren Env espikulan deskribatu, eta Influenza edo Ebola birusak bezalako giza-patogeno garrantzitsuen glukoproteinetan ere presente daude (Walker & Burton, 2018).

PhD tesi lan honek aurkezten dituen emaitzen arabera, antigorputzen eta mintzen interfasearen arteko elkarrekintzen sustapena prozedura orokorra izan daiteke itu terapeutiko desberdinetan mintzetik gertu edo mintzez inguratuta dauden epitopoen ezagumendu molekularra emendatzeko.

Chapter 5

REFERENCES

5. REFERENCES

Ahmad, M., Ahmed, O. M., Schnepp, B., & Johnson, P. R. (2017). Engineered Expression of Broadly Neutralizing Antibodies Against Human Immunodeficiency Virus. Annual Review of Virology, 4(1), 491–510. https://doi.org/10.1146/annurev-virology-101416-041929

Alam, S. M., McAdams, M., Boren, D., Rak, M., Scearce, R. M., Gao, F., Camacho, Z. T., Gewirth, D., Kelsoe, G., Chen, P., & Haynes, B. F. (2007). The Role of Antibody Polyspecificity and Lipid Reactivity in Binding of Broadly Neutralizing Anti-HIV-1 Envelope Human Monoclonal Antibodies 2F5 and 4E10 to Glycoprotein 41 Membrane Proximal Envelope Epitopes. The Journal of Immunology, 178(7), 4424–4435. https://doi.org/10.4049/jimmunol.178.7.4424

Alam, S. M., Morelli, M., Dennison, S. M., Liao, H. X., Zhang, R., Xia, S. M., Rits-Volloch, S., Sun, L., Harrison, S. C., Haynes, B. F., & Chen, B. (2009). Role of HIV membrane in neutralization by two broadly neutralizing antibodies. Proceedings of the National Academy of Sciences of the United States of America, 106(48), 20234–20239. https://doi.org/10.1073/pnas.0908713106

Aloia, R. C., Jensen, F. C., Curtain, C. C., Mobley, P. W., & Gordon, L. M. (1988). Lipid composition and fluidity of the human immunodeficiency virus. Proceedings of the National Academy of Sciences of the United States of America, 85(3), 900–904. https://doi.org/10.1073/pnas.85.3.900

Aloia, R. C., Tian, H., & Jensen, F. C. (1993). Lipid composition and fluidity of the human immunodeficiency virus envelope and host cell plasma membranes. Proceedings of the National Academy of Sciences of the United States of America, 90(11), 5181–5185. https://doi.org/10.1073/pnas.90.11.5181

Andersen, O., & Koeppe, R. E. (2008). The preference of tryptophan for membrane interfaces: Insights from N-methylation of tryptophans in gramicidin channels. Article in Journal of Biological Chemistry. https://doi.org/10.1074/jbc.M802074200

Apellániz, B., Huarte, N., Largo, E., & Nieva, J. L. (2014). The three lives of viral fusion peptides. In Chemistry and Physics of Lipids (Vol. 181, pp. 40–55). Elsevier Ireland Ltd. https://doi.org/10.1016/j.chemphyslip.2014.03.003

Apellániz, B., Rujas, E., Carravilla, P., Requejo-Isidro, J., Huarte, N., Domene, C., & Nieva, J. L. (2014). Cholesterol-Dependent Membrane Fusion Induced by the gp41 Membrane-Proximal External Region-Transmembrane Domain Connection Suggests a Mechanism for Broad HIV-1 Neutralization. Journal of Virology, 88(22), 13367–13377. https://doi.org/10.1128/jvi.02151-14

Apellániz, B., Rujas, E., Serrano, S., Morante, K., Tsumoto, K., Caaveiro, J. M. M., Jiménez, M. Á., & Nieva, J. L. (2015). The atomic structure of the HIV-1 gp41 transmembrane domain and its connection to the immunogenic membrane-proximal external region. Journal of Biological Chemistry, 290(21), 12999–13015. https://doi.org/10.1074/jbc.M115.644351

Arbuzova, A., Wang, J., Murray, D., Jacob, J., Cafiso, D. S., & McLaughlin, S. (1997). Kinetics of interaction of the myristoylated alanine-rich C kinase substrate, membranes, and calmodulin. Journal of Biological Chemistry, 272(43), 27167–27177. https://doi.org/10.1074/jbc.272.43.27167

Arbuzova, A., Wang, L., Wang, J., Hangyas-Mihalyne, G., Murray, D., Honig, B., & McLaughlin, S. (2000). Membrane binding of peptides containing both basic and aromatic residues. Experimental studies with peptides corresponding to the scaffolding region of caveolin and the effector region of MARCKS. Biochemistry, 39(33), 10330–10339. https://doi.org/10.1021/bi001039j

Aricescu, A. R., Lu, W., & Jones, E. Y. (2006). A time- and cost-efficient system for high-level protein production in mammalian cells. Acta Crystallographica Section D: Biological Crystallography, 62(10), 1243–1250. https://doi.org/10.1107/S0907444906029799

Armbruster, C., Stiegler, G. M., Vcelar, B. A., Jäger, W., Köller, U., Jilch, R., Ammann, C. G., Pruenster, M., Stoiber, H., & Katinger, H. W. D. (2004). Passive immunization with the anti-HIV-1 human monoclonal antibody (hMAb) 4E10 and the hMAb combination 4E10/2F5/2G12. Journal of Antimicrobial Chemotherapy, 54(5), 915–920. https://doi.org/10.1093/jac/dkh428

Arnaout, R., Lee, W., Cahill, P., Honan, T., Sparrow, T., Weiand, M., Nusbaum, C., Rajewsky, K., & Koralov, S. B. (2011). High-Resolution Description of Antibody Heavy-Chain Repertoires in Humans. PLoS ONE, 6(8), e22365. https://doi.org/10.1371/journal.pone.0022365

Asokan, M., Rudicell, R. S., Louder, M., McKee, K., O'Dell, S., Stewart-Jones, G., Wang, K., Xu, L., Chen, X., Choe, M., Chuang, G., Georgiev, I. S., Joyce, M. G., Kirys, T., Ko, S., Pegu, A., Shi, W., Todd, J. P., Yang, Z., … Mascola, J. R. (2015). Bispecific

Antibodies Targeting Different Epitopes on the HIV-1 Envelope Exhibit Broad and Potent Neutralization. Journal of Virology, 89(24), 12501–12512. https://doi.org/10.1128/jvi.02097-15

Atwell, S., Ridgway, J. B. B., Wells, J. A., & Carter, P. (1997). Stable heterodimers from remodeling the domain interface of a homodimer using a phage display library. Journal of Molecular Biology, 270(1), 26–35. https://doi.org/10.1006/jmbi.1997.1116

Baba, T. W., Liska, V., Hofmann-Lehmann, R., Vlasak, J., Xu, W., Ayehunie, S., Cavacini, L. A., Posner, M. R., Katinger, H., Stiegler, G., Bernacky, B. J., Rizvi, T. A., Schmidt, R., Hill, L. R., Keeling, M. E., Lu, Y., Wright, J. E., Chou, T. C., & Ruprecht, R. M. (2000). Human neutralizing monoclonal antibodies of the IgG1 subtype protect against mucosal simian-human immunodeficiency virus infection. Nature Medicine, 6(2), 200–206. https://doi.org/10.1038/72309

Barbas, C. F., Kang, A. S., Lerner, R. A., & Benkovic, S. J. (1991). Assembly of combinatorial antibody libraries on phage surfaces: The gene III site. Proceedings of the National Academy of Sciences of the United States of America, 88(18), 7978–7982. https://doi.org/10.1073/pnas.88.18.7978

Barbian, H. J., Decker, J. M., Bibollet-Ruche, F., Galimidi, R. P., West, A. P., Learn, G. H., Parrish, N. F., Iyer, S. S., Li, Y., Pace, C. S., Song, R., Huang, Y., Denny, T. N., Mouquet, H., Martin, L., Acharya, P., Zhang, B., Kwong, P. D., Mascola, J. R., … Hahn, B. H. (2015). Neutralization properties of simian immunodeficiency viruses infecting chimpanzees and gorillas. MBio, 6(2), 1–22. https://doi.org/10.1128/mBio.00296-15

Bar-On, Y., Gruell, H., Schoofs, T., Pai, J. A., Nogueira, L., Butler, A. L., Millard, K., Lehmann, C., Suárez, I., Oliveira, T. Y., Karagounis, T., Cohen, Y. Z., Wyen, C., Scholten, S., Handl, L., Belblidia, S., Dizon, J. P., Vehreschild, J. J., Witmer-Pack, M., … Nussenzweig, M. C. (2018). Safety and antiviral activity of combination HIV-1 broadly neutralizing antibodies in viremic individuals. Nature Medicine, 24(11), 1701–1707. https://doi.org/10.1038/s41591-018-0186-4

Barouch, D. H., Whitney, J. B., Moldt, B., Klein, F., Oliveira, T. Y., Liu, J., Stephenson, K. E., Chang, H. W., Shekhar, K., Gupta, S., Nkolola, J. P., Seaman, M. S., Smith, K. M., Borducchi, E. N., Cabral, C., Smith, J. Y., Blackmore, S., Sanisetty, S., Perry, J. R., … Burton, D. R. (2013). Therapeutic efficacy of potent neutralizing HIV-1-specific monoclonal antibodies in SHIV-infected rhesus monkeys. Nature, 503(7475), 224–228. https://doi.org/10.1038/nature12744

Barré-Sinoussi, F., Chermann, J. C., Rey, F., Nugeyre, M. T., Chamaret, S., Gruest, J., Dauguet, C., Axler-Blin, C., Vézinet-Brun, F., Rouzioux, C., Rozenbaum, W., & Montagnier, L. (1983). Isolation of a T-lymphotropic retrovirus from a patient at risk for acquired immune deficiency syndrome (AIDS). Science, 220(4599), 868–871. https://doi.org/10.1126/science.6189183

Bartlett, G. R. (1958). Phosphorus Assay in Column Chromatography*. http://www.jbc.org/

Bebenek, K., Abbotts, J., Wilson, S. H., Kunkelg, T. A., & Biol, J. (1993). Error-prone Polymerization by HIV-1 Reverse Transcriptase: Contribution of template-primer misalignment, miscoding, and termination probability to mutational hot spots*. In The journal of Biological Chemistry (Vol. 268, Issue 14).

Behrens, A. J., & Crispin, M. (2017). Structural principles controlling HIV envelope glycosylation. In Current Opinion in Structural Biology (Vol. 44, pp. 125–133). Elsevier Ltd. https://doi.org/10.1016/j.sbi.2017.03.008

Behrens, A. J., Vasiljevic, S., Pritchard, L. K., Harvey, D. J., Andev, R. S., Krumm, S. A., Struwe, W. B., Cupo, A., Kumar, A., Zitzmann, N., Seabright, G. E., Kramer, H. B., Spencer, D. I. R., Royle, L., Lee, J. H., Klasse, P. J., Burton, D. R., Wilson, I. A., Ward, A. B., … Crispin, M. (2016). Composition and Antigenic Effects of Individual Glycan Sites of a Trimeric HIV-1 Envelope Glycoprotein. Cell Reports, 14(11), 2695–2706. https://doi.org/10.1016/j.celrep.2016.02.058

Belzile, O., Huang, X., Gong, J., Carlson, J., Schroit, A., Brekken, R., & Freimark, B. (2018). Antibody targeting of phosphatidylserine for the detection and immunotherapy of cancer. ImmunoTargets and Therapy, Volume 7, 1–14. https://doi.org/10.2147/itt.s134834

Bessette, P. H., Åslund, F., Beckwith, J., & Georgiou, G. (1999). Efficient folding of proteins with multiple disulfide bonds in the Escherichia coli cytoplasm. Proceedings of the National Academy of Sciences of the United States of America, 96(24), 13703–13708. https://doi.org/10.1073/pnas.96.24.13703

Binley, J. M., Sanders, R. W., Clas, B., Schuelke, N., Master, A., Guo, Y., Kajumo, F., Anselma, D. J., Maddon, P. J., Olson, W. C., & Moore, J. P. (2000). A Recombinant Human Immunodeficiency Virus Type 1 Envelope Glycoprotein Complex Stabilized by an Intermolecular Disulfide Bond between the gp120 and gp41 Subunits Is an Antigenic Mimic of the Trimeric Virion-Associated Structure. Journal of Virology, 74(2), 627–643. https://doi.org/10.1128/jvi.74.2.627-643.2000

Binley, J. M., Wrin, T., Korber, B., Zwick, M. B., Wang, M., Chappey, C., Stiegler, G., Kunert, R., Zolla-Pazner, S., Katinger, H., Petropoulos, C. J., & Burton, D. R. (2004). Comprehensive Cross-Clade Neutralization Analysis of a Panel of Anti-Human Immunodeficiency Virus Type 1 Monoclonal Antibodies. Journal of Virology, 78(23), 13232–13252. https://doi.org/10.1128/jvi.78.23.13232-13252.2004

Blumenthal, R., Durell, S., & Viard, M. (2012). HIV entry and envelope glycoprotein-mediated fusion. In Journal of Biological Chemistry (Vol. 287, Issue 49, pp. 40841–40849). American Society for Biochemistry and Molecular Biology. https://doi.org/10.1074/jbc.R112.406272

Bobardt, M. D., Cheng, G., de Witte, L., Selvarajah, S., Chatterji, U., Sanders-Beer, B. E., Geijtenbeek, T. B. H., Chisari, F. v., & Gallay, P. A. (2008). Hepatitis C virus NS5A anchor peptide disrupts human immunodeficiency virus. Proceedings of the National Academy of Sciences of the United States of America, 105(14), 5525–5530. https://doi.org/10.1073/pnas.0801388105

Bonomelli, C., Doores, K. J., Dunlop, D. C., Thaney, V., Dwek, R. A., Burton, D. R., Crispin, M., & Scanlan, C. N. (2011). The glycan shield of HIV is predominantly oligomannose independently of production system or viral clade. PLoS ONE, 6(8). https://doi.org/10.1371/journal.pone.0023521

Bonsignori, M., Hwang, K.-K., Chen, X., Tsao, C.-Y., Morris, L., Gray, E., Marshall, D. J., Crump, J. A., Kapiga, S. H., Sam, N. E., Sinangil, F., Pancera, M., Yongping, Y., Zhang, B., Zhu, J., Kwong, P. D., O'Dell, S., Mascola, J. R., Wu, L., … Haynes, B. F. (2011). Analysis of a Clonal Lineage of HIV-1 Envelope V2/V3 Conformational Epitope-Specific Broadly Neutralizing Antibodies and Their Inferred Unmutated Common Ancestors. Journal of Virology, 85(19), 9998–10009. https://doi.org/10.1128/jvi.05045-11

Böttcher, C. J. F., Pries, C., & van Gent, C. M. (1961). A rapid and sensitive colorimetric microdetermination of free and bound choline. Recueil Des Travaux Chimiques Des Pays-Bas, 80(11), 1169–1178. https://doi.org/10.1002/recl.19610801102

Bournazos, S., Gazumyan, A., Seaman, M. S., Nussenzweig, M. C., & Ravetch, J. v. (2016). Bispecific Anti-HIV-1 Antibodies with Enhanced Breadth and Potency. Cell, 165(7), 1609–1620. https://doi.org/10.1016/j.cell.2016.04.050

Bournazos, S., Klein, F., Pietzsch, J., Seaman, M. S., Nussenzweig, M. C., & Ravetch, J. v. (2014). Broadly neutralizing anti-HIV-1 antibodies require Fc effector functions for in vivo activity. Cell, 158(6), 1243–1253. https://doi.org/10.1016/j.cell.2014.08.023

Breden, F., Lepik, C., Longo, N. S., Montero, M., Lipsky, P. E., & Scott, J. K. (2011). Comparison of antibody repertoires produced by HIV-1 infection, other chronic and acute infections, and systemic autoimmune disease. PLoS ONE, 6(3). https://doi.org/10.1371/journal.pone.0016857

Brezski, R. J., Kinder, M., Grugan, K. D., Soring, K. L., Carton, J., Greenplate, A. R., Petley, T., Capaldi, D., Brosnan, K., Emmell, E., Watson, S., & Jordan, R. E. (2014). A monoclonal antibody against hinge-cleaved IgG restores effector function to proteolytically inactivated IgGs in vitro and in vivo. MAbs, 6(5), 1265–1273. https://doi.org/10.4161/mabs.29825

Briggs, J. A. G., & Kräusslich, H. G. (2011). The molecular architecture of HIV. In Journal of Molecular Biology (Vol. 410, Issue 4, pp. 491–500). Academic Press. https://doi.org/10.1016/j.jmb.2011.04.021

Briney, B. S., Willis, J. R., & Crowe, J. E. (2012). Human peripheral blood antibodies with long HCDR3s are established primarily at original recombination using a limited subset of germline genes. PLoS ONE, 7(5). https://doi.org/10.1371/journal.pone.0036750

Brügger, B., Glass, B., Haberkant, P., Leibrecht, I., Wieland, F. T., & Kräusslich, H. G. (2006). The HIV lipidome: A raft with an unusual composition. Proceedings of the National Academy of Sciences of the United States of America, 103(8), 2641–2646. https://doi.org/10.1073/pnas.0511136103

Buchacher, A., Predl, R., Strutzenberger, K., Steinfellner, W., Trkola, A., Purtscher, M., Gruber, G., Tauer, C., Steindl, F., Jungbauer, A., & Katinger, H. (1994). Generation of Human Monoclonal Antibodies against HIV-1 Proteins; Electrofusion and Epstein-Barr Virus Transformation for Peripheral Blood Lymphocyte Immortalization. AIDS Research and Human Retroviruses, 10(4), 359–369. https://doi.org/10.1089/aid.1994.10.359

Buchner, C., Bryant, C., Eslami, A., & Lakos, G. (2014). Anti-nuclear antibody screening using HEp-2 cells. Journal of Visualized Experiments, 88(88), 51211. https://doi.org/10.3791/51211

Burges, A., Wimberger, P., Kümper, C., Gorbounova, V., Sommer, H., Schmalfeldt, B., Pfisterer, J., Lichinitser, M., Makhson, A., Moiseyenko, V., Lahr, A., Schulze, E., Jäger, M., Ströhlein, M. A., Heiss, M. M., Gottwald, T., Lindhofer, H., & Kimmig, R. (2007). Effective relief of malignant ascites in patients with advanced ovarian cancer by a trifunctional anti-EpCAM x anti-CD3 antibody: A phase I/II study. Clinical Cancer Research, 13(13), 3899–3905. https://doi.org/10.1158/1078-0432.CCR-06-2769

Burton, D. R. (2002). Antibodies, viruses and vaccines. In Nature Reviews Immunology (Vol. 2, Issue 9, pp. 706–713). Nature Publishing Group. https://doi.org/10.1038/nri891

Burton, D. R. (2017). What are the most powerful immunogen design vaccine strategies?: Reverse vaccinology 2.0 shows great promise. Cold Spring Harbor Perspectives in Biology, 9(11). https://doi.org/10.1101/cshperspect.a030262

Burton, D. R., & Hangartner, L. (2016). Broadly Neutralizing Antibodies to HIV and Their Role in Vaccine Design. Annual Review of Immunology, 34(1), 635–659. https://doi.org/10.1146/annurev-immunol-041015-055515

Burton, D. R., & Mascola, J. R. (2015). Antibody responses to envelope glycoproteins in HIV-1 infection. In Nature Immunology (Vol. 16, Issue 6, pp. 571–576). Nature Publishing Group. https://doi.org/10.1038/ni.3158

Cale, E. M., Gorman, J., Radakovich, N. A., Crooks, E. T., Osawa, K., Tong, T., Li, J., Nagarajan, R., Ozorowski, G., Ambrozak, D. R., Asokan, M., Bailer, R. T., Bennici, A. K., Chen, X., Doria-Rose, N. A., Druz, A., Feng, Y., Joyce, M. G., Louder, M. K., … Binley, J. M. (2017). Virus-like Particles Identify an HIV V1V2 Apex-Binding Neutralizing Antibody that Lacks a Protruding Loop. Immunity, 46(5), 777-791.e10. https://doi.org/10.1016/j.immuni.2017.04.011

Cao, L., Diedrich, J. K., Kulp, D. W., Pauthner, M., He, L., Park, S. K. R., Sok, D., Su, C. Y., Delahunty, C. M., Menis, S., Andrabi, R., Guenaga, J., Georgeson, E., Kubitz, M., Adachi, Y., Burton, D. R., Schief, W. R., Yates, J. R., & Paulson, J. C. (2017). Global site-specific N-glycosylation analysis of HIV envelope glycoprotein. Nature Communications, 8(1), 1–13. https://doi.org/10.1038/ncomms14954

Cardoso, R. M. F., Zwick, M. B., Stanfield, R. L., Kunert, R., Binley, J. M., Katinger, H., Burton, D. R., & Wilson, I. A. (2005). Broadly neutralizing anti-HIV antibody 4E10 recognizes a helical conformation of a highly conserved fusion-associated motif in gp41. Immunity, 22(2), 163–173. https://doi.org/10.1016/j.immuni.2004.12.011

Carravilla, P., Chojnacki, J., Rujas, E., Insausti, S., Largo, E., Waithe, D., Apellaniz, B., Sicard, T., Julien, J. P., Eggeling, C., & Nieva, J. L. (2019). Molecular recognition of the native HIV-1 MPER revealed by STED microscopy of single virions. Nature Communications, 10(1), 1–11. https://doi.org/10.1038/s41467-018-07962-9

Carravilla, P., Darré, L., Oar-Arteta, I. R., Vesga, A. G., Rujas, E., de las Heras-Martínez, G., Domene, C., Nieva, J. L., & Requejo-Isidro, J. (2020). The Bilayer Collective

Properties Govern the Interaction of an HIV-1 Antibody with the Viral Membrane. Biophysical Journal, 118(1), 44–56. https://doi.org/10.1016/j.bpj.2019.11.005

Carravilla, P., & Nieva, J. L. (2018). HIV antivirals: Targeting the functional organization of the lipid envelope. In Future Virology (Vol. 13, Issue 2, pp. 129–140). Future Medicine Ltd. https://doi.org/10.2217/fvl-2017-0114

Caskey, M., Klein, F., Lorenzi, J. C. C., Seaman, M. S., West, A. P., Buckley, N., Kremer, G., Nogueira, L., Braunschweig, M., Scheid, J. F., Horwitz, J. A., Shimeliovich, I., Ben-Avraham, S., Witmer-Pack, M., Platten, M., Lehmann, C., Burke, L. A., Hawthorne, T., Gorelick, R. J., … Nussenzweig, M. C. (2015). Viraemia suppressed in HIV-1-infected humans by broadly neutralizing antibody 3BNC117. Nature, 522(7557), 487–491. https://doi.org/10.1038/nature14411

Caskey, M., Klein, F., & Nussenzweig, M. C. (2019). Broadly neutralizing anti-HIV-1 monoclonal antibodies in the clinic. In Nature Medicine (Vol. 25, Issue 4, pp. 547–553). Nature Publishing Group. https://doi.org/10.1038/s41591-019-0412-8

Caskey, M., Schoofs, T., Gruell, H., Settler, A., Karagounis, T., Kreider, E. F., Murrell, B., Pfeifer, N., Nogueira, L., Oliveira, T. Y., Learn, G. H., Cohen, Y. Z., Lehmann, C., Gillor, D., Shimeliovich, I., Unson-O'Brien, C., Weiland, D., Robles, A., Kümmerle, T., … Klein, F. (2017). Antibody 10-1074 suppresses viremia in HIV-1-infected individuals. Nature Medicine, 23(2), 185–191. https://doi.org/10.1038/nm.4268

Cerutti, N., Loredo-Varela, J. L., Caillat, C., & Weissenhorn, W. (2017). Antigp41 membrane proximal external region antibodies and the art of using the membrane for neutralization. In Current Opinion in HIV and AIDS (Vol. 12, Issue 3, pp. 250–256). Lippincott Williams and Wilkins. https://doi.org/10.1097/COH.0000000000000364

Chan, R., Uchil, P. D., Jin, J., Shui, G., Ott, D. E., Mothes, W., & Wenk, M. R. (2008). Retroviruses Human Immunodeficiency Virus and Murine Leukemia Virus Are Enriched in Phosphoinositides. Journal of Virology, 82(22), 11228–11238. https://doi.org/10.1128/jvi.00981-08

Checkley, M. A., Luttge, B. G., & Freed, E. O. (2011). HIV-1 envelope glycoprotein biosynthesis, trafficking, and incorporation. In Journal of Molecular Biology (Vol. 410, Issue 4, pp. 582–608). Academic Press. https://doi.org/10.1016/j.jmb.2011.04.042

Chen, B., & Chou, J. J. (2017). Structure of the transmembrane domain of HIV-1 envelope glycoprotein. In FEBS Journal (Vol. 284, Issue 8, pp. 1171–1177). Blackwell Publishing Ltd. https://doi.org/10.1111/febs.13954

Chen, J., Frey, G., Peng, H., Rits-Volloch, S., Garrity, J., Seaman, M. S., & Chen, B. (2014). Mechanism of HIV-1 Neutralization by Antibodies Targeting a Membrane-Proximal Region of gp41. Journal of Virology, 88(2), 1249–1258. https://doi.org/10.1128/jvi.02664-13

Chernomordik, L. v., & Kozlov, M. M. (2008). Mechanics of membrane fusion. In Nature Structural and Molecular Biology (Vol. 15, Issue 7, pp. 675–683). Nat Struct Mol Biol. https://doi.org/10.1038/nsmb.1455

Chiliveri, S. C., Louis, J. M., Ghirlando, R., Baber, J. L., & Bax, A. (2018). Tilted, Uninterrupted, Monomeric HIV-1 gp41 Transmembrane Helix from Residual Dipolar Couplings. Journal of the American Chemical Society, 140(1), 34–37. https://doi.org/10.1021/jacs.7b10245

Chojnacki, J., Waithe, D., Carravilla, P., Huarte, N., Galiani, S., Enderlein, J., & Eggeling, C. (2017). Envelope glycoprotein mobility on HIV-1 particles depends on the virus maturation state. Nature Communications, 8(1), 1–10. https://doi.org/10.1038/s41467-017-00515-6

Chothia, C., & Lesk, A. M. (1987). Canonical Structures for the Hypervariable Regions of Immunoglobulins. In Mol. Biol (Vol. 196).

Coffin, J., A, H., JA, L., L, M., S, O., N, T., H, T., K, T., H, V., & P, V. (1986). What to call the AIDS virus? Nature, 321(6065), 10. https://doi.org/10.1038/321010a0

Cohen, M. S., & Kashuba, A. D. M. (2008). Antiretroviral therapy for prevention of HIV infection: New clues from an animal model. In PLoS Medicine (Vol. 5, Issue 2, pp. 0190–0192). Public Library of Science. https://doi.org/10.1371/journal.pmed.0050030

Cohen, M. S., Shaw, G. M., Mcmichael, A. J., Ch, B., & Haynes, B. F. (2011). Acute HIV-1 Infection. https://doi.org/10.1056/NEJMra1011874

Collet, J. F., & Bardwell, J. C. A. (2002). Oxidative protein folding in bacteria. In Molecular Microbiology (Vol. 44, Issue 1, pp. 1–8). John Wiley & Sons, Ltd. https://doi.org/10.1046/j.1365-2958.2002.02851.x

Croney, J. C., Jameson, D. M., & Learmonth, R. P. (2001). Fluorescence spectroscopy in biochemistry: teaching basic principles with visual demonstrations. Biochemistry and Molecular Biology Education, 29(2), 60–65. https://doi.org/10.1111/j.1539-3429.2001.tb00071.x

Dean, P. N. (2001). Confocal Microscopy: Principles and Practices. Current Protocols in Cytometry, 5(1), 2.8.1-2.8.12. https://doi.org/10.1002/0471142956.cy0208s05

de Groot, A. S., & Scott, D. W. (2007). Immunogenicity of protein therapeutics. In Trends in Immunology (Vol. 28, Issue 11, pp. 482–490). Elsevier Current Trends. https://doi.org/10.1016/j.it.2007.07.011

DeKruyff, R. H., Bu, X., Ballesteros, A., Santiago, C., Chim, Y.-L. E., Lee, H.-H., Karisola, P., Pichavant, M., Kaplan, G. G., Umetsu, D. T., Freeman, G. J., & Casasnovas, J. M. (2010). T Cell/Transmembrane, Ig, and Mucin-3 Allelic Variants Differentially Recognize Phosphatidylserine and Mediate Phagocytosis of Apoptotic Cells. The Journal of Immunology, 184(4), 1918–1930. https://doi.org/10.4049/jimmunol.0903059

Dellavance, A., & Andrade, L. E. C. (2019). Detection of autoantibodies by indirect immunofluorescence cytochemistry on Hep-2 cells. In Methods in Molecular Biology (Vol. 1901, pp. 19–46). Humana Press Inc. https://doi.org/10.1007/978-1-4939-8949-2_3

Deng, H. K., Liu, R., Ellmeier, W., Choe, S., Unutmaz, D., Burkhart, M., di Marzio, P., Marmon, S., Sutton, R. E., Mark Hill, C., Davis, C. B., Peiper, S. C., Schall, T. J., Littman, D. R., & Landau, N. R. (1996). Identification of a major co-receptor for primary isolates of HIV-1. Nature, 381(6584), 661–666. https://doi.org/10.1038/381661a0

Dev, J., Park, D., Fu, Q., Chen, J., Ha, H. J., Ghantous, F., Herrmann, T., Chang, W., Liu, Z., Frey, G., Seaman, M. S., Chen, B., & Chou, J. J. (2016). Structural basis for membrane anchoring of HIV-1 envelope spike. Science, 353(6295), 172–175. https://doi.org/10.1126/science.aaf7066

Diskin, R., Scheid, J. F., Marcovecchio, P. M., West, A. P., Klein, F., Gao, H., Gnanapragasam, P. N. P., Abadir, A., Seaman, M. S., Nussenzweig, M. C., & Bjorkman, P. J. (2011). Increasing the potency and breadth of an HIV antibody by using structure-based rational design. Science, 334(6060), 1289–1293. https://doi.org/10.1126/science.1213782

Doria-Rose, N. A., Altae-Tran, H. R., Roark, R. S., Schmidt, S. D., Sutton, M. S., Louder, M. K., Chuang, G. Y., Bailer, R. T., Cortez, V., Kong, R., McKee, K., O'Dell, S., Wang, F., Abdool Karim, S. S., Binley, J. M., Connors, M., Haynes, B. F., Martin, M. A., Montefiori, D. C., … Georgiev, I. S. (2017). Mapping Polyclonal HIV-1 Antibody Responses via Next-Generation Neutralization Fingerprinting. PLoS Pathogens, 13(1). https://doi.org/10.1371/journal.ppat.1006148

Doria-Rose, N. A., Klein, R. M., Manion, M. M., O'Dell, S., Phogat, A., Chakrabarti, B., Hallahan, C. W., Migueles, S. A., Wrammert, J., Ahmed, R., Nason, M., Wyatt, R. T., Mascola, J. R., & Connors, M. (2009). Frequency and Phenotype of Human Immunodeficiency Virus Envelope-Specific B Cells from Patients with Broadly Cross-

Neutralizing Antibodies. Journal of Virology, 83(1), 188–199. https://doi.org/10.1128/jvi.01583-08

Doria-Rose, N. A., & Landais, E. (2019). Coevolution of HIV-1 and broadly neutralizing antibodies. In Current Opinion in HIV and AIDS (Vol. 14, Issue 4, pp. 286–293). Lippincott Williams and Wilkins. https://doi.org/10.1097/COH.0000000000000550

Doria-Rose, N. A., Schramm, C. A., Gorman, J., Moore, P. L., Bhiman, J. N., DeKosky, B. J., Ernandes, M. J., Georgiev, I. S., Kim, H. J., Pancera, M., Staupe, R. P., Altae-Tran, H. R., Bailer, R. T., Crooks, E. T., Cupo, A., Druz, A., Garrett, N. J., Hoi, K. H., Kong, R., … Mascola, J. R. (2014). Developmental pathway for potent V1V2-directed HIV-neutralizing antibodies. Nature, 508(7498), 55–62. https://doi.org/10.1038/nature13036

Dowall, S., Taylor, I., Yeates, P., Smith, L., Rule, A., Easterbrook, L., Bruce, C., Cook, N., Corbin-Lickfett, K., Empig, C., Schlunegger, K., Graham, V., Dennis, M., & Hewson, R. (2013). Catheterized guinea pigs infected with Ebola Zaire virus allows safer sequential sampling to determine the pharmacokinetic profile of a phosphatidylserine-targeting monoclonal antibody. Antiviral Research, 97(2), 108–111. https://doi.org/10.1016/j.antiviral.2012.11.003

Elgundi, Z., Reslan, M., Cruz, E., Sifniotis, V., & Kayser, V. (2017). The state-of-play and future of antibody therapeutics. In Advanced Drug Delivery Reviews (Vol. 122, pp. 2–19). Elsevier B.V. https://doi.org/10.1016/j.addr.2016.11.004

Emu, B., Fessel, J., Schrader, S., Kumar, P., Richmond, G., Win, S., Weinheimer, S., Marsolais, C., & Lewis, S. (2018). Phase 3 Study of Ibalizumab for Multidrug-Resistant HIV-1. New England Journal of Medicine, 379(7), 645–654. https://doi.org/10.1056/NEJMoa1711460

Feng, Y., Broder, C. C., Kennedy, P. E., & Berger, E. A. (1996). HIV-1 entry cofactor: Functional cDNA cloning of a seven-transmembrane, G protein-coupled receptor. Science, 272(5263), 872–877. https://doi.org/10.1126/science.272.5263.872

Ferrantelli, F., Hofmann-Lehmann, R., Rasmussen, R. A., Wang, T., Xu, W., Li, P. L., Montefiori, D. C., Cavacini, L. A., Katinger, H., Stiegler, G., Anderson, D. C., McClure, H. M., & Ruprecht, R. M. (2003). Post-exposure prophylaxis with human monoclonal antibodies prevented SHIV89.6P infection or disease in neonatal macaques. AIDS, 17(3), 301–309. https://doi.org/10.1097/00002030-200302140-00003

Fery-Forgues, S., Fayet, J. P., & Lopez, A. (1993). Drastic changes in the fluorescence properties of NBD probes with the polarity of the medium: involvement of a TICT state?

Journal of Photochemistry and Photobiology, A: Chemistry, 70(3), 229–243. https://doi.org/10.1016/1010-6030(93)85048-D

Finney, J., & Kelsoe, G. (2018). Poly-and autoreactivity of HIV-1 bNAbs: Implications for vaccine design. In Retrovirology (Vol. 15, Issue 1, p. 53). BioMed Central Ltd. https://doi.org/10.1186/s12977-018-0435-0

Fiske, C. H. (1925). The colorimetric determination of phosphorus. J. Biol. Chem, 66. https://www.jbc.org/content/66/2/375.citation

Flyak, A. I., Kuzmina, N., Murin, C. D., Bryan, C., Davidson, E., Gilchuk, P., Gulka, C. P., Ilinykh, P. A., Shen, X., Huang, K., Ramanathan, P., Turner, H., Fusco, M. L., Lampley, R., Kose, N., King, H., Sapparapu, G., Doranz, B. J., Ksiazek, T. G., … Crowe, J. E. (2018). Broadly neutralizing antibodies from human survivors target a conserved site in the ebola virus glycoprotein hr2-mper region. Nature Microbiology, 3(6), 670–677. https://doi.org/10.1038/s41564-018-0157-z

Freed, E. O. (2015). HIV-1 assembly, release and maturation. In Nature Reviews Microbiology (Vol. 13, Issue 8, pp. 484–496). Nature Publishing Group. https://doi.org/10.1038/nrmicro3490

Freeman, G. J., Casasnovas, J. M., Umetsu, D. T., & Dekruyff, R. H. (2010). TIM genes: A family of cell surface phosphatidylserine receptors that regulate innate and adaptive immunity. In Immunological Reviews (Vol. 235, Issue 1, pp. 172–189). https://doi.org/10.1111/j.0105-2896.2010.00903.x

Fugmann, S. D., Lee, A. I., Shockett, P. E., Villey, I. J., & Schatz, D. G. (2000). The RAG Proteins and V(D)J Recombination: Complexes, Ends, and Transposition. Annual Review of Immunology, 18(1), 495–527. https://doi.org/10.1146/annurev.immunol.18.1.495

Fu, Q., Shaik, M. M., Cai, Y., Ghantous, F., Piai, A., Peng, H., Rits-Volloch, S., Liu, Z., Harrison, S. C., Seaman, M. S., Chen, B., & Chou, J. J. (2018). Structure of the membrane proximal external region of HIV-1 envelope glycoprotein. Proceedings of the National Academy of Sciences of the United States of America, 115(38), E8892–E8899. https://doi.org/10.1073/pnas.1807259115

Galiani, S., Waithe, D., Reglinski, K., Cruz-Zaragoza, L. D., Garcia, E., Clausen, M. P., Schliebs, W., Erdmann, R., & Eggeling, C. (2016). Super-resolution microscopy reveals compartmentalization of peroxisomal membrane proteins. Journal of Biological Chemistry, 291(33), 16948–16962. https://doi.org/10.1074/jbc.M116.734038

Gallo, R. C., Salahuddin, S. Z., Popovic, M., Shearer, G. M., Kaplan, M., Haynes, B. F., Palker, T. J., Redfield, R., Oleske, J., Safai, B., White, G., Foster, P., & Markham, P. D. (1984). Frequent detection and isolation of cytopathic retroviruses (HTLV-III) from patients with AIDS and at risk for AIDS. Science, 224(4648), 500–503. https://doi.org/10.1126/science.6200936

Ganser-Pornillos, B. K., Yeager, M., & Pornillos, O. (2012). Assembly and architecture of HIV. Advances in Experimental Medicine and Biology, 726, 441–465. https://doi.org/10.1007/978-1-4614-0980-9_20

Gautam, R., Nishimura, Y., Pegu, A., Nason, M. C., Klein, F., Gazumyan, A., Golijanin, J., Buckler-White, A., Sadjadpour, R., Wang, K., Mankoff, Z., Schmidt, S. D., Lifson, J. D., Mascola, J. R., Nussenzweig, M. C., & Martin, M. A. (2016). A single injection of anti-HIV-1 antibodies protects against repeated SHIV challenges. Nature, 533(7601), 105–109. https://doi.org/10.1038/nature17677

Gerald D Fasman. (1996). Circular Dichroism and the Conformational Analysis of Biomolecules. In Circular Dichroism and the Conformational Analysis of Biomolecules. https://doi.org/10.1007/978-1-4757-2508-7

Go, E. P., Herschhorn, A., Gu, C., Castillo-Menendez, L., Zhang, S., Mao, Y., Chen, H., Ding, H., Wakefield, J. K., Hua, D., Liao, H.-X., Kappes, J. C., Sodroski, J., & Desaire, H. (2015). Comparative Analysis of the Glycosylation Profiles of Membrane-Anchored HIV-1 Envelope Glycoprotein Trimers and Soluble gp140. Journal of Virology, 89(16), 8245–8257. https://doi.org/10.1128/jvi.00628-15

Gray, E. S., Madiga, M. C., Hermanus, T., Moore, P. L., Wibmer, C. K., Tumba, N. L., Werner, L., Mlisana, K., Sibeko, S., Williamson, C., Abdool Karim, S. S., & Morris, L. (2011). The Neutralization Breadth of HIV-1 Develops Incrementally over Four Years and Is Associated with CD4+ T Cell Decline and High Viral Load during Acute Infection. Journal of Virology, 85(10), 4828–4840. https://doi.org/10.1128/jvi.00198-11

Grobben, M., Stuart, R. al, & van Gils, M. J. (2019). The potential of engineered antibodies for HIV-1 therapy and cure. Current Opinion in Virology, 38(Table 1), 70–80. https://doi.org/10.1016/j.coviro.2019.07.007

Gruell, H., & Klein, F. (2018). Antibody-mediated prevention and treatment of HIV-1 infection. In Retrovirology (Vol. 15, Issue 1, p. 73). BioMed Central Ltd. https://doi.org/10.1186/s12977-018-0455-9

Hallenberger, S., Bosch, V., Angliker, H., Shaw, E., Klenk, H. D., & Garten, W. (1992). Inhibition of furin-mediated cleavage activation of HIV-1 glycoprotein gpl60. Nature, 360(6402), 358–361. https://doi.org/10.1038/360358a0

Halper-Stromberg, A., Lu, C. L., Klein, F., Horwitz, J. A., Bournazos, S., Nogueira, L., Eisenreich, T. R., Liu, C., Gazumyan, A., Schaefer, U., Furze, R. C., Seaman, M. S., Prinjha, R., Tarakhovsky, A., Ravetch, J. v., & Nussenzweig, M. C. (2014). Broadly neutralizing antibodies and viral inducers decrease rebound from HIV-1 latent reservoirs in humanized mice. Cell, 158(5), 989–999. https://doi.org/10.1016/j.cell.2014.07.043

Harrison, S. C. (2008). Viral membrane fusion. In Nature Structural and Molecular Biology (Vol. 15, Issue 7, pp. 690–698). Nature Publishing Group. https://doi.org/10.1038/nsmb.1456

Haynes, B. F., Fleming, J., st. Clair, E. W., Katinger, H., Stiegler, G., Kunert, R., Robinson, J., Scearce, R. M., Plonk, K., Staats, H. F., Ortel, T. L., Liao, H. X., & Alam, S. M. (2005). Cardiolipin polyspecific autoreactivity in two broadly neutralizing HIV-1 antibodies. Science, 308(5730), 1906–1908. https://doi.org/10.1126/science.1111781

Haynes, B. F., & Mascola, J. R. (2017). The quest for an antibody-based HIV vaccine. In Immunological Reviews (Vol. 275, Issue 1, pp. 5–10). Blackwell Publishing Ltd. https://doi.org/10.1111/imr.12517

Haynes, B. F., Nicely, N. I., & Alam, S. M. (2010). HIV-1 autoreactive antibodies: Are they good or bad for HIV-1 prevention? In Nature Structural and Molecular Biology (Vol. 17, Issue 5, pp. 543–545). NIH Public Access. https://doi.org/10.1038/nsmb0510-543

Henderson, R., Lu, M., Zhou, Y., Mu, Z., Parks, R., Han, Q., Hsu, A. L., Carter, E., Blanchard, S. C., Edwards, R. J., Wiehe, K., Saunders, K. O., Borgnia, M. J., Bartesaghi, A., Mothes, W., Haynes, B. F., Acharya, P., & Munir Alam, S. (2020). Disruption of the HIV-1 Envelope allosteric network blocks CD4-induced rearrangements. Nature Communications, 11(1), 1–14. https://doi.org/10.1038/s41467-019-14196-w

Hendriks, D., Choi, G., de Bruyn, M., Wiersma, V. R., & Bremer, E. (2017). Antibody-Based Cancer Therapy: Successful Agents and Novel Approaches. In International Review of Cell and Molecular Biology (Vol. 331, pp. 289–383). Elsevier Inc. https://doi.org/10.1016/bs.ircmb.2016.10.002

Hessell, A. J., Poignard, P., Hunter, M., Hangartner, L., Tehrani, D. M., Bleeker, W. K., Parren, P. W. H. I., Marx, P. A., & Burton, D. R. (2009). Effective, low-titer antibody

protection against low-dose repeated mucosal SHIV challenge in macaques. Nature Medicine, 15(8), 951–954. https://doi.org/10.1038/nm.1974

Hessell, A. J., Rakasz, E. G., Tehrani, D. M., Huber, M., Weisgrau, K. L., Landucci, G., Forthal, D. N., Koff, W. C., Poignard, P., Watkins, D. I., & Burton, D. R. (2010). Broadly Neutralizing Monoclonal Antibodies 2F5 and 4E10 Directed against the Human Immunodeficiency Virus Type 1 gp41 Membrane-Proximal External Region Protect against Mucosal Challenge by Simian-Human Immunodeficiency Virus SHIVBa-L. Journal of Virology, 84(3), 1302–1313. https://doi.org/10.1128/jvi.01272-09

Heuck, A. P., Hotze, E. M., Tweten, R. K., & Johnson, A. E. (2000). Mechanism of membrane insertion of a multimeric β-barrel protein: Perfringolysin O creates a pore using ordered and coupled conformational changes. Molecular Cell, 6(5), 1233–1242. https://doi.org/10.1016/S1097-2765(00)00119-2

Huang, J., Kang, B. H., Ishida, E., Zhou, T., Griesman, T., Sheng, Z., Wu, F., Doria-Rose, N. A., Zhang, B., McKee, K., O'Dell, S., Chuang, G. Y., Druz, A., Georgiev, I. S., Schramm, C. A., Zheng, A., Joyce, M. G., Asokan, M., Ransier, A., … Connors, M. (2016). Identification of a CD4-Binding-Site Antibody to HIV that Evolved Near-Pan Neutralization Breadth. Immunity, 45(5), 1108–1121. https://doi.org/10.1016/j.immuni.2016.10.027

Huang, J., Kang, B. H., Pancera, M., Lee, J. H., Tong, T., Feng, Y., Imamichi, H., Georgiev, I. S., Chuang, G. Y., Druz, A., Doria-Rose, N. A., Laub, L., Sliepen, K., van Gils, M. J., de La Peña, A. T., Derking, R., Klasse, P. J., Migueles, S. A., Bailer, R. T., … Connors, M. (2014). Broad and potent HIV-1 neutralization by a human antibody that binds the gp41-gp120 interface. Nature, 515(7525), 138–142. https://doi.org/10.1038/nature13601

Huang, J., Ofek, G., Laub, L., Louder, M. K., Doria-Rose, N. A., Longo, N. S., Imamichi, H., Bailer, R. T., Chakrabarti, B., Sharma, S. K., Alam, S. M., Wang, T., Yang, Y., Zhang, B., Migueles, S. A., Wyatt, R., Haynes, B. F., Kwong, P. D., Mascola, J. R., & Connors, M. (2012). Broad and potent neutralization of HIV-1 by a gp41-specific human antibody. Nature, 491(7424), 406–412. https://doi.org/10.1038/nature11544

Huang, Y., Yu, J., Lanzi, A., Yao, X., Andrews, C. D., Tsai, L., Gajjar, M. R., Sun, M., Seaman, M. S., Padte, N. N., & Ho, D. D. (2016). Engineered Bispecific Antibodies with Exquisite HIV-1-Neutralizing Activity. Cell, 165(7), 1621–1631. https://doi.org/10.1016/j.cell.2016.05.024

Huarte, N., Carravilla, P., Cruz, A., Lorizate, M., Nieto-Garai, J. A., Kräusslich, H. G., Pérez-Gil, J., Requejo-Isidro, J., & Nieva, J. L. (2016). Functional organization of the HIV lipid envelope. Scientific Reports, 6. https://doi.org/10.1038/srep34190

Hutchings, C. J., Colussi, P., & Clark, T. G. (2019). Ion channels as therapeutic antibody targets. In mAbs (Vol. 11, Issue 2, pp. 265–296). Taylor and Francis Inc. https://doi.org/10.1080/19420862.2018.1548232

Hutchings, C. J., Koglin, M., Olson, W. C., & Marshall, F. H. (2017). Opportunities for therapeutic antibodies directed at G-protein-coupled receptors. In Nature Reviews Drug Discovery (Vol. 16, Issue 11, pp. 787–810). Nature Publishing Group. https://doi.org/10.1038/nrd.2017.91

Igarashi, T., Brown, C., Azadegan, A., Haigwood, N., Dimitrov, D., Martin, M. A., & Shibata, R. (1999). Human immunodeficiency virus type 1 neutralizing antibodies accelerate clearance of cell-free virions from blood plasma. Nature Medicine, 5(2), 211–216. https://doi.org/10.1038/5576

Igawa, T., Tsunoda, H., Kuramochi, T., Sampei, Z., Ishii, S., & Hattori, K. (2011). Engineering the variable region of therapeutic IgG antibodies. In mAbs (Vol. 3, Issue 3, pp. 243–252). Landes Bioscience. https://doi.org/10.4161/mabs.3.3.15234

Irimia, A., Sarkar, A., Stanfield, R. L., & Wilson, I. A. (2016). Crystallographic Identification of Lipid as an Integral Component of the Epitope of HIV Broadly Neutralizing Antibody 4E10. Immunity, 44(1), 21–31. https://doi.org/10.1016/j.immuni.2015.12.001

Irimia, A., Serra, A. M., Sarkar, A., Jacak, R., Kalyuzhniy, O., Sok, D., Saye-Francisco, K. L., Schiffner, T., Tingle, R., Kubitz, M., Adachi, Y., Stanfield, R. L., Deller, M. C., Burton, D. R., Schief, W. R., & Wilson, I. A. (2017). Lipid interactions and angle of approach to the HIV-1 viral membrane of broadly neutralizing antibody 10E8: Insights for vaccine and therapeutic design. PLoS Pathogens, 13(2), 1–20. https://doi.org/10.1371/journal.ppat.1006212

Isenegger, P. G., & Davis, B. G. (2020). Concepts of catalysis in site-selective protein modifications. In Journal of the American Chemical Society (Vol. 141, Issue 20, pp. 8005–8013). American Chemical Society. https://doi.org/10.1021/jacs.8b13187

Jacob, R. A., Moyo, T., Schomaker, M., Abrahams, F., Grau Pujol, B., & Dorfman, J. R. (2015). Anti-V3/Glycan and Anti-MPER Neutralizing Antibodies, but Not Anti-V2/Glycan Site Antibodies, Are Strongly Associated with Greater Anti-HIV-1 Neutralization Breadth

and Potency. Journal of Virology, 89(10), 5264–5275. https://doi.org/10.1128/jvi.00129-15

Jen, E. Y., Xu, Q., Schetter, A., Przepiorka, D., Shen, Y. L., Roscoe, D., Sridhara, R., Deisseroth, A., Philip, R., Farrell, A. T., & Pazdur, R. (2019). FDA approval: Blinatumomab for Patients with B-cell Precursor Acute Lymphoblastic Leukemia in Morphologic Remission with Minimal Residual Disease. Clinical Cancer Research, 25(2), 473–477. https://doi.org/10.1158/1078-0432.CCR-18-2337

Jiménez-Díaz, M. B., Mulet, T., Viera, S., Gómez, V., Garuti, H., Ibáñez, J., Alvarez-Doval, A., Shultz, L. D., Martínez, A., Gargallo-Viola, D., & Angulo-Barturen, I. (2009). Improved murine model of malaria using Plasmodium falciparum competent strains and non-myelodepleted NOD-scid IL2Rgammanull mice engrafted with human erythrocytes. *Antimicrobial agents and chemotherapy*, *53*(10), 4533–4536. https://doi.org/10.1128/AAC.00519-09

Johnson, W. E., & Desrosiers, R. C. (2002). Viral Persistence: HIV's Strategies of Immune System Evasion. Annual Review of Medicine, 53(1), 499–518. https://doi.org/10.1146/annurev.med.53.082901.104053

Joos, B., Trkola, A., Kuster, H., Aceto, L., Fischer, M., Stiegler, G., Armbruster, C., Vcelar, B., Katinger, H., & Günthard, H. F. (2006). Long-term multiple-dose pharmacokinetics of human monoclonal antibodies (MAbs) against human immunodeficiency virus type 1 envelope gp120 (MAb 2G12) and gp41 (MAbs 4E10 and 2F5). Antimicrobial Agents and Chemotherapy, 50(5), 1773–1779. https://doi.org/10.1128/AAC.50.5.1773-1779.2006

Julg, B., Sok, D., Schmidt, S. D., Abbink, P., Newman, R. M., Broge, T., Linde, C., Nkolola, J., Le, K., Su, D., Torabi, J., Pack, M., Pegu, A., Allen, T. M., Mascola, J. R., Burton, D. R., & Barouch, D. H. (2017). Protective Efficacy of Broadly Neutralizing Antibodies with Incomplete Neutralization Activity against Simian-Human Immunodeficiency Virus in Rhesus Monkeys. Journal of Virology, 91(20). https://doi.org/10.1128/jvi.01187-17

Julien, J. P., Cupo, A., Sok, D., Stanfield, R. L., Lyumkis, D., Deller, M. C., Klasse, P. J., Burton, D. R., Sanders, R. W., Moore, J. P., Ward, A. B., & Wilson, I. A. (2013). Crystal structure of a soluble cleaved HIV-1 envelope trimer. Science, 342(6165), 1477–1483. https://doi.org/10.1126/science.1245625

Julien, J. P., Huarte, N., Maeso, R., Taneva, S. G., Cunningham, A., Nieva, J. L., & Pai, E. F. (2010). Ablation of the Complementarity-Determining Region H3 Apex of the Anti-

HIV-1 Broadly Neutralizing Antibody 2F5 Abrogates Neutralizing Capacity without Affecting Core Epitope Binding. Journal of Virology, 84(9), 4136–4147. https://doi.org/10.1128/jvi.02357-09

Julien, J. P., Sok, D., Khayat, R., Lee, J. H., Doores, K. J., Walker, L. M., Ramos, A., Diwanji, D. C., Pejchal, R., Cupo, A., Katpally, U., Depetris, R. S., Stanfield, R. L., McBride, R., Marozsan, A. J., Paulson, J. C., Sanders, R. W., Moore, J. P., Burton, D. R., … Wilson, I. A. (2013). Broadly Neutralizing Antibody PGT121 Allosterically Modulates CD4 Binding via Recognition of the HIV-1 gp120 V3 Base and Multiple Surrounding Glycans. PLoS Pathogens, 9(5), e1003342. https://doi.org/10.1371/journal.ppat.1003342

Kang, T. H., & Jung, S. T. (2019). Boosting therapeutic potency of antibodies by taming Fc domain functions. In Experimental and Molecular Medicine (Vol. 51, Issue 11, pp. 1–9). Springer Nature. https://doi.org/10.1038/s12276-019-0345-9

Kaur, J., Kumar, A., & Kaur, J. (2018). Strategies for optimization of heterologous protein expression in E. coli: Roadblocks and reinforcements. In International Journal of Biological Macromolecules (Vol. 106, pp. 803–822). Elsevier B.V. https://doi.org/10.1016/j.ijbiomac.2017.08.080

Keele, B. F., van Heuverswyn, F., Li, Y., Bailes, E., Takehisa, J., Santiago, M. L., Bibollet-Ruche, F., Chen, Y., Wain, L. v., Liegeois, F., Loul, S., Ngole, E. M., Bienvenue, Y., Delaporte, E., Brookfield, J. F. Y., Sharp, P. M., Shaw, G. M., Peeters, M., & Hahn, B. H. (2006). Chimpanzee reservoirs of pandemic and nonpandemic HIV-1. Science, 313(5786), 523–526. https://doi.org/10.1126/science.1126531

Kepler, T. B., Liao, H. X., Alam, S. M., Bhaskarabhatla, R., Zhang, R., Yandava, C., Stewart, S., Anasti, K., Kelsoe, G., Parks, R., Lloyd, K. E., Stolarchuk, C., Pritchett, J., Solomon, E., Friberg, E., Morris, L., Karim, S. S. A., Cohen, M. S., Walter, E., … Haynes, B. F. (2014). Immunoglobulin gene insertions and deletions in the affinity maturation of HIV-1 broadly reactive neutralizing antibodies. Cell Host and Microbe, 16(3), 304–313. https://doi.org/10.1016/j.chom.2014.08.006

Khan, S. N., Sok, D., Tran, K., Movsesyan, A., Dubrovskaya, V., Burton, D. R., & Wyatt, R. T. (2018). Targeting the HIV-1 Spike and Coreceptor with Bi- and Trispecific Antibodies for Single-Component Broad Inhibition of Entry. Journal of Virology, 92(18), 384–402. https://doi.org/10.1128/jvi.00384-18

Kim, A. S., Leaman, D. P., & Zwick, M. B. (2014). Antibody to gp41 MPER Alters Functional Properties of HIV-1 Env without Complete Neutralization. PLoS Pathogens, 10(7), e1004271. https://doi.org/10.1371/journal.ppat.1004271

Klatzmann, D., Champagne, E., Chamaret, S., Gruest, J., Guetard, D., Hercend, T., Gluckman, J. C., & Montagnier, L. (1984). T-lymphocyte T4 molecule behaves as the receptor for human retrovirus LAV. Nature, 312(5996), 767–768. https://doi.org/10.1038/312767a0

Klein, C., Lammens, A., Schäfer, W., Georges, G., Schwaiger, M., Mössner, E., Hopfner, K. P., Umaña, P., & Niederfellner, G. (2013). Epitope interactions of monoclonal antibodies targeting CD20 and their relationship to functional properties. MAbs, 5(1), 22–33. https://doi.org/10.4161/mabs.22771

Klein, F., Diskin, R., Scheid, J. F., Gaebler, C., Mouquet, H., Georgiev, I. S., Pancera, M., Zhou, T., Incesu, R. B., Fu, B. Z., Gnanapragasam, P. N. P., Oliveira, T. Y., Seaman, M. S., Kwong, P. D., Bjorkman, P. J., & Nussenzweig, M. C. (2013). Somatic mutations of the immunoglobulin framework are generally required for broad and potent HIV-1 neutralization. Cell, 153(1), 126–138. https://doi.org/10.1016/j.cell.2013.03.018

Klein, F., Halper-Stromberg, A., Horwitz, J. A., Gruell, H., Scheid, J. F., Bournazos, S., Mouquet, H., Abadir, A., Diskin, R., Abadir, A., Zang, T., Dorner, M., Billerbeck, E., Labitt, R. N., Gaebler, C., Marcovecchio, P. M., Incesu, R. B., Eisenreich, T. R., Bieniasz, P. D., … Nussenzweig, M. C. (2012). HIV therapy by a combination of broadly neutralizing antibodies in humanized mice. In Nature (Vol. 492, Issue 7427, pp. 118–122). https://doi.org/10.1038/nature11604

Klein, F., Mouquet, H., Dosenovic, P., Scheid, J. F., Scharf, L., & Nussenzweig, M. C. (2013). Antibodies in HIV-1 vaccine development and therapy. Science, 341(6151), 1199–1204. https://doi.org/10.1126/science.1241144

Klein, J. S., Gnanapragasam, P. N. P., Galimidi, R. P., Foglesong, C. P., West, A. P., & Bjorkman, P. J. (2009). Examination of the contributions of size and avidity to the neutralization mechanisms of the anti-HIV antibodies b12 and 4E10. Proceedings of the National Academy of Sciences of the United States of America, 106(18), 7385–7390. https://doi.org/10.1073/pnas.0811427106

Köhler, G., & Milstein, C. (1975). Continuous cultures of fused cells secreting antibody of predefined specificity. Nature, 256(5517), 495–497. https://doi.org/10.1038/256495a0

Kolchinsky, P., Kiprilov, E., & Sodroski, J. (2001). Increased Neutralization Sensitivity of CD4-Independent Human Immunodeficiency Virus Variants. Journal of Virology, 75(5), 2041–2050. https://doi.org/10.1128/jvi.75.5.2041-2050.2001

Kong, L., Lee, J. H., Doores, K. J., Murin, C. D., Julien, J. P., McBride, R., Liu, Y., Marozsan, A., Cupo, A., Klasse, P. J., Hoffenberg, S., Caulfield, M., King, C. R., Hua, Y., Le, K. M., Khayat, R., Deller, M. C., Clayton, T., Tien, H., … Wilson, I. A. (2013). Supersite of immune vulnerability on the glycosylated face of HIV-1 envelope glycoprotein gp120. Nature Structural and Molecular Biology, 20(7), 796–803. https://doi.org/10.1038/nsmb.2594

Kong, R., Xu, K., Zhou, T., Acharya, P., Lemmin, T., Liu, K., Ozorowski, G., Soto, C., Taft, J. D., Bailer, R. T., Cale, E. M., Chen, L., Choi, C. W., Chuang, G. Y., Doria-Rose, N. A., Druz, A., Georgiev, I. S., Gorman, J., Huang, J., … Mascola, J. R. (2016). Fusion peptide of HIV-1 as a site of vulnerability to neutralizing antibody. Science, 352(6287), 828–833. https://doi.org/10.1126/science.aae0474

Ko, S. Y., Pegu, A., Rudicell, R. S., Yang, Z. Y., Joyce, M. G., Chen, X., Wang, K., Bao, S., Kraemer, T. D., Rath, T., Zeng, M., Schmidt, S. D., Todd, J. P., Penzak, S. R., Saunders, K. O., Nason, M. C., Haase, A. T., Rao, S. S., Blumberg, R. S., … Nabel, G. J. (2014). Enhanced neonatal Fc receptor function improves protection against primate SHIV infection. Nature, 514(7524), 642–645. https://doi.org/10.1038/nature13612

Koyanagi, Y., Miles, S., Mitsuyasu, R. T., Merrill, J. E., Vinters, H. v., & Chen, I. S. Y. (1987). Dual infection of the central nervous system by AIDS viruses with distinct cellular tropisms. Science, 236(4803), 819–822. https://doi.org/10.1126/science.3646751

Krall, N., da Cruz, F. P., Boutureira, O., & Bernardes, G. J. L. (2016). Site-selective protein-modification chemistry for basic biology and drug development. Nature Chemistry, 8(2), 103–113. https://doi.org/10.1038/nchem.2393

Krebs, S. J., Kwon, Y. D., Schramm, C. A., Law, W. H., Donofrio, G., Zhou, K. H., Gift, S., Dussupt, V., Georgiev, I. S., Schätzle, S., McDaniel, J. R., Lai, Y. T., Sastry, M., Zhang, B., Jarosinski, M. C., Ransier, A., Chenine, A. L., Asokan, M., Bailer, R. T., … Doria-Rose, N. A. (2019). Longitudinal Analysis Reveals Early Development of Three MPER-Directed Neutralizing Antibody Lineages from an HIV-1-Infected Individual. Immunity, 50(3), 677-691.e13. https://doi.org/10.1016/j.immuni.2019.02.008

Kreer, C., Gruell, H., Mora, T., Walczak, A. M., & Klein, F. (2020). Exploiting B Cell Receptor Analyses to Inform on HIV-1 Vaccination Strategies. Vaccines, 8(1), 13. https://doi.org/10.3390/vaccines8010013

Kumaraswamy, S., & Tobias, R. (2015). Label-Free Kinetic Analysis of an Antibody–Antigen Interaction Using Biolayer Interferometry. In Protein-Protein Interactions: Methods and Applications: Second Edition (pp. 165–182). Springer New York. https://doi.org/10.1007/978-1-4939-2425-7_10

Kwon, B., Lee, M., Waring, A. J., & Hong, M. (2018). Oligomeric Structure and Three-Dimensional Fold of the HIV gp41 Membrane-Proximal External Region and Transmembrane Domain in Phospholipid Bilayers. Journal of the American Chemical Society, 140(26), 8246–8259. https://doi.org/10.1021/jacs.8b04010

Kwon, Y. do, Chuang, G. Y., Zhang, B., Bailer, R. T., Doria-Rose, N. A., Gindin, T. S., Lin, B., Louder, M. K., McKee, K., O'Dell, S., Pegu, A., Schmidt, S. D., Asokan, M., Chen, X., Choe, M., Georgiev, I. S., Jin, V., Pancera, M., Rawi, R., … Kwong, P. D. (2018). Surface-Matrix Screening Identifies Semi-specific Interactions that Improve Potency of a Near Pan-reactive HIV-1-Neutralizing Antibody. Cell Reports, 22(7), 1798–1809. https://doi.org/10.1016/j.celrep.2018.01.023

Kwon, Y. do, Finzi, A., Wu, X., Dogo-Isonagie, C., Lee, L. K., Moore, L. R., Schmidt, S. D., Stuckey, J., Yang, Y., Zhou, T., Zhu, J., Vicic, D. A., Debnath, A. K., Shapiro, L., Bewley, C. A., Mascola, J. R., Sodroski, J. G., & Kwong, P. D. (2012). Unliganded HIV-1 gp120 core structures assume the CD4-bound conformation with regulation by quaternary interactions and variable loops. Proceedings of the National Academy of Sciences of the United States of America, 109(15), 5663–5668. https://doi.org/10.1073/pnas.1112391109

Kwon, Y. do, Georgiev, I. S., Ofek, G., Zhang, B., Asokan, M., Bailer, R. T., Bao, A., Caruso, W., Chen, X., Choe, M., Druz, A., Ko, S.-Y., Louder, M. K., McKee, K., O'Dell, S., Pegu, A., Rudicell, R. S., Shi, W., Wang, K., … Kwong, P. D. (2016). Optimization of the Solubility of HIV-1-Neutralizing Antibody 10E8 through Somatic Variation and Structure-Based Design. Journal of Virology, 90(13), 5899–5914. https://doi.org/10.1128/jvi.03246-15

Kwong, P. D. (2017). What are the most powerful immunogen design vaccine strategies?: A structural biologist's perspective. Cold Spring Harbor Perspectives in Biology, 9(11). https://doi.org/10.1101/cshperspect.a029470

Kwong, P. D., & Mascola, J. R. (2012). Human Antibodies that Neutralize HIV-1: Identification, Structures, and B Cell Ontogenies. Immunity, 37(3), 412–425. https://doi.org/10.1016/j.immuni.2012.08.012

Kwon, Y. D., Pancera, M., Acharya, P., Georgiev, I. S., Crooks, E. T., Gorman, J., Joyce, M. G., Guttman, M., Ma, X., Narpala, S., Soto, C., Terry, D. S., Yang, Y., Zhou, T., Ahlsen, G., Bailer, R. T., Chambers, M., Chuang, G. Y., Doria-Rose, N. A., … Kwong, P. D. (2015). Crystal structure, conformational fixation and entry-related interactions of mature ligand-free HIV-1 Env. Nature Structural and Molecular Biology, 22(7), 522–531. https://doi.org/10.1038/nsmb.3051

Ladokhin, A. S., Jayasinghe, S., & White, S. H. (2000). How to Measure and Analyze Tryptophan Fluorescence in Membranes Properly, and Why Bother? Analytical Biochemistry, 285, 235–245. https://doi.org/10.1006/abio.2000.4773

Lai, Y. T., Wang, T., O'Dell, S., Louder, M. K., Schön, A., Cheung, C. S. F., Chuang, G. Y., Druz, A., Lin, B., McKee, K., Peng, D., Yang, Y., Zhang, B., Herschhorn, A., Sodroski, J., Bailer, R. T., Doria-Rose, N. A., Mascola, J. R., Langley, D. R., & Kwong, P. D. (2019). Lattice engineering enables definition of molecular features allowing for potent small-molecule inhibition of HIV-1 entry. Nature Communications, 10(1). https://doi.org/10.1038/s41467-018-07851-1

Land, A., Zonneveld, D., & Braakman, I. (2003). Folding of HIV-1 Envelope glycoprotein involves extensive isomerization of disulfide bonds and conformation-dependent leader peptide cleavage. The FASEB Journal, 17(9), 1058–1067. https://doi.org/10.1096/fj.02-0811com

Lanzavecchia, A., Corti, D., & Sallusto, F. (2007). Human monoclonal antibodies by immortalization of memory B cells. In Current Opinion in Biotechnology (Vol. 18, Issue 6, pp. 523–528). Elsevier Current Trends. https://doi.org/10.1016/j.copbio.2007.10.011

Lee, Jeong Hyun, Andrabi, R., Su, C. Y., Yasmeen, A., Julien, J. P., Kong, L., Wu, N. C., McBride, R., Sok, D., Pauthner, M., Cottrell, C. A., Nieusma, T., Blattner, C., Paulson, J. C., Klasse, P. J., Wilson, I. A., Burton, D. R., & Ward, A. B. (2017). A Broadly Neutralizing Antibody Targets the Dynamic HIV Envelope Trimer Apex via a Long, Rigidified, and Anionic β-Hairpin Structure. Immunity, 46(4), 690–702. https://doi.org/10.1016/j.immuni.2017.03.017

Lee, Jeong Hyun, Ozorowski, G., & Ward, A. B. (2016). Cryo-EM structure of a native, fully glycosylated, cleaved HIV-1 envelope trimer. Science, 351(6277), 1043–1048. https://doi.org/10.1126/science.aad2450

Lee, Jun Ho, Park, C. K., Chen, G., Han, Q., Xie, R. G., Liu, T., Ji, R. R., & Lee, S. Y. (2014). A monoclonal antibody that targets a NaV1.7 channel voltage sensor for pain and itch relief. Cell, 157(6), 1393–1404. https://doi.org/10.1016/j.cell.2014.03.064

Lefranc, M.-P., & Lefranc, G. (2001). The Immunoglobulin FactsBook. 2001. https://books.google.es/books?hl=en&lr=&id=3GN3V7UJ8isC&oi=fnd&pg=PP1&dq=the+immunoglobulin+factsbook&ots=Pv9a3O9JTI&sig=C4pxaooMKDmlGQ_CXOS8IGStSXY#v=onepage&q=the immunoglobulin factsbook&f=false

Liao, H. X., Lynch, R., Zhou, T., Gao, F., Munir Alam, S., Boyd, S. D., Fire, A. Z., Roskin, K. M., Schramm, C. A., Zhang, Z., Zhu, J., Shapiro, L., Mullikin, J. C., Gnanakaran, S., Hraber, P., Wiehe, K., Kelsoe, G., Yang, G., Xia, S. M., … Young, A. (2013). Co-evolution of a broadly neutralizing HIV-1 antibody and founder virus. Nature, 496(7446), 469–476. https://doi.org/10.1038/nature12053

Li, M., Ablan, S. D., Miao, C., Zheng, Y. M., Fuller, M. S., Rennert, P. D., Maury, W., Johnson, M. C., Freed, E. O., & Liu, S. L. (2014). TIM-family proteins inhibit HIV-1 release. Proceedings of the National Academy of Sciences of the United States of America, 111(35). https://doi.org/10.1073/pnas.1404851111

Liu, Q., Lai, Y. T., Zhang, P., Louder, M. K., Pegu, A., Rawi, R., Asokan, M., Chen, X., Shen, C. H., Chuang, G. Y., Yang, E. S., Miao, H., Wang, Y., Fauci, A. S., Kwong, P. D., Mascola, J. R., & Lusso, P. (2019). Improvement of antibody functionality by structure-guided paratope engraftment. Nature Communications, 10(1), 1–13. https://doi.org/10.1038/s41467-019-08658-4

Li, Z., Li, W., Lu, M., Bess, J., Chao, C. W., Gorman, J., Terry, D. S., Zhang, B., Zhou, T., Blanchard, S. C., Kwong, P. D., Lifson, J. D., Mothes, W., & Liu, J. (2020). Subnanometer structures of HIV-1 envelope trimers on aldrithiol-2-inactivated virus particles. Nature Structural and Molecular Biology, 1–9. https://doi.org/10.1038/s41594-020-0452-2

Lobstein, J., Emrich, C. A., Jeans, C., Faulkner, M., Riggs, P., & Berkmen, M. (2012). SHuffle, a novel Escherichia coli protein expression strain capable of correctly folding disulfide bonded proteins in its cytoplasm. Microbial Cell Factories, 11, 56. https://doi.org/10.1186/1475-2859-11-56

Lu, M., Ma, X., Castillo-Menendez, L. R., Gorman, J., Alsahafi, N., Ermel, U., Terry, D. S., Chambers, M., Peng, D., Zhang, B., Zhou, T., Reichard, N., Wang, K., Grover, J. R., Carman, B. P., Gardner, M. R., Nikić-Spiegel, I., Sugawara, A., Arthos, J., … Mothes, W. (2019). Associating HIV-1 envelope glycoprotein structures with states on the virus observed by smFRET. Nature, 568(7752), 415–419. https://doi.org/10.1038/s41586-019-1101-y

Lutje Hulsik, D., Liu, Y. ying, Strokappe, N. M., Battella, S., el Khattabi, M., McCoy, L. E., Sabin, C., Hinz, A., Hock, M., Macheboeuf, P., Bonvin, A. M. J. J., Langedijk, J. P. M., Davis, D., Forsman Quigley, A., Aasa-Chapman, M. M. I., Seaman, M. S., Ramos, A., Poignard, P., Favier, A., … Rutten, L. (2013). A gp41 MPER-specific Llama VHH Requires a Hydrophobic CDR3 for Neutralization but not for Antigen Recognition. PLoS Pathogens, 9(3). https://doi.org/10.1371/journal.ppat.1003202

Lynch, R. M., Boritz, E., Coates, E. E., DeZure, A., Madden, P., Costner, P., Enama, M. E., Plummer, S., Holman, L., Hendel, C. S., Gordon, I., Casazza, J., Conan-Cibotti, M., Migueles, S. A., Tressler, R., Bailer, R. T., McDermott, A., Narpala, S., O'Dell, S., … Ledgerwood, J. E. (2015). Virologic effects of broadly neutralizing antibody VRC01 administration during chronic HIV-1 infection. Science Translational Medicine, 7(319). https://doi.org/10.1126/scitranslmed.aad5752

Lyumkis, D., Julien, J. P., de Val, N., Cupo, A., Potter, C. S., Klasse, P. J., Burton, D. R., Sanders, R. W., Moore, J. P., Carragher, B., Wilson, I. A., & Ward, A. B. (2013). Cryo-EM structure of a fully glycosylated soluble cleaved HIV-1 envelope trimer. Science, 342(6165), 1484–1490. https://doi.org/10.1126/science.1245627

Magnus, C., Rusert, P., Bonhoeffer, S., Trkola, A., & Regoes, R. R. (2009). Estimating the Stoichiometry of Human Immunodeficiency Virus Entry. Journal of Virology, 83(3), 1523–1531. https://doi.org/10.1128/jvi.01764-08

Mahlangu, J. N. (2018). Bispecific Antibody Emicizumab for Haemophilia A: A Breakthrough for Patients with Inhibitors. BioDrugs, 32(6), 561–570. https://doi.org/10.1007/s40259-018-0315-0

Malbec, M., Porrot, F., Rua, R., Horwitz, J., Klein, F., Halper-Stromberg, A., Scheid, J. F., Eden, C., Mouquet, H., Nussenzweig, M. C., & Schwartz, O. (2013). Broadly neutralizing antibodies that inhibit HIV-1 cell to cell transmission. Journal of Experimental Medicine, 210(13), 2813–2821. https://doi.org/10.1084/jem.20131244

Manrique, A., Rusert, P., Joos, B., Fischer, M., Kuster, H., Leemann, C., Niederöst, B., Weber, R., Stiegler, G., Katinger, H., Günthard, H. F., & Trkola, A. (2007). In Vivo and In Vitro Escape from Neutralizing Antibodies 2G12, 2F5, and 4E10. Journal of Virology, 81(16), 8793–8808. https://doi.org/10.1128/jvi.00598-07

Mao, Y., Wang, L., Gu, C., Herschhorn, A., Désormeaux, A., Finzi, A., Xiang, S. H., & Sodroski, J. G. (2013). Molecular architecture of the uncleaved HIV-1 envelope glycoprotein trimer. Proceedings of the National Academy of Sciences of the United States of America, 110(30), 12438–12443. https://doi.org/10.1073/pnas.1307382110

Marasco, W. A., & Sui, J. (2007). The growth and potential of human antiviral monoclonal antibody therapeutics. In Nature Biotechnology (Vol. 25, Issue 12, pp. 1421–1434). Nat Biotechnol. https://doi.org/10.1038/nbt1363

Ma, X., Lu, M., Gorman, J., Terry, D. S., Hong, X., Zhou, Z., Zhao, H., Altman, R. B., Arthos, J., Blanchard, S. C., Kwong, P. D., Munro, J. B., & Mothes, W. (2018). HIV-1 env trimer opens through an asymmetric intermediate in which individual protomers adopt distinct conformations. ELife, 7. https://doi.org/10.7554/eLife.34271

Mayer, K. H., Seaton, K. E., Huang, Y., Grunenberg, N., Isaacs, A., Allen, M., Ledgerwood, J. E., Frank, I., Sobieszczyk, M. E., Baden, L. R., Rodriguez, B., van Tieu, H., Tomaras, G. D., Deal, A., Goodman, D., Bailer, R. T., Ferrari, G., Jensen, R., Hural, J., … Montefiori, D. C. (2017). Safety, pharmacokinetics, and immunological activities of multiple intravenous or subcutaneous doses of an anti-HIV monoclonal antibody, VRC01, administered to HIV-uninfected adults: Results of a phase 1 randomized trial. PLoS Medicine, 14(11). https://doi.org/10.1371/journal.pmed.1002435

Mayer, L. (1986). Vesicles of variable sizes produced by a rapid extrusion procedure. In Bioehimica et Biophysica Acta (Vol. 858).

McCafferty, J., Griffiths, A. D., Winter, G., & Chiswell, D. J. (1990). Phage antibodies: filamentous phage displaying antibody variable domains. Nature, 348(6301), 552–554. https://doi.org/10.1038/348552a0

McDonald, S. K., & Fleming, K. G. (2016). Aromatic Side Chain Water-to-Lipid Transfer Free Energies Show a Depth Dependence across the Membrane Normal. Journal of the American Chemical Society, 138(25), 7946–7950. https://doi.org/10.1021/jacs.6b03460

McLaughlin, S. (1989). The Electrostatic Properties of Membranes. Annual Review of Biophysics and Biophysical Chemistry, 18(1), 113–136. https://doi.org/10.1146/annurev.bb.18.060189.000553

Mehandru, S., Vcelar, B., Wrin, T., Stiegler, G., Joos, B., Mohri, H., Boden, D., Galovich, J., Tenner-Racz, K., Racz, P., Carrington, M., Petropoulos, C., Katinger, H., & Markowitz, M. (2007). Adjunctive Passive Immunotherapy in Human Immunodeficiency Virus Type 1-Infected Individuals Treated with Antiviral Therapy during Acute and Early Infection. Journal of Virology, 81(20), 11016–11031. https://doi.org/10.1128/jvi.01340-07

Melikyan, G. B. (2010). Driving a wedge between viral lipids blocks infection. In Proceedings of the National Academy of Sciences of the United States of America (Vol.

107, Issue 40, pp. 17069–17070). National Academy of Sciences. https://doi.org/10.1073/pnas.1012748107

Melikyan, G. B. (2011). Membrane Fusion Mediated by Human Immunodeficiency Virus Envelope Glycoprotein. In Current Topics in Membranes (Vol. 68). Academic Press Inc. https://doi.org/10.1016/B978-0-12-385891-7.00004-0

Mendoza, P., Gruell, H., Nogueira, L., Pai, J. A., Butler, A. L., Millard, K., Lehmann, C., Suárez, I., Oliveira, T. Y., Lorenzi, J. C. C., Cohen, Y. Z., Wyen, C., Kümmerle, T., Karagounis, T., Lu, C. L., Handl, L., Unson-O'Brien, C., Patel, R., Ruping, C., … Nussenzweig, M. C. (2018). Combination therapy with anti-HIV-1 antibodies maintains viral suppression. Nature, 561(7724), 479–484. https://doi.org/10.1038/s41586-018-0531-2

Montefiori, D. C. (2009). Measuring HIV neutralization in a luciferase reporter gene assay. Methods in Molecular Biology, 485, 395–405. https://doi.org/10.1007/978-1-59745-170-3_26

Montefiori, D. C. (2016). Bispecific Antibodies Against HIV. In Cell (Vol. 165, Issue 7, pp. 1563–1564). Cell Press. https://doi.org/10.1016/j.cell.2016.06.004

Montefiori, D. C., Roederer, M., Morris, L., & Seaman, M. S. (2018). Neutralization tiers of HIV-1. In Current Opinion in HIV and AIDS (Vol. 13, Issue 2, pp. 128–136). Lippincott Williams and Wilkins. https://doi.org/10.1097/COH.0000000000000442

Montero, M., van Houten, N. E., Wang, X., & Scott, J. K. (2008). The Membrane-Proximal External Region of the Human Immunodeficiency Virus Type 1 Envelope: Dominant Site of Antibody Neutralization and Target for Vaccine Design. Microbiology and Molecular Biology Reviews, 72(1), 54–84. https://doi.org/10.1128/mmbr.00020-07

Moore, P. L., Crooks, E. T., Porter, L., Zhu, P., Cayanan, C. S., Grise, H., Corcoran, P., Zwick, M. B., Franti, M., Morris, L., Roux, K. H., Burton, D. R., & Binley, J. M. (2006). Nature of Nonfunctional Envelope Proteins on the Surface of Human Immunodeficiency Virus Type 1. Journal of Virology, 80(5), 2515–2528. https://doi.org/10.1128/jvi.80.5.2515-2528.2006

Muñoz-Barroso, I., Salzwedel, K., Hunter, E., & Blumenthal, R. (1999). Role of the Membrane-Proximal Domain in the Initial Stages of Human Immunodeficiency Virus Type 1 Envelope Glycoprotein-Mediated Membrane Fusion. Journal of Virology, 73(11), 9693–9693. https://doi.org/10.1128/jvi.73.11.9693-9693.1999

Munro, J. B., Gorman, J., Ma, X., Zhou, Z., Arthos, J., Burton, D. R., Koff, W. C., Courter, J. R., Smith, A. B., Kwong, P. D., Blanchard, S. C., & Mothes, W. (2014). Conformational dynamics of single HIV-1 envelope trimers on the surface of native virions. Science, 346(6210), 759–763. https://doi.org/10.1126/science.1254426

Neuberger, M. S. (2008). Antibody diversification by somatic mutation: from Burnet onwards. Immunology & Cell Biology, 86(2), 124–132. https://doi.org/10.1038/sj.icb.7100160

Nyamweya, S., Hegedus, A., Jaye, A., Rowland-Jones, S., Flanagan, K. L., & Macallan, D. C. (2013). Comparing HIV-1 and HIV-2 infection: Lessons for viral immunopathogenesis. Reviews in Medical Virology, 23(4), 221–240. https://doi.org/10.1002/rmv.1739

Ofek, G., Tang, M., Sambor, A., Katinger, H., Mascola, J. R., Wyatt, R., & Kwong, P. D. (2004). Structure and Mechanistic Analysis of the Anti-Human Immunodeficiency Virus Type 1 Antibody 2F5 in Complex with Its gp41 Epitope. Journal of Virology, 78(19), 10724–10737. https://doi.org/10.1128/jvi.78.19.10724-10737.2004

Ota, T., Doyle-Cooper, C., Cooper, A. B., Huber, M., Falkowska, E., Doores, K. J., Hangartner, L., Le, K., Sok, D., Jardine, J., Lifson, J., Wu, X., Mascola, J. R., Poignard, P., Binley, J. M., Chakrabarti, B. K., Schief, W. R., Wyatt, R. T., Burton, D. R., & Nemazee, D. (2012). Anti-HIV B Cell Lines as Candidate Vaccine Biosensors. The Journal of Immunology, 189(10), 4816–4824. https://doi.org/10.4049/jimmunol.1202165

Pace, M., & Frater, J. (2019). Curing HIV by 'kick and kill': from theory to practice? In Expert Review of Anti-Infective Therapy (Vol. 17, Issue 6, pp. 383–386). Taylor and Francis Ltd. https://doi.org/10.1080/14787210.2019.1617697

Padte, N. N., Yu, J., Huang, Y., & Ho, D. D. (2018). Engineering multi-specific antibodies against HIV-1. In Retrovirology (Vol. 15, Issue 1, p. 60). BioMed Central Ltd. https://doi.org/10.1186/s12977-018-0439-9

Pahuja, K. B., Nguyen, T. T., Jaiswal, B. S., Prabhash, K., Thaker, T. M., Senger, K., Chaudhuri, S., Kljavin, N. M., Antony, A., Phalke, S., Kumar, P., Mravic, M., Stawiski, E. W., Vargas, D., Durinck, S., Gupta, R., Khanna-Gupta, A., Trabucco, S. E., Sokol, E. S., … Seshagiri, S. (2018). Actionable Activating Oncogenic ERBB2/HER2 Transmembrane and Juxtamembrane Domain Mutations. Cancer Cell, 34(5), 792-806.e5. https://doi.org/10.1016/j.ccell.2018.09.010

Pegu, A., Yang, Z. Y., Boyington, J. C., Wu, L., Ko, S. Y., Schmidt, S. D., McKee, K., Kong, W. P., Shi, W., Chen, X., Todd, J. P., Letvin, N. L., Huang, J., Nason, M. C., Hoxie, J. A., Kwong, P. D., Connors, M., Rao, S. S., Mascola, J. R., & Nabel, G. J. (2014). Neutralizing antibodies to HIV-1 envelope protect more effectively in vivo than those to the CD4 receptor. Science Translational Medicine, 6(243). https://doi.org/10.1126/scitranslmed.3008992

Pejchal, R., Doores, K. J., Walker, L. M., Khayat, R., Huang, P. S., Wang, S. K., Stanfield, R. L., Julien, J. P., Ramos, A., Crispin, M., Depetris, R., Katpally, U., Marozsan, A., Cupo, A., Maloveste, S., Liu, Y., McBride, R., Ito, Y., Sanders, R. W., … Wilson, I. A. (2011). A potent and broad neutralizing antibody recognizes and penetrates the HIV glycan shield. Science, 334(6059), 1097–1103. https://doi.org/10.1126/science.1213256

Pettersen, E. F., Goddard, T. D., Huang, C. C., Couch, G. S., Greenblatt, D. M., Meng, E. C., & Ferrin, T. E. (2004). UCSF Chimera - A visualization system for exploratory research and analysis. Journal of Computational Chemistry, 25(13), 1605–1612. https://doi.org/10.1002/jcc.20084

Pinto, D., Fenwick, C., Caillat, C., Silacci, C., Guseva, S., Dehez, F., Chipot, C., Barbieri, S., Minola, A., Jarrossay, D., Tomaras, G. D., Shen, X., Riva, A., Tarkowski, M., Schwartz, O., Bruel, T., Dufloo, J., Seaman, M. S., Montefiori, D. C., … Weissenhorn, W. (2019). Structural Basis for Broad HIV-1 Neutralization by the MPER-Specific Human Broadly Neutralizing Antibody LN01. Cell Host and Microbe, 26(5), 623-637.e8. https://doi.org/10.1016/j.chom.2019.09.016

Preston, B. D., Poiesz, B. J., & Loeb, L. A. (1988). Fidelity of HIV-1 reverse transcriptase. Science, 242(4882), 1168–1171. https://doi.org/10.1126/science.2460924

Rajewsky, K. (1996). Clonal selection and learning in the antibody system. In Nature (Vol. 381, Issue 6585, pp. 751–758). Nature. https://doi.org/10.1038/381751a0

Rantalainen, K., Berndsen, Z. T., Antanasijevic, A., Schiffner, T., Zhang, X., Lee, W. H., Torres, J. L., Zhang, L., Irimia, A., Copps, J., Zhou, K. H., Kwon, Y. D., Law, W. H., Schramm, C. A., Verardi, R., Krebs, S. J., Kwong, P. D., Doria-Rose, N. A., Wilson, I. A., … Ward, A. B. (2020). HIV-1 Envelope and MPER Antibody Structures in Lipid Assemblies. Cell Reports, 31(4), 107583. https://doi.org/10.1016/j.celrep.2020.107583

Rantalainen, K., Berndsen, Z. T., Murrell, S., Cao, L., Omorodion, O., Torres, J. L., Wu, M., Umotoy, J., Copps, J., Poignard, P., Landais, E., Paulson, J. C., Wilson, I. A., & Ward, A. B. (2018). Co-evolution of HIV Envelope and Apex-Targeting Neutralizing

Antibody Lineage Provides Benchmarks for Vaccine Design. Cell Reports, 23(11), 3249–3261. https://doi.org/10.1016/j.celrep.2018.05.046

Reardon, P. N., Sage, H., Dennison, S. M., Martin, J. W., Donald, B. R., Alam, S. M., Haynes, B. F., & Spicer, L. D. (2014). Structure of an HIV-1-neutralizing antibody target, the lipid-bound gp41 envelope membrane proximal region trimer. Proceedings of the National Academy of Sciences of the United States of America, 111(4), 1391–1396. https://doi.org/10.1073/pnas.1309842111

Ridgway, J. B. B., Presta, L. G., & Carter, P. (1996). “Knobs-into-holes” engineering of antibody C(H)3 domains for heavy chain heterodimerization. Protein Engineering, 9(7), 617–621. https://doi.org/10.1093/protein/9.7.617

Riss, T., Niles, A., Moravec, R., Karassina, N., & Vidugiriene, J. (2019). Cytotoxicity Assays: In Vitro Methods to Measure Dead Cells. In Assay Guidance Manual. Eli Lilly & Company and the National Center for Advancing Translational Sciences. http://www.ncbi.nlm.nih.gov/pubmed/31070879

Ritz, D., Lim, J., Reynolds, C. M., Poole, L. B., & Beckwith, J. (2001). Conversion of a peroxiredoxin into a disulfide reductase by a triplet repeat expansion. Science, 294(5540), 158–160. https://doi.org/10.1126/science.1063143

Robbie, G. J., Criste, R., Dall’Acqua, W. F., Jensen, K., Patel, N. K., Losonsky, G. A., & Griffin, M. P. (2013). A novel investigational Fc-modified humanized monoclonal antibody, motavizumab-YTE, has an extended half-life in healthy adults. Antimicrobial Agents and Chemotherapy, 57(12), 6147–6153. https://doi.org/10.1128/AAC.01285-13

Rudicell, R. S., Kwon, Y. D., Ko, S.-Y., Pegu, A., Louder, M. K., Georgiev, I. S., Wu, X., Zhu, J., Boyington, J. C., Chen, X., Shi, W., Yang, Z. -y., Doria-Rose, N. A., McKee, K., O’Dell, S., Schmidt, S. D., Chuang, G.-Y., Druz, A., Soto, C., … Nabel, G. J. (2014). Enhanced Potency of a Broadly Neutralizing HIV-1 Antibody In Vitro Improves Protection against Lentiviral Infection In Vivo. Journal of Virology, 88(21), 12669–12682. https://doi.org/10.1128/jvi.02213-14

Rujas, E., Caaveiro, J. M. M., Insausti, S., García-Porras, M., Tsumoto, K., & Nieva, J. L. (2017). Peripheral membrane interactions boost the engagement by an anti-HIV-1 broadly neutralizing antibody. Journal of Biological Chemistry, 292(13), 5571–5583. https://doi.org/10.1074/jbc.M117.775429

Rujas, E., Caaveiro, J. M. M., Partida-Hanon, A., Gulzar, N., Morante, K., Apellániz, B., García-Porras, M., Bruix, M., Tsumoto, K., Scott, J. K., Jiménez, M. Á., & Nieva, J. L.

(2016). Structural basis for broad neutralization of HIV-1 through the molecular recognition of 10E8 helical epitope at the membrane interface. Scientific Reports, 6(1), 38177. https://doi.org/10.1038/srep38177

Rujas, E., Gulzar, N., Morante, K., Tsumoto, K., Scott, J. K., Nieva, J. L., & Caaveiro, J. M. M. (2015). Structural and Thermodynamic Basis of Epitope Binding by Neutralizing and Nonneutralizing Forms of the Anti-HIV-1 Antibody 4E10. Journal of Virology, 89(23), 11975–11989. https://doi.org/10.1128/jvi.01793-15

Rujas, E., Insausti, S., García-Porras, M., Sánchez-Eugenia, R., Tsumoto, K., Nieva, J. L., & Caaveiro, J. M. M. (2017). Functional Contacts between MPER and the Anti-HIV-1 Broadly Neutralizing Antibody 4E10 Extend into the Core of the Membrane. Journal of Molecular Biology, 429(8), 1213–1226. https://doi.org/10.1016/j.jmb.2017.03.008

Rujas, E., Leaman, D. P., Insausti, S., Ortigosa-Pascual, L., Zhang, L., Zwick, M. B., & Nieva, J. L. (2018). Functional Optimization of Broadly Neutralizing HIV-1 Antibody 10E8 by Promotion of Membrane Interactions. Journal of Virology, 92(8), 1–18. https://doi.org/10.1128/jvi.02249-17

Sakamoto, S., & Hamachi, I. (2019). Recent Progress in Chemical Modification of Proteins. Analytical Sciences, 35(1), 5–27. https://doi.org/10.2116/analsci.18R003

Salzwedel, K., West, J. T., & Hunter, E. (1999). A Conserved Tryptophan-Rich Motif in the Membrane-Proximal Region of the Human Immunodeficiency Virus Type 1 gp41 Ectodomain Is Important for Env-Mediated Fusion and Virus Infectivity. Journal of Virology, 73(3), 2469–2480. https://doi.org/10.1128/jvi.73.3.2469-2480.1999

Sánchez-Martínez, S., Lorizate, M., Katinger, H., Kunert, R., Basañez, G., & Nieva, J. L. (2006). Specific phospholipid recognition by human immunodeficiency virus type-1 neutralizing anti-gp41 2F5 antibody. FEBS Letters, 580(9), 2395–2399. https://doi.org/10.1016/j.febslet.2006.03.067

Sanders, R. W., Derking, R., Cupo, A., Julien, J. P., Yasmeen, A., de Val, N., Kim, H. J., Blattner, C., de la Peña, A. T., Korzun, J., Golabek, M., de los Reyes, K., Ketas, T. J., van Gils, M. J., King, C. R., Wilson, I. A., Ward, A. B., Klasse, P. J., & Moore, J. P. (2013). A Next-Generation Cleaved, Soluble HIV-1 Env Trimer, BG505 SOSIP.664 gp140, Expresses Multiple Epitopes for Broadly Neutralizing but Not Non-Neutralizing Antibodies. PLoS Pathogens, 9(9). https://doi.org/10.1371/journal.ppat.1003618

Sanders, R. W., Schiffner, L., Master, A., Kajumo, F., Guo, Y., Dragic, T., Moore, J. P., & Binley, J. M. (2000). Variable-Loop-Deleted Variants of the Human Immunodeficiency

Virus Type 1 Envelope Glycoprotein Can Be Stabilized by an Intermolecular Disulfide Bond between the gp120 and gp41 Subunits. Journal of Virology, 74(11), 5091–5100. https://doi.org/10.1128/jvi.74.11.5091-5100.2000

Sanders, R. W., Vesanen, M., Schuelke, N., Master, A., Schiffner, L., Kalyanaraman, R., Paluch, M., Berkhout, B., Maddon, P. J., Olson, W. C., Lu, M., & Moore, J. P. (2002). Stabilization of the Soluble, Cleaved, Trimeric Form of the Envelope Glycoprotein Complex of Human Immunodeficiency Virus Type 1. Journal of Virology, 76(17), 8875–8889. https://doi.org/10.1128/jvi.76.17.8875-8889.2002

Santiago, C., Ballesteros, A., Martínez-Muñoz, L., Mellado, M., Kaplan, G. G., Freeman, G. J., & Casasnovas, J. M. (2007). Structures of T Cell Immunoglobulin Mucin Protein 4 Show a Metal-Ion-Dependent Ligand Binding Site where Phosphatidylserine Binds. Immunity, 27(6), 941–951. https://doi.org/10.1016/j.immuni.2007.11.008

Scanlan, C. N., Offer, J., Zitzmann, N., & Dwek, R. A. (2007). Exploiting the defensive sugars of HIV-1 for drug and vaccine design. In Nature (Vol. 446, Issue 7139, pp. 1038–1045). Nature Publishing Group. https://doi.org/10.1038/nature05818

Scharf, L., Wang, H., Gao, H., Chen, S., McDowall, A. W., & Bjorkman, P. J. (2015). Broadly Neutralizing Antibody 8ANC195 Recognizes Closed and Open States of HIV-1 Env. Cell, 162(6), 1379–1390. https://doi.org/10.1016/j.cell.2015.08.035

Scheid, J. F., Horwitz, J. A., Bar-On, Y., Kreider, E. F., Lu, C. L., Lorenzi, J. C. C., Feldmann, A., Braunschweig, M., Nogueira, L., Oliveira, T., Shimeliovich, I., Patel, R., Burke, L., Cohen, Y. Z., Hadrigan, S., Settler, A., Witmer-Pack, M., West, A. P., Juelg, B., … Caskey, M. (2016). HIV-1 antibody 3BNC117 suppresses viral rebound in humans during treatment interruption. Nature, 535(7613), 556–560. https://doi.org/10.1038/nature18929

Scheid, J. F., Mouquet, H., Feldhahn, N., Seaman, M. S., Velinzon, K., Pietzsch, J., Ott, R. G., Anthony, R. M., Zebroski, H., Hurley, A., Phogat, A., Chakrabarti, B., Li, Y., Connors, M., Pereyra, F., Walker, B. D., Wardemann, H., Ho, D., Wyatt, R. T., … Nussenzweig, M. C. (2009). Broad diversity of neutralizing antibodies isolated from memory B cells in HIV-infected individuals. Nature, 458(7238), 636–640. https://doi.org/10.1038/nature07930

Scherer, E. M., Leaman, D. P., Zwick, M. B., McMichael, A. J., & Burton, D. R. (2010). Aromatic residues at the edge of the antibody combining site facilitate viral glycoprotein recognition through membrane interactions. Proceedings of the National Academy of

Sciences of the United States of America, 107(4), 1529–1534. https://doi.org/10.1073/pnas.0909680107

Schibli, D. J., Montelaro, R. C., & Vogel, H. J. (2001). The membrane-proximal tryptophan-rich region of the HIV glycoprotein, gp41, forms a well-defined helix in dodecylphosphocholine micelles. Biochemistry, 40(32), 9570–9578. https://doi.org/10.1021/bi010640u

Schommers, P., Gruell, H., Abernathy, M. E., Tran, M. K., Dingens, A. S., Gristick, H. B., Barnes, C. O., Schoofs, T., Schlotz, M., Vanshylla, K., Kreer, C., Weiland, D., Holtick, U., Scheid, C., Valter, M. M., van Gils, M. J., Sanders, R. W., Vehreschild, J. J., Cornely, O. A., … Klein, F. (2020). Restriction of HIV-1 Escape by a Highly Broad and Potent Neutralizing Antibody. Cell, 180(3), 471-489.e22. https://doi.org/10.1016/j.cell.2020.01.010

Schoofs, T., Barnes, C. O., Suh-Toma, N., Golijanin, J., Schommers, P., Gruell, H., West, A. P., Bach, F., Lee, Y. E., Nogueira, L., Georgiev, I. S., Bailer, R. T., Czartoski, J., Mascola, J. R., Seaman, M. S., McElrath, M. J., Doria-Rose, N. A., Klein, F., Nussenzweig, M. C., & Bjorkman, P. J. (2019). Broad and Potent Neutralizing Antibodies Recognize the Silent Face of the HIV Envelope. Immunity, 50(6), 1513-1529.e9. https://doi.org/10.1016/j.immuni.2019.04.014

Schroeder, H. W., & Cavacini, L. (2010). Structure and function of immunoglobulins. Journal of Allergy and Clinical Immunology, 125(2 SUPPL. 2), S41. https://doi.org/10.1016/j.jaci.2009.09.046

Seigneuret, M., & Devaux, P. F. (1984). ATP-dependent asymmetric distribution of spin-labeled phospholipids in the erythrocyte membrane: Relation to shape changes. Proceedings of the National Academy of Sciences of the United States of America, 81(12 I), 3751–3755. https://doi.org/10.1073/pnas.81.12.3751

Serrano, S., Araujo, A., Apellániz, B., Bryson, S., Carravilla, P., de La Arada, I., Huarte, N., Rujas, E., Pai, E. F., Arrondo, J. L. R., Domene, C., Jiménez, M. A., & Nieva, J. L. (2014). Structure and immunogenicity of a peptide vaccine, including the complete HIV-1 gp41 2F5 epitope: Implications for antibody recognition mechanism and immunogen design. Journal of Biological Chemistry, 289(10), 6565–6580. https://doi.org/10.1074/jbc.M113.527747

Shepard, L. A., Heuck, A. P., Hamman, B. D., Rossjohn, J., Parker, M. W., Ryan, K. R., Johnson, A. E., & Tweten, R. K. (1998). Identification of a membrane-spanning domain of the thiol-activated pore-forming toxin Clostridium perfringens perfringolysin O: An α-

helical to β-sheet transition identified by fluorescence spectroscopy. Biochemistry, 37(41), 14563–14574. https://doi.org/10.1021/bi981452f

Shnyrova, A. v., Bashkirov, P. v., Akimov, S. A., Pucadyil, T. J., Zimmerberg, J., Schmid, S. L., & Frolov, V. A. (2013). Geometric catalysis of membrane fission driven by flexible dynamin rings. Science, 339(6126), 1433–1436. https://doi.org/10.1126/science.1233920

Simek, M. D., Rida, W., Priddy, F. H., Pung, P., Carrow, E., Laufer, D. S., Lehrman, J. K., Boaz, M., Tarragona-Fiol, T., Miiro, G., Birungi, J., Pozniak, A., McPhee, D. A., Manigart, O., Karita, E., Inwoley, A., Jaoko, W., DeHovitz, J., Bekker, L.-G., … Koff, W. C. (2009). Human Immunodeficiency Virus Type 1 Elite Neutralizers: Individuals with Broad and Potent Neutralizing Activity Identified by Using a High-Throughput Neutralization Assay together with an Analytical Selection Algorithm. Journal of Virology, 83(14), 7337–7348. https://doi.org/10.1128/jvi.00110-09

Simon, V., Ho, D. D., & Abdool Karim, Q. (2006). HIV/AIDS epidemiology, pathogenesis, prevention, and treatment. In Lancet (Vol. 368, Issue 9534, pp. 489–504). NIH Public Access. https://doi.org/10.1016/S0140-6736(06)69157-5

Slim, J., Sulkowski, MS., and Sham, J. S. (2011). Monoclonal Antibody Bavituximab Well-Tolerated by HIV/HCV Coinfected People. 46th Annual Meeting of the European Association for the Study of the Liver (EASL). http://www.hivandhepatitis.com/2011_conference/easl2011/docs/0415_2010_b.html

Soares, M. M., King, S. W., & Thorpe, P. E. (2008). Targeting inside-out phosphatidylserine as a therapeutic strategy for viral diseases. Nature Medicine, 14(12), 1357–1362. https://doi.org/10.1038/nm.1885

Sok, D., & Burton, D. R. (2018). Recent progress in broadly neutralizing antibodies to HIV. In Nature Immunology (Vol. 19, Issue 11, pp. 1179–1188). Nature Publishing Group. https://doi.org/10.1038/s41590-018-0235-7

Sok, D., Gils, M. J. V., Pauthner, M., Julien, J. P., Saye-Francisco, K. L., Hsueh, J., Briney, B., Lee, J. H., Le, K. M., Lee, P. S., Hua, Y., Seaman, M. S., Moore, J. P., Ward, A. B., Wilson, I. A., Sanders, R. W., & Burton, D. R. (2014). Recombinant HIV envelope trimer selects for quaternary-dependent antibodies targeting the trimer apex. Proceedings of the National Academy of Sciences of the United States of America, 111(49), 17624–17629. https://doi.org/10.1073/pnas.1415789111

Sok, D., Pauthner, M., Briney, B., Lee, J. H., Saye-Francisco, K. L., Hsueh, J., Ramos, A., Le, K. M., Jones, M., Jardine, J. G., Bastidas, R., Sarkar, A., Liang, C. H., Shivatare, S. S., Wu, C. Y., Schief, W. R., Wong, C. H., Wilson, I. A., Ward, A. B., … Burton, D. R. (2016). A Prominent Site of Antibody Vulnerability on HIV Envelope Incorporates a Motif Associated with CCR5 Binding and Its Camouflaging Glycans. Immunity, 45(1), 31–45. https://doi.org/10.1016/j.immuni.2016.06.026

Speck, R. F., Wehrly, K., Platt, E. J., Atchison, R. E., Charo, I. F., Kabat, D., Chesebro, B., & Goldsmith, M. A. (1997). Selective employment of chemokine receptors as human immunodeficiency virus type 1 coreceptors determined by individual amino acids within the envelope V3 loop. Journal of Virology, 71(9).

Stamatatos, L., Morris, L., Burton, D. R., & Mascola, J. R. (2009). Neutralizing antibodies generated during natural hiv-1 infection: Good news for an hiv-1 vaccine? Nature Medicine, 15(8), 866–870. https://doi.org/10.1038/nm.1949

Steinhardt, J. J., Guenaga, J., Turner, H. L., McKee, K., Louder, M. K., O'Dell, S., Chiang, C. I., Lei, L., Galkin, A., Andrianov, A. K., Doria-Rose, N. A., Bailer, R. T., Ward, A. B., Mascola, J. R., & Li, Y. (2018). Rational design of a trispecific antibody targeting the HIV-1 Env with elevated anti-viral activity. Nature Communications, 9(1), 1–12. https://doi.org/10.1038/s41467-018-03335-4

Steinitz, M., Klein, G., Koskimies, S., & Makel, O. (1977). EB virus-induced B lymphocyte cell lines producing specific antibody. Nature, 269(5627), 420–422. https://doi.org/10.1038/269420a0

Stiegler, G., Kunert, R., Purtscher, M., Wolbank, S., Voglauer, R., Steindl, F., & Katinger, H. (2001). A potent cross-clade neutralizing human monoclonal antibody against a novel epitope on gp41 of human immunodeficiency virus type 1. AIDS Research and Human Retroviruses, 17(18), 1757–1765. https://doi.org/10.1089/08892220152741450

Struwe, W. B., Chertova, E., Allen, J. D., Seabright, G. E., Watanabe, Y., Harvey, D. J., Medina-Ramirez, M., Roser, J. D., Smith, R., Westcott, D., Keele, B. F., Bess, J. W., Sanders, R. W., Lifson, J. D., Moore, J. P., & Crispin, M. (2018). Site-Specific Glycosylation of Virion-Derived HIV-1 Env Is Mimicked by a Soluble Trimeric Immunogen. Cell Reports, 24(8), 1958-1966.e5. https://doi.org/10.1016/j.celrep.2018.07.080

st. Vincent, M. R., Colpitts, C. C., Ustinov, A. v., Muqadas, M., Joyce, M. A., Barsby, N. L., Epand, R. F., Epand, R. M., Khramyshev, S. A., Valueva, O. A., Korshun, V. A., Tyrrell, D. L. J., & Schang, L. M. (2010). Rigid amphipathic fusion inhibitors, small

molecule antiviral compounds against enveloped viruses. Proceedings of the National Academy of Sciences of the United States of America, 107(40), 17339–17344. https://doi.org/10.1073/pnas.1010026107

Sundquist, W. I., & Kräusslich, H. G. (2012). HIV-1 assembly, budding, and maturation. In Cold Spring Harbor Perspectives in Medicine (Vol. 2, Issue 7). Cold Spring Harbor Laboratory Press. https://doi.org/10.1101/cshperspect.a006924

Sun, Z. Y. J., Oh, K. J., Kim, M., Yu, J., Brusic, V., Song, L., Qiao, Z., Wang, J. huai, Wagner, G., & Reinherz, E. L. (2008). HIV-1 Broadly Neutralizing Antibody Extracts Its Epitope from a Kinked gp41 Ectodomain Region on the Viral Membrane. Immunity, 28(1), 52–63. https://doi.org/10.1016/j.immuni.2007.11.018

Tao, M. H., Smith, R. I. F., & Morrison, S. L. (1993). Structural features of human immunoglobulin G that determine isotype-specitic differences in complement activation. Journal of Experimental Medicine, 178(2), 661–667. https://doi.org/10.1084/jem.178.2.661

Teese, M. G., & Langosch, D. (2015). Role of GxxxG Motifs in Transmembrane Domain Interactions. Biochemistry, 54(33), 5125–5135. https://doi.org/10.1021/acs.biochem.5b00495

Tiller, T., Meffre, E., Yurasov, S., Tsuiji, M., Nussenzweig, M. C., & Wardemann, H. (2008). Efficient generation of monoclonal antibodies from single human B cells by single cell RT-PCR and expression vector cloning. Journal of Immunological Methods, 329(1–2), 112–124. https://doi.org/10.1016/j.jim.2007.09.017

Tonegawa, S. (1983). Somatic generation of antibody diversity. Nature, 302(5909), 575–581. https://doi.org/10.1038/302575a0

Trkola, A., Kuster, H., Rusert, P., Joos, B., Fischer, M., Leemann, C., Manrique, A., Huber, M., Rehr, M., Oxenius, A., Weber, R., Stiegler, G., Vcelar, B., Katinger, H., Aceto, L., & Günthard, H. F. (2005). Delay of HIV-1 rebound after cessation of antiretroviral therapy through passive transfer of human neutralizing antibodies. Nature Medicine, 11(6), 615–622. https://doi.org/10.1038/nm1244

van Anken, E., Sanders, R. W., Liscaljet, I. M., Land, A., Bontjer, I., Tillemans, S., Nabatov, A. A., Paxton, W. A., Berkhout, B., & Braakman, I. (2008). Only five of 10 strictly conserved disulfide bonds are essential for folding and eight for function of the HIV-1 envelope glycoprotein. Molecular Biology of the Cell, 19(10), 4298–4309. https://doi.org/10.1091/mbc.E07-12-1282

van Gils, M. J., & Sanders, R. W. (2014). In vivo protection by broadly neutralizing HIV antibodies. In Trends in Microbiology (Vol. 22, Issue 10, pp. 550–551). Elsevier Ltd. https://doi.org/10.1016/j.tim.2014.08.006

Verkoczy, L., & Diaz, M. (2014). Autoreactivity in HIV-1 broadly neutralizing antibodies: Implications for their function and induction by vaccination. In Current Opinion in HIV and AIDS (Vol. 9, Issue 3, pp. 224–234). Lippincott Williams and Wilkins. https://doi.org/10.1097/COH.0000000000000049

Wagh, K., Seaman, M. S., Zingg, M., Fitzsimons, T., Barouch, D. H., Burton, D. R., Connors, M., Ho, D. D., Mascola, J. R., Nussenzweig, M. C., Ravetch, J., Gautam, R., Martin, M. A., Montefiori, D. C., & Korber, B. (2018). Potential of conventional & bispecific broadly neutralizing antibodies for prevention of HIV-1 subtype A, C & D infections. PLOS Pathogens, 14(3), e1006860. https://doi.org/10.1371/journal.ppat.1006860

Walker, L. M., & Burton, D. R. (2018). Passive immunotherapy of viral infections: “super-antibodies” enter the fray. In Nature Reviews Immunology (Vol. 18, Issue 5, pp. 297–308). Nature Publishing Group. https://doi.org/10.1038/nri.2017.148

Walker, L. M., Huber, M., Doores, K. J., Falkowska, E., Pejchal, R., Julien, J. P., Wang, S. K., Ramos, A., Chan-Hui, P. Y., Moyle, M., Mitcham, J. L., Hammond, P. W., Olsen, O. A., Phung, P., Fling, S., Wong, C. H., Phogat, S., Wrin, T., Simek, M. D., … Poignard, P. (2011). Broad neutralization coverage of HIV by multiple highly potent antibodies. Nature, 477(7365), 466–470. https://doi.org/10.1038/nature10373

Wang, Y., Kaur, P., Sun, Z. Y. J., Elbahnasawy, M. A., Hayati, Z., Qiao, Z. S., Bui, N. N., Chile, C., Nasr, M. L., Wagner, G., Wang, J. H., Song, L., Reinherz, E. L., & Kim, M. (2019). Topological analysis of the gp41 MPER on lipid bilayers relevant to the metastable HIV-1 envelope prefusion state. Proceedings of the National Academy of Sciences of the United States of America, 116(45), 22556–22566. https://doi.org/10.1073/pnas.1912427116

Ward, A. B., & Wilson, I. A. (2015). Insights into the trimeric HIV-1 envelope glycoprotein structure. In Trends in Biochemical Sciences (Vol. 40, Issue 2, pp. 101–107). Elsevier Ltd. https://doi.org/10.1016/j.tibs.2014.12.006

Watson, H. (2015). Biological membranes. Essays in Biochemistry, 59, 43–70. https://doi.org/10.1042/BSE0590043

Wei, X., Decker, J. M., Wang, S., Hui, H., Kappes, J. C., Wu, X., Salazar-Gonzalez, J. F., Salazar, M. G., Kilby, J. M., Saag, M. S., Komarova, N. L., Nowak, M. A., Hahn, B. H., Kwong, P. D., & Shaw, G. M. (2003). Antibody neutralization and escape by HIV-1. Nature, 422(6929), 307–312. https://doi.org/10.1038/nature01470

West, A. P., Scharf, L., Scheid, J. F., Klein, F., Bjorkman, P. J., & Nussenzweig, M. C. (2014). Structural insights on the role of antibodies in HIV-1 vaccine and therapy. In Cell (Vol. 156, Issue 4, pp. 633–648). NIH Public Access. https://doi.org/10.1016/j.cell.2014.01.052

White, S. H., Ladokhin, A. S., Jayasinghe, S., & Hristova, K. (2001). How Membranes Shape Protein Structure. In Journal of Biological Chemistry (Vol. 276, Issue 35, pp. 32395–32398). J Biol Chem. https://doi.org/10.1074/jbc.R100008200

White, S. H., & Wimley, W. C. (1999). Membrane protein folodinig and stability: Physical Principles. Annual Review of Biophysics and Biomolecular Structure, 28(1), 319–365. https://doi.org/10.1146/annurev.biophys.28.1.319

Wilker, P. R., Sedy, J. R., Grigura, V., Murphy, T. L., & Murphy, K. M. (2007). Evidence for carbohydrate recognition and homotypic and heterotypic binding by the TIM family. International Immunology, 19(6), 763–773. https://doi.org/10.1093/intimm/dxm044

Williams, L. T. D., Ofek, G., Schätzle, S., McDaniel, J. R., Lu, X., Nicely, N. I., Wu, L., Lougheed, C. S., Bradley, T., Louder, M. K., McKee, K., Bailer, R. T., O'Dell, S., Georgiev, I. S., Seaman, M. S., Parks, R. J., Marshall, D. J., Anasti, K., Yang, G., … Haynes, B. F. (2017). Potent and broad HIV-neutralizing antibodies in memory B cells and plasma. Science Immunology, 2(7), eaal2200. https://doi.org/10.1126/sciimmunol.aal2200

Williamson, P., & Schlegel, R. A. (1994). Back and Forth: The regulation and function of transbilayer phospholipid movement in eukaryotic cells (review). Molecular Membrane Biology, 11(4), 199–216. https://doi.org/10.3109/09687689409160430

Wimley, W. C., & White, S. H. (1996). Experimentally determined hydrophobicity scale for proteins at membrane interfaces. In Nature Structural Biology (Vol. 3, Issue 10, pp. 842–848). Nature Publishing Group. https://doi.org/10.1038/nsb1096-842

Wren, L. H., Chung, A. W., Isitman, G., Kelleher, A. D., Parsons, M. S., Amin, J., Cooper, D. A., Stratov, I., Navis, M., & Kent, S. J. (2013). Specific antibody-dependent cellular cytotoxicity responses associated with slow progression of HIV infection. Immunology, 138(2), 116–123. https://doi.org/10.1111/imm.12016

Wu, X., Parast, A. B., Richardson, B. A., Nduati, R., John-Stewart, G., Mbori-Ngacha, D., Rainwater, S. M. J., & Overbaugh, J. (2006). Neutralization Escape Variants of Human Immunodeficiency Virus Type 1 Are Transmitted from Mother to Infant. Journal of Virology, 80(5), 2585–2585. https://doi.org/10.1128/jvi.80.5.2585.2006

Wu, X., Yang, Z. Y., Li, Y., Hogerkorp, C. M., Schief, W. R., Seaman, M. S., Zhou, T., Schmidt, S. D., Wu, L., Xu, L., Longo, N. S., McKee, K., O'Dell, S., Louder, M. K., Wycuff, D. L., Feng, Y., Nason, M., Doria-Rose, N., Connors, M., … Mascola, J. R. (2010). Rational design of envelope identifies broadly neutralizing human monoclonal antibodies to HIV-1. Science, 329(5993), 856–861. https://doi.org/10.1126/science.1187659

Xiao, X., Chen, W., Feng, Y., Zhu, Z., Prabakaran, P., Wang, Y., Zhang, M. Y., Longo, N. S., & Dimitrov, D. S. (2009). Germline-like predecessors of broadly neutralizing antibodies lack measurable binding to HIV-1 envelope glycoproteins: Implications for evasion of immune responses and design of vaccine immunogens. Biochemical and Biophysical Research Communications, 390(3), 404–409. https://doi.org/10.1016/j.bbrc.2009.09.029

Xu, L., Pegu, A., Rao, E., Doria-Rose, N., Beninga, J., McKee, K., Lord, D. M., Wei, R. R., Deng, G., Louder, M., Schmidt, S. D., Mankoff, Z., Wu, L., Asokan, M., Beil, C., Lange, C., Leuschner, W. D., Kruip, J., Sendak, R., … Nabel, G. J. (2017). Trispecific broadly neutralizing HIV antibodies mediate potent SHIV protection in macaques. Science, 358(6359), 85–90. https://doi.org/10.1126/science.aan8630

Xu, S. Z., Zeng, F., Lei, M., Li, J., Gao, B., Xiong, C., Sivaprasadarao, A., & Beech, D. J. (2005). Generation of functional ion-channel tools by E3 targeting. Nature Biotechnology, 23(10), 1289–1293. https://doi.org/10.1038/nbt1148

Yu, L., & Guan, Y. (2014). Immunologic basis for long HCDR3s in broadly neutralizing antibodies against HIV-1. In Frontiers in Immunology (Vol. 5, Issue JUN, p. 250). Frontiers Research Foundation. https://doi.org/10.3389/fimmu.2014.00250

Zalevsky, J., Chamberlain, A. K., Horton, H. M., Karki, S., Leung, I. W. L., Sproule, T. J., Lazar, G. A., Roopenian, D. C., & Desjarlais, J. R. (2010). Enhanced antibody half-life improves in vivo activity. Nature Biotechnology, 28(2), 157–159. https://doi.org/10.1038/nbt.1601

Zanetti, G., Briggs, J. A. G., Grünewald, K., Sattentau, Q. J., & Fuller, S. D. (2006). Cryo-Electron Tomographic Structure of an Immunodeficiency Virus Envelope Complex In Situ. PLoS Pathogens, 2(8), e83. https://doi.org/10.1371/journal.ppat.0020083

Zhang, L., Irimia, A., He, L., Landais, E., Rantalainen, K., Leaman, D. P., Vollbrecht, T., Stano, A., Sands, D. I., Kim, A. S., Miiro, G., Serwanga, J., Pozniak, A., McPhee, D., Manigart, O., Mwananyanda, L., Karita, E., Inwoley, A., Jaoko, W., … Zwick, M. B. (2019). An MPER antibody neutralizes HIV-1 using germline features shared among donors. Nature Communications, 10(1), 1–16. https://doi.org/10.1038/s41467-019-12973-1

Zhou, T., Lynch, R. M., Chen, L., Acharya, P., Wu, X., Doria-Rose, N. A., Joyce, M. G., Lingwood, D., Soto, C., Bailer, R. T., Ernandes, M. J., Kong, R., Longo, N. S., Louder, M. K., McKee, K., O'Dell, S., Schmidt, S. D., Tran, L., Yang, Z., … Kwong, P. D. (2015). Structural repertoire of HIV-1-neutralizing antibodies targeting the CD4 supersite in 14 donors. Cell, 161(6), 1280–1292. https://doi.org/10.1016/j.cell.2015.05.007

Zhu, P., Liu, J., Bess, J., Chertova, E., Lifson, J. D., Grisé, H., Ofek, G. A., Taylor, K. A., & Roux, K. H. (2006). Distribution and three-dimensional structure of AIDS virus envelope spikes. Nature, 441(7095), 847–852. https://doi.org/10.1038/nature04817

Zhu, Z., Qin, H. R., Chen, W., Zhao, Q., Shen, X., Schutte, R., Wang, Y., Ofek, G., Streaker, E., Prabakaran, P., Fouda, G. G., Liao, H.-X., Owens, J., Louder, M., Yang, Y., Klaric, K.-A., Moody, M. A., Mascola, J. R., Scott, J. K., … Dimitrov, D. S. (2011). Cross-Reactive HIV-1-Neutralizing Human Monoclonal Antibodies Identified from a Patient with 2F5-Like Antibodies. Journal of Virology, 85(21), 11401–11408. https://doi.org/10.1128/jvi.05312-11

Zwaal, R. F. A., Comfurius, P., & Bevers, E. M. (2005). Surface exposure of phosphatidylserine in pathological cells. In Cellular and Molecular Life Sciences (Vol. 62, Issue 9, pp. 971–988). Springer. https://doi.org/10.1007/s00018-005-4527-3

Zwick, M. B. (2005). The membrane-proximal external region of HIV-1 gp41: A vaccine target worth exploring. In AIDS (Vol. 19, Issue 16, pp. 1725–1737). Lippincott Williams and Wilkins. https://doi.org/10.1097/01.aids.0000189850.83322.41

Zwick, M. B., Labrijn, A. F., Wang, M., Spenlehauer, C., Saphire, E. O., Binley, J. M., Moore, J. P., Stiegler, G., Katinger, H., Burton, D. R., & Parren, P. W. H. I. (2001). Broadly Neutralizing Antibodies Targeted to the Membrane-Proximal External Region of Human Immunodeficiency Virus Type 1 Glycoprotein gp41. Journal of Virology, 75(22), 10892–10905. https://doi.org/10.1128/jvi.75.22.10892-10905.2001